University of London

Imperial College London

In Vitro Osteogenic and Chondrogenic Differentiation of Embryonic Stem Cells for Bone and Cartilage Tissue Engineering

Yu-Shik Hwang

Submitted for PhD Degree Chemical Engineering

BIB. LONDON UNIV

ABSTRACT

Tissue engineering, which has emerged as a new discipline that amalgamates aspects from biology, engineering, materials science, and medicine, aims to produce functional replacement tissues that can be used to restore damaged ones. In view of the ageing population and the worldwide shortage of donor tissue, tissue engineering are expected to alter the practice of modern medicine.

Recently, embryonic stem cells (ESCs) are considered as potent cell source for skeletal tissue engineering due to several biological advantages. However, although considerable progress to direct ESC differentiation to specific lineages has been made, before ESCs may be used as a suitable cell source in cell and tissue therapy, there are still remaining obstacles which have to be resolved regarding ESC differentiation: 1) the requirement for more efficient methods for increasing the differentiation efficiency to the desired cell type; and 2) the requirement of developing time and cost effective culture systems for controlling ESC differentiation is essential.

The overall aim of this thesis was the development of an efficient method to control mesodermal differentiation and enhance osteogenic/chondrogenic differentiation of mESCs for application to skeletal tissue engineering. The initial focus of this thesis was the investigation of the effect of the HepG2 conditioned medium on the early differentiation of mESCs to primitive streak/nascent mesoderm-like cells, which could be potent progenitor cells of osteogenic/chondrogenic differentiation. Next, the focus was to investigate the control and enhancement of osteogenic and chondrogenic differentiation from mESC-derived primitive streak/nascent mesoderm-like cells by modulating the

culture conditions and process. Finally, the focus became the development of efficient bioprocessing for the three-dimensional (3D) osteogenic and chondrogenic differentiation of mESC in alginate hydrogels and the culture in HARV bioreactors for the purpose of achieving 3D bone/cartilage-like tissue formation, resulting in an efficient and reproducible culture system for bone and cartilage tissue engineering applications.

ACKNOWLEDGEMENTS

This thesis is the result of four and half years of work whereby I have been accompanied and supported by many people. It is a pleasant aspect that I have now the opportunity to express my gratitude for all of them. Especially, I would like to express my deep and sincere gratitude to my direct supervisor Dr Anathathios Mantalaris. I owe him lots of gratitude for having me shown this way of research. He could not even realize how much I have learned from him. I would also like to thank to my second supervisor Professor Dame Julia M Polak who monitored my work. Without her encouragement and understanding it would have been impossible for me to finish this work. Furthermore, I warmly thank the referees Professor Robert Brown and Dr. Xuebin Yang who took effort in reading and providing me with valuable advices and comments on this thesis.

During this work I have collaborated with many colleagues Wesley, Nick, Mark, Siti, Jaemin, Yunyi, Maya, Teresa, Carolyn, Iliana, Osama, Hugo, Michalis, Ines, Sandeep, Ming, Yiping, Chen, and Supacharn for whom I have great regard, and I wish to extend my sincere thanks to all those who have helped me and shared many experiences and thoughts with me throughout the last years. I would also like to gratefully acknowledge the support of all of my Korean friends Jaemin, Ji Eun, Johann, Joonsik, Sang Baek and others in Imperial College London. They helped me immensely by giving me encouragement, friendship, and the feeling of being at home at work. I was lucky to have such a good friends and collegues at work.

Finally, I feel a deep sense of gratitude for my father, my mother, my systers and their families who formed part of my vision and taught me the good things that really matter in life. I really appreciate for their loving support.

STATEMENT OF ORIGINALITY

I declare that this thesis was conducted and written by myself and that the work that it presents is my own except where stated otherwise.

Signed: 

Date: 14th March 2008

ABBREVIATIONS

[A]

ACI: Autologous chondrocyte implantation

ALPase: Alkaline phosphatase

α-MEM: Alpha modified Minimal Essential Medium

ARS: Alizarin Red S

ATR-FTIR: Micro attenuated total reflection - Fourier transformed infrared (FT-IR)

ATP: Adenosine triphosphate

ATCC: American Type Culture Collection

[B]

BCA: Bicinchoninic acid

bFGF: Basic fibroblast growth factor

bHLH: Basic helix-loop-helix

BMP-4: Bone morphogenic protein 4 (also known as BMP-2b or DVR-4)

βNGF : β nerve growth factor

BSA: Bovine serum albumin

[C]

Calcein AM: 3',6'-Di(O-acetyl)-2',7'-bis[N,N-bis(carboxymethyl) aminomethyl] fluorescein, tetraacetoxymethyl ester

Cbfa1: Core binding factor

cDNA: Complementary DNA

CM: Conditioned Medium

CM-mESCs: mESCs treated with HepG2 CM

CM-mESC-EB1: CM-mESCs allowed to form EBs for 1 day

CM-mESC-EB3: CM-mESCs allowed to form EBs for 3 days

CM-mESC-EB5: CM-mESCs allowed to form EBs for 5 days

CM-mESC-rr: mESCs were treated HepG2 CM for 3 days, and then replated and cultured in mESC maintenance medium

CM-mESC-rd: mESCs were treated HepG2 CM for 3 days and then cultured in mESC maintenance medium by direct media replacement without replating

CPC: Cetylpyridinium chloride

[D]

DAPI: 4',6 diamidino-2-phenylindole
DEX: Dexamethasone
DMEM: Dulbecco's Modified Eagles Medium
DMMB: 1,9-Dimethlmethylene Blue
DNA: Deoxynucleic acid
dNTP: 2'-deoxynucleoside 5'-triphosphate

[E]
EB5: mESCs allowed to form EBs for 5 days
ECM: Extracellular matrix
EC: Embryonic carcinoma
EG: Embryonic germ
EGF: Epidermal growth factor
EMT: Epithelial to mesenchyme transition
EB: Embryoid body
EDTA: Ethylenediaminetetraacetic acid
END-2: Visceral endoderm-like cell line
EPL: Early Primitive ectoderm Like cells
ERK: Extracellular receptor kinase
ESCs: Embryonic stem cells
EtBr: Ethidium bromide
EthD-1: Ethidium homodimer-1
E14Tg2a: E14 thioguanine resistance 2a mESC cell line

[F]
FACS: Fluorecence activated cell sorting
FBS: Foetal bovine serum
FDA: Food and Drug Administration
FITC: Fluorescein isothiocyanate)
Flk-1: Foetal liver kinase-1
FPA: Focal plane array

[G]
GAG: Glycosaminoglycans
GAPDH: Glyceraldehyde-3-phosphate dehydrogenase
gp: Glycoprotein

[H]

HA : Hydroxyapatite ($Ca_{10}(PO_4)_6(OH)_2$)
HARV: Horizontal Aspect Ratio Vessel
H&E: Haematoxylin & Eosin
HEPES: N-(2-hydroxyethyl) piperazine-N-(2- ethane sulfonic acid)
HepG2: Hepatocarcinoma cell line (ATCC HB-8605)
HGF: Hepatocyte growth factor
HMG: High-mobility group

[I]
ICM: Inner cell mass
IGF-I: Insulin-like growth factor I
IgG: Immunoglobulin G
ITS: Insulin-transferrin-selenium

[L]
LIF: Leukaemia inhibitory factor
LIFRβ: LIF receptor β

[M]
MAPK: Mitogen-activated protein kinase
mESCs: Mouse ESCs
mRNA: Massenger RNA
MSCs: Mesenchymal stem cells
MTS: 3-(4,5- dimethylthiazol-2-yl)-5-(3-carboxymethoxyphenyl)-2-(4-sulfophenyl)-2H-tetrazolium)

[O]
Oct4: Octamer binding factor 4 (also known as Oct-3, Oct-3/4, Pou5f1)
OB-cadherin: Osteoblast cadherin
OCN: Osteocalcin
OPN: Osteopontin

[P]
PA: Peptide–amphiphile
PBS: Phosphate buffered saline
PCR: Polymerase chain reaction
PDGF-BB: Platelet derived growth factor-BB
PEG: Poly(ethylene glycol)-based
PEGDA: Poly(ethylene glycol)-diacrylate

PI: Propidium iodide
PLGA: Poly(lactic-co-glycolic acid)

[R]
R: Rhodamine
RGD: Arginine-glycine-aspartate
RNA: Ribonucleic acid
RT: Reverse transcription
RWV: Rotating Wall Vessel
Runx2: Runt related transcription factor

[S]
SD: Standard deviation
SDS: Sodium dodecyl sulfate
SEM-EDS: Scanning Electron Microscope - Energy Dispersive spectroscopy
STAT3: Signal transducers and activators of transcription
SSEA-1: Stage-specific embryonic antigen

[T]
TBST: 20mM Tris-HCl, 0.15M NaCl and 0.05% Tween-20, pH 7.4
TCA: Tricarboxylic acid
TGF-β1: Transforming growth factor β1
TR: Texas Red
TSB: 1.0M Tris-2.0M NaCl-50mM $CaCl_2$, pH 7.8 - 8.0

[U]
UV: Ultraviolet

LIST OF FIGURES

Figure 1. Bone and cartilage defects 2

Figure 2. Bone remodelling 4

Figure 3. Articular cartilage structure 6

Figure 4. Principle of skeletal tissue engineering 8

Figure 5. MSC differentiation strategy 13

Figure 6. ESCs pluripotency in embryogenesis 18

Figure 7. *In vivo* differentiation process for mesoderm formation 20

Figure 8. *In vivo* mesodermal differentiation strategy of ESCs 21

Figure 9. The process of chondrogenesis 23

Figure 10. *In vitro* skeletal lineage differentiation of ESCs 71

Figure 11. Schematic diagram of experimental process for the generation of primitive streak/nascent mesoderm like cells from mESCs 75

Figure 12. Assessment of undifferentiation marker expression of mESCs in 2D expansion 76

Figure 13. mESC growth kinetics in accordance with cell seeding density 77

Figure 14. Morphological evaluation of ES cell (mESC) and conditioned media treated mESC (CM-mESC) under light microscope 78

Figure 15. mESC adhesion in HepG2 conditioned media (CM) and normal maintenance media (BM) 79

Figure 16. mESC proliferation in HepG2 conditioned media (CM) and normal maintenance media (BM) 80

Figure 17. Assessment of ALPase expression using Alkaline Phosphatase Detection Kit (Chemicon, USA) 81

Figure 18. Colorimetric assay for assessing ALPase activity 82

Figure 19. Immunostaining of mESCs and conditioned media treated mESCs

(CM-mESC) 83

Figure 20. Morphological evaluation of mESC and conditioned media treated mESC (CM-mESC) derived EBs under light microscope 85

Figure 21. Molecular analysis (RT-PCR) of brachyury, goosecoid, nodal and cripto gene expression with GAPDH control lanes 87

Figure 22. Morphological observation of mESCs in various culture conditions 88

Figure 23. Immunostaining of mESCs in various culture conditions 88-89

Figure 24. Current *in vitro* culture strategy for osteogenic and chondrogenic differentiation through EB formation 96

Figure 25. Schematic diagram of experimental process for EB-mediated osteogenic and chondrogenic differentiation of mESCs 100

Figure 26. Morphology of beating colony 102

Figure 27. Effect of EB formation time on beating colony formation 103

Figure 28. Immunocytochemical staining for sarcomeric α-actinin and tropomyosin in the CM-treated mESCs 104

Figure 29. RT-PCR analysis of cardiogenic (Nkx-2.5) gene expression at day 11 of culture 105

Figure 30. Morphology of mineralised bone nodule 106

Figure 31. Alizarin red S stained bone nodules in a light microscope 107

Figure 32. Alizarin red S stained bone nodules under UV light 108

Figure 33. Bone nodule formation 109

Figure 34. Immunocytochemical staining for OB-cadherin in CM-treated mESC-derived cultures 110

Figure 35. Alkaline phosphatase activity 111

Figure 36. RT-PCR analysis of osteogenic (Cbfa1/Runx2) gene expression at day 11 of culture 112

Figure 37. Morphology of cartilage nodules 114

Figure 38. Quantification of the Alcian blue stained areas of cartilage nodules 115

Figure 39. Alcian blue and Alizarin red-S double staining 116

Figure 40. Quantification of relative matrix sulfated GAG amount produced by culture 118

Figure 41. Immunostaining of cartilage nodules with type II collagen antibody 119

Figure 42. Molecular analysis (RT-PCR) of type II collagen, aggrecan, sox-9 and type X collagen gene expression with GAPDH control lanes 120

Figure 43. Schematic illustration of cystic EB formation 131

Figure 44. Schematic illustration of direct *in vitro* osteogenesis and chondrogenesis without EB formation process 134

Figure 45. Alizarin red S quantification for evaluating bone nodule formation 135

Figure 46. Characterisation of mineralised bone nodules 136

Figure 47. Assessment of ALPase expression using Alkaline Phosphatase Detection Kit (Chemicon, USA) 137-138

Figure 48. Colorimetric assay for assessing ALPase activity 139

Figure 49. Immunocytochemical staining for type I collagen and osteopontin in CM-treated mESC-derived cultures 140

Figure 50. RT-PCR analysis of osteogenic gene expression 142

Figure 51. Morphology of cartilage nodules and other cell lineages 143

Figure 52. Quantification of the Alcian blue stained areas of cartilage nodules 144

Figure 53. Quantification of relative matrix sulfated GAG amount produced by culture 145

Figure 54. Quantification of relative matrix collagen amount produced by culture

146

Figure 55. Immunostaining of cartilage nodules with type II collagen and sox-9 antibody 147

Figure 56. Molecular analysis (RT-PCR) of type II collagen, scleraxis, sox-9 aggrecan, and link-protein gene expression with GAPDH control lanes 148

Figure 57. RWV bioreactor and influencing factor diagram for particle move 160

Figure 58. Schematic representation of the different gel network structures of a Ca-alginate hydrogel 162

Figure 59. Experimental process for single step 3D osteogenesis and chondrogenesis in a HARV bioreactor 164

Figure 60. Alginate beads and HARV bioreactor system 165

Figure 61. Live/dead assay and morphology of cells within alginate beads in 3D osteogenesis 166-167

Figure 62. The change of pH, glucose, ammonia and lactate concentration in medium in accordance with culture time during 3D osteogenesis 168

Figure 63. RT-PCR analysis of osteogenic gene expression in 3D osteogenesis 169

Figure 64. Various staining and immuno-staining for mineralised bone nodules and osteogenic differentiation 171-173

Figure 65. The FTIR images and ATR-FTIR spectra of cell + alginate construct 175

Figure 66. SEM and EDS microanalysis spectra for the composition of mineralised bone nodules formed within alginate beads in the osteogenic culture of mESCs after 21 days 176

Figure 67. Mechanical strength of bone like construct 177

Figure 68. Live/dead assay and morphology of cells within alginate beads 178

Figure 69. The change of pH, glucose, ammonia and lactate concentration in medium in accordance with culture time during 3D chondrogenesis 179

Figure 70. RT-PCR analysis of chondrogenic gene expression in 3D chondrogenesis 181

Figure 71. Various staining and immuno-staining for 3D cartilage like construct 182-185

LIST OF TABLES

Table 1. Oligonucleotide primers for RT-PCR analysis for mESCs early differentiation 39

Table 2. Oligonucleotide primers for RT-PCR analysis for osteogenic and spontaneous cardiogenic differentiation through EB formation 45

Table 3. Oligonucleotide primers for RT-PCR analysis for chondrogenic differentiation through EB formation 49

Table 4. Oligonucleotide primers for RT-PCR analysis for direct osteogenesis 52

Table 5. Oligonucleotide primers for RT-PCR analysis for direct chondrogenesis 57

Table 6. Oligonucleotide primers for RT-PCR analysis for 3D osteogenesis 62

Table 7. Oligonucleotide primers for RT-PCR analysis for 3D chondrogenesis 62

Table 8. Current approaches for *in vitro* EB mediated osteogenesis and chondrogenesis 129

TABLE OF CONTENTS

ABSTRACT

ACKNOWLEDGEMENTS

STATEMENT OF ORIGINALITY

ABBREVIATIONS

LIST OF FIGURES

LIST OF TABLES

CHAPTER I. LITERATURE RVIEW 1

1.1. Clinical Needs in Bone and Cartilage Regeneration 2
- 1.1.1. Bone and Current Approaches for Bone Regeneration 3
- 1.1.2. Cartilage and Current Approaches for Cartilage Regeneration 5

1.2. Principle of Tissue Engineering 7

1.3. Cells for Bone and Cartilage Tissue Engineering 10
- 1.3.1. Adult Differentiated Cell 11
- 1.3.2. Adult Stem Cell 12
- 1.3.3. Embryonic Stem Cell 15

1.4. *In Vivo* Osteogenesis and Chondrogenesis of Embryonic Stem Cells 19
- 1.4.1. *In Vivo* Mesoderm Formation of ESCs 19
- 1.4.2. *In vivo* Osteogenesis and Chondrogenesis 22

1.5. Aims and Objectives 24

CHAPTER II. MATERIALS AND METHODS 26

2.1. Overview of Experiment 27

2.2. Basic Materials and Common Assay Techniques 27
2.2.1. Media 27
2.2.1.1. mESC maintenance medium 27
2.2.1.2. HepG2 maintenance medium 27
2.2.1.3. EB formation medium 28
2.2.2. Cell Culture 28
2.2.2.1. mESC maintenance and expansion 28
2.2.2.2. HepG2 maintenance and expansion 28
2.2.2.3. Collection of HepG2 conditioned media 28
2.2.3. Common Assay Techniques 29
2.2.3.1. Immunocytochemical staining 29
2.2.3.2. Ribonucleic acid (RNA) extraction 30
2.2.3.3. Reverse transcription (RT) 30
2.2.3.4. Polymerase chain reaction (PCR) amplification 31
2.2.3.5. Agarose gel electrophoresis 31

2.3. Early Differentiation of Murine Embryonic Stem Cells into Primitive Streak/Nascent Mesoderm Like Cells 33
2.3.1. mESCs Expansion and Characterisation 33
2.3.2. Induction of mESC Early Differentiation by HepG2 Conditioned Media 35
2.3.3. Embryoid Body (EB) Formation 35
2.3.4. Characterisation 35
2.3.4.1. Morphological observation 35
2.3.4.2. Cell adhesion and proliferation assay 36
2.3.4.3. ALPase expression and ALPase activity 36
2.3.4.4. Immunocytochemistry 38
2.3.4.5. Reverse transcription and polymerase chain reaction (RT-PCR) 38
2.3.4.6. Reversibility of early differentiation and characterisation 40

2.4. *In Vitro* Osteogenic and Chondrogenic Differentiation of Murine Embryonic Stem Cells through EB Formation 42
2.4.1. Osteogenic and Spontaneous Cardiogenic Differentiation 42

2.4.1.1. Osteogenic Media 42
2.4.1.2. Experimental groups 42
2.4.1.3. Osteogenic differentiation 43
2.4.1.4. Beating colony formation and quantification 43
2.4.1.5. Bone nodule formation and quantification (ARS staining) 43
2.4.1.6. Immunocytochemical staining 44
2.4.1.7. Reverse transcription and polymerase chain reaction (RT-PCR) 44
2.4.1.8. Colorimetric quantification of ALPase activity 45
2.4.2. Chondrogenic Differentiation 45
2.4.2.1. Chondrogenic Media 45
2.4.2.2. Experimental groups 46
2.4.2.3. Micromass culture for chondrogenesis 46
2.4.2.4. Measurement of Alcian blue-stained areas 46
2.4.2.5. Measurement of sulfated GAG content (1,9-DimethImethylene Blue (DMMB) assay) and DNA content 47
2.4.2.6. Immunocytochemical staining 48
2.4.2.7. Reverse transcription and polymerase chain reaction (RT-PCR) 49

2.5. *In Vitro* Osteogenic and Chondrogenic Differentiation of Murine Embryonic Stem Cells without EB Formation 50
2.5.1. Direct Osteogenic Differentiation without EB Formation 50
2.5.1.1. Direct osteogenic differentiation 50
2.5.1.2. Bone nodule formation (ARS staining) and ARS quantification 50
2.5.1.3. ALPase expression and ALPase activity 51
2.5.1.4. Immunocytochemical staining 51
2.5.1.5. Reverse transcription and polymerase chain reaction (RT-PCR) 52
2.5.2. Direct Chondrogenic Differentiation without EB Formation 53
2.5.2.1. Chondrogenic medium 53
2.5.2.2. Direct osteogenic differentiation 53
2.5.2.3. Morphological observation 54
2.5.2.4. Measurement of Alcian blue-stained areas 54
2.5.2.5. Measurement of sulfated GAG content (1,9- DimethImethylene Blue (DMMB) assay) and DNA content 54
2.5.2.6. Measurement of collagen content and DNA content 55
2.5.2.7. Immunocytochemical staining 56
2.5.2.8. Reverse transcription and polymerase chain reaction (RT-PCR) 56

2.6. Bioprocessing for Three Dimensional (3D) Bone and Cartilage Tissue Like Construct Formation Using Alginate Encapsulated Murine Embryonic Stem

Cells and HARV Bioreactors 58
2.6.1. 3D mESC Encapsulation 58
2.6.2. Operation of Single-Step Bioprocess Using HARV Bioreactors 59
2.6.3. Characterisation of 3D Osteogenesis and Chondrogenesis 59
2.6.3.1. Observation of cell viability (Live/Dead assay) 60
2.6.3.2. Bioprofiling 60
2.6.3.3. Reverse transcription and polymerase chain reaction (RT-PCR) 61
2.6.3.4. Staining of paraffin embedded section of alginate beads 63
2.6.3.4.1. Paraffin embedding of alginate beads 63
2.6.3.4.2. Haematoxylin & Eosin staining 63
2.6.3.4.3. Alizarin Red S staining (3D osteogenesis) 64
2.6.3.4.4. Alcian Blue and Safranin O staining (3D chondrogenesis) 64
2.6.3.4.5. Immuno-staining (3D osteogenesis and chondrogenesis) 65
2.6.3.4.6. Physicochemical and mechanical characterisation of alginate beads (3D osteogenesis) 66
2.6.3.4.6.1. SEM-EDS analysis 66
2.6.3.4.6.2. FT-IR analysis 67
2.6.3.4.6.3. Compression study 67
2.7. Statistical Analysis 68

CHAPTER III: EARLY DIFFERENTIATION OF MURNE EMBRYONIC STEM CELLS INTO PRIMITIVE STREAK / NASCENT MESODERM LIKE CELL 69

3.1. Introduction: Current Approaches for *In Vitro* Early Differentiation of Embryonic Stem Cells into Mesoderm 70
3.1.1. EB mediated in vitro spontaneous early differentiation 70
3.1.2. *In vitro* early differentiation using exogenous cytokines and growth factors 72
3.1.3. *In vitro* early differentiation using conditioned media 73

3.2. Objectives 74

3.3. Experimental Process 75

3.4. Results 75
3.4.1. mESCs expansion and maintenance 75
3.4.2. mESCs morphological studies 77

3.4.3. Cell adhesion and growth 78
3.4.4. ALPase expression in mESC and CM-mESCs 80
3.4.5. Molecular expression relating with ESCs pluripotency and early differentiation 83
3.4.6. EB formation capacity 84
3.4.7. Gene expression 86
3.4.8. Reversibility of early differentiation 87

3.5. Discussion 90

3.6. Conclusion 94

CHAPTER IV: *IN VITRO* OSTEOGENIC AND CHONDROGENIC DIFFERENTIATION OF MURINE EMBRYONIC STEM CELLS THROUGH EB FORMATION 95

4.1. Introduction: Current Approaches for *In Vitro* EB-Mediated Osteogenic and Chondrogenic Differentiation of Embryonic Stem Cells 96

4.2. Objectives 99

4.3. Experimental Process 99

4.4. Results 101
4.4.1. *In vitro* EB-mediated cardiogenic differentiation 101
4.4.1.1. Morphology of beating colonies 101
4.4.1.2. Beating colony formation 102
4.4.1.3. Immuno-staining for cardiogenic differentiation 103
4.4.1.4. Cardiogenic gene expression 105
4.4.2. *In vitro* EB-mediated osteogenic differentiation 105
4.4.2.1. Morphology of mineralised bone nodules 106
4.4.2.2. Bone nodule formation 106
4.4.2.3. Immuno-staining for osteogenic differentiation 109
4.4.2.4. Alkaline phosphatase activity 110
4.4.2.5. Osteogenic gene expression 112
4.4.3. *In vitro* EB-mediated chondrogenic differentiation 113
4.4.3.1. Morphology of cartilage nodule 113
4.4.3.2. Cartilage nodule formation 114

4.4.3.3. Glycosaminoglycan (GAG) synthesis 117
4.4.3.4. Immuno-staining for chondrogenic differentiation 118
4.4.3.5. Chondrogenic gene expression 119

4.5. Discussion 121

4.6. Conclusion 127

CHAPTER V: *IN VITRO* DIRECT OSTEOGENIC AND CHONDROGENIC DIFFERENTIATION OF MURINE EMBRYONIC STEM CELLS WITHOUT EB FORMATION PROCESS 128

5.1. Introduction 129

5.2. Objectives 132

5.3. Experimental Process 133

5.4. Results 134
5.4.1. Direct osteogenic differentiation 134
5.4.1.1. Bone nodule formation and quantification 134
5.4.1.2. Characterisation of mineralised bone nodule 135
5.4.1.3. ALPase expression and activity quantification 137
5.4.1.4. Immuno-staining for osteogenic differentiation 140
5.4.1.5. Osteogenic gene expression 141
5.4.2. Direct chondrogenic differentiation 142
5.4.2.1. Morphological evaluation 142
5.4.2.2. Cartilage nodule formation 143
5.4.2.3. Extracellular matrix synthesis 144
5.4.2.4. Immuno-staining for chondrogenic differentiation 146
5.4.2.5. Chondrogenic gene expression 147

5.5. Discussion 149

5.6. Conclusion 155

CHAPTER VI: BIOPROCESSING FOR THREE DIMENSIONAL BONE AND CARTILAGE TISSUE LIKE CONSTRUCT FORMATION USING ALGINATE

ENCAPSULATED MURINE EMBRYONIC STEM CELLS AND HARV BIOREACTORS 157

6.1. Introduction 158

6.2. Objectives 163

6.3. Experimental Process 163

6.4. Results 165
6.4.1. Alginate beads and HARV bioreactor system 165
6.4.2. *In vitro* single step 3D osteogenesis in a HARV bioreactor 165
6.4.2.1. Observation of cell viability 166
6.4.2.2. Bioprofiling 167
6.4.2.3. Osteogenic gene expression 168
6.4.2.4. Staining and immuno staining 170
6.4.2.5. Physicochemical characterisation of alginate beads 173
6.4.2.5.1. The micro attenuated total reflection-Fourier transformed infrared (ATR-FTIR) analysis of mineralised nodules 173
6.4.2.5.2. Scanning Electron Microscope (SEM) and Energy Dispersive spectroscopy (EDS) analysis of mineralised bone nodules 176
6.4.2.5.3. Mechanical property of 3D bone like construct 177
6.4.3. *In vitro* single step 3D chondrogenesis in a HARV bioreactor 177
6.4.3.1. Observation of cell viability 177
6.4.3.2. Bioprofiling 178
6.4.3.3. Chondrogenic gene expression 180
6.4.3.4. Staining and immuno-staining 181

6.5. Discussion 185

6.6. Conclusion 193

CONCLUSION AND FUTURE WORK 194

REFERENCES 200

APPENDIX 225

ACHIEVEMENTS DERIVED FROM THIS STUDY 234

CHAPER I

LITERATURE REVIEW

1.1. Clinical Needs in Bone and Cartilage Regeneration

Therapeutic repair of skeletal tissues has received significant interest by the scientific community. Advances in reconstructive orthopaedic surgery, such as total hip replacement, spinal fusion and plastic surgery, resulting from progress in surgical procedures and the increase in an ageing population, have lead to a demand for bone and cartilage grafts that exceeds the current available supply. Therefore, the loss of bone and cartilage tissue due to congenital defects, trauma and following tumour resection represents a major clinical problem. Specifically, trauma and diseases of the bones or cartilage, frequently involving structural damage to both the subchondral bone and the articular cartilage surface (Figure 1), result in pain and disability for millions of people worldwide and affect the quality of life of patients [South-Paul JE 2001, Percival M 1999, Bobic V 2000, Buckwalter JA 2002].

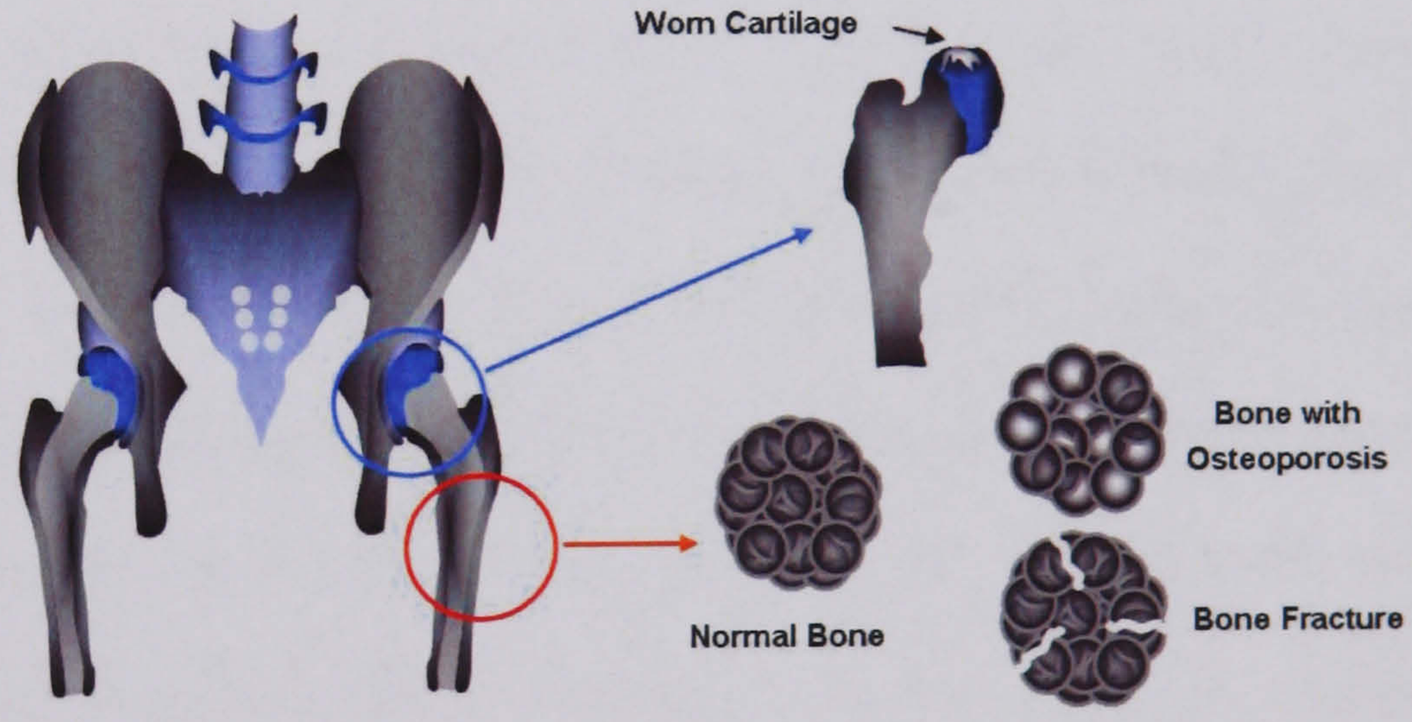


Figure 1. Bone and cartilage defects

Furthermore, the deterioration of bone and cartilage tissue due to age related degenerative diseases, such as osteoporosis and osteoarthritis, is a major public health issue for the elderly [Percival M 1999, Martin JA 2002]. However, despite recent advances in surgical and non-surgical therapies, the treatment of

bone and cartilage regions still remains an intractable problem. Therefore, regeneration of skeletal tissues represents one of the most promising areas of biological repair that could provide a broad spectrum of potential clinical applications.

1.1.1. Bone and Current Approaches to Bone Regeneration

Bone is rigid substance with an intricate structure. The periosteum, a fibrous membrane, covers the outside of bone. This membrane is rich with capillaries, which are responsible for nourishing bone. The outer layer of bone is termed compact bone – eighty percent of skeletal bone mass is compact bone Compact bone is mainly composed of a hollow, laminated rod of collagen and calcium phosphate, which is optimised to handle compressive and bending forces. Near the end of the bones, where the stresses become more complex, there is a meshwork of cancellous, or spongy bone, which is an inner spongy structure that resembles a honeycomb and accounts for 20% of bone mass. The inner bone cavities contain bone marrow, where all blood cells are produced [Weiner S 1992]. Bone performs several key functions within the body. Being composed of hard tissue, bone provides mechanical resistance and structural support to the body; its hard matrix mainly composed of calcium salts deposited around protein fibres. Minerals provide rigidity to bone whereas proteins, such as collagen, provide strength and elasticity. Furthermore, bone is engaged in a continuous cycle of remodelling. Bone absorbing cells, termed osteoclasts, break bone down and discard worn cells. After a few weeks, the osteoclasts disappear and osteoblasts recruite to repair bone (Figure 2). During this cycle, calcium is deposited and withdrawn from the blood [Seeman, 2006]. Consequently, bone is capable of

maintaining an optimal shape and structure throughout life via this continual process of renewal through which it is able to respond to changes in its mechanical environment thus maintaining an optimal balance between form and function.

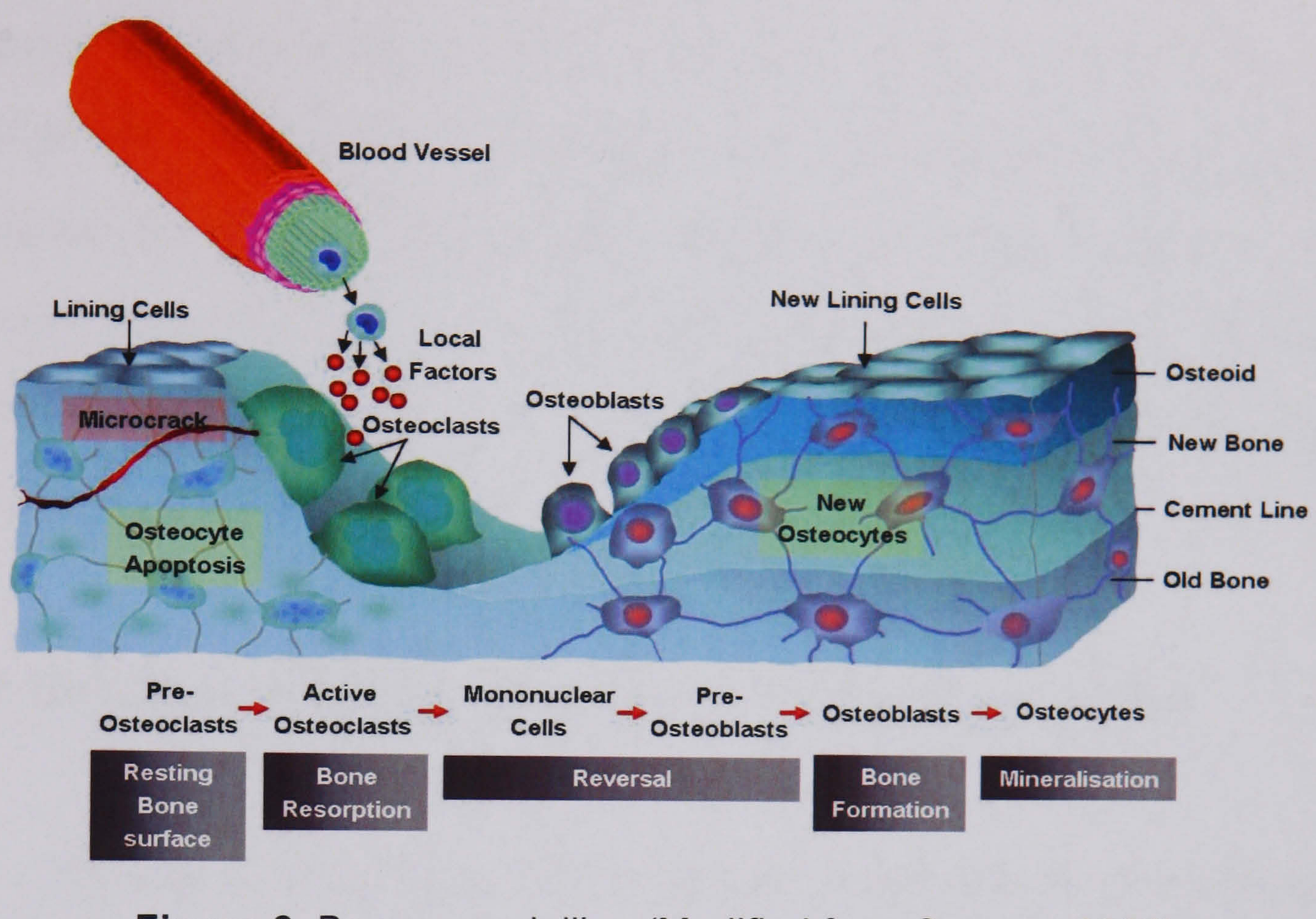


Figure 2. Bone remodelling (Modified from Seeman 2006)

Bone defects can occur in a wide variety of situations; their reconstruction being important in the patient's rehabilitation. The current golden standard for bone regeneration and reconstruction, the autogenous bone graft, works well in many circumstances. However, autograft reconstructions, along with the available alternatives of allogenous bone graft or bone cement, do not solve all instances of bone deficiency. Furthermore, patients with bone disease, such as osteoporosis, have poor bone regeneration capacity since the disease deters bone regeneration - normal haemostatic remodelling being abrogated in osteoporosis [Hollinger, 2000]. In addition, clinical treatments for critical-sized defects are problematic and often yield poor healing due to the complicated anatomy and physiology of bone

tissue. Therefore, although autologous or allogenic bone grafts have been employed for many years [Giannoudis PV 2005], a number of disadvantages to their use exist, including the failure of complete resorption of autologous bone, difficulties in shaping the bone graft to fill the defect, possible immune reaction in allograft, and, often, a lack of sufficient available material. In certain instances of patients with osteoporosis, cell therapy has been suggested as an effective alternative, but this has not been widely accepted for clinical practice due to the shortage of donor cells [Betz RR 2002]. Consequently, tissue engineered therapies, uniquely tailored to the bone regeneration requirements of individual patients, are extremely important.

1.1.2. Cartilage and Current Approaches to Cartilage Regeneration

Articular cartilage consists of the cellular component, the matrix-secreting chondrocytes, and the extracellular matrix (ECM) they secrete, mainly type II collagen, hyaluronic acid, and chondroitin sulphate, which accounts for the tissue's characteristic rigidity and flexibility. Articular cartilage (Figure 3) is typically depicted in 4 zones [James CB 2001] - each zone having its own distinct matrix region. The superficial zone includes the gliding surface of the joint. This layer of cell-free matrix contains fine fibrils with few polysaccharides and is adjoined by a layer of elongated chondrocytes organised parallel to the articular surface. The next layer is the transitional zone, which includes active chondrocytes. The collagen fibrils of this zone are larger than those of the superficial zone. In this layer, collagen fibre orientation transitions from parallel to columnar. The deep zone contains chondrocytes that are similar to those of the transitional zone but are organized in a columnar pattern perpendicular to the joint surface. These cells

contain large amounts of intermediate filaments and glycogen granules. Furthermore, the largest collagen fibrils of articular cartilage and the highest content of proteoglycans are also contained here. The deepest zone of calcified cartilage separates the softer cartilage from subchondral bone.

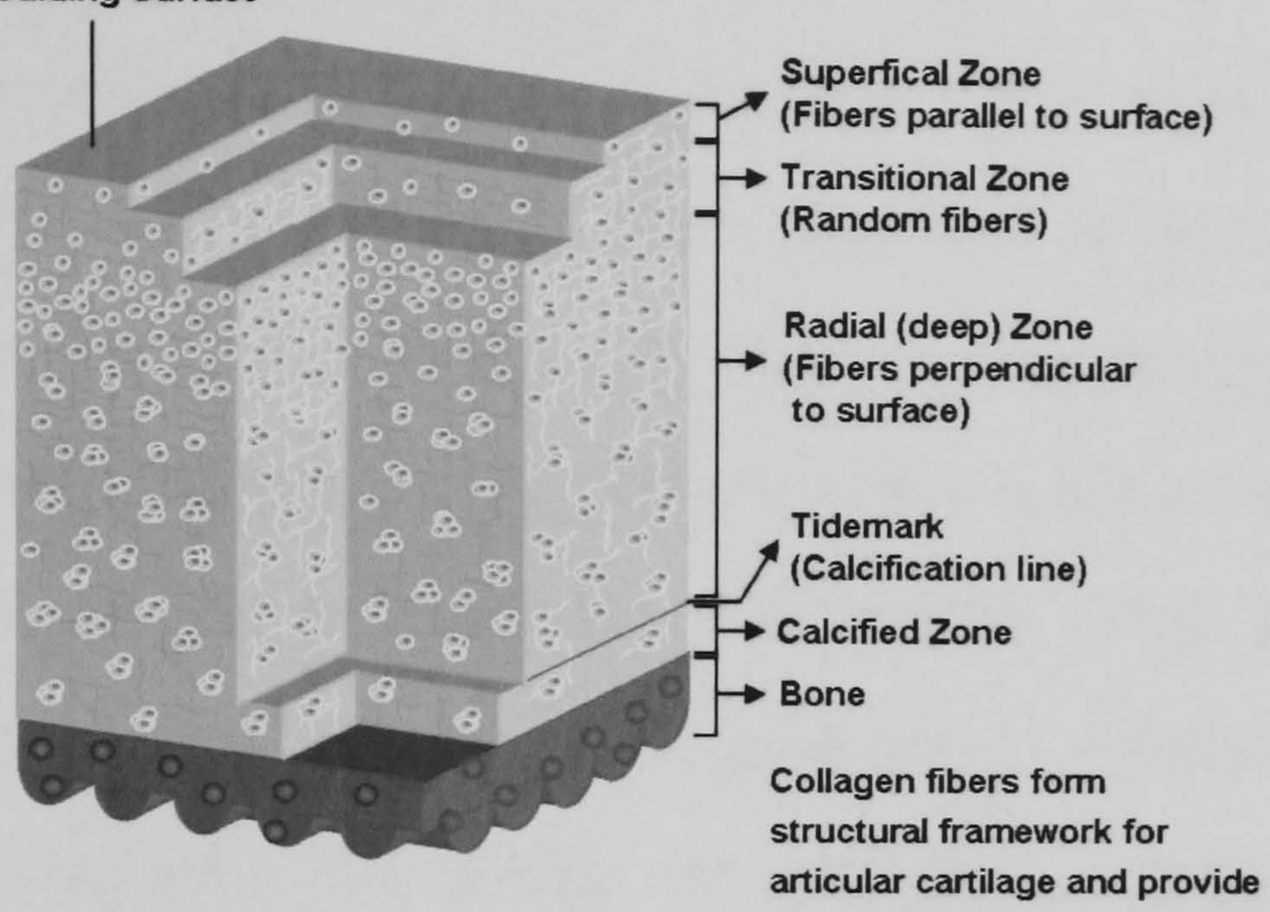


Figure 3. Articular cartilage structure (Modified from ref: James CB 2001)

These components are required for the survival and functionality of the cartilage tissue, especially in the joints where cartilage has to endure pressure forces caused by movement. Joint pain, often a consequence of joint degeneration due to primary osteoarthritis resulting in cartilage loss, is a major healthcare problem affecting, in particular, elderly people [Martin JA 2002]. The self-regeneration capacity of articular cartilage is very limited; attempts to repair articular cartilage defects, including transplantation of autologous chondrocyte or mesenchymal cells from bone marrow, have been investigated [Hambly K 2006, Yoo J 2001]. Recently, autologous chondrocyte implantation (ACI) has been widely used to improve cartilage repair. The first step of ACI is to perform an arthroscopic surgery to identify the area of cartilage damage, where during the arthroscopic

procedure chondrocytes are harvested. The harvested chondrocytes are expanded *in vitro* for approximately 4-6 weeks in order to generate enough cells. Following expansion, a second surgery is required where a larger incision is made to access the area of cartilage damage. In addition, an incision over the thin bone is required in order to harvest periosteum tissue, which will provide the periosteal patch required to cover the cartilage-damaged area. The periosteal patch is sewn over the area of damaged cartilage. Once a tight seal is created between the patch and the surrounding cartilage, the cultured chondrocytes are injected underneath the patch [Hambly K 2006]. However, this approach is limited due to the collection of autolougus cartilage tissue, which causes further cartilage defects in the peripheral area and suffers from the availability of suitable tissue and cell source. As an alternative cell source for autologous cartilage implantation, mesenchymal stem cells (MSCs) isolated from the bone marrow have been employed due to their potential to differentiate towards the chondrogenic lineage [Yoo J 2001]. However, the use of MSCs is also limited since their self-renewal, proliferative capacity and population is restricted and decrease with age [Tsuji T 1990, Dodson SA 1996]. Thus, the search for new cell sources is ongoing. Thus, the development of new therapies that involve bone and cartilage regeneration has focused on bone and cartilage tissue engineering strategies that may provide alternative solutions of “living” constructs that possess the potential to integrate with the surrounding native tissue.

1.2. Principle of Tissue Engineering

Tissue engineering is a new discipline that combines knowledge and

technology from biology, chemical engineering, materials science, and surgery. The aim of tissue engineering is the fabrication of functional living tissues to replace damaged tissues. Although advances in tissue engineering have been rapid, it is acknowledged that research that is more basic is necessary to develop its full potential. In recent years, skeletal tissue engineering progress includes methods for the harvest, expansion, lineage specific differentiation and transplantation of tissue-forming cells, the use of bioactive matrix materials as tissue scaffolds, local or systemic delivery of various hormones and growth factors or other chemical compounds, and other methods to control the culture environment [Petite H 2000, Tamura S 2001, Karen JLB 2001]. In particular, the *in vitro* expansion and differentiation of cells, most commonly in bioreactors and the utilisation of appropriate 3-dimensional (3D) polymeric or natural scaffolds has been explored [Freed LE 1997]. In general, the general principle of skeletal tissue engineering (Figure 4), specifically bone and cartilage tissue engineering, involves combining bone and cartilage forming cells, such as osteoblasts and chondrocytes, with a natural or synthetic support or scaffold to produce a three-dimensional living tissue construct that is functionally, structurally, and mechanically equal to bone or cartilage it has been designed to replace [Cancedda R 2003].

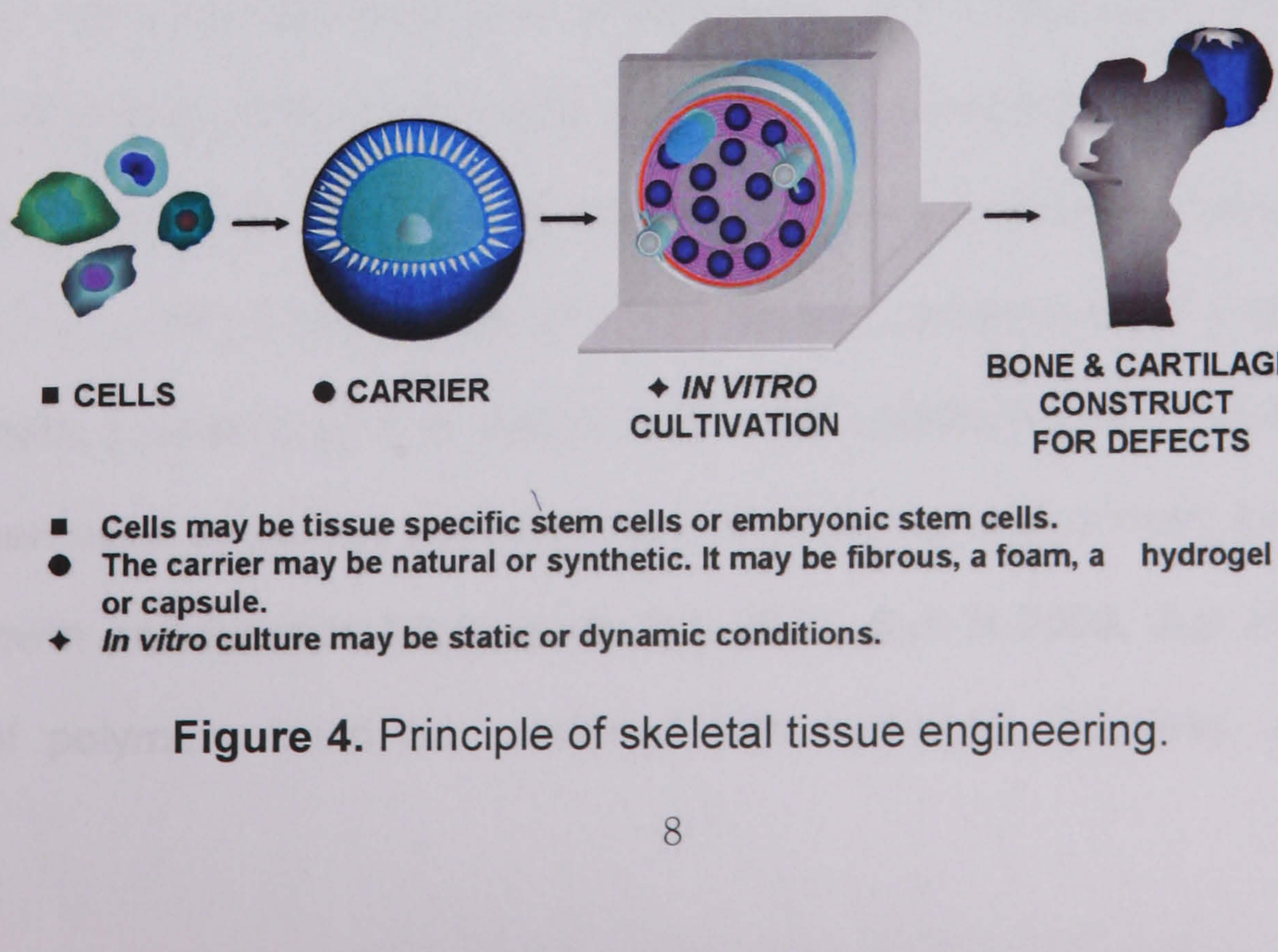


Figure 4. Principle of skeletal tissue engineering.

Tissue engineered constructs are mainly composed of two components: (i) tissue-forming cells, and (ii) a biocompatible carrier scaffold on which these cells can grow and differentiate. Numerous cell and scaffold choices are available with unique advantages and disadvantages. Research and clinical therapies have explored using cells alone, cells in combination with a biomaterial scaffold, and biomaterials that induce host cell activities [Yoo J 2001, Tamura S 2001, Karen JLB 2000]. The cells are important for the production of new tissue through ECM synthesis and are responsible for the long-term stability of this matrix. The scaffold material provides mechanical strength of the construct and a template for 3D growth. Addition of a cellular component to the scaffold may aid in repairing tissue at a faster rate as well as in repairing larger defects. Thus, the interaction of scaffolds and cells, cell adhesion on the matrix surface, cell maturation, ECM production, and cell proliferation are all important for the success of a tissue engineered construct.

To date, there has been significant progress in developing tissue engineered constructs using various scaffolds and cells. For instance, in bone tissue engineering, many suitable materials have been generated, including synthetic hydroxyapatite/tricalcium phosphates and polyglycolic and polylactic acids. Transplants of hydroxyapatite ceramics supplemented with periosteal cells or bone marrow cells appear to be effective for forming bone-like tissue [Brook IM 1991, Mankani MH 2004, Bianco P 2001]. Other commonly used materials, such as synthetic polylactic acid or poly L-lactic acid hybridized with natural collagen, have been used as porous scaffold to provide suitable environment for osteogenic cells growth and function [Hutmacher DW 2000, Suh H 2000, Suh H 2001], and some of polymers could be combined with hydrogels, bioglass, or ceramics

[Endres M 2003, Blaker JJ 2005, Chen OZ 2006].

Similarly, in cartilage tissue engineering, the development of various polymeric, such as the biodegradable and biocompatible poly(α-hydroxy esters) – namely, polyglycolic acid, polylactic acid, and copolymer poly(lactic-co-glycolic acid) (PLGA), has resulted in approval by the US Food and Drug Administration (FDA) for clinical use [Li WJ 2006]. Several studies have reported the morphological maintenance of chondrocytes and the synthesis of cartilage specific ECM by chondrogenic cells in these scaffolds [Vacanti CA 1991, Mahmoudifar N 2005, Mouw JK 2005]. In addition, hydrogels, which are crosslinked polymer networks that have the ability to absorb large amounts of water making these materials attractive scaffolds for engineering tissues with high water content, such as cartilage. For instance, alginate, a seaweed-derived polysaccharide approved by the FDA for medical use [Atala A 2005], has been identified as such a suitable candidate and has been used to culture annular chondrocytes in hydrostatic loading experiments [Kuo CK 2001, Wenger KH 2005]. However, no clinical application has materialised, yet.

Despite the advances in biomaterials and culture systems for bone/ cartilage tissue engineering, identification of an appropriate cell source that is easily obtainable, has good expansion ability, and can be differentiated into the desired cell type, still remains a significant challenge.

1.3. Cells for Bone and Cartilage Tissue Engineering

In vivo, cells are essential for the construction, remodelling, and maintenance of tissues. Furthermore, they contribute to tissue repair by various

mechanisms, including the secretion of soluble signals and the production of matrix molecules. Cells used in tissue engineering applications can be derived from numerous sources, including primary tissues as well as cell lines. The ideal properties are non-immunogenic, highly proliferative (since large numbers may be required), easy to harvest, and able to differentiate into specific cell types with specialized functions [Marler JJ, 1998]. Both autologous and allogenic cells have been considered as cell sources, including adult differentiated cells, adult stem cells and embryonic stem cells (ESCs).

1.3.1. Adult Differentiated Cells

The most obvious cell source is the tissue itself; hence, autologous adult differentiated cells, such as mature osteoblasts and chondrocytes, have been used extensively and are considered the “golden” standard. However, the use of human derived osteoblasts has been primarily confined to laboratory studies and no clinical application exist yet. In contrast, chondrocytes have been widely used as an adult differentiated cell source and currently autologous chondrocyte implantation (ACI) is approved by the FDA as a cell-based cartilage repair product [Brittberg M 1994, Brittberg M 2001].

However, in most cases, differentiated cells released from adult tissues exhibit a very limited proliferation capacity, which could be due to the accelerated telomere shortening associated with age resulting in replicative senescence of cells [Muschler GF 2004, Harley CB 1990, Martin JA 2001]. This presents serious limitations to their expansion in culture in order to generate sufficient cell numbers for use in the *in vitro* reconstruction of engineered tissues that are to be transplanted back to the patients. In addition, lack of source and the harvesting of

adequate numbers of adult differentiated cells for extracorporeal expansion are also problematic. Specifically, harvesting osteogenic cells is time consuming and relatively few cells are available after dissociation of bone tissue in addition to exhibiting relatively low cellular expansion rates [Salgado AJ 2004]. Furthermore, even though chondrocytes have already been utilised in ACI, certain limitations exist such as the amount of tissue that can be harvested as well as donor site morbidity [Temenoff JS 2000, Schreiber RE 2000]. When chondrocytes are removed from their native tissue environment and expanded in monolayer, they lose their chondrogenic phenotype as evidenced by loss of spherical cell shape, production of type I collagen instead of type II collagen, and aggrecan gene expression [Schnabel M 2002]. Consequently, ACI is applicable to cartilage defects with only small degenerated areas. Therefore, more rapidly proliferating cell sources such as foetal, neonatal, genetically manipulated, or stem cells are being explored [Vacanti JP 1999].

1.3.2. Adult Stem Cells

Adult stem cells are capable of self-renewal and of differentiating into tissue-specific cell lineages as directed by appropriate inducers. Progenitor or precursor cells in foetal or adult tissues are partly differentiated cells that divide and give rise to fully differentiated cells. Such cells are usually regarded as "committed" to differentiation along a particular cellular development pathway. The primary function of adult stem cells is to homeostasis and to replace cells that die because of injury or disease. Adult stem cells are present in most tissues but the capacity to which they contribute to normal homeostasis and repair varies widely [Rando TA 2006]. Ideally, adult stem cells are also defined as clonogenic cells

where a single adult stem cell generates a line of genetically identical cells, which then give rise to all the appropriate, differentiated cell types of the tissue in which they reside [Hennessy B 2004].

To date, bone marrow cells are the most frequently used cell source in bone and cartilage tissue engineering. The marrow (Figure 5) contains mesenchymal stem cells (MSCs), which contribute to the regeneration of mesenchymal tissues such as bone, cartilage, muscle, ligament, tendon, adipose, and stroma [Pittenger MF 1999, Caplan AI 2005].

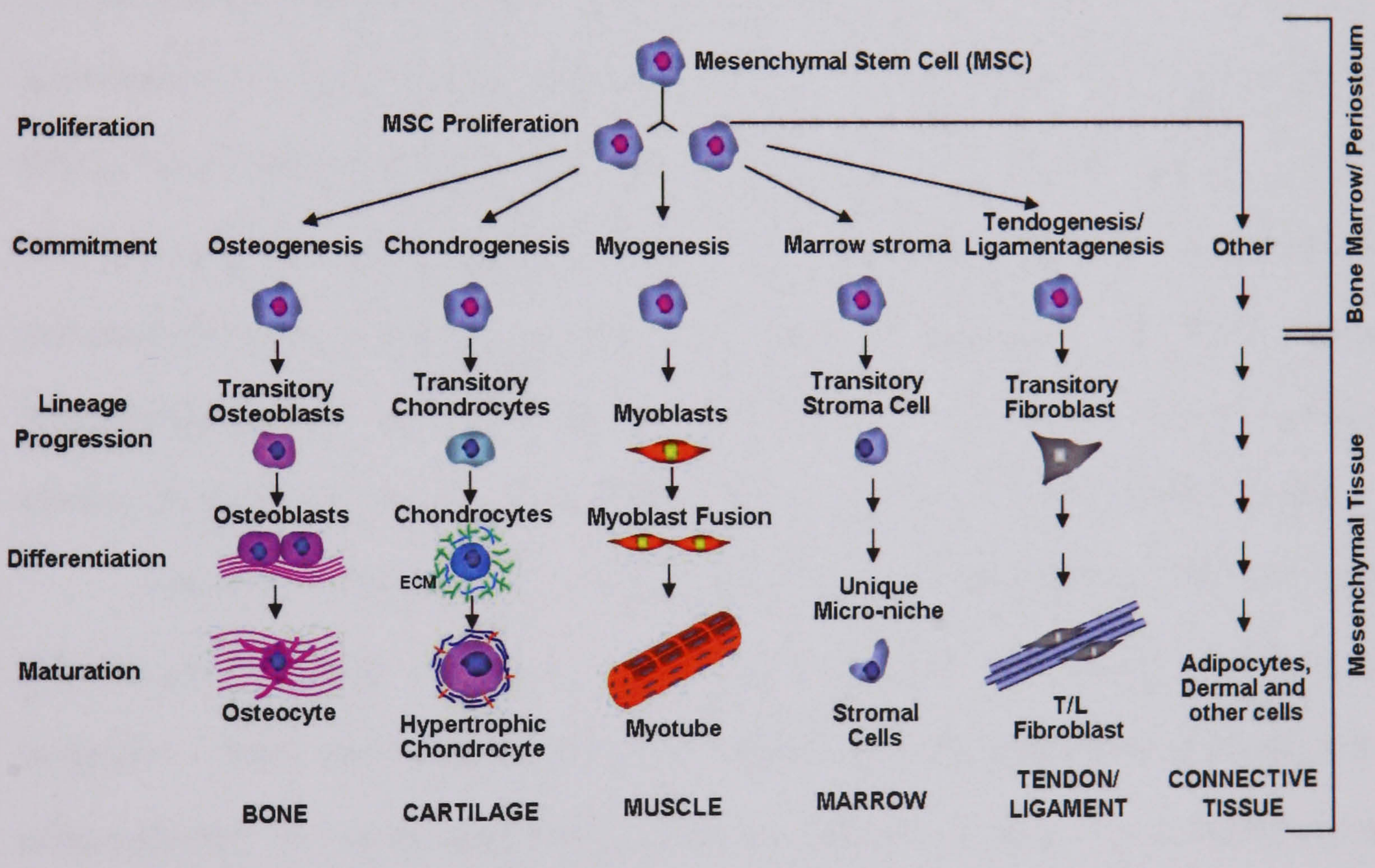


Figure 5. MSC differentiation strategy (Modified from Ref: Caplan AI 2005)

MSCs have been isolated and expanded *in vitro* while maintaining their ability to differentiate into chondrogenic and osteogenic lineages. Extensive research into the *in vitro* osteogenic and chondrogenic differentiation of MSCs for the fabrication of tissue engineered bone and cartilage tissue-like structures using various three dimensional supporting matrices as well as enhanced culture system

such as bioreactors has been conducted. For instance, a recent study reported that the combination of perfusion culture system with MSCs seeded on three dimensional collagen sponges and self-assembled peptide–amphiphile (PA) nanofibers hybrid scaffold significantly enhanced the *in vitro* and *in vivo* osteogenic differentiation of MSCs compared with conventional static tissue culture plates [Hosseinkhani H 2006]. Others have reported that the osteogenic potential of MSCs is affected by the size and microporosity of hydroxyapatite (HA) microparticles, which is clinically used as an injectable bone filler, and indicated that MSCs-HA particle hybrids may be used for the development of injectable formulations of tissue engineered bone constructs [Fisher EM, 2003]. Furthermore, MSCs have been harvested from the patient's bone marrow, expanded *in vitro*, and then induced to differentiate towards the osteogenic cell lineage followed by mineralised bone formation on three dimensional HA ceramics. These tissue engineered bone constructs were then implanted into the original patients demonstrating bone healing potential without any side effects [Morishita T 2006].

Efficient protocols for directing MSC differentiation towards the chondrogenic lineage as well as suitable biomaterials – coated with type II collagen – have been developed. It has been demonstrated that chondrogenic differentiation is enhanced using type II collagen based three-dimensional hydrogel scaffolds in the presence of transforming growth factor β1 (TGF-β1) [Bosnakovski D 2006]. One of the widely accepted culture methods for culturing chondrocytes is the pellet culture technique since MSCs are able to differentiate into chondrocytes resulting in the formation of three dimensional cartilage tissue-like structures [Bosnakovski D 2004]. Furthermore, the utilisation of mechanical stimuli has been explored to induce MSC differentiation towards the chondrogenic lineage [Schumann D 2006] and three-dimensional polymeric scaffolds have been

used to produce cartilage-like tissues using MSCs [Wang Y 2005].

As described previously, the main three advantages for the clinical use of adult stem cells, especially bone marrow derived MSCs, is availability, autologous nature, and multi-lineage differentiation capacity. However, in many cases, relatively few MSCs are available in BM aspirates, especially from elderly or diseased patients. It has been reported that the proportion of MSCs in bone marrow is 0.01% to 0.001% [Friedenstein AJ 1982] and Wexlel et al have reported a 1 in 3.4×10^4 frequency for these cells [Wexler SA 2003]. In addition, several studies have suggested that the number of marrow-derived progenitors declines as a function of donor age [Tsuji T 1990. Dodson SA 1996]. Furthermore, it has also been reported that *in vitro* expansion induced rapid aging of MSCs resulting in a limited passage capability and loss of their multi-differentiation potential [Bonab MM 2006, Baxter MA 2007], which limits their usefulness in treating age-related degenerative diseases such as osteoporosis and osteoarthritis.

1.3.3. Embryonic Stem Cells

Recently, the use of embryonic stem cells (ESCs) as a potential cell source for cell-based therapies has been suggested. The derivation of pluripotent cell lines from mouse embryos was reported in 1981 [Evans MJ 1981]. ESCs were originally derived from the inner cell mass (ICM) of blastocysts by plating embyros at the expanded blastocyst stage, either intact or following immunosurgical isolation of ICM, onto a feeder layer. After several days of culture, the epiblast-derived cell mass is dissected and disaggregated and then replated onto fresh feeders. Various types of differentiated cell colonies arise along with colonies of a characteristic undifferentiated morphology [Robertson EJ 1997]. These

undifferentiated cell colonies are individually dissociated and replated, resulting in further expansion and the establishment of ESCs. Mouse ESCs (mESCs) are maintained in the undifferentiated (and pluripotent) state in the presence of the leukaemia inhibitory factor (LIF). LIF sustains mESCs self-renewal activity in the absence of feeders [Smith 1988]. On withdrawal of LIF (or feeders), proliferation continues but differentiation is induced and stem cells do not persist beyond a few days. Therefore, ESCs are characterized by two unique properties, namely their "unlimited self-renewal capacity" and "pluripotency," which allows them the ability to generate all foetal and adult cell types *in vivo* and *in vitro*. These properties make ESCs, potentially, an invaluable cell source for diverse, "off-the-shelf" tissue-engineering and clinical applications.

Many signalling pathway molecules participate in the control of ESCs self-renewal activity and pluripotency. Octamer binding factor 4 (also known as Oct-3, Oct-3/4, Pou5f1) is a POU family transcriptional regulator restricted to early embryos, germ line cells, and undifferentiated embryonic carcinoma (EC), embryonic germ (EG) line cells, and ESCs [Pesce M 1998]. *In vivo*, zygotic expression of Oct-3/4 is essential for the initial development of pluripotential capacity in the ICM [Nichols J 1998]. In ESCs, continuous function of Oct-3/4 is necessary to maintain pluripotency and control differentiation [Niwa H 2000]. However, it has been well established that maintenance of Oct-3/4 expression is not in itself sufficient to sustain the pluripotent phenotype. Competition and co-ordination between various transcriptional complexes involving Oct-3/4 are involved in guiding cell determination. These include the transcription factor Oct-3/4, signal transducers and activators of transcription (STAT3), stage-specific embryonic antigen (SSEA)-1, and alkaline phosphatase (ALPase) [Saito S 2004]. It has been demonstrated that potential downstream effectors of the LIF signal in

mESCs include kinases of the Src, Jak, and mitogen-activated protein families and the signal transducer and transcriptional activator STAT3 [Raz R 1999]. Activation of the signal transducer STAT3 via LIF receptor (LIFRβ) and glycoprotein (gp)130 signalling appears to be essential for maintenance of mESC pluripotency [Matsuda T 1999]. Therefore, propagation of the pluripotent mESCs phenotype requires both the intrinsic activity of Oct-3/4 and the cytokine-induced action of STAT3. In addition, it has been recently identified that the homeodomain protein Nanog is among the intrinsic regulators of the pluripotency of mESCs. When overexpressed, Nanog displays the unique role of maintaining mESC self-renewal activity in the absence of the requisite extracellular stimulation by LIF; Nanog overexpression can maintain self-renewal of mESCs independently of LIF/gp130/STAT3 signalling pathway [Yates A 2005]. However, in contrast to mESCs, recent reports demonstrated that STAT3 activation is not sufficient to inhibit human ESCs (hESCs) spontaneous differentiation. Loss of the pluripotency markers Nanog and Oct-4 was detected in hESCs on the mouse feeder cell layer during gp130-dependent signalling, indicating that signalling through this pathway is insufficient to prevent the onset of differentiation [Humphrey RK 2004, Dahéron L 2004]. This fact suggests the existence of an unidentified factor from mouse feeder layer cells that acts to maintain hESC self-renewal independently of STAT3 signalling pathway. Hence, the totality of factors and signalling pathways that regulate self-renewal activity and pluripotency in hESCs remain to be elucidated.

The term pluripotent describes stem cells that can give rise to cells derived from all three embryonic germ layers - mesoderm, endoderm, and ectoderm (Figure 6). During embryogenesis, ESCs specialize into many derivatives of the three germ layers including gut epithelium (endoderm); cartilage, bone, smooth muscle and striated muscle (mesoderm); and neural, epithelium, embryonic

ganglia, and stratified squamous epithelium (ectoderm) [Suemori H 1990]. In contrast to adult stem and differentiated cells, ESCs are able to divide continually in culture while maintaining their ability to generate any cell type desired provided they are supplied with the proper supplements such as growth factors or cytokines and placed in the appropriate culture environment.

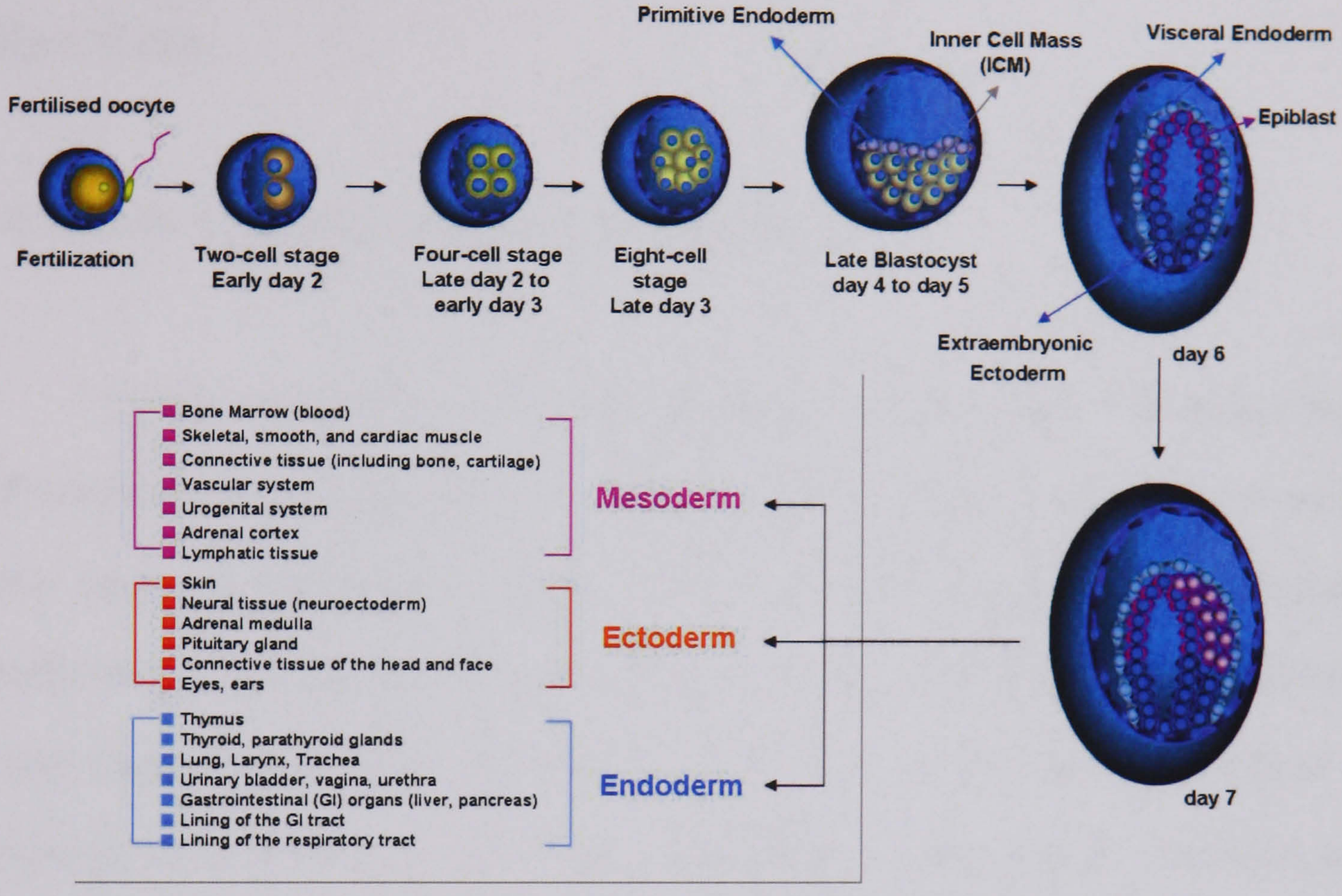


Figure 6. ESCs pluripotency in embryogenesis [Illustrated by author]

Although it is possible to direct ESC differentiation towards certain desired lineages *in vitro*, it has been difficult to control ESC growth and differentiation into higher order structures that are composed of multiple cell types that grow and differentiate together to form an integrated functional tissue. Furthermore, the inherent ESC properties of self-renewal and differentiation pose a significant problem for their clinical usage in the form of uncontrolled growth and differentiation, known as teratogenesis. It has been demonstrated that ESCs form complex teratomas when engrafted into an immune-deficient host [Gertow K 2004]. Transplanted hESCs into immune-deficient mice form complex teratomas

consisting of a range of differentiated somatic tissues, some of which appear highly organized and resemble structures normally identified in the embryo and adult [Przyborski SA 2005].

1.4. *In Vivo* Osteogenesis and Chondrogenesis of Embryonic Stem Cells

1.4.1. *In Vivo* Mesoderm Formation of ESCs

During embryogenesis, undifferentiated ESCs from the ICM initiate lineage differentiation though gastrulation, which is the process by which the embryo at an early stage of development produces the three primary germ layers: ectoderm, mesoderm, and endoderm [Lu CC 2001]. Embryogenesis mainly consists of four major stages: a) fertilized egg division (cleavage), b) formation of a ball of cells (morula), c) development of a cavity (blastocyst stage), and d) formation of the three primary germ layers that will give rise to all the cell types of the body (gastrula stage) and ultimately generate all the specialized tissues and organs of a mature organism [Tam PP 1993]. Prior to gastrulation, the majority of cells in the pre-implantation blastocyst are composed of the trophectoderm and the primitive endoderm. The pre-implantation embryo consists of the inner cell mass or epiblast cells. Subsequently, three differentiated cell types exist: the trophoblast, the epiblast (also called the embryonic ectoderm or primitive ectoderm at this stage), and the primitive endoderm. During the developmental step, namely gastrulation, the primitive endoderm differentiates into two different types of endoderm, parietal and visceral endoderm, in the anterior region, which is essential in regulating development during gastrulation (Figure 7). In the next phase, the forward

migration of the posterior epiblast cells occurs into the space between the epiblast and the visceral endoderm resulting in formation of primitive streak in a specific region of the epiblast along the posterior axis of the embryo [Lawson A 2003]. Mesendoderm, the precursor of mesoderm and endoderm, is derived from primitive streak, as is ectoderm. At this stage, the three primary germ layers that will generate the body of the embryo are finally formed [Niederlander C 2001].

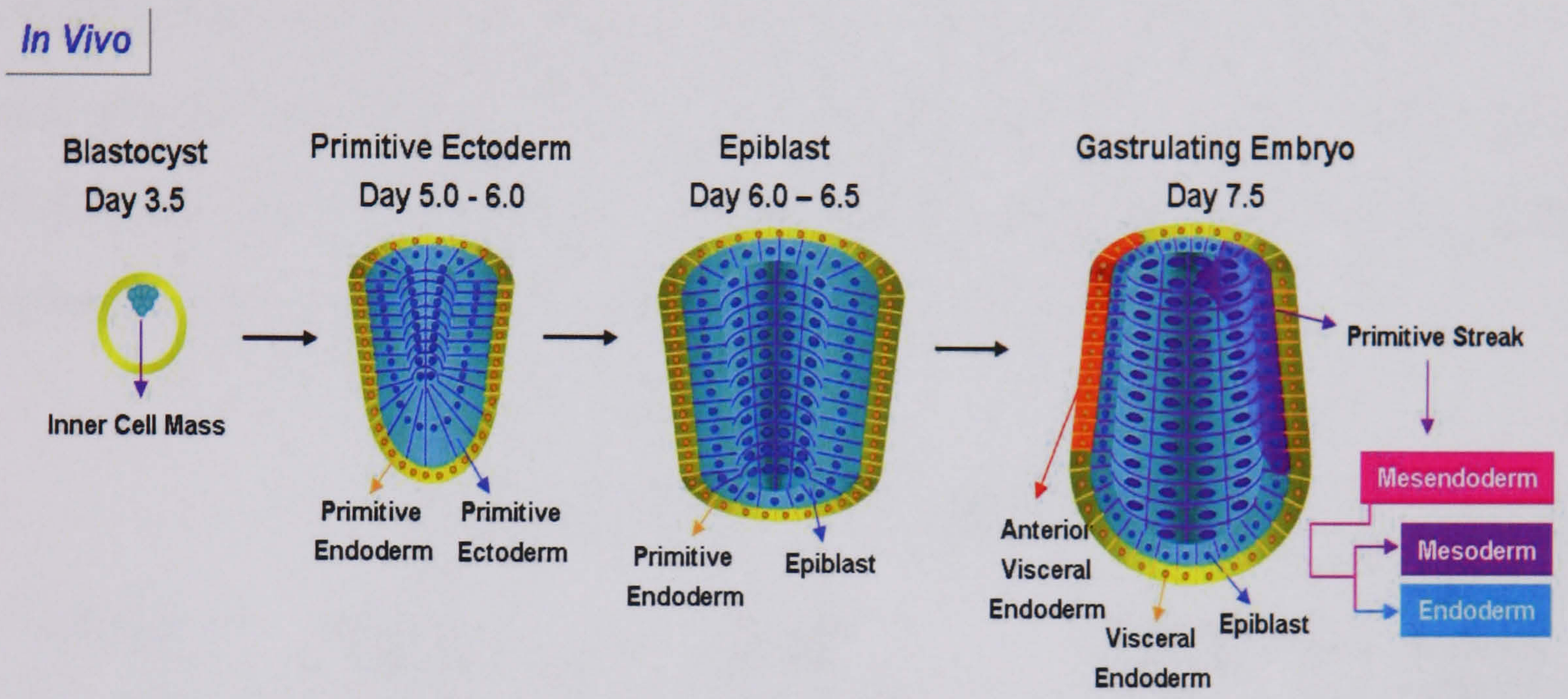


Figure 7. *In vivo* differentiation process for mesoderm formation [modified from Ref: Tam PP 2007]

The developmental process of the mesoderm formation and the role of visceral endoderm on mesoderm formation *in vivo* are relatively well understood. Visceral endoderm is an extraembryonic cell layer that appears prior to gastrulation and performs critical functions during embryogenesis. The traditional role ascribed to the visceral endoderm entails nutrient uptake and transport. Besides synthesizing a number of specialized molecules that facilitate uptake, digestion, and secretion of nutrients, the extraembryonic visceral endoderm coordinates blood cell differentiation and vessel formation in the adjoining mesoderm, thereby facilitating efficient exchange of nutrients and gases between

the mother and embryo [Bielinska M 1999]. Around day 6.5 of gastrulation in the mouse, epiblast cells start to migrate in the space between the epiblast and the visceral endoderm, and undergo an epithelial to mesenchyme transition (EMT) and form the transient primitive. Molecules secreted by the visceral endoderm are required for activation of mesoderm development, but the exact pathways still remain undetermined [Lu CC 2001, Tam PP 1993, Lawson A 2003, Bielinska M 1999]. These complex processes result in the formation of the tissues and organs and require the activation/inactivation of specific genes at specific times, highly integrated cell-cell interactions, and interactions between cells and the ECM [Pfendler KC 2005, Grover A 1995], as shown in Figure 8.

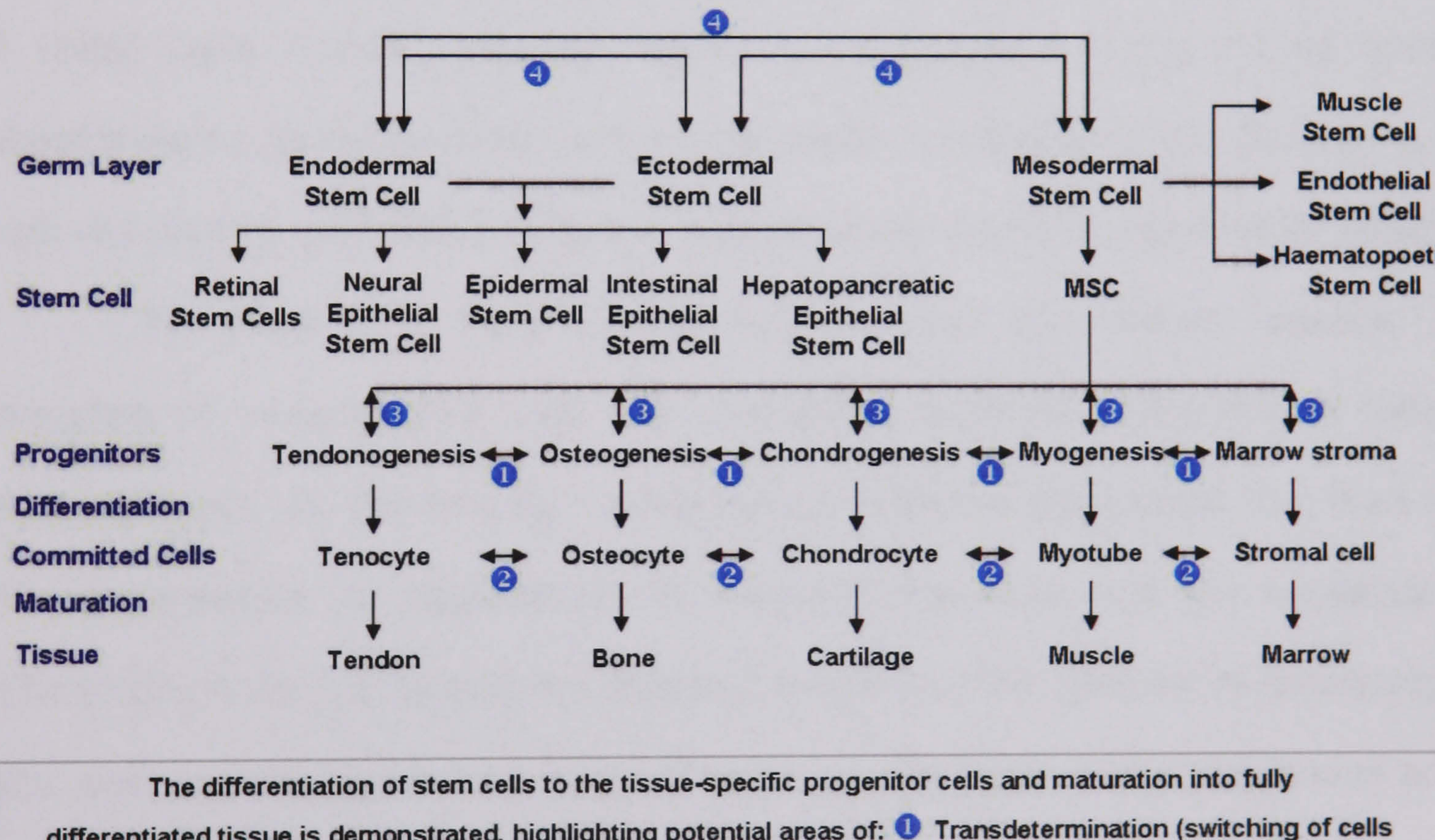


Figure 8. *In vivo* mesodermal differentiation strategy of ESCs [Modified from Ref: Raghunath J 2005].

1.4.2. *In Vivo* Osteogenesis and Chondrogenesis

Ultimately, morphogenesis of the skeleton is the outcome of the regulated differentiation, function, and interactions of its component cell types. Two major cell types contribute to the skeleton: the osteoblasts, which deposit bone matrix, and chondrocytes, which form cartilage. As stated earlier, they are both of mesenchymal origin [Colnot C, 2005]. During embryogenesis, osteogenic and chondrogenic cells may arise from the sclerotomal cells of the somatic mesoderm, the somitomeres of the hindbrain or the mesectodermal cells of the neural crest. They are believed to derive from a common embryonic progenitor cell, mesodermal progenitor cell/mesenchymal progenitor cell [Colnot C 2005, Poliard A 1995]. Cells in these lineages migrate to the locations in the embryo where skeletal elements will develop, form characteristic mesenchymal condensations of high cell density, and differentiate into osteoblasts or chondrocytes [Hall BK1992].

The process of bone development involves four distinct phases: (i) migration of mesenchymal cells with osteogenic potential to the site of future skeletogenesis, (ii) followed by mesenchymal–epithelial interactions that lead to, (iii) condensation (or aggregation) of mesenchymal cells, and (iv) subsequent differentiation into the osteogenic lineage [Heng BC 2004]. Descriptive embryology and anatomy distinguish two types of bone development: intramembranous and endochondral. Intramembranous ossification occurs when mesenchymal precursor cells differentiate directly into bone forming osteoblasts, a process employed in generating the flat bones of the skull as well as in adding new bone to the outer surfaces of long bones. In contrast, endochondral bone formation entails the conversion of an initial cartilage template into bone and is responsible for generating most bones in the skeleton [Colnot C 2005].

Chondrogenesis (Figure 9) results in the formation of the cartilage intermediate, anlagen, and leads to endochondral ossification during skeletal development. It occurs in stages beginning with mesenchymal cell recruitment and migration, proliferation, and condensation, which are regulated by mesenchymal-epithelial cell interactions [Hall BK 2000, Tuan RS 2004]. The aggregation of chondroprogenitors from mesenchymal cells into precartilage condensations represents one of the earliest events in chondrogenesis. The differentiation of chondroprogenitors is required for subsequent stages of skeletogenesis and is characterized by the deposition of cartilage matrix containing collagen types II, IX, and XI as well as aggrecan. Subsequently, the differentiated chondrocytes can then proliferate and undergo the complex process of hypertrophic maturation. Finally, the development of long bones from the cartilage anlagen occurs by a process termed endochondral ossification, which involves terminal differentiation of chondrocytes to the hypertrophic phenotype, cartilage matrix calcification, vascular invasion, and ossification [Goldring MB 2006].

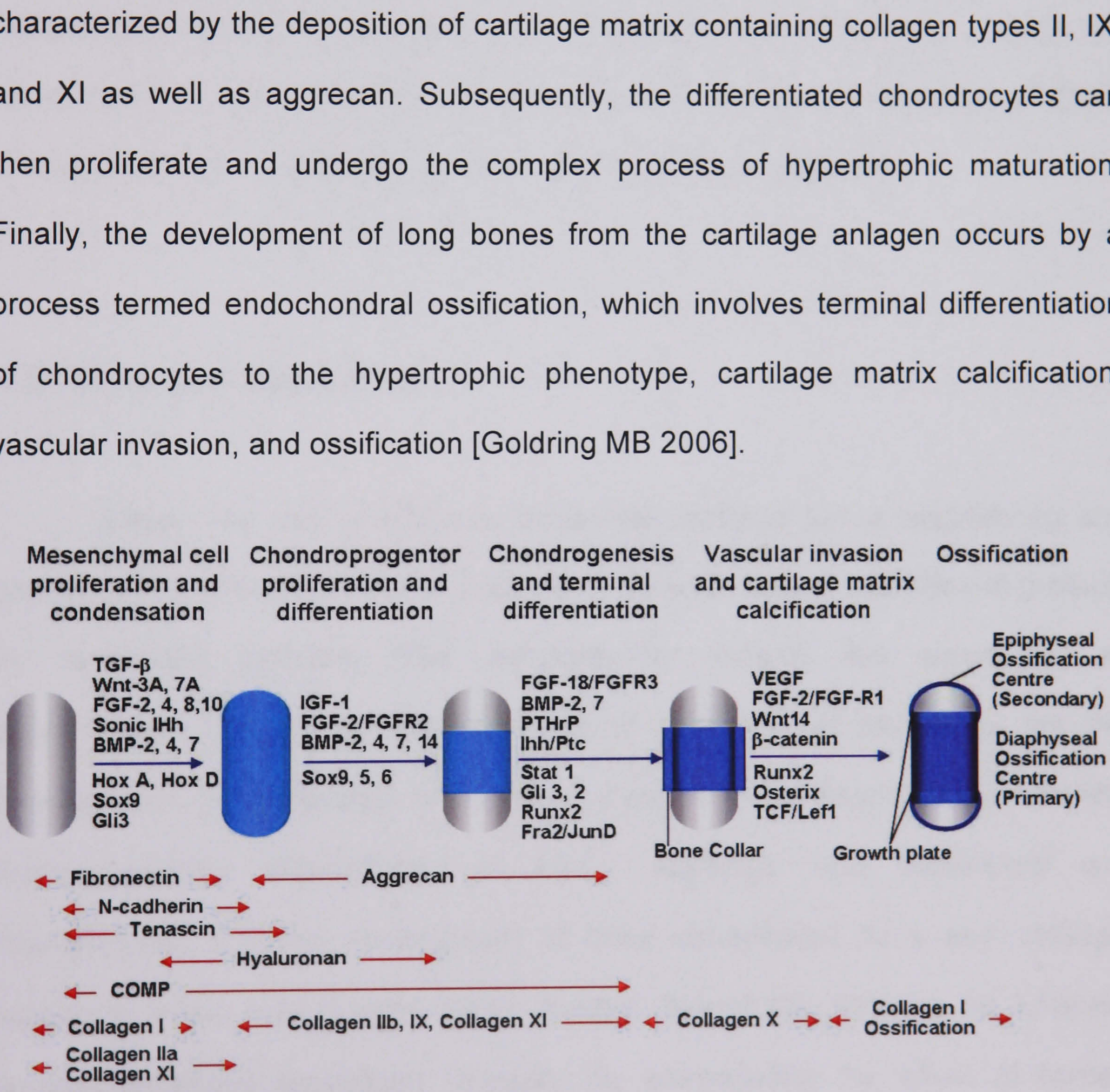


Figure 9. The process of chondrogenesis (Modified from Ref: Goldring MB, 2006).

The molecular and cellular mechanisms underlying the sequential differentiation of mesodermal cells into osteogenic and chondrogenic lineages have been the object of numerous studies. Studies have identified several factors that influence these processes, such as Insulin-like growth factor I (IGF-I), BMP-2, -4, and -5 and the TGF-β superfamilies [Erlebacher A 1995, Baker J 1993, Wozney JM 1992, Kingsley DM 1992]. Furthermore, at the molecular level certain cellular transcription factors are closely associated to skeletal lineage differentiation, such as the sry-related transcription factor Sox-9 and the runt-related transcription factor Runx-2 [Frank Eamesa B 2004]. However, despite the identification of several factors involved in skeletal lineage differentiation of ESCs *in vivo*, the precise mechanism still remains to be fully elucidated.

1.5. Aims and Objectives

Aims: The use of ESCs in bone and cartilage tissue engineering and regeneration necessitates the development of a well-defined and efficient protocol for selectively directing ESC differentiation towards the osteogenic or chondrogenic lineages *in vitro*. The overall objectives of this thesis are the development and evaluation of a culture process for enhancing and controlling lineage specific differentiation of ESCs, especially into osteoblasts and chondrocytes, and the development of three dimensional bone and cartilage constructs within a bioreactor culture system. Specifically, this can be achieved through enhanced mesoderm formation by investigating the effect of human hepatocarcinoma cell line (HepG2) conditioned medium on early differentiation of mESCs to primitive streak/nascent mesoderm cells. Subsequently, the focus

would be on the development of an integrated, single step culture process for direct osteogenic and chondrogenic differentiation of mESC by encapsulation in alginate hydrogels and culture in bioreactors, resulting in an efficient and reproducible culture system for bone and cartilage tissue engineering applications.

The specific objectives are:

- Development of the *in vitro* protocol for the generation of a specific cell population with high osteogenic and chondrogenic potential from mESCs: Enhancement of mesoderm formation.
- Enhancement and control of *in vitro* osteogenic and chondrogenic differentiation of mESCs
- Establishment of an 2D efficient single-step culture system for direct differentiation of mESCs into osteogenic and chondrogenic lineages
- Development of 3D bone and cartilage tissue like constructs through a 3D single-step culture system using alginate encapsulation and culture in the Horizontal Aspect Ratio Vessel (HARV) bioreactor.

CHAPER II

MATERIALS AND METHODS

2.1. Overview of Experiment

The pivotal element of the proposed experiment was divided into four main phases; Phase I: Early differentiation of murine embryonic stem cells (mESCs) into primitive streak/nascent mesoderm like cell. Phase II: *In vitro* osteogenic and chondrogenic differentiation of murine embryonic stem cells through Embryoid body (EB) formation. Phase III: *In vitro* direct osteogenic and chondrogenic differentiation of murine embryonic stem cells without EB formation process. Phase IV: Bioprocessing for three dimensional bone and cartilage tissue like construct formation using alginate encapsulated murine embryonic stem cells and HARV bioreactor

2.2. Basic Materials and Common Assay Techniques

2.2.1. Media

2.2.1.1. mESC maintenance medium

Dulbecco's Modified Eagles Medium (DMEM; Gibco, UK) high glucose / no sodium pyruvate was supplemented with 10% foetal bovine serum (FBS; Gibco), and 100 units/ml penicillin and 100 μg/ml streptomycin, 2 mM L-glutamine (all supplied by Gibco, UK), 0.1 mM β-Mercaptoethanol (Sigma, UK) and 1000 U/ml Esgro™ LIF (Chemicon, UK).

2.2.1.2. HepG2 maintenance medium

DMEM high glucose / no sodium pyruvate was supplemented with 10% FBS, 2 mM L-glutamine and 100 units/ml penicillin and 100 μg/ml streptomycin (all

supplied by Gibco, UK).

2.2.1.3. EB formation medium

Alpha Minimal Essential Medium (α-MEM; Gibco, UK) was supplemented with 15% FBS, and 100 units/ml penicillin and 100 μg/ml streptomycin.

2.2.2. Cell Culture

2.2.2.1. mESC maintenance and expansion

Prior to mESCs culture, tissue culture plastics were coated with 0.1 % gelatin (Sigma, UK) in phosphate buffered saline (PBS; Gibco, UK). mESCs (E14/TG2a cell line) was routinely cultured and passaged on 0.1% gelatin coated tissue culture plastic at 37°C in a 5% CO_2 humidified incubator. Undifferentiated mESCs (<p20) were passaged every two or three days and fed everyday with fresh mESC maintenance medium. To detach the mESCs from the flasks, 0.5% (v/v) trypsin-ethylenediaminetetraacetic acid (Trypsin-EDTA; Gibco, UK) was administrated to the mESCs for 5 minutes at 37°C, after medium aspiration and a single wash with pre-warmed 1X PBS.

2.2.2.2. HepG2 maintenance and expansion

Human hepatocarcinoma cell line (HepG2; ATCC HB-8605) were cultured on tissue culture plastic at 37°C in a 5% CO_2 humidified incubator. HepG2 cells were passaged every three or four days and fed every 2 days with HepG2 maintenance medium.

2.2.2.3. Collection of HepG2 conditioned media

HepG2 cells were cultured in tissue-culture flasks in a 5% CO_2 humidified

incubator using HepG2 maintenance medium at a seeding density of 5.0×10^4 cells/cm^2. The conditioned medium (CM) was collected after three or four days of culture, and the collected media was filter-sterilised through a 0.22 μm filter unit (Nalgene, UK), and then filtered conditioned media was supplemented with 0.1 mM β-mercaptoethanol (Sigma, UK), and stored at -20°C prior to use.

2.2.3. Common Assay Techniques

2.2.3.1. Immunocytochemical staining

Immunocytochemical staining was generally done according to following protocol throughout all experiment. Firstly, cells in 4 or 8 well chamber slides were fixed with 4% paraformaldehyde (Sigma, UK) for 30 minutes, washed three times with 1X PBS, followed by permeabilisation with 0.2% triton X-100 (Sigma, UK), and blocking of non-specific binding by incubation with 10% (v/v) rabbit/goat/mouse serum (Vector Laboratory, USA), which serum was selected according to the origin of primary antibodies. The primary antibodies (diluted to proper concentration with bovine serum albumin (BSA)/Azide solution) were incubated overnight at 4°C. Following a wash with PBS, the secondary fluorescent-conjugated antibodies were incubated for 1 hr at room temperature which secondary antibodies were selected according to the origin of primary antibodies. The cells were counter-stained with 4',6 diamidino-2-phenylindole (DAPI) or Propidium iodide (PI) (Vector Laboratory, USA) to visualize the cell nucleus and were observed using epi-fluorescence on a BX-60 microscope and images were captured using a Zeiss Axiocam digital camera and analysed using KS-300 software.

2.2.3.2. Ribonucleic acid (RNA) extraction

For the analysis of gene expression profile, firstly total RNA was extracted from each cell culture or sample using the total RNA isolation kit (Quiagen Ltd, UK) according to manufacturer's instruction. Briefly, each sample was kept in ice throughout the whole process and was dissolved by 350 or 600μl Lysis buffer containing 10μl/ml β-mercaptoetanol, which volume of Lysis buffer depends on the sample amount. Following vigorous vortexing until no visible sign of cell clumps, sample solution was transferred to purple column and was centrifuged at max speed for 2 min. Equal volume of 70% ethanol was added to sample solution, gently mixed and then transferred into pink isolation column. After following centrifuge at 15000 rpm for 15 sec, solution was discarded and RNA could be present on the membrane of column. 700μl RW1 buffer was added into pink column and then centrifuged at max speed for 15 sec. After discarding solution, pink column was transferred to 2ml new tube and then 500μl RPE solution was added into pink column and centrifuged at max speed for 15 sec. After discarding solution, 500μl RPE solution was added again into pink column and centrifuged at 15000 rpm for 2 min. The pink column was transferred to a new tube and then 30μl RNase free water added in the middle of membrane carefully, and then centrifuged at max speed for 1 min. Finally, extracted RNA was diluted 20 times and then the concentration of RNA was measured UV spectrophotometer (Eppendorf BioPhotometer, Germany). Samples were stored at –80 °C until further use.

2.2.3.3. Reverse transcription (RT)

1μg RNA was used as a template for AMV reverse transcriptase. RNA was reversed transcribed into complementary deoxynucleic acid (cDNA) using the

reverse Transcription System (Promega, UK) according to the manufacturer's recommendations. Single-stranded cDNA synthesis was performed with total RNA in the presence of 5 mM $MgCl_2$, 1 mM of dNTP mixture, 1 unit/μl recombinant RNasin ribonuclease inhibitor, 15 units/μl AMV reverse transcriptase and 0.5 μg/μl random primers in a total volume of 20 μl per reaction. Diluted RNA samples were heated at 70 °C for 10 min, briefly centrifuged and cooled on ice for 5 min. The Mastermix + RNA was incubated at 22 °C for 10min, reverse transcription was performed at 42 °C for 40 min, followed by denaturation at 99 °C for 5 min and a cooling step at 4 °C for 5 min using a thermocycler (Eppendorf Mastercycler, Germany). Samples of cDNA were diluted 5-fold to a final volume of 100 μl and stored at -20 °C until further use.

2.2.3.4. Polymerase chain reaction (PCR) amplification

10 μl of the diluted cDNA samples were used for PCR amplification in 20 μl reactions. PCRs consisted of 1×Amplitaq Gold Buffer, 1.5 mM $MgCl_2$, 200 μM each dNTP, 0.2 units of Amplitaq DNA polymerase (PE biosystem) and 0.5 μM of each of 'forward' and 'reverse' primers (Invitrogen custom primers, UK). Reactions were incubated in a thermocycler (Eppendorf Mastercycler, Germany) as follows; at 94 °C for 10 min for one cycle, then 94 °C (30 sec); specific primer annealing temperature (30 sec), 72 °C (60 sec) for optimal cycles, and/or with a final 10 min extension at 72 °C. The number of amplification cycles used was optimised to ensure that product concentration was within the exponential part of the amplification reaction. Products were then held at 4 °C.

2.2.3.5. Agarose gel electrophoresis

After amplification, PCR products were analyzed by electrophoresis.

Aliquots of 9.6 μl of amplified cDNA were mixed with 2.4 μl of 6x loading buffer and electrophoresed on a 1.5% (w/v) agarose gel (made up with 10X TAE buffer from Invitrogen, UK; 0.4 M Tris acetate, 10 mM EDTA, pH 8.3), containing 0.001 μg/mL ethidium bromide (EtBr). When exposed to Ultraviolet (UV) illumination, the gel showed a single band when the mRNA was expressed. Images of the gel were captured digitally using a BioRad Fluor-S multi-imager (BioRad/Zeiss, UK).

2.3. Early Differentiation of Murine Embryonic Stem Cells into Primitive Streak/Nascent Mesoderm Like Cells

2.3.1. mESCs Expansion and Characterisation

As a test for characterising the undifferentiation stage prior to the induction of early differentiation, mESCs were expanded in mESC maintenance medium at 37°C and 5% CO_2 and were immuno-stained for Oct-4, CD9 and E-cadherin, and expression of alkaline phosphatase (ALPase) was evaluated. Prior to antibody reaction, the fixed cells were then incubated with 10% (v/v) blocking goat or rabbit serum (Vector Laboratories) for 30 min at room temperature. The primary antibodies, goat anti E-cadherin (diluted 1:50 with BSA/Azide solution; Santa Cruz Biotechnology, UK), rabbit anti Oct 4 (diluted 1:50 with BSA/Azide solution; Santa Cruz Biotechnology, UK) and rat anti CD 9 (diluted 1:50 with BSA/Azide solution; Research Diagnostics, USA) were incubated overnight at 4 °C. In secondary antibody reaction, the secondary Fluorescein isothiocyanate (FITC)-conjugated anti-goat immunoglobulin G (IgG) (Santa Cruz Biotechnology, UK) or Texas Red (TR)-conjugated anti-rabbit IgG (Santa Cruz Biotechnology, UK) or Rhodamine (R)-conjugated anti-rat IgG (Chemicon, USA) antibodies were incubated for 1 hr at room temperature. The cells were counter-stained with DAPI to visualize the cell nucleus, and other procedure was done according to previously described method in the section of 2.2.3.1. Immunocytochemical staining.

The assessment of alkaline phosphatase (ALPase) expression was done using Alkaline Phosphatase Detection Kit (Chemicon, USA). Briefly, the cells were fixed with 4% paraformaldehyde (Sigma, UK) for 1 min followed by three washes with 1X TBST buffer (20mM Tris-HCl, 0.15M NaCl and 0.05% Tween-20, pH 7.4). The fixed cells were stained with Naphtal/Fast Red Violet solution, which was

prepared according to manufacturer's instruction, for 15 min in dark and then washed with 1X PBS. Images of stained cells were captured using Leica inverted microscope (Leica, UK) equipped with Olympus DP50 digital camera (Olympus Optical Co, Tokyo, Japan) and analyzed using analySIS® imaging software (Soft Image System GmbH, Germany).

In addition, in order to establish the optimal condition for mESC expansion, the mESC growth in accordance with initial cell seeding density was evaluated using the CellTiter 96® AQueous non-radioactive cell proliferation assay (Promega, UK). mESCs were seeded on 0.1% (v/v) gelatin coated 24 well plates with initial cell seeding density of 7500, 15000 and 30000 cells/cm^2, and cultured in mESC maintenance medium for 1, 2, 3, 4, and 5 days at 37°C in a 5% CO_2 incubator. After culture, unattached cells were removed by thoroughly washing 3 times with 1X PBS. Cell proliferation were evaluated by quantifying the metabolically active adherent or proliferating cells by measuring the level of the endogenous mitochondrial dehydrogenase by addition of 200 μl/well of DMEM without phenol red (Gibco, UK) and 40 μl/well of mitochondrial dehydrogenase substrate (Promega, UK). Following 2 hrs incubation, mitochondrial dehydrogenase activity was stopped by addition of 50 μl/well 10% (w/v) sodium dodecyl sulfate (SDS; Sigma, UK) in 1X PBS. The plates were read at a 490 nm wavelength using an ELISA reader (MRX II, Dynex Technology, USA). A standard curve (Appendix 1) was generated by measuring the level of the endogenous mitochondrial dehydrogenase of mESCs after 4 hrs of seeding in accordance with serial cell seeding density using the same protocol above mentioned in order to determine the number of adherent or proliferating cells. Data were expressed as number of cells/cm^2.

2.3.2. Induction of mESCs Early Differentiation by HepG2 Conditioned Media

For the early differentiation of mESCs, mESCs were cultured for three days in tissue-culture flasks coated with 0.1% (v/v) gelatin using a 1:1 mixture containing the HepG2 conditioned medium (CM) and the standard mESC maintenance medium containing LIF described earlier. CM treated mESCs is denominated as CM-mESCs in further experimental protocol.

2.3.3. Embryoid Body (EB) Formation

Prior to establishment of EB formation process, two different EB formation medium were tested to provide suitable environment for efficient EB formation of undifferentiated mESCs and CM-mESCs; DMEM with high glucose/no sodium pyruvate was supplemented with 15% FBS, and 100 units/ml penicillin and 100 μg/ml streptomycin or α-MEM was supplemented with 15% FBS, and 100 units/ml penicillin and 100 μg/ml streptomycin.

The CM-mESCs and undifferentiated mESCs were trypsinised to detach cells from flasks; trypsinisation was stopped through addition of prewarmed serum containing medium before the dispersion of single cells became apparent. The cell colonies were very gently centrifuged for 10 sec and re-suspended in pre-warmed EB formation medium. The re-suspended cells were plated onto non-tissue culture treated petri dishes and cultured at 37°C in a 5% CO_2 humidified incubator. The cultures were fed every two days by replacing with fresh medium.

2.3.4. Characterisation

2.3.4.1. Morphological observation

After culture of mESCs in mESC maintenance medium or 50% of CM and

EB culture in EB formation media, cells and EBs morphology were observed routinely using an inverted phase microscope (Olympus IX70, UK) equipped with analysisD soft imaging system (Soft imaging system GmbH, Germany). The change of mESCs and EBs morphology was captured.

2.3.4.2. Cell adhesion and proliferation assay

The cell adhesion and proliferation activity of mESCs in standard mESC maintenance culture medium and in 50% HepG2 CM were compared as follows: 24-well tissue culture polystyrene plates were coated with 0.1% (v/v) gelatin for 30 min. For cell adhesion studies, mESCs were seeded onto the plates at the density of 3.0×10^4 cells/cm^2 and allowed to adhere for 1, 2, and 4 hr in standard mESC culture medium or 50% HepG2 conditioned medium at 37°C in a 5% CO_2 humidified incubator. For cell proliferation studies, mESCs were seeded onto the plates at the density of 3.0×10^4 cells/cm^2 and cultured for 1, 2, 3, 4, and 5 days in standard mESC maintenance culture medium or 50% HepG2 conditioned medium at 37°C in a 5% CO_2 humidified incubator. Unattached cells were removed by thoroughly washing 3 times with 1X PBS. Cell adhesion and proliferation were evaluated using the CellTiter 96® AQueous non-radioactive cell proliferation assay according to previously described method in the section of 2.3.1.

2.3.4.3. ALPase expression and ALPase activity

The undifferentiation/differentiation stage of mESCs in 50% HepG2 conditioned medium was evaluated by assessing ALPase expression and ALPase activity in comparison with undifferentiated mESCs in mESC maintenance medium. mESCs were seeded onto the plates at the density of 3.0×10^4 cells/cm^2 and cultured for 3 days in standard mESC maintenance culture medium or 50%

HepG2 conditioned medium at 37°C in a 5% CO_2 humidified incubator. Unattached cells were removed by thoroughly washing 3 times with 1X PBS. After 1 and 3 days of culture, the assessment of ALPase expression was done with same protocol as previously described in the section of 2.3.1. Images of stained cells were captured using Leica inverted microscope (Leica, UK) equipped with Olympus DP50 digital camera (Olympus Optical Co, Tokyo, Japan) and analyzed using analySIS® imaging software (Soft Image System GmbH, Germany).

In the parallel experiment of ALPase expression, the ALPase activity for mESCs in 50% HepG2 conditioned medium or mESC maintenance medium was determined at day 3 of culture, in order to capture the temporal nature of ALPase activity. Briefly, unattached cells were removed by gentle washing with1X PBS. The cells were then incubated with pre-warmed 150 μl/well of ALPase buffer (Sigma) and 150 μl/well of a p-nitrophenyl phosphate solution (Sigma) for 30 min in a 5% CO_2 humidified incubator at 37 °C. The reaction was stopped by adding 200 μl/well of 0.5N NaOH solution. The production of p-nitrophenol was determined by absorption at 405 nm using an ELISA reader (MRX II, Dynex Technology). A calibration curve (Appendix 2) was generated using standard p-nitrophenol solution (Sigma, UK) and the amount of total p-nitrophenol produced from cultured cells was enumerated from the calibration curve. In addition, the content of cellular protein in culture was evaluated at each experimental time point using Lowry or Bicinchoninic acid (BCA) method. Calibration curves (Appendix 3) were generated using bovine serum albumin (Sigma, UK) and Bio-Rad DC protein assay kit (Bio-Rad, USA) and BCA™ protein assay kit (Pierce, USA) according to the manufacturer's instruction, and the amount of total protein produced from cultured cells was enumerated from the calibration curve. Finally, the enzyme activity was expressed as micromoles of reaction product (p-nitrophenol) per

minute per mg of total cellular protein.

2.3.4.4. Immunocytochemistry

The effect of HepG2 conditioned media on mESCs early differentiation was evaluated by specific staining for Oct-4 and E-cadherin. mESCs were cultured in mESC maintenance medium and 50% HepG2 conditioned medium at 37°C in a 5% CO_2 humidified incubator and were immuno-stained for Oct-4 and E-cadherin. Prior to antibody reaction, the fixed cells were then incubated with 10% (v/v) blocking goat or rabbit serum (Vector Laboratories) for 30 min at room temperature. The primary antibodies, goat anti E-cadherin (diluted 1:50 with BSA/Azide solution; Santa Cruz Biotechnology, UK), and rabbit anti Oct 4 (diluted 1:50 with BSA/Azide solution; Santa Cruz Biotechnology, UK) were incubated overnight at 4°C. In secondary antibody reaction, the secondary FITC-conjugated anti-goat IgG (Santa Cruz Biotechnology, UK) or TR-conjugated anti-rabbit IgG (Santa Cruz Biotechnology, UK) antibodies were incubated for 1 hr at room temperature. The cells were counter-stained with DAPI to visualize the cell nucleus and were observed using epi-fluorescence on a BX-60 microscope and images were captured using a Zeiss Axiocam digital camera and analysed using KS-300 software, and other procedure was done according to previously described method in the section of 2.2.3.1.

2.3.4.5. Reverse transcription and polymerase chain reaction (RT-PCR)

For evaluating the change of gene expression profile in CM-mESCs and its derived EBs in comparison with undifferentiated mESCs and its derived EBs, mESCs were cultured in standard mESC culture medium or 50% HepG2 conditioned medium at 37°C in a 5% CO_2 humidified incubator for 3 days.

Following monolayer culture, HepG2 conditioned medium treated mESCs (CM-mESCs) were trypsinised to detach cells from flasks; trypsinisation was stopped through addition of serum containing medium before the dispersion of single cells became apparent. The cell colonies were very gently centrifuged for 10 sec and re-suspended in pre-warmed EB formation medium. The re-suspended cells were plated onto non-tissue culture treated petri dishes and were allowed to form EBs for 1-day (CM-mESC-EB1), 3-days (CM-mESC-EB3), or 5-days (CM-mESC-EB5) in suspension culture at 37°C in a 5% CO_2 humidified incubator . The cultures were fed every two days by replacing with fresh medium. Non-treated mESCs were allowed to form EB for 5 days as control group After culture, total RNA was extracted from cells of each test group, and RNA extraction and RT-PCR procedure was done according to previously described method in the sections of 2.2.3.2-2.2.3.5. Primers which used in this experiment and the expected product size are detailed in Table 1

Table 1. Oligonucleotide primers for RT-PCR analysis for mESCs early differentiation

Gene		Sequence	Product (bp)
mBrachyury	sense	5'-AAGGAACCACCGGTCATC-3'	319
	antisense	5'-GTGTCGTCAGTGGTGTGTAATG-3'	
mGoosecoid	sense	5'-GCACCATCTTCACCGATGAG-3'	523
	antisense	5'-AGGAGGATCGCTTCTGTCGT-3'	
mNodal	sense	5'-TGTGTCTATCCAGGGAGCAGAA-3'	195
	antisense	5'-CAAGCAGTTCATAAACCCTATTTCC-3'	
mCritpo-1	sense	5'-GTCCCTGATAGTCTCTGATATTC-3'	240
	antisense	5'-GAAATGTAAGAGAAGTCATGGG-3'	
mGAPDH	sense	5'-CATCACCATCTTCCAGGAGC-3'	500
	antisense	5'-ATGCCAGTGAGCTTCCCGTC-3'	

2.3.4.6. Reversibility of early differentiation and characterisation

The reversible differentiation of CM-mESCs to undifferentiated mESCs was tested by morphological observation and immuno-staining with several markers indicating undifferentiation/differentiation stage. mESCs were cultured in various conditions at 37°C in a 5% CO_2 humidified incubator; Four experimental groups were set-up. Group 1 is mESCs culture in standard mESC maintenance medium (denominated as mESC), Group 2 is mESCs culture in 50% HepG2 conditioned medium for 3 days (denominated as CM-mESC), Group 3 is mESCs which were replated and cultured in mESC maintenance medium following HepG2 conditioned medium treatment for 3 days (denominated as CM-mESC-rr), and Group 4 is mESCs which were cultured in mESC maintenance media following HepG2 conditioned media treatment for 3 days with direct media replacement without replating (denominated as CM-mESC-rd).

After culture, morphological change of each groups were observed using an inverted phase microscope (Olympus IX70, UK) equipped with analysisD soft imaging system (Soft imaging system GmbH, Germany).

In addition, as a test for characterising the undifferentiation/differentiation stage of mESCs in various culture conditions in molecular level, each groups were immuno-stained for Oct-4, CD9 and E-cadherin. Prior to antibodies reaction, the fixed cells were then incubated with 10% (v/v) blocking goat or rabbit serum for 30 min at room temperature. The primary antibodies, goat anti E-cadherin (diluted 1:50 with BSA/Azide solution), rabbit anti Oct 4 (diluted 1:50 with BSA/Azide solution) and rat anti CD 9 (diluted 1:50 with BSA/Azide solution) were incubated overnight at 4°C. In secondary antibody reaction, the secondary FITC-conjugated anti-goat IgG or TR-conjugated anti-rabbit IgG or R-conjugated anti-rat IgG antibodies were incubated for 1 hr at room temperature. The cells were counter-

stained with DAPI to visualize the cell nucleus, and other procedure was done according to previously described method in the section of 2.2.3.1.

2.4. *In Vitro* Osteogenic and Chondrogenic Differentiation of Murine Embryonic Stem Cells through EB Formation

2.4.1. Osteogenic and Spontaneous Cardiogenic Differentiation

2.4.1.1. Osteogenic Media

α-MEM was supplemented with 15% FBS, and 100 units/ml penicillin and 100 μg/ml streptomycin containing 50 μg/ml ascorbic acid (Sigma, UK) in 1X PBS and 10 mM β-glycerophosphate (Sigma, UK) in 1X PBS. After 14 days of culture, the medium was further supplemented with 1 μM dexamethasone (Sigma, UK) in 1X PBS.

2.4.1.2. Experimental groups

Three experimental groups and one control group were set-up. The experimental groups consisted of CM-mESCs allowed to form EBs for 1-day (CM-mESC-EB1), 3-days (CM-mESC-EB3), or 5-days (CM-mESC-EB5), followed by a further 21 days of culture in the osteogenic medium detailed above. The control group (EB5) consisted of mESCs maintained for 3 days in the standard mESC maintenance medium, followed by EB formation for 5 days. The control group represents the standard protocol for development of mesoderm required for skeletal cell lineage differentiation, which EB formation for 5 days is generally accepted method to induce spontaneous mesoderm formation for further mesodermal lineage differentiation [Nakayama N 2003, Kramer J 2000 & 2005, Kawaguchi J 2005, Tanaka H 2004, Buttery LD 2001, Xu C 2002], prior to being cultured for a further 21 days in the osteogenic medium previously described.

2.4.1.3. Osteogenic differentiation

After EB formation, the EBs of each test group were very gently centrifuged and then trypsinised to release single cells; trypsinisation was stopped through addition of serum containing medium before the dispersion of single cells became apparent. The single cell dispersion was centrifuged at 1000 rpm for 10 min and re-suspended, and then re-suspended cells were plated in tissue culture plates at a cell density of 30,000 cells/cm^2 in our previously described basic osteogenic medium. The cultures were maintained at 37 °C in a 5% CO_2 humidified incubator and fed every two days up to 21 days.

2.4.1.4. Beating colony formation and quantification

During the culture, spontaneous cardiogenic differentiation was evaluated. Beating colonies were counted at day 11, 16, and 21 of culture using an inverted phase microscope (Olympus IX70) equipped with a Nikon CoolPix 950 digital camera. Data were expressed as number of beating colonies/well in each well of a 6-well plate.

2.4.1.5. Bone nodule formation and quantification (Alizarin Red-S staining)

Bone nodule formation was evaluated at day 11, 16, and 21 of osteogenic culture. After culture, cells in each test group were fixed with 4% paraformaldehyde (Sigma, UK) for 20 min followed by three washes with 1X PBS. The fixed cells were stained with 40 mM Alizarin Red S (ARS; Sigma, UK) solution (pH4.2) for 20 min at room temperature and then washed with 1X PBS three times and with tap water. Bone nodules were counted using an inverted epi-fluorescence microscope (BX-60, Olympus, Japan) and images were captured using a Zeiss Axiocam digital camera and analysed using KS-300 software (Imaging Associates,

UK). Only bone nodules fluorescent were counted as positive when ARS stained area was exposed to filtered UV light (excitation at 530-560 nm and emission at 580 nm) to exclude non-specific staining.

2.4.1.6. Immunocytochemical staining

Osteogenic and spontaneous cardiogenic differentiation in molecular level was characterised by immunostaining for OB-cadherin, and sarcomeric α-actinin and tropomyosin, respectively. Prior to antibodies reaction, the fixed cells were then incubated with 10% (v/v) blocking goat or mouse serum (Vector Laboratories) for 30 min at room temperature. The primary antibodies, goat anti OB-cadherin (diluted 1:50 with BSA/azide solution; Santa Cruz Biotechnology, UK), mouse anti sarcomeric α-actinin (diluted 1:800 with BSA/Azide solution; Sigma), and mouse anti tropomyosin (diluted 1:50 with BSA/Azide solution; Sigma) were incubated overnight at 4°C. In secondary antibodies reaction, the secondary FITC-conjugated goat anti-mouse IgG (Jackson Immunoresearch laboratory, USA) or FITC-conjugated rabbit anti-goat IgG (Santa Cruz Biotechnology) antibodies were incubated for 1 hr at room temperature. The cells were counter-stained with DAPI to visualize the cell nucleus and were observed using epi-fluorescence on a BX-60 microscope and images were captured using a Zeiss Axiocam digital camera and analysed using KS-300 software, and other procedure was done according to previously described method in the section of 2.2.3.1.

2.4.1.7. Reverse transcription and polymerase chain reaction (RT-PCR)

For evaluating the change of gene expression profile in osteogenic differentiation and spontaneous cardiogenic differentiation of each test groups, after 11 days of culture, total RNA was extracted from cells of each test group, and

RNA extraction and RT-PCR procedure was done according to previously described method in the sections of 2.2.3.2-2.2.3.5. Primers which used in this experiment and the expected product size are detailed in Table 2.

Table 2. Oligonucleotide primers for RT-PCR analysis for osteogenic and spontaneous cardiogenic differentiation through EB formation

Gene		Sequence	Product (bp)
mCbfa1/ Runx2	sense	5'- CATGGTGGAGATCATCGC -3'	
	antisense	5'- ACTCTTGCCTCGTCCACTC -3'	285
mNkx-2.5	sense	5'- TGGCGTCGGGGACTTGAAC -3'	
	antisense	5'- AGGCTACGTCAATAAAGTGG -3'	259
mGAPDH	sense	5'-CATCACCATCTTCCAGGAGC-3'	
	antisense	5'-ATGCCAGTGAGCTTCCCGTC-3'	500

2.4.1.8. Colorimetric quantification of ALPase activity

ALPase activity for each test group was determined at day 6, 11, 16 and 21 of osteogenic culture, in order to capture the temporal nature of ALPase activity. Briefly, unattached cells were removed by gentle washing with 1X PBS. Following ALPase activity assay was done according to previously described method in the sections of 2.3.4.3.

2.4.2. Chondrogenic Differentiation

2.4.2.1. Chondrogenic media

α-MEM was supplemented with 15% FBS, 100 units/ml penicillin and 100 μg/ml streptomycin, 0.4 mM L-proline (Sigma, UK), 1X Non essential amino acid (Gibco, UK), 4500 mg/L glucose, 1X insulin-transferrin-selenium (ITS; Sigma, UK), 50 μg/ml ascorbic acid (Sigma, UK), 1 μM dexamethasone (Sigma, UK) and 50

ng/ml insulin like growth factor (IGF-I, Sigma, UK).

2.4.2.2. Experimental groups

Three experimental groups and one control group were set-up. The experimental groups consisted of CM-mESCs allowed to form EBs for 1-day (CM-mESC-EB1), 3-days (CM-mESC-EB3), or 5-days (CM-mESC-EB5), followed by a further 15 days of culture in the chondrogenic medium detailed above. The control group (EB5) consisted of mESCs maintained for 3 days in the standard mESC maintenance medium, followed by EB formation for 5 days.

2.4.2.3. Micromass culture for chondrogenesis

For high cell density micromass culture, after EB formation, the CM-mESC-EBs and control EBs were gently centrifuged and then trypsinized to release single cells; trypsinisation was stopped by addition of serum-containing EB formation medium before the dispersion of single cells became apparent. The single cell dispersion was centrifuged and resuspended at density of 10×10^6 cells/ml and 20 μl drops (2×10^5 cells: 380000 cells/cm^2) spotted onto 24 well plates. In addition, for RT-PCR and immunocytochemistry, cells were plated in 6 well plates and 8 well chamber slides at a cell density of 380000 cells/cm^2. After 30 min, wells were flooded with 2 ml chondrogenic medium. The cultures were fed everyday by replacing half the volume with fresh medium and maintained in a 5% CO_2 humidified incubator.

2.4.2.4. Measurement of Alcian blue-stained areas

Cartilage nodule formation in chondrogenic culture was evaluated at day 15 of culture by the measurement of GAG-specific Alcian blue stained area. Cells

were fixed with 4% paraformaldehyde for 20 min, washed in 1X PBS, and stained with 1% (w/v in 3% Acetic acid, pH 2.5) Alcian blue 8 GX (Sigma, UK) for 20 min and then washed with 1X PBS. Stained cartilage nodules were observed using an inverted microscope (BX-60, Olympus, Japan). The area of stained nodule was calculated from randomly taken pictures using Photoshop program (Adobe, USA). The area of the stained region was expressed relative to the whole area of the picture including stained region.

To exclude the possibility that any Alcian blue-stained region derived from bone or other cell colonies rather than cartilage, we performed dual staining with Alcian blue and Alrizarin red-S. After Alcian blue staining, the nodules were stained with 40 mM Alizarin Red S (ARS) solution (pH4.2) for 20 min at room temperature and then washed with 1X PBS. The stained cell cultures were observed using an inverted epi-fluorescence microscope (BX-60, Olympus, Japan) and images were captured using a Zeiss Axiocam digital camera and analysed using KS-300 software (Imaging Associates, UK)

2.4.2.5. Measurement of sulfated GAG content (1,9-DimethImethylene Blue (DMMB) assay) and DNA content

To measure sulfated glycosaminoglycans (GAG) produced by cells, DMMB assay was performed as documented in [Barbosa I 2003] with a slight adaptation. Briefly, after culture for chondrogenic differentiation, all cell cultures were digested with Proteinase K solution (50 μg/ml proteinase K in 100 mM K_2HPO_4 (pH 8.0), Sigma, UK) at 37°C overnight with shaking in a CO_2 incubator. After digestion, samples were transferred to 1.5 ml centrifuge tubes, and then proteinase K activity was inactivated by heating at 90 °C for 10 min. After centrifugation at 12,000g for 10 min, supernatant was collected to use in GAG quantification and DNA content

measurement. 100 μl Proteinase K-treated samples solution were reacted with 1.4 ml DMMB solution (Sigma) through vigorous vortexing for 30 min resulting in complexation of GAG with DMMB. After centrifugation at 12,000g for 10 min, precipitates of insoluble GAG-DMMB complex were dissolved with 1 ml DMMB decomplexation solution with vortexing for 10 min, and the OD_{650} of the solution was measured using an ELISA Plate Peader (MRX II, Dynex Technology, Finland). A calibration curve (Appendix 4) was generated using the chondroitin sulfate solution (Sigma, UK), and the amount of total GAG produced from cultured cells was enumerated from the calibration curve.

From the Proteinase K-treated samples solution, 100μl of the sample supernatant was placed in a DNA/RNA free eppendorf tube along with 100μl of Hoescht 33258 solution (2 μg/ml; Sigma, UK) and vortexed for 2-3 min. An aliquot (100μl) of the solution was then read using a microtiter plate fluorometer (MFX, Dynex Technology, Finland) with the excitation wavelength being at 365 nm and the emission wavelength at 460 nm. A calibration curve (Appendix 5) was generated using highly polymerised calf-thymus DNA (Sigma, UK) and the amount of total DNA produced from routinely cultured cells was enumerated from the calibration curve.

For the final data analysis, GAG values were normalized to total values of DNA content determined by Hoechst 33258 assay. The GAG content was expressed as relative GAG content at each culture time to GAG content at 0 day culture of each test group.

2.4.2.6. Immunocytochemical staining

Chondrogenic differentiation in molecular level was evaluated by immunostaining for type II collagen. Prior to antibodies reaction, the fixed cells

were then incubated with 10% (v/v) blocking goat serum (Vector Laboratories) for 30 min at room temperature. The primary antibodies, goat anti type II collagen (diluted 1:50 with BSA/Azide solution; Santa Cruz Biotechnology, UK) were incubated overnight at 4°C. In secondary antibodies reaction, the secondary FITC-conjugated rabbit anti-goat IgG (Santa Cruz Biotechnology) antibodies were incubated for 1 hr at room temperature. The cells were countered stained with DAPI to visualize the cell nucleus.

2.4.2.7. Reverse transcription and polymerase chain reaction (RT-PCR)

For evaluating the change of gene expression profile in chondrogenic differentiation of CM-mESC-EB1, after 5, 10 or 15 days of culture, total RNA was extracted from cells of each test group, and RNA extraction and RT-PCR procedure was done according to previously described method in the sections of 2.2.3.2-2.2.3.5. Primers which used in this experiment and the expected product size are detailed in Table 3.

Table 3. Oligonucleotide primers for RT-PCR analysis for chondrogenic differentiation through EB formation

Gene		Sequence	Product (bp)
mCol II	sense	5'-GCGCTCACGCCGCGGTCCTA-3'	463(IIA)
	antisense	5'-AGGGGTACCAGGTTCTCCATC-3'	222(IIB)
mCol X	sense	5'-CCTGGGTTAGATGGAAAA-3'	579
	antisense	5'-AATCTCATAAATGGGATGGG-3'	
mAggrecan	sense	5'-AGGGTGAGAAGGTAAGGGGT-3'	102
	antisense	5'-GAGGCGAAGTAACCAACCAT-3'	
mSox-9	sense	5'-GTGGCAAGTATTGGTCAA-3'	320
	antisense	5'-GAACAGACTCACATCTCT-3'	
mGAPDH	sense	5'-CATCACCATCTTCCAGGAGC-3'	500
	antisense	5'-ATGCCAGTGAGCTTCCCGTC-3'	

2.5. *In Vitro* Osteogenic and Chondrogenic Differentiation of Murine Embryonic Stem Cells without EB Formation

2.5.1. Direct Osteogenic Differentiation without EB Formation

2.5.1.1. Direct osteogenic differentiation

For *in vitro* direct osteogenesis, mESCs were directly plated at a cell density of 10,000 cells/cm^2, and were cultured for 3 days in the culture condition of a 1:1 (v/v) mixture of HepG2 CM and the standard mESC maintenance medium in a same manner with the section of 2.3.2. Induction of mESCs early differentiation by HepG2 conditioned media. After 3 days, the conditioned media was directly replaced by osteogenic medium previously described in the section of 2.4.1.1. The cultures were maintained at 37°C in a 5% CO_2 humidified incubator and fed every 2 days up to 21 days. As a comparative control group, mESCs were cultured in mESC maintenance medium for 3 days, and then cultured in osteogenic medium up to 21 days.

2.5.1.2. Bone nodule formation (ARS staining) and ARS quantification

Bone nodule formation assay was done by mineralised nodule specific Alizarin red S (ARS) staining and the quantification of extracted ARS from stained bone nodules using cetylpyridinium chloride (CPC) extraction method [Gregory CA 2004] with a slight adaptation. After 6, 11, 16, and 21 days of osteogenic culture, each test group were fixed with 4% paraformaldehyde for 20 min followed by three washes with 1X PBS, and then were stained with ARS in a same way previously described in the section of 2.4.1.5. These ARS stained bone nodules were captured were captured using a Zeiss Axiocam digital camera in an inverted epi-

fluorescence microscope (BX-60, Olympus, Japan). In addition, for the quantification of bone nodule formation, ARS from stained bone nodules in 6 well plates were extracted with 2ml CPC buffer (10% (w/v) CPC in 10mM Na_2PO_4 (pH 7.0)) for 1hr with shaking at 37°C, and then 200μl aliquots were transferred to a 96-well plate and the OD_{550} of the solution was measured using an microplate reader (ELx 808, Bio-Tek Instrument, USA).

2.5.1.3. ALPase expression and ALPase activity

Direct osteogenic differentiation of mESCs and CM-mESCs was evaluated by assessing ALPase expression and ALPase activity. mESCs were seeded onto the 48 well plates at the concentration of 1.0×10^4 cells/cm^2 and cultured for 3 days in standard mESC maintenance culture medium or 50% HepG2 conditioned medium and then were induced to differentiate osteogenic lineage in osteogenic medium for 21 days at 37°C in a 5% CO_2 humidified incubator. At day 6, 11, 16, and 21 of culture, ALPase expression and its activity was measured using the same method as previously described in the section of 2.3.4.3.

2.5.1.4. Immunocytochemical staining

Direct Osteogenic differentiation in molecular level was characterised by immunostaining for type I collagen and osteopontin, respectively. Prior to antibody reaction, the fixed cells were then incubated with 10% (v/v) blocking goat serum (Vector Laboratories) for 30 min at room temperature. The primary antibodies, goat anti type I collagen (diluted 1:50 with BSA/azide solution; Santa Cruz Biotechnology, UK), and goat anti osteopontin (diluted 1:50 with BSA/Azide solution; Sigma) were incubated overnight at 4°C. In secondary antibody reaction, the secondary FITC-conjugated rabbit anti-goat IgG (Santa Cruz Biotechnology)

antibodies were incubated for 1 hr at room temperature. The cells were counter-stained with DAPI to visualize the cell nucleus and were observed using epi-fluorescence on a BX-60 microscope and images were captured using a Zeiss Axiocam digital camera and analysed using KS-300 software, and other procedure was done according to previously described method in the section of 2.2.3.1.

2.5.1.5. Reverse transcription and polymerase chain reaction (RT-PCR)

For evaluating the change of gene expression profile in direct osteogenic differentiation of mESCs and CM-mESCs, after 6, 11, 16 and 21 days of culture, total RNA was extracted from cells of each group, and RNA extraction and RT-PCR procedure was done according to previously described method in the sections of 2.2.3.2-2.2.3.5. Primers which used in this experiment and the expected product size are detailed in Table 4.

Table 4. Oligonucleotide primers for RT-PCR analysis for direct osteogenesis

Gene		Sequence	Product (bp)
mOsteocalcin	sense	5'-CGGCCCTGAGTCTGACAAA-3'	50
	antisense	5'-ACCTTATTGCCCTCCTGCTT-3'	
mCbfa1/Runx2	sense	5'- CATGGTGGAGATCATCGC -3'	285
	antisense	5'- ACTCTTGCCTCGTCCACTC -3'	
mOsterix	sense	5'-CAGGCATCCACGCAGGCATCTC-3'	398
	antisense	5'-TGGGGCAGTCGCAGGTAGAACG-3'	
mGAPDH	sense	5'-CATCACCATCTTCCAGGAGC-3'	500
	antisense	5'-ATGCCAGTGAGCTTCCCGTC-3'	

2.5.2. Direct Chondrogenic Differentiation without EB Formation

2.5.2.1. Chondrogenic medium

α-MEM supplemented with 15% (v/v) FBS, 100 units/ml penicillin and 100 μg/ml streptomycin, 0.4 mM L-proline (Sigma), 1X non essential amino acid (Gibco), 4.5 g/L glucose (Sigma), 1X insulin-transferrin-selenium (ITS; Sigma, UK), 50 μg/ml ascorbic acid (Sigma), 1 μM dexamethasone (Sigma) and 50 ng/ml transforming growth factor-β1 (TGF-β1; Sigma, UK) were added. TGF-β1 was reconstituted in 4 mM HCl, which activates TGF-β1 from its latent form, containing 1 mg/ml of bovine serum albumin, prior to the addition of the TGF-β1 to the medium.

2.5.2.2. Direct chondrogenic differentiation

For *in vitro* direct chondrogenesis, mESCs were directly plated at a cell density of 30,000 cells/cm^2, and were cultured for 3 days in the culture condition of a 1:1 (v/v) mixture of HepG2 CM and the standard mESC maintenance medium in a same manner with the section of 2.3.2. After 3 days, the conditioned media was directly replaced by chondrogenic medium previously described in the section of 2.5.2.1. The cultures were maintained at 37°C in a 5% CO_2 humidified incubator and fed everyday up to 15 days. As a comparative control group, mESCs were seeded at a cell density of 30,000 cells/cm^2, and cultured in mESC maintenance medium for 3 days, and the conditioned media was directly replaced by chondrogenic medium previously described in the section of 2.5.2.1., and cultured in chondrogenic medium upto 15 days.

2.5.2.3. Morphological observation

During the direct chondrogenic differentiation, morphological change of mESCs and CM-mESCs were observed routinely using an inverted phase microscope (Olympus IX70, UK) equipped with analysisD soft imaging system (Soft imaging system GmbH, Germany). The change of mESCs and CM-mESCs morphology was captured.

2.5.2.4. Measurement of Alcian blue-stained areas

Cartilage nodule formation in the culture for direct chondrogenic differentiation was evaluated at day 15 of culture by the measurement of GAG-specific Alcian blue stained area. After culture, mESCs and CM-mESCs were fixed with 4% paraformaldehyde for 20 min, washed in 1X PBS, and stained with 1% (w/v in 3% Acetic acid, pH 2.5) Alcian blue 8 GX for 20 min and then excessive staining was washed with 1X PBS several times. Stained cartilage nodules were observed using an inverted microscope (BX-60, Olympus, Japan). The area of stained nodule was calculated from randomly taken pictures using Photoshop program (Adobe, USA). The area of the stained region was expressed relative to the whole area of the picture including stained region.

2.5.2.5. Measurement of sulfated GAG content (1,9-DimethImethylene Blue (DMMB) assay) and DNA content

After 5, 10, 15 days of culture for direct chondrogenic differentiation, the content of sulfated glycosaminoglycans (GAG) produced by mESCs and CM-mESCs and DNA content was measured using DMMB assay method and Hoechst 33258 DNA assay method previously described in the section of 2.4.2.5. GAG values were normalized to total values of DNA content determined by Hoechst

33258 assay.

2.5.2.6. Measurement of collagen content and DNA content

In addition to the measurement of GAG content, after 5, 10, 15 days of culture for direct chondrogenic differentiation, collagen content was quantified using the collagen detection kit (Sircol Collagen Assay S 1000, Biocolor Ltd, Ireland) according to manufacturer's instruction. Briefly, following chondrogenic differentiation for 5, 10 and 15 days, non-attached cells were removed by washing with 1X PBS, and all cultures were digested with 0.5 ml (starting volume) of pepsin (Sigma, UK) solution (2 mg/ml dissolved in 0.05M acetic acid) at 4°C overnight with gentle mixing on a rotator. After pepsin digestion, 1/10 the starting volume of 10X TSB (1.0M Tris-2.0M NaCl-50mM $CaCl_2$, pH 7.8 - 8.0) was added and mixed vigorously, and then 1/10 the starting volume of pancreatic elastase (Sigma, UK) (1 mg/ml dissolved in 1X TSB, pH 7.8 - 8.0) was added and incubated at 35°C for 30 min with gentle mixing on a rotator. Finally, digested samples were centrifuged at 10,000 rpm for 5 min at room temperature. After centrifuge, only supernatant was acquired for assay for collagen content with the collagen detection kit (Sircol Collagen Assay S 1000, Biocolor Ltd, Ireland), and then 200μl aliquots were transferred to a 96-well plate and the OD_{540} of the solution was measured using an ELISA Plate Peader (MRX II, Dynex Technology, Finland). A calibration curve (Appendix 6) was generated using the supplied reference collagen standard solution, and the amount of total collagen produced from cultured cells was enumerated from the calibration curve.

In addition, the DNA content was measured using Hoechst 33258 DNA assay method previously described in the section of 2.4.2.5. Collagen values were

normalized to total values of DNA content determined by Hoechst 33258 assay.

2.5.2.7. Immunocytochemical staining

Chondrogenic differentiation in molecular level was evaluated by immunostaining for type II collagen and sox-9. Prior to antibody reaction, the fixed cells were then incubated with 10% (v/v) blocking goat serum (Vector Laboratories) for 30 min at room temperature. The primary antibodies, goat anti type II collagen (diluted 1:50 with BSA/Azide solution; Santa Cruz Biotechnology, UK) or goat anti Sox-9 (diluted 1:50 with BSA/Azide solution; Santa Cruz Biotechnology, UK) were incubated overnight at 4°C. In secondary antibody reaction, the secondary FITC-conjugated rabbit anti-goat IgG (Santa Cruz Biotechnology) or Alexa Fluor 350-conjugated donkey anti-goat IgG (Invitrogen, UK) antibodies were incubated for 1 hr at room temperature. The cells were counter-stained with PI to visualize the cell nucleus and were observed using epi-fluorescence on a BX-60 microscope and images were captured using a Zeiss Axiocam digital camera and analysed using KS-300 software, and other procedure was done according to previously described method in the section of 2.2.3.1.

2.5.2.8. Reverse transcription and polymerase chain reaction (RT-PCR)

For evaluating the change of gene expression profile in direct chondrogenic differentiation of mESCs and CM-mESCs, after 5, 10 and 15 days of culture, total RNA was extracted from cells of each group, and RNA extraction and RT-PCR procedure was done according to previously described method in the sections of 2.2.3.2-2.2.3.5. Primers which used in this experiment and the expected product size are detailed in Table 5.

Table 5. Oligonucleotide primers for RT-PCR analysis for direct chondrogenesis

Gene		Sequence	Product (bp)
mCol II	sense	5'-GCGCTCACGCCGCGGTCCTA-3'	463
	antisense	5'-AGGGGTACCAGGTTCTCCATC-3'	
mAggrecan	sense	5'-AGGGTGAGAAGGTAAGGGGT-3'	102
	antisense	5'-GAGGCGAAGTAACCAACCAT-3'	
mLink-protein	sense	5'-TTCTGGGCTATGACCGCTG-3'	80
	antisense	5'-AGCGCCTTCTTGGTCGAGA-3'	
mSox-9	sense	5'-GTGGCAAGTATTGGTCAA-3'	320
	antisense	5'-GAACAGACTCACATCTCT-3'	
mScleraxis	sense	5'-GTGGACCCTCCTCCTTCTAATTCG-3'	376
	antisense	5'-GACCGCACCAACAGCGTGAA-3'	
mGAPDH	sense	5'-CATCACCATCTTCCAGGAGC-3'	500
	antisense	5'-ATGCCAGTGAGCTTCCCGTC-3'	

2.6. Bioprocessing for Three Dimensional (3D) Bone and Cartilage Tissue Like Construct Formation Using Alginate Encapsulated Murine Embryonic Stem Cells and HARV Bioreactors

2.6.1. 3D mESC Encapsulation

After expansion on T75 tissue culture flasks, undifferentiated mESCs were trypsinised, counted, and resuspended in 0.2μm sterile filtered 1.1% (w/v) low viscosity alginic acid (Sigma, UK) and 0.1% (v/v) porcine gelatin (Sigma, UK) (all dissolved in 1X PBS, pH 7.4) solution at room temperature. With a peristaltic pump (Model P-1, Amersham Biosciences, UK), a flow rate producing single droplets, a drop height of 30 mm (tubing autoclaved and then sterilised with 1 M NaOH for 30 min and washed three times with sterile 1X PBS) the cell-gel solution was passed through the peristaltic pump and dropped using a 25-gauge needle (Becton Dickinson, UK) into sterile alginate gelation solution which is composed of 100 mM calcium chloride solution ($CaCl_2$; Sigma, UK), 10 mM N-(2-hydroxyethyl) piperazine-N-(2- ethane sulfonic acid) (HEPES; Sigma, UK), and 0.01% Tween (Sigma, UK) in distilled water at pH 7.4, at room temperature with stirring. The cell-gel solution gelled immediately on contact with the $CaCl_2$ solution, forming spherical beads resulting in encapsulating cells. The beads remained in gently stirred $CaCl_2$ solution for 6-10 min at room temperature. The beads were washed three times in 1X PBS and placed into a 1:1 (v/v) mixture of HepG2 CM and the standard mESC maintenance medium.

For the 3D osteogenic differentiation, 25000 cells were encapsulated in each alginate beads through the cell suspension at the approximate cell density of 3.90×10^7 cells/ml alginate solution, which was calculated from that the approximate volume of a drop of alginate solution passing though needle is 6.4 μl

for making an alginate bead.

For the 3D chondrogenic differentiation, 50000 cells were encapsulated in each alginate beads through the cell suspension at the approximate cell density of 7.81 x 10^7 cells/ml alginate solution, which was calculated from that the approximate volume of a drop of alginate solution passing though needle is 6.4 μl for making an alginate bead.

2.6.2. Operation of Single-Step Bioprocess Using HARV Bioreactors

Undifferentiated mESCs encapsulated in alginate beads were cultured for 3 days in a 1:1 (v/v) mixture of HepG2 CM and the standard mESC maintenance medium in 50 ml horizontal aspect ratio vessel (HARV) bioreactors (Synthecon, USA) with daily refreshment of medium to induce early differentiation. Each vessel contained 600 beads and was rotated anticlockwise at 25 rpm throughout the whole culture period.

To initiate 3D osteogenic differentiation, the 50% HepG2 conditioned medium was replaced in the HARV with osteogenic medium which was described previously in the section of 2.4.1.1. on day 3 until day 24 of culture and changed every 2 days.

To initiate 3D chondrogenic differentiation, the 50% HepG2 conditioned medium was replaced in the HARV with chondrogenic medium which was described previously in the section of 2.5.2.1. on day 3 until day 18 of culture and changed everyday.

2.6.3. Characterisation of 3D Osteogenesis and Chondrogenesis

2.6.3.1. Observation of cell viability (Live/Dead assay)

Time course cell viability within alginate beads during 3D osteogenic and chondrogenic culture in 3D single step culture system was visualized using a two-colour fluorescence cell viability assay, EthD-1/ Calcein AM live/dead assay (Molecular Probes, UK), that is based on the simultaneous determination of live and dead cells that measure intracellular esterase activity and plasma membrane integrity. Membrane permeable 3',6'-Di(O-acetyl)-2',7'-bis[N,N-bis(carboxymethyl) aminomethyl] fluorescein, tetraacetoxymethyl ester (Calcein AM) is cleaved by intracellular esterases to brightly label live cells with green fluorescence. Ethidium homodimer (EthD-1) enters cells that have lost plasma membrane integrity, producing bright red fluorescent labelling of dead cells. This assay was done according to the manufacturer's instruction. Briefly, a 4 mM EthD-1 and 2 mM calcein AM solution diluted in 1X PBS was added to 1X PBS washed, cells encapsulated by alginate were incubated at room temperature for 30 min, in the dark. After incubation, the solution was aspirated and washed with 1X PBS and a small amount of 1X PBS was added to the cells to prevent dehydration. The cells were then photographed, within 30 min using a BX-60 microscope and images were captured using a Zeiss Axiocam digital camera and analysed using KS-300 software to visualise the proportion of live and dead cells.

2.6.3.2. Bioprofiling

Following live and dead assay, the consumption of nutrient by cells within alginate beads in the osteogenic and chondrogenic media in a HARV bioreactor was evaluated by measuring time-course concentration of glucose, ammonia, lactate and by detecting pH of media during whole culture. Media samples of 1.5 ml were collected every two days during the duration of cultures. Glucose,

ammonia, lactate concentrations, and pH were measured using a BioProfile Analyser 200 (Nova Biomedical, USA). In this study, the osteogenic and chondrogenic media was refreshed every two days just after measuring the concentration of nutrients in cultured media. As a control, osteogenic medium and chondrogenic medium was collected at day 0 and glucose, ammonia, lactate concentrations, and pH were measured in the same way.

2.6.3.3. Reverse transcription and polymerase chain reaction (RT-PCR)

For extracting RNA from encapsulated cells, after osteogenic and chondrogenic culture, around 100 alginate beads were collected and then alginate beads containing cells were dissolved in a sterile depolymerisation buffer consisting of 50 mM tri-sodium citrate dihydrate (Fluka, UK), 77 mM sodium chloride (BDH Laboratory supplies, UK) and 10 mM HEPES. The dissolution buffer (Ca^{2+}-depletion) was added to 1X PBS washed beads for 15-20 min while stirring gently. The solution was centrifuged at 400g for 10 min and the pellet was washed with 1X PBS and centrifuged again, at 300g for 3 min. These cell pellets were stored at -80°C prior to use for the extraction of RNA. Total RNA was extracted from these cell pellets, and RNA extraction and RT-PCR procedure was done according to previously described method in the sections of 2.2.3.2-2.2.3.5.

Primers which used for evaluating gene expression profile of 3D osteogenic differentiation in HARV bioreactor culture system and the expected product size are detailed in Table 6.

Primers which used for evaluating gene expression profile of 3D chondrogenic differentiation in HARV bioreactor culture system and the expected product size are detailed in Table 7.

Table 6. Oligonucleotide primers for RT-PCR analysis for 3D osteogenesis

Gene		Sequence	Product (bp)
mOsteocalcin	sense	5'-CGGCCCTGAGTCTGACAAA-3'	50
	antisense	5'-ACCTTATTGCCCTCCTGCTT-3'	
mCbfa1/Runx2	sense	5'- CATGGTGGAGATCATCGC -3'	285
	antisense	5'- ACTCTTGCCTCGTCCACTC -3'	
mOsterix	sense	5'-CAGGCATCCACGCAGGCATCTC-3'	398
	antisense	5'-TGGGGCAGTCGCAGGTAGAACG-3'	
mOct4	sense	5'-TGGAGACTTTGCAGCCTGAG-3'	798
	antisense	5'-TGAATGCATGGGAGAGCCCA-3'	
mBrachyury	sense	5'-GTGTGCGTCAGTGGTGTGTAATC-3'	299
	antisense	5'-AAGGAACCACCGGTCATC-3'	
mGATA-4	sense	5'-CTCCTACTCCAGCCCCTACC-3'	590
	antisense	5'-GTGGCATTGCTGGAGTTACC-3'	
mNestin	sense	5'-CGGCCCACGCATCCCCCATCC-3'	253
	antisense	5'-AGCGGCCTTCCAATCTCTGTTCC-3'	
mGAPDH	sense	5'-CATCACCATCTTCCAGGAGC-3'	500
	antisense	5'-ATGCCAGTGAGCTTCCCGTC-3'	

Table 7. Oligonucleotide primers for RT-PCR analysis for 3D chondrogenesis

Gene		Sequence	Product (bp)
mCol II	sense	5'-GCGCTCACGCCGCGGTCCTA-3'	463
	antisense	5'-AGGGGTACCAGGTTCTCCATC-3'	
mAggrecan	sense	5'-AGGGTGAGAAGGTAAGGGGT-3'	102
	antisense	5'-GAGGCGAAGTAACCAACCAT-3'	
mLink-protein	sense	5'-TTCTGGGCTATGACCGCTG-3'	80
	antisense	5'-AGCGCCTTCTTGGTCGAGA-3'	
mSox-9	sense	5'-GTGGCAAGTATTGGTCAA-3'	320
	antisense	5'-GAACAGACTCACATCTCT-3'	
mScleraxis	sense	5'-GTGGACCCTCCTCCTTCTAATTCG-3'	376
	antisense	5'-GACCGCACCAACAGCGTGAA-3'	
mOct4	sense	5'-TGGAGACTTTGCAGCCTGAG-3'	798
	antisense	5'-TGAATGCATGGGAGAGCCCA-3'	
mBrachyury	sense	5'-GTGTGCGTCAGTGGTGTGTAATC-3'	299
	antisense	5'-AAGGAACCACCGGTCATC-3'	
mGATA-4	sense	5'-CTCCTACTCCAGCCCCTACC-3'	590
	antisense	5'-GTGGCATTGCTGGAGTTACC-3'	
mNestin	sense	5'-CGGCCCACGCATCCCCCATCC-3'	253
	antisense	5'-AGCGGCCTTCCAATCTCTGTTCC-3'	
mGAPDH	sense	5'-CATCACCATCTTCCAGGAGC-3'	500
	antisense	5'-ATGCCAGTGAGCTTCCCGTC-3'	

2.6.3.4. Staining of paraffin embedded section of alginate beads

2.6.3.4.1. Paraffin embedding of alginate beads

After culture for 3D osteogenic and chondrogenic differentiation, the alginate beads were fixed with 10% (w/v) PFA for 30 min at room temperature and then placed in 1X PBS for 15 min prior to dehydration. The beads were dehydrated by placing in a sequential series of increasing ethanol concentrations to remove all the water. The ethanol was then completely replaced with increasing xylene concentration, finally 100% xylene, followed by incubation with paraffin saturated xylene at room temperature overnight. The beads in paraffin saturated xylene were then placed in an oven (60 °C) for 20 min. The xylene was then completely replaced with pre-warmed liquid paraffin. The beads were then serially sectioned (4 µm) and left at room temperature overnight to adhere to Vectabonded™ (Vector Laboratories, UK) glass slides.

For staining, the paraffin was completely removed from the sections by immersion in xylene, decreasing ethanol concentrations and then by washing with tap water.

For immuno-staining, the deparaffinised sections were immersed in pre-heated antigen retrieval reagent (R&D systems, USA) and allowed to cool in order to retrieve the antigens.

2.6.3.4.2. Haematoxylin & Eosin staining

The slides of sectioned alginate beads were dipped in haematoxylin (Harris' solution; BDH Laboratory Supplies, UK) for 30 sec following fixation. The slides were washed in running tap water for 2-3 min and examined for sufficient staining. Excess stain was removed by decolourising in 0.5-1% HCl in 70%

ethanol for a few seconds and then washed in tap water for 5 min. The slides were finally dipped in 1% eosin (BDH Laboratory Supplies, UK) for 2 min and washed briefly in tap water. The tissue was dehydrated by dipping in ethanol (70% (v/v) once and anhydrous or 100% twice), cleared in xylene and mounted in 1,3-diethyl-8-phenylxanthine mountant (DPX; BDH Laboratories, UK), and examined using Leica inverted microscope (Leica, UK) equipped with Olympus DP50 digital camera (Olympus Optical Co, Tokyo, Japan) and analyzed using analySIS® imaging software (Soft Image System GmbH, Germany).

2.6.3.4.3. Alizarin Red S staining (3D osteogenesis)

The sections of alginate beads from 3D culture for osteogenic differentiation were immersed in a 2% (w/v) Alizarin Red S (ARS), (Sigma, UK) solution (pH4.2) for 5 min at room temperature, and excessive staining was washed in tap water, rinsed once in distilled water, and the stained slides were dipped in acetone 20 times and then in 1:1 acetone/xylene for 20 times, followed by clearing in xylene and mounting with DPX solution. The slides were counterstained with Mayer's haematoxylin, and examined using Leica inverted microscope (Leica, UK) equipped with Olympus DP50 digital camera (Olympus Optical Co, Tokyo, Japan) and analyzed using analySIS® imaging software (Soft Image System GmbH, Germany).

2.6.3.4.4. Alcian Blue and Safranin O staining (3D chondrogenesis)

The sections of alginate beads from 3D culture for chondrogenic differentiation were pre-treated with 3% (v/v) acetic acid and then were stained with 1% Alcian blue at pH 2.5 for 2 hr at room temperature and excessive staining was washed in tap water, rinsed once in distilled water, and the stained slides

were dipped in acetone 20 times and then in 1:1 acetone/xylene for 20 times, followed by clearing in xylene and mounting with DPX solution. The slides were counterstained with Mayer's haematoxylin, and examined using Leica inverted microscope (Leica, UK) equipped with Olympus DP50 digital camera (Olympus Optical Co, Tokyo, Japan) and analyzed using analySIS® imaging software (Soft Image System GmbH, Germany).

Alternatively, the sections of alginate beads from 3D culture for chondrogenic differentiation were stained with 0.1% safranin O solution (Sigma, UK) for 5 min at room temperature. and excessive staining was washed in tap water, rinsed once in distilled water, and the stained slides were dipped in acetone 20 times and then in 1:1 acetone/xylene for 20 times, followed by clearing in xylene and mounting with DPX solution. The slides were counterstained with Mayer's haematoxylin, and examined using Leica inverted microscope (Leica, UK) equipped with Olympus DP50 digital camera (Olympus Optical Co, Tokyo, Japan) and analyzed using analySIS® imaging software (Soft Image System GmbH, Germany).

2.6.3.4.5. Immuno-staining (3D osteogenesis and chondrogenesis)

Immuno-staining was performed on sections using goat polyclonal antibodies to type I collagen (diluted 1:50 with BSA/Azide solution; Santa Cruz Biotechnology, UK), osteocalcin (diluted 1:50 with BSA/Azide solution; Santa Cruz Biotechnology, UK) for the characterisation of 3D osteogenic differentiation and type II collagen (diluted 1:50 with BSA/Azide solution; Santa Cruz Biotechnology, UK) for the characterisation of 3D chondrogenic differentiation. Briefly, the slides were immersed in 0.3% (v/v) H_2O_2 for 15 min to quench endogenous peroxidase activity from sectioned tissues on slides. Sections were then placed in 10% (v/v)

goat serum (Vector laboratory, USA) for 30 min at room temperature to block non-specific staining. The primary antibodies were applied and allowed to react for overnight at 4°C. Sections were then incubated with biotinylated antibodies to goat IgG (R&D systems, USA). After colour development using ant-goat HRP-AEC Cell & Tissue Staining kit (R&D systems, USA) according to the manufacturer's instruction, the slides were counterstained with Mayer's haematoxylin, and examined using Leica inverted microscope (Leica, UK) equipped with Olympus DP50 digital camera (Olympus Optical Co, Tokyo, Japan) and analyzed using analySIS® imaging software (Soft Image System GmbH, Germany).

2.6.3.4.6. Physicochemical and mechanical characterisation of alginate beads (3D osteogenesis)

2.6.3.4.6.1. Scanning Electron Microscope - Energy Dispersive X-ray Spectroscopy (SEM-EDS) analysis

The cross-section of alginate beads from the 3D culture for osteogenic differentiation were fixed with 10% PFA, thoroughly washed with distilled water, and then freeze-dried. Specimens were mounted and sputter-coated with gold using an ion coater and observed at an accelerating voltage of 20kV. In order to characterise the morphology and the chemical composition of mineralized nodules within alginate beads, Energy-dispersive X-ray Spectroscopy (EDS) analysis on cross sections of alginate beads was carried out with a LEO Gemini Field Emission Gun-Scanning Electron Microscope (FEG-SEM, Carl Zeiss, Hertfordshire, UK). Samples for SEM analysis were either imaged directly.

2.6.3.4.6.2. Micro attenuated total reflection - Fourier transformed infrared

(ATR-FTIR) analysis

The cross-section of alginate beads from the 3D culture for osteogenic differentiation was further characterized by the micro attenuated total reflection - Fourier transformed infrared (ATR-FTIR) spectroscopy. FT-IR images were collected with a system described previously [Chan KLA 2003]. The FT-IR images were collected with a Bruker Optics imaging spectrometer (Bruker Optics Inc, Germany). The whole system is made up of an IFS 66/S step scan FT-IR spectrometer, an infrared microscope (IRscope II) with a Ge ATR objective, and a 64 X 64 focal-plane array (FPA) detector. In this configuration, the field of view of the image was 500 X 700 μm^2. All images were taken with a nominal spectral resolution of 8 cm^{-1} in the range 4000 – 900 cm^{-1} using 20 scans. The cross-sections were supported on a BaF_2 window and the background was taken with the same window without the sample. The chemical images were obtained by attributing a color to each pixel according to the absorbance of a spectral band characteristic of a given compound.

2.6.3.4.6.3. Compression study

A micro-deformation apparatus, developed in Dr. Williams' earlier work [Andrei DC 1996, Briscoe BJ 1998], was used to measure the force-displacement characteristics of the alginate hydrogels that are compressed between two rigid parallel plates. The alginate hydrogels were prepared with one test group and two control groups (Test group: 3D bone construct: alginate hydrogels encapsulating mESCs-derived osteogenic cells by osteogenic culture for 21 days in HARV bioreactor, Control group 1: pure alginate hydrogels, Control group 2; alginate hydrogels encapsulating undifferentiated mESCs with the cell density of approximate 1800,000 cells, which are almost identical to the cell number in 3D

bone construct). A detailed description of the micro-deformation apparatus is presented elsewhere [Andrei DC 1996, Briscoe BJ 1998, Liu KK 1998]. The apparatus permits continuous and simultaneous measurements on the responsive force (measured with a cantilever transducer of 10 μN resolution) and the applied displacement (monitored by the computer with a resolution of 0.1 μm). During the experiment, the alginate hydrogels are fully immersed in α-MEM supplemented with 15% FBS, and 100 units/ml penicillin and 100 μg/ml streptomycin. The alginate hydrogels were subjected to a maximum deformation of up to 20%, and were continuously monitored by a high-resolution video camera during manipulation and deformation to ensure that the alginate hydrogels were not damaged. Deformation measurements were carried out immediately on the alginate hydrogels after harvest to minimise effects on the alginate hydrogel compliance due to swelling. At least eight force-displacement measurements were taken for each type of alginate hydrogels, and all experiments were conducted under ambient conditions (T = 20 ± 2 °C).

2.7. Statistical Analysis

The results were expressed as mean ± standard deviation (SD) and analysed using a Student's unpaired two-tailed *t*-test, comparing all data pairs. Statistical significance was considered at $P < 0.05$.

CHAPER III

EARLY DIFFERENTIATION OF MURINE EMBRYONIC STEM CELLS INTO PRIMITIVE STREAK / NASCENT MESODERM LIKE CELLS

3.1. INTRODUCTION: Current Approaches to *In Vitro* Differentiation of Embryonic Stem Cells into Mesoderm

Induction of mesoderm formation has been identified as the early differentiation step required for further specific lineage differentiation towards the haematopoietic, cardiogenic, osteogenic, and chondrogenic lineages with various conditions having been established for the efficient and reproducible induction and differentiation into mesoderm *in vitro*.

3.1.1. EB-mediated i*n vitro* spontaneous early differentiation

Undifferentiated mESCs can be induced to differentiate *in vitro* by removal of the feeder-cell layer and LIF, and subsequent transfer into suspension culture [Eldor JI 2000]. Under these conditions, ESCs undergo differentiation into spheroid structures termed embryoid bodies (EBs). Currently, the most established methodology for ESC differentiation requires the formation of EBs. EB formation is considered to mimic the differentiation in the blastocyst *in vivo*. Much of our current understanding on mesoderm induction is dependent on EBs recapitulating several aspects of early development, displaying regional-specific differentiation processes into derivatives of all three embryonic germ layers, namely ectoderm, endoderm and mesoderm [Eldor JI 2000]. Consequently, EB formation has been utilised as a basic step in a wide range of studies aimed at differentiating ESCs into specific and desired cell types. Formation of EBs represents several phase of differentiation (Figure 10). Within 2–4 days in suspension culture, endoderm forms a rim on the surface of the inner cell mass cells, giving rise to three dimensional spheroid structures. Around day 4 or 5, differentiation of a columnar epithelium with a basal lamina and formation of a central cavity occurs. Upon continued *in vitro* culture of EBs, mesodermal cells appear, and subsequently a variety of the

early embryonal lineages develop [Eldor JI 2000, Tanaka H 2004, Buttery LD 2001, Mummery C 2002].

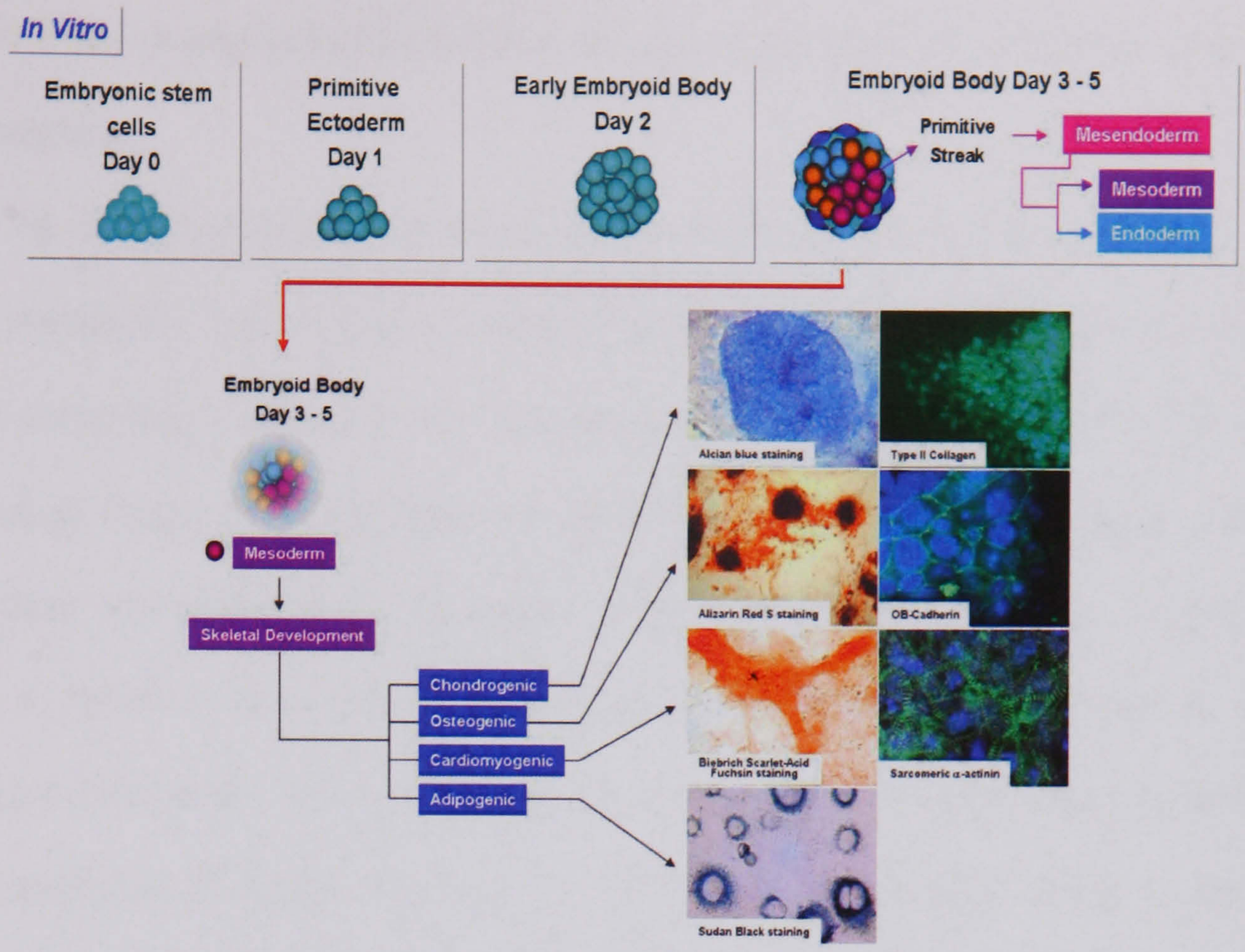


Figure 10. *In vitro* skeletal lineage differentiation of ESCs.

Differentiation studies have suggested that structural organization and the dynamics of developmental processes are maintained during EB formation. The first two days of EB formation are equivalent to the period between implantation and beginning of gastrulation in mouse embryos. Gastrulation-related cell types appear to be present in the EBs between days 3 and 5. It has been well known that early organogenesis is stretched out during EB formation between days 3 and 8 [Leahy A 1999]. Therefore, differentiation of ESCs through EB formation in suspension culture provides a powerful *in vitro* system for studying early lineage determination during mammalian development. Consequently, most protocols for skeletal lineage differentiation require EB formation for approximately 5 days followed by replating of the EB-derived cells onto tissue culture dishes and terminal differentiation induction into the various specialized cells, such as osteoblasts, chondrocytes and cardiomyocytes, using the appropriate culture

conditions [Tanaka H 2004, Buttery LD 2001, Mummery C 2002].

3.1.2. *In vitro* early differentiation using exogenous cytockines and growth factors

The use of growth factors has been investigated in order to develop defined culture media for directing the mesodermal differentiation of ESCs or EB-derived cells. A promising candidate for inducing mesoderm formation is the transforming growth factor beta (TGF-β) family of cytokines. Specifically, Activin A was shown to mediate dorsoanterior mesoderm differentiation and bone morphogenetic protein 4 (BMP-4; also known as BMP-2b or DVR-4) was shown to mediate mesoderm formation of a more ventral character, including hematopoietic cells [Valdimarsdotter G 2005, Huber BTL 1998, Johansson BM 1995]. In addition, it has been well reported that Nodal plays a role of inducing mesoderm formation during the development of embryos [Jones CM 1995, Vincent SD 2003, Pfendler KC 2005]. In addition to the TGF-β superfamily, it has been demonstrated that binding of IGF-II, a member of insulin-like growth factor (IGF) family, to its signalling receptor, IGF1R, at the surface of mesoderm precursor cells increased mesoderm formation [Morali OG 2000].

Although several growth factors have been identified to influence mesoderm formation *in vivo* and *in vitro*, the reports in literature are conflicting. Hence, activin A also functions to maintain ESCs undifferentiation [Beattie GM 2005] and the self-renewal activity of ESCs was sustained by BMP-4 addition to the ESC maintenance medium by inhibiting both the extracellular receptor kinase (ERK) and p38 mitogen-activated protein kinase (MAPK) pathways [Qi X 2004]. Furthermore, Johansson et al demonstrated that members of both the TGF-β and the fibroblast growth factor (FGF) families, such as TGF-β1, -β2, and -β3, acidic

FGF, and basic FGF, when applied individually, did not produce any marked consistent increase in the expression of the mesoderm markers. They suggested that these factors normally operate in conjunction with others [Johansson BM 1995]. These observations are consistent with the fact that mesoderm formation and subsequent development involve multiple dynamic, overlapping signals that progressively give rise to pattern formation [Kimelman D 1992, Wolpert L 1969].

3.1.3. *In vitro* early differentiation using conditioned media

An alternative strategy for inducing mesoderm formation or other early differentiation of ESCs is the use of conditioned culture media. Recently, it has been shown that visceral endoderm plays a critical role in establishing anterior-posterior polarity in the mouse embryo and the primitive streak followed by mesoderm formation during embryogenesis [Lu CC 2001]. Furthermore, similarities between liver cell lines and visceral endoderm in their biological functionality and gene expression profiles were observed [Rathjen J 1999]. These observations have resulted in the use of the human hepatocarcinoma cell line (HepG2)-conditioned medium [Rathjen J 1999, Lake J 2003] or of the visceral endoderm-like cell line, END-2 [Mummery C 2000], in studies of early ESC differentiation, suggesting that these conditioned media recapitulate the visceral endoderm-like signalling. In particular, HepG2 conditioned medium treatment induced mESC early differentiation into a primitive ectoderm like cell, termed the early primitive ectoderm like cell (EPL), as evidenced by the gene expression profile of conditioned medium-treated ESCs that was similar to primitive ectoderm. Furthermore, they also reported a restricted repertoire of cell types comprising of mainly mesodermal cell types and parietal endoderm [Rathjen J 1999, Lake J 2003]; mesoderm consisting up to 90% of EBs. In contrast, others have shown

that treatment of hESCs with HepG2-conditioned medium directed differentiation to a cell type with a gene expression profile resembling that of primitive streak/nascent mesoderm-stage cells while retaining the pluripotency markers [Calhoun JD 2004]. Although there are conflicting reports on the cell type generated by treatment with the HepG2 conditioned medium, mesoderm formation was certainly enhanced. Similarly, Mummery and colleagues reported that when ESCs were cultured on the visceral endoderm-like cell line (END-2), they aggregated and spontaneously differentiated to cardiomyocyte-forming beating-heart muscle colonies. This spontaneous differentiation towards cardiomyocytes was induced not only by co-culture with the END-2 cells but also by the END-2 conditioned medium suggesting that soluble factors secreted by END-2 cells can act as cues for cardiac differentiation [Mummery C 2000]. In addition, it has been reported that avian precardiac explant-conditioned medium induces cardiomyocyte differentiation presumably by mimicking the cues from the explanted endoderm/mesoderm [Rudy-Reil D 2004]. The utilisation of conditioned media has highlighted an efficient methodology for inducing mesoderm formation as the primary potent cell source for terminal skeletal lineage differentiation with concomitant reduction in the formation of other contaminating lineages.

3.2. Objectives

Despite progress in developing efficient strategies for osteogenic or chondrogenic differentiation of ESCs, little has been achieved in establishing optimal conditions for the efficient induction of mesoderm. Hence, the focus of this chapter is on the development of an *in vitro* protocol for the generation of a specific cell population with high osteogenic and chondrogenic potential from mESCs by investigating the effects of the HepG2 conditioned medium on early

differentiation of mESCs to primitive streak/nascent mesoderm cells, which could be potent progenitor cells for osteogenic and chondrogenic differentiation.

3.3. Experimental Process

In this chapter, prior to osteogenic or chondrogenic differentiation, mESCs were treated with 50% HepG2 conditioned medium, which was collected by culturing the HepG2 cells for 3 days. Following HepG2 exposure, the conditioned medium-treated mESCs were allowed to form EBs to achieve spontaneous differentiation. The experimental and control groups (untreated mESCs) were evaluated for change in morphology, gene expression, ALPase activity, EB formation capacity as detailed in chapter II. In brief, the overall experimental process is illustrated in Figure 11.

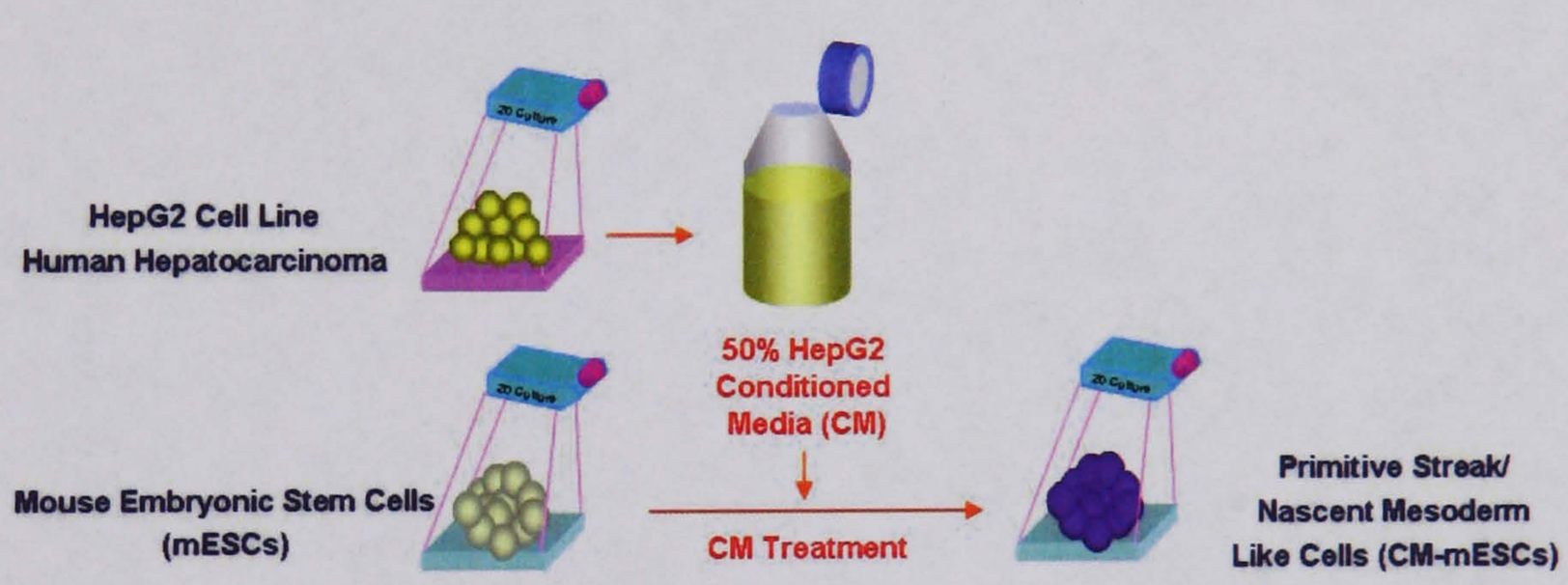


Figure 11. Schematic diagram of experimental process for the generation of primitive streak/nascent mesoderm like cells from mESCs.

3.4. Results

3.4.1. mESCs expansion and maintenance

The maintenance and expansion of undifferentiated mESCs, while retaining their pluripotency, is an important step since it provides the starting material for osteogenic and chondrogenic differentiation. Pluripotent ESCs can be characterized by high level expression of the Oct3/4 transcription factor (POU

domain, class 5, transcription factor 1, Pou5f1) [Niwa H 2000], and CD9 [Oka M 2002] and E-cadherin [Bloor DJ 2002] cell-surface makers. Oct3/4 expression is required to sustain stem-cell pluripotency and its expression is down-regulated as cells differentiate [Niwa H 2000]. E-cadherin plays a role in cell colony and EB formation of ESCs; constitutive expression of E-cadherin in early stage embryo is down-regulated as the cells differentiate [Bloor DJ 2002, Dang SM 2004]. mESCs showed typical three dimensional colony formation with colony size increasing during the culture. Furthermore, Oct-4, CD9 and E-cadherin were strongly expressed in the nucleus and periphery of cells in the cell colonies (Figure 12A-C). In addition, high expression of ALPase was observed in mESC colonies (Figure 12D).

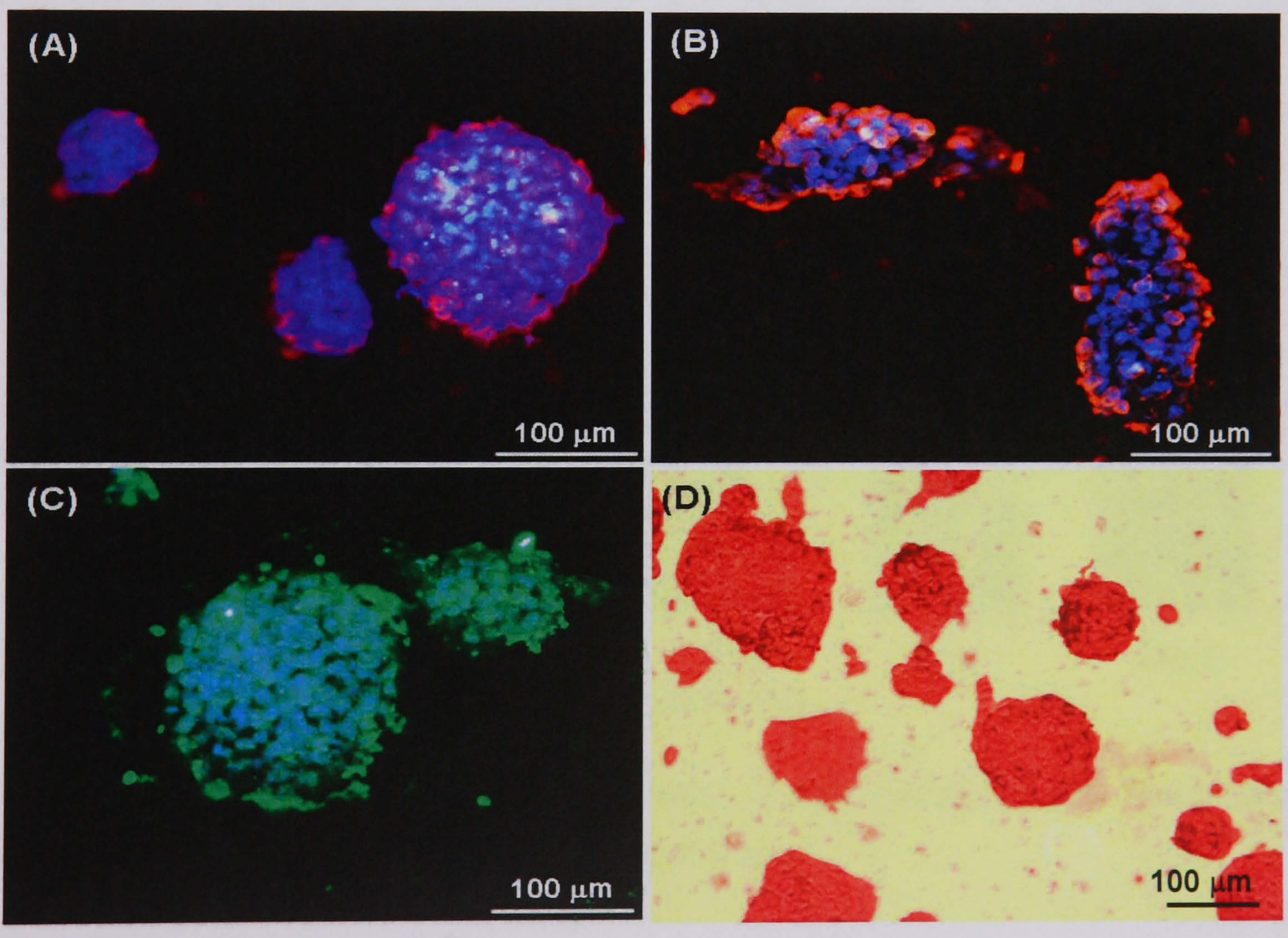


Figure 12. Assessment of undifferentiation marker expression of mESCs in 2D expansion. mESCs expressed Oct-4 (pink) (A), CD9 (Orange/red) (B), and E-cadherin (Green) (C) with DAPI counterstaining (nuclear staining, blue). mESCs expressed ALPase as well (D).

In addition, in order to establish the optimal conditions for mESC expansion, mESC growth was correlated to initial cell seeding density. As shown in Figure 13, high initial cell seeding density of approximately 30,000 cells/cm^2 showed rapid growth rate resulting in achieving 80% confluent cell density within 3 days of culture in comparison with medium (15,000 cells/cm^2) and low (7,500 cells/cm^2) cell densities. Consequently, the high cell seeding density was used in all further studies.

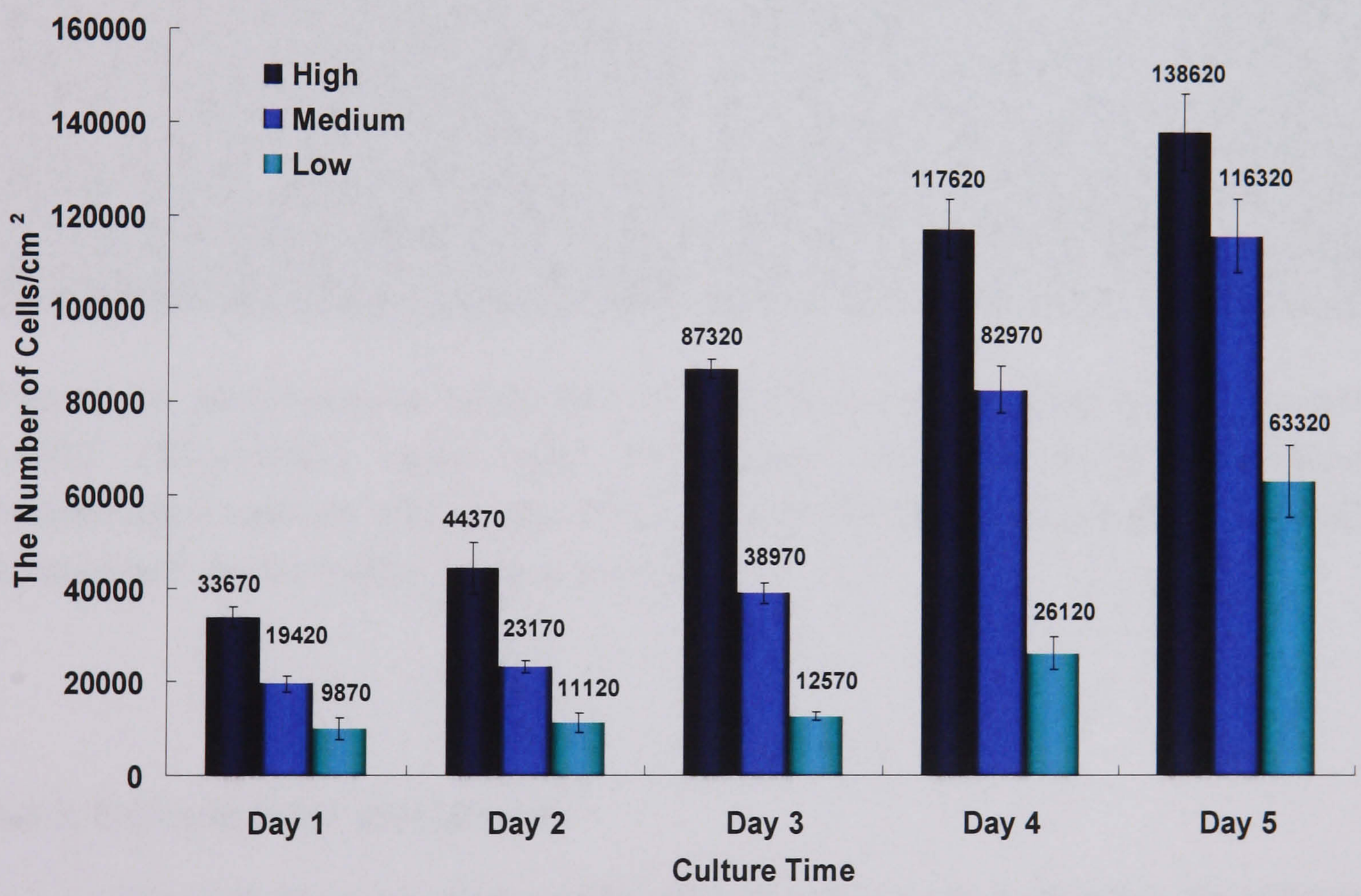


Figure 13. mESC growth kinetics as a function of cell seeding density. Each value represents the mean±SD cells/cm^2 in six samples.

3.4.2. mESCs morphology studies

The morphology of untreated mESCs (control group) was compared to

those treated with the HepG2 conditioned medium (experimental group). Control mESC cultures formed colonies with typical morphology of round multi-layers with tight phase bright boundaries. Individual cells were difficult to identify within the colonies of undifferentiated mESC (Figure 14A). In contrast, mESCs grown in conditioned medium exhibited a more flattened morphology with relatively larger nucleoli. Individual cells were clearly visible within the colonies (Figure 14B).

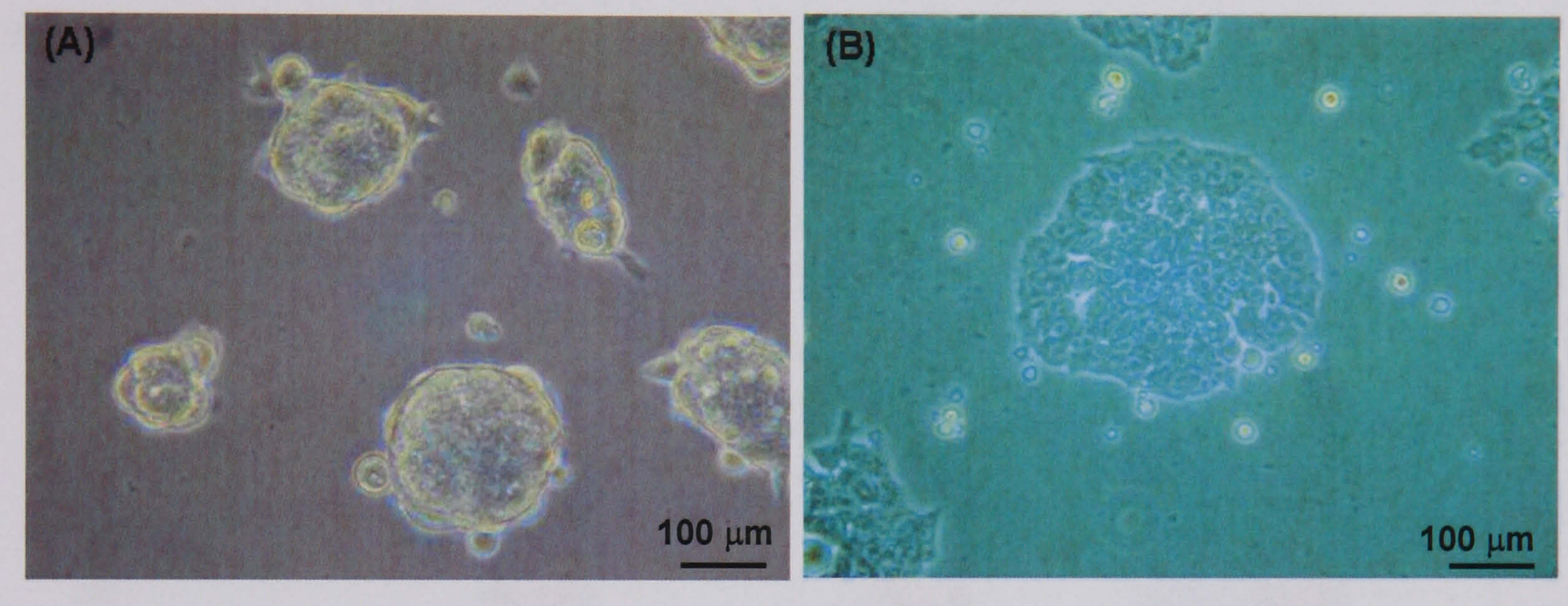
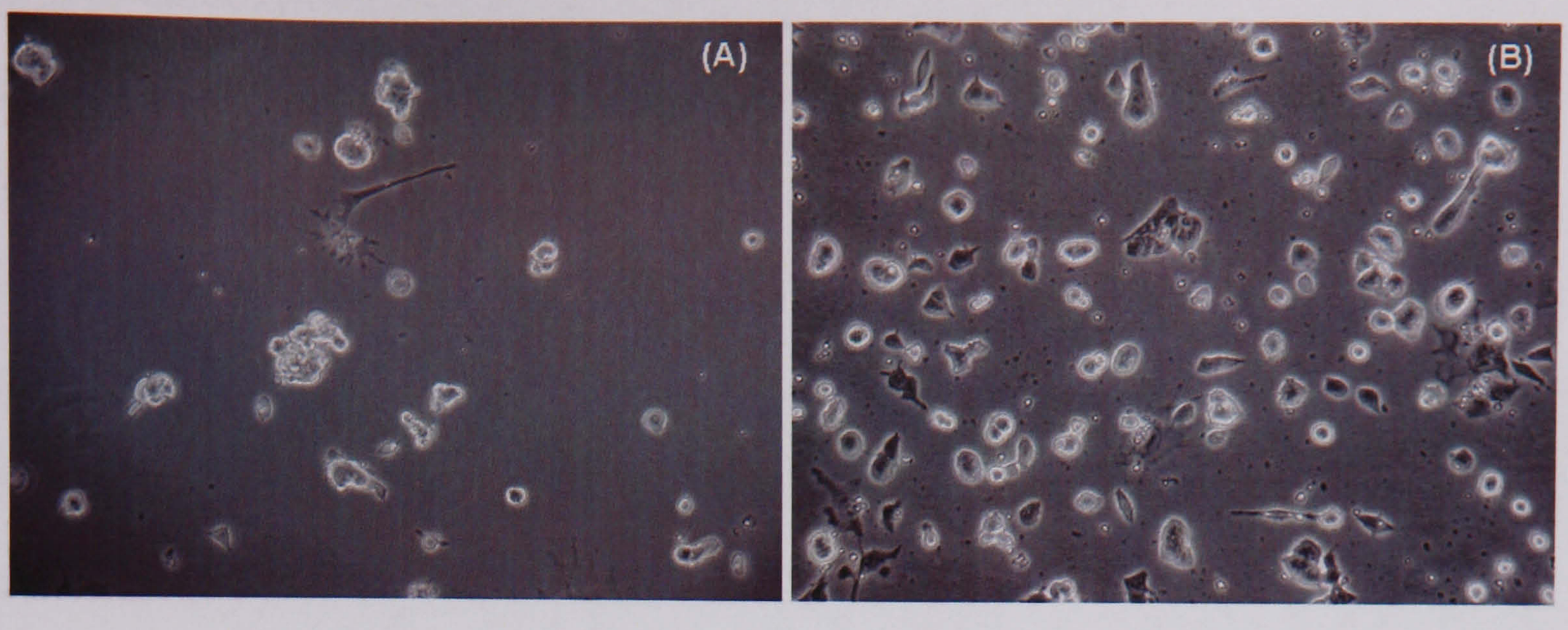


Figure 14. Morphological evaluation of mESCs and conditioned medium-treated mESC (CM-mESC) under light microscopy. (A) mESCs in conventional maintenance medium after 1 day of culture and (B) CM-mESCs in 50% of HepG2 conditioned medium after 1 day of culture

3.4.3. Cell adhesion and growth

The cell adhesion and proliferation capacity were evaluated. Specifically, adhesion was rapid - 67% of the cells adhered in 1 hr and 95% in 2 hrs ($P < 0.05$) – in the CM-mESC group as compared to the control mESC group where 10% of the cells adhered in 1 hr and 40% in 2 hrs (Figure 15). After 4 hrs the difference was less marked, with 95% of mESCs in CM adhering as compared with 80% of control mESCs.



(C)

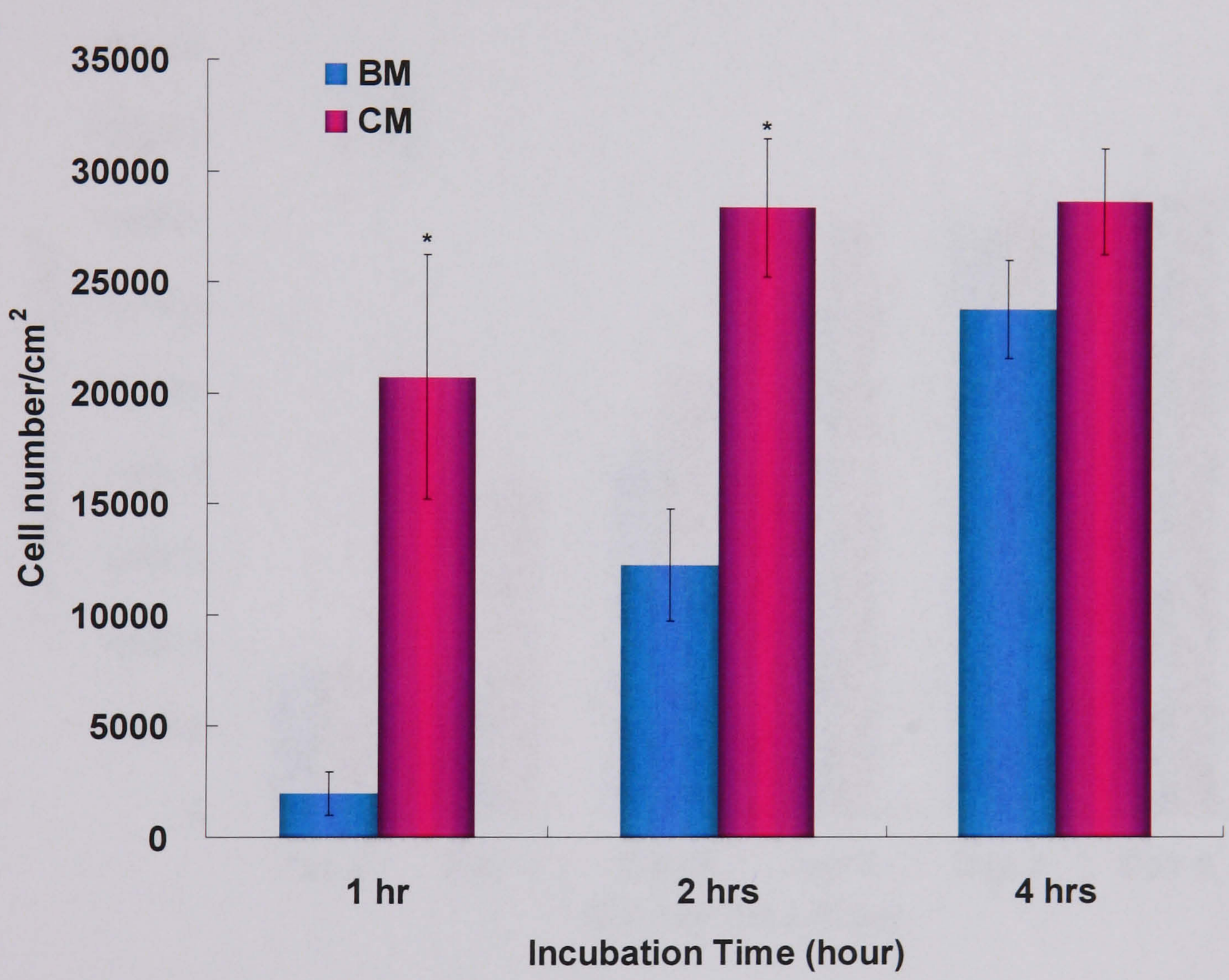


Figure 15. mESC adhesion in HepG2 conditioned medium (CM) and normal maintenance medium (BM). (A) mESC morphology in BM after 1hr of seeding. (B) mESC morphology in CM after 1hr of seeding. (C) Cell adhesion assay: each value represents the mean±SD cells/cm^2 in six samples. (*: significantly different compared to the control BM, $P<0.05$).

Similarly, cell proliferation, as determined by the 3-(4,5- dimethylthiazol-2-

yl)-5-(3-carboxymethoxyphenyl)-2-(4-sulfophenyl)-2H-tetrazolium; MTS) assay, [Ber S 2005] was more rapid in the CM-mESC group as compared with control mESCs early in the culture (days 1 and 2), as shown in Figure 16. Specifically, the cell proliferation rate of mESCs exposed to CM was almost two fold higher ($P < 0.05$) than that of the control mESCs at day 1 of culture. As culture time increased, no significant difference in the cell proliferation could be observed, and at day 5 both reached the same cell density.

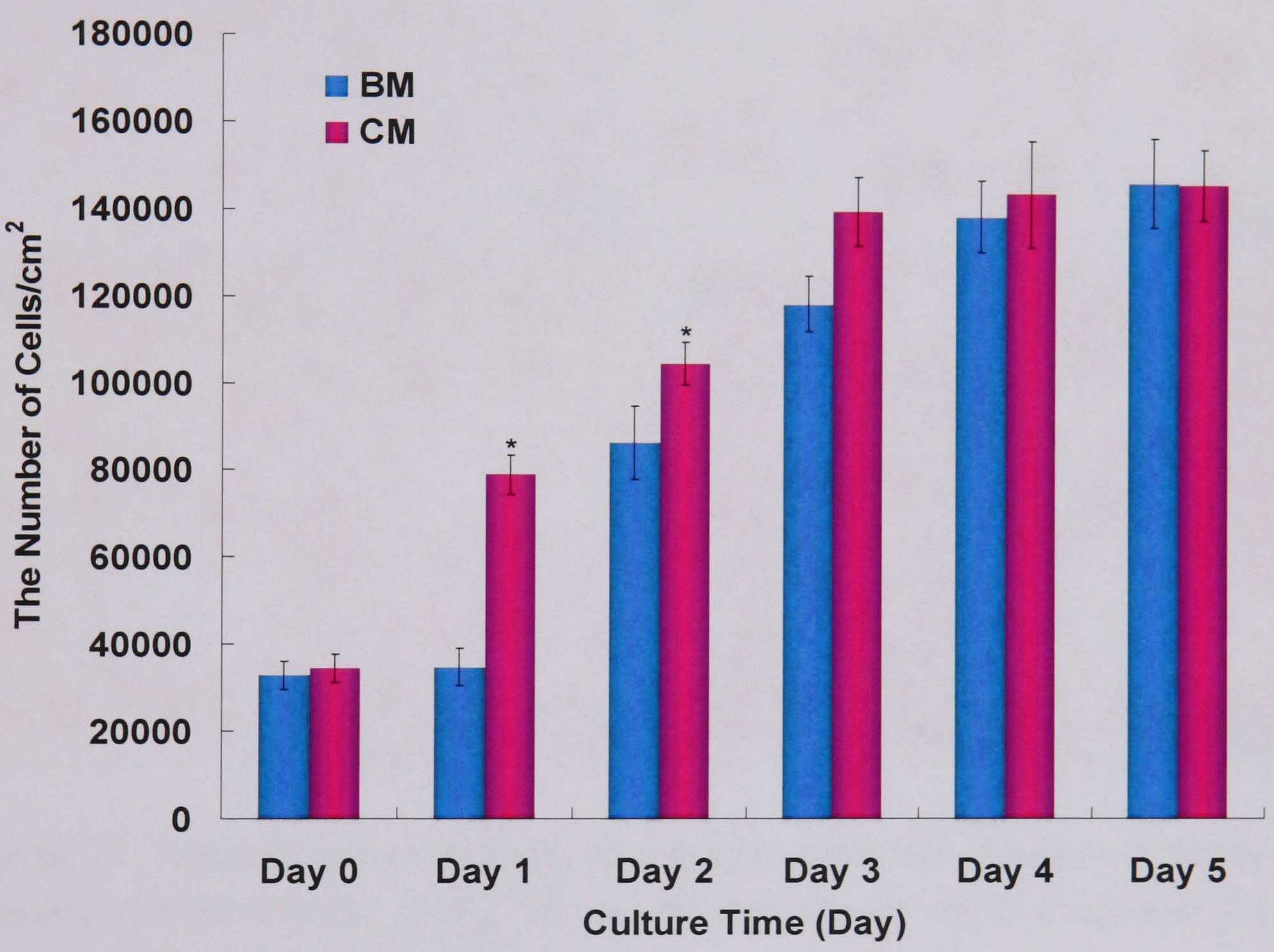


Figure 16. mESC proliferation in HepG2 conditioned medium (CM) and normal maintenance medium (BM). Each value represents the mean±SD cells/cm^2 in six samples. (*: significantly different compared to the control BM, $P < 0.05$).

3.4.4. ALPase expression

The undifferentiated/differentiated state of the embryonic stem cells is characterized by a high level of expression of alkaline phosphatase (ALPase), one of the classical markers of pluripotent ESCs [Thomson JA 1998]. Expression levels

of ALPase decrease following stem cell differentiation. As shown in Figure 17, mESCs expressed high ALPase activity whereas CM-mESCs showed relatively weak ALPase expression at day 3 of culture.

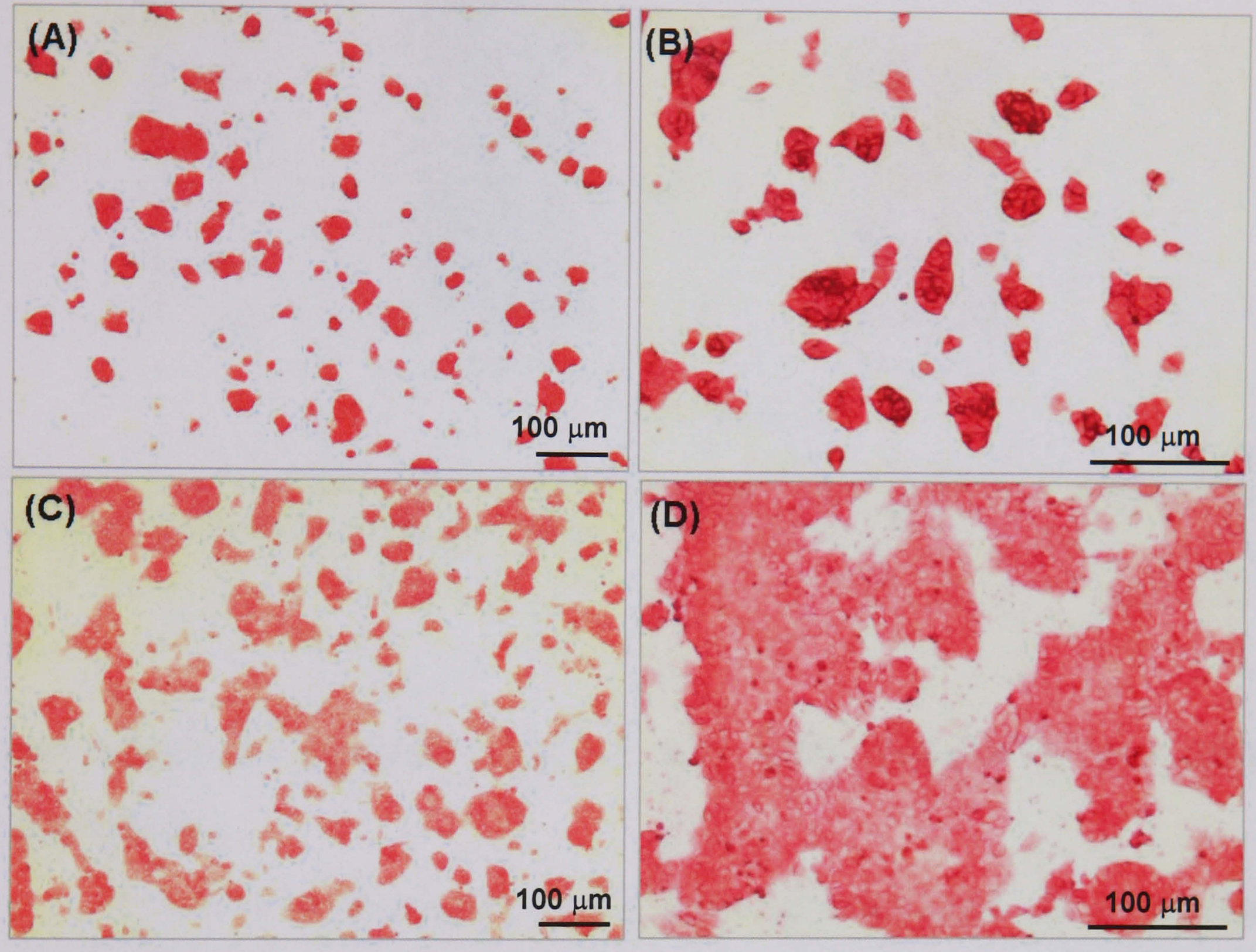


Figure 17. Assessment of ALPase Expression using the Alkaline Phosphatase Detection Kit (Chemicon, USA). (A) and (B): mESCs at day 3 of culture, (C) and (D): CM-mESCs at day 3 of culture.

The expression of ALPase was supported by the quantification of ALPase activity using the colorimetric assay. Consistent with expression, CM-mESCs showed relatively low level of ALPase activity in comparison with mESCs at day 3 of culture, indicating the early differentiation stage of CM-mESCs (Figure 18).

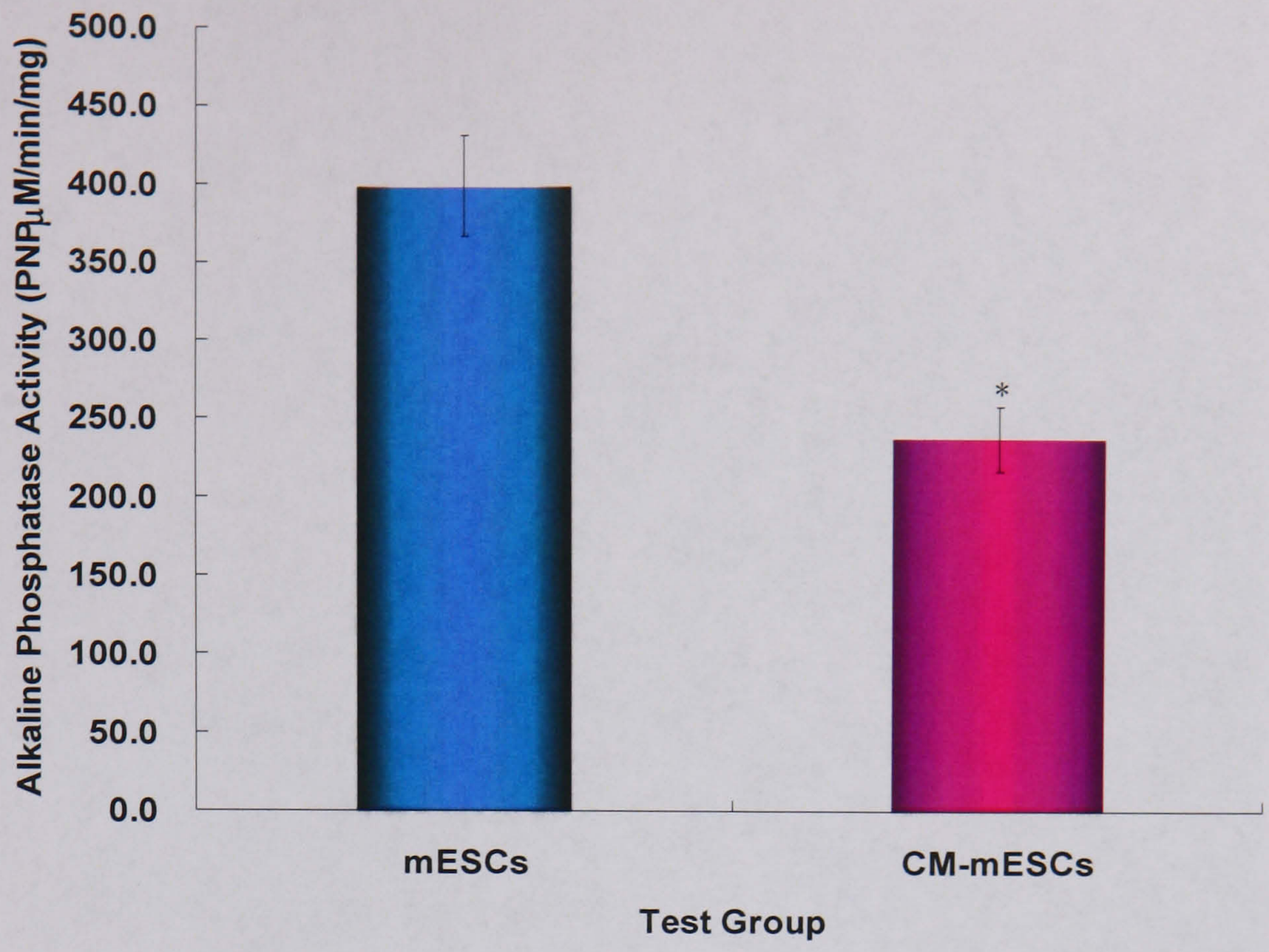


Figure 18. Colorimetric assay for assessing ALPase activity. (*: significantly different compared to mESCs, $P < 0.05$).

3.4.5. Molecular expression relating with ESCs pluripotency and early differentiation

To determine development stage of the mESCs treated with the HepG2 conditioned medium, immunostaining for undifferentiation and early differentiation cellular markers was performed (Figure 19). Control mESCs showed typical three dimensional colonies with strong expression of Oct-4 and E-cadherin at both days 1 and 3 culture, as well as Oct-4 transcription factor, which was localised in the nucleus. Similarly, CM-mESCs, after 1 day of culture, expressed Oct-4 and E-cadherin strongly, even though some of the cells displayed a relatively more flat and elongated morphology. However, after 3 days of culture, very few cells in the large CM-mESCs colonies expressed weak Oct-4 and E-cadherin, with most confluent CM-mESC colonies not expressing Oct-4 and E-cadherin.

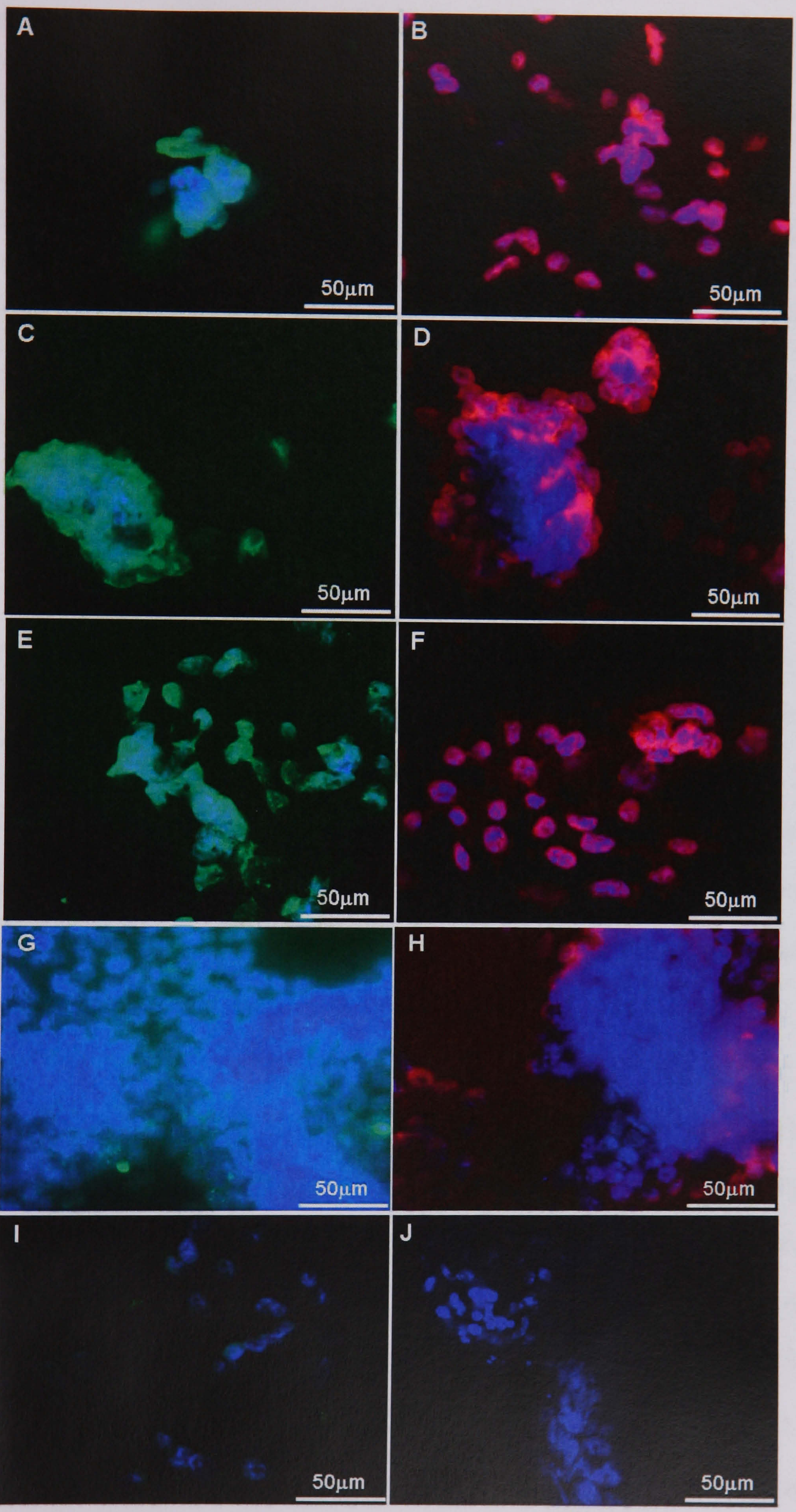

A
50μm
B
50μm
C
50μm
D
50μm
E
50μm
F
50μm
G
50μm
H
50μm
I
50μm
J
50μm

Figure 19. Immunostaining of mESCs and conditioned media treated mESCs (CM-mESC). (A) and (B) mESCs after 1 day of culture with the use of anti E-cadherin (Green) and anti Oct-4 (pink) antibodies and DAPI (nuclear staining, blue); X400 magnification. (C) and (D) mESCs after 3 days of culture with the use of anti E-cadherin (Green) and anti Oct-4 (pink) antibodies and DAPI (nuclear staining, blue); X400 magnification. (E) and (F) CM-mESCs after 1 day of culture with the use of anti E-cadherin (Green) and anti Oct-4 (pink) antibodies and DAPI (nuclear staining, blue); X400 magnification. (G) and (H) CM-mESCs after 3 days of culture with the use of anti E-cadherin (Green) and anti Oct-4 (pink) antibodies and DAPI (nuclear staining, blue); X 400 magnification. (I) and (J) Negative staining with the use of anti E-cadherin and Oct-4 antibodies and DAPI.

3.4.6. EB formation capacity

EB formation, where ESCs spontaneously differentiate into multi-lineage cells as tissue-like spheroids in suspension culture, is the most accepted practice in inducing ESC differentiation. Recently, it has been shown that EB formation is driven by cell to cell adhesion of undifferentiated ESCs through E-cadherin interactions [Dang SM 2004]. The EB formation capacity of mESCs and CM-mESCs was evaluated; their EB formation capacity could be influenced by different culture media and supplements (Figure 20A-F & A'-F'). Specifically, three different culture media were evaluated: DMEM containing 15% FBS, DMEM containing 15% FBS and 50 μg/ml ascorbic acid (same as that of α-MEM), and α-MEM containing 15% FBS. Based on morphology, the EB formation capacity of mESCs was not influenced by the different culture conditions with the EBs displaying spherical shape with smooth surfaces. However, CM-mESCs demonstrated different EB formation capabilities dependent on the culture media used. Specifically, CM-mESCs could not form EBs efficiently in the DMEM and DMEM containing ascorbic acid media. In contrast, in α-MEM, CM-mESCs displayed high EB formation capacity with EBs assuming spherical shape, albeit

with a relatively rough surface. Following 5 days of EB formation, agglomeration was observed by the mESC-derived EBs resulting in larger EBs with either spherical or rod shapes in all culture media. However, agglomeration was not prevalent in EBs generated by the CM-mESCs derived EB formation; only a few EB agglomerates were detected in α-MEM and EB agglomeration was hardly detected in DMEM and DMEM containing ascorbic acid.

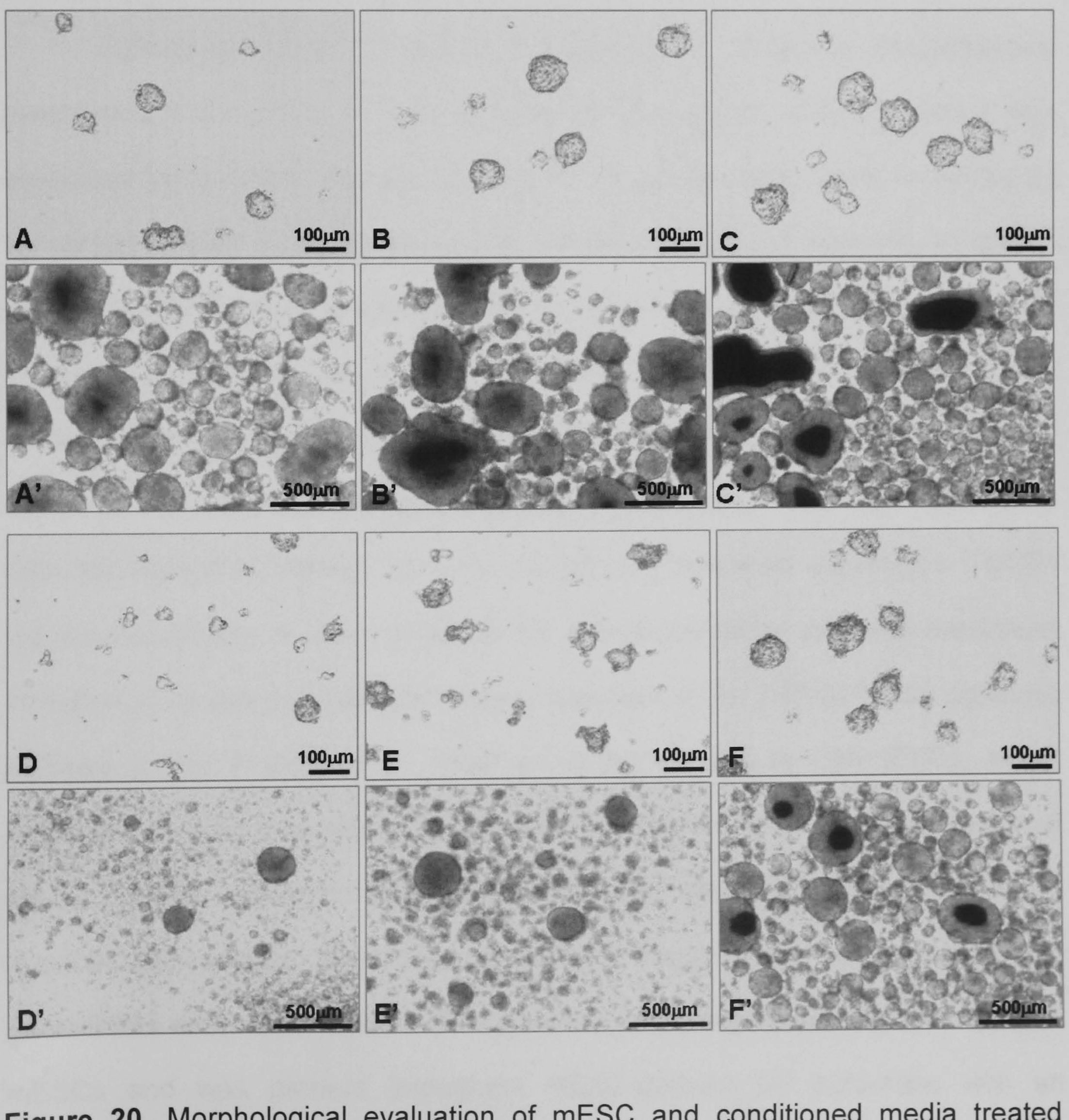


Figure 20. Morphological evaluation of mESC and conditioned media treated mESC (CM-mESC) derived EBs under light microscope. (A) and (A') mESC derived EBs for 1 day and for 5 days in DMDM containing 15% FBS; (B) and (B')

mESC derived EBs for 1 day and 5 days in DMDM containing 50 μg/ml ascorbic acid and 15% FBS; (C) and (C') mESC derived EBs for 1 day and 5 days in α-MEM containing and 15% FBS. (D) and (D') CM-mESC derived EBs for 1 day and for 5 days in DMDM containing 15% FBS; (E) and (E') CM-mESC derived EBs for 1 day and 5 days in DMDM containing 50 μg/ml ascorbic acid and 15% FBS; (F) and (F') CM-mESC derived EBs for 1 day and 5 days in α-MEM containing 15% FBS. (A, B, C, D, E, F) X100 magnification under light microscope. (A', B', C', D', E', F') X40 magnification under light microscope.

3.4.7. Gene expression

Differential gene expression, indicative of primitive streak/nascent mesoderm of CM-ESCs as well as different time points of EB formation was evaluated by RT-PCR analysis (Figure 21). A much higher level of brachyury expression, which is restricted to the primitive streak and nascent mesoderm [Wilkinson DG 1990], was detected from day 0 to day 3 of CM-mESC-derived EBs; thereafter it gradually decreased. In contrast, brachyury expression in control mESCs was not detected and mESC-derived EBs expressed brachyury temporally from day 1 to day 5 with a distinct increase at day 3 yet at relatively lower levels than the CM-mESC-derived EBs. Consistent with brachyury expression, TDGF1 (cripto) expression, a gene essential for anterior-posterior axis and mesoderm formation in mouse embryos and a key component of the TGF-β1/Nodal signalling pathway [Dono R 1993], was observed at high levels in CM-mESCs, which remained constant throughout EB formation. On the contrary, cripto expression in control mESCs was hardly detected and increased gradually from day 3 to day 5 in mESC-derived EBs. Nodal was continuously transcribed at high levels in both CM-mESCs and mESC-derived EBs, whereas it was expressed at lower levels in mESCs and was present throughout mESC-derived EB cultivation with an apparent high expression at day 3. Goosecoid, a gene that is expressed as an

immediate early response to mesoderm induction [Niehrs C 1994], was present in CM-mESCs though not in mESCs. Goosecoid expression was observed in EBs derived from both mESCs and CM-mESCs.

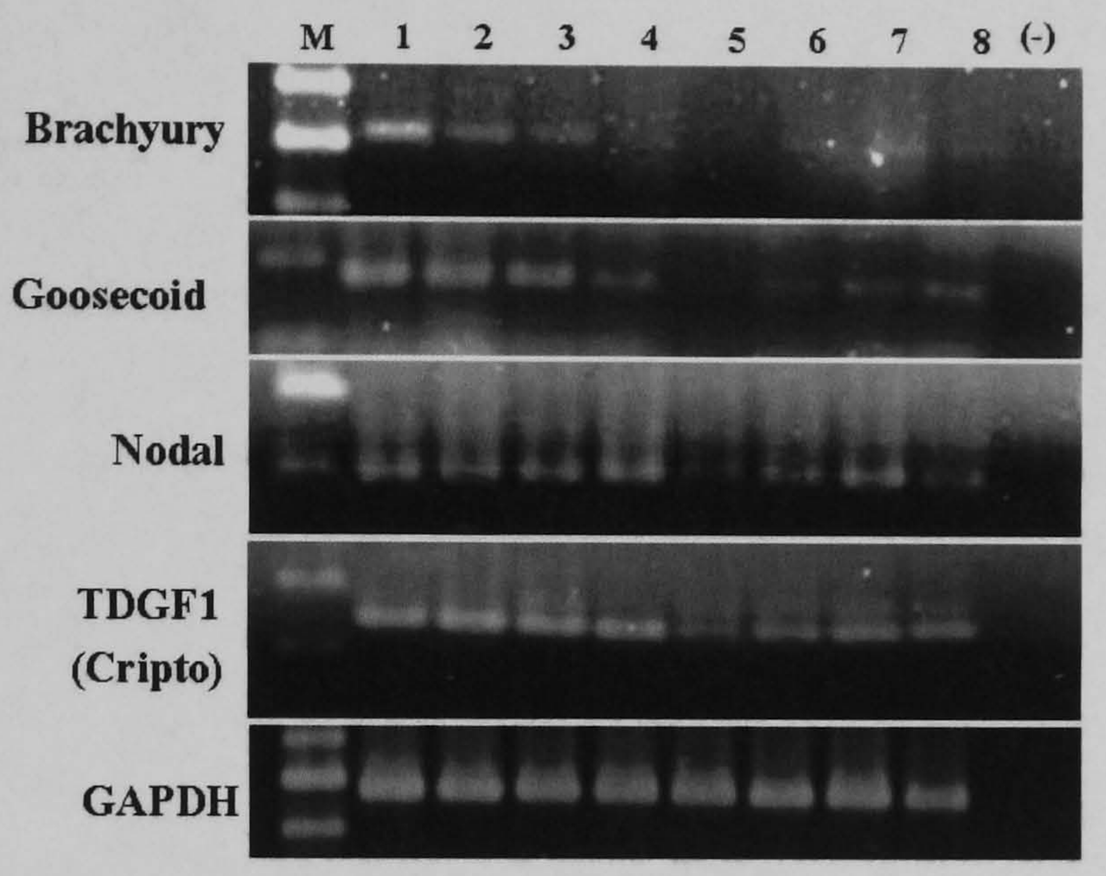


Figure 21. Molecular analysis (RT-PCR). Lane M: EZ Load 100 bp Molecular Ruler. Lane 1: CM-mESC. Lane 2: CM-mESC derived EB for 1 day (CM-mESC-EB1). Lane 3: CM-mESC derived EB for 3 days (CM-mESC-EB3). Lane 4: CM-mESC derived EB for 5 days (CM-mESC-EB5), Lane 5: mESC, Lane 6: mESC derived EB for 1 day (EB1), Lane 7: mESC derived EB for 3 days (EB3), Lane 8: mESC derived EB for 5 days (EB5).

3.4.8. Reversibility of early differentiation

The results thus far suggest that the CM-mESCs represent a cell population with characteristics similar to primitive streak/nascent mesoderm. Furthermore, when CM-mESCs were cultured in mESC maintenance medium, a reversal in morphology to undifferentiated mESCs was observed (Figure 22), as evidenced by the distinct colony morphology of round multilayer with tight phase bright boundaries, which is considered as typical morphology of undifferentiated mESCs with variations in their colony size.

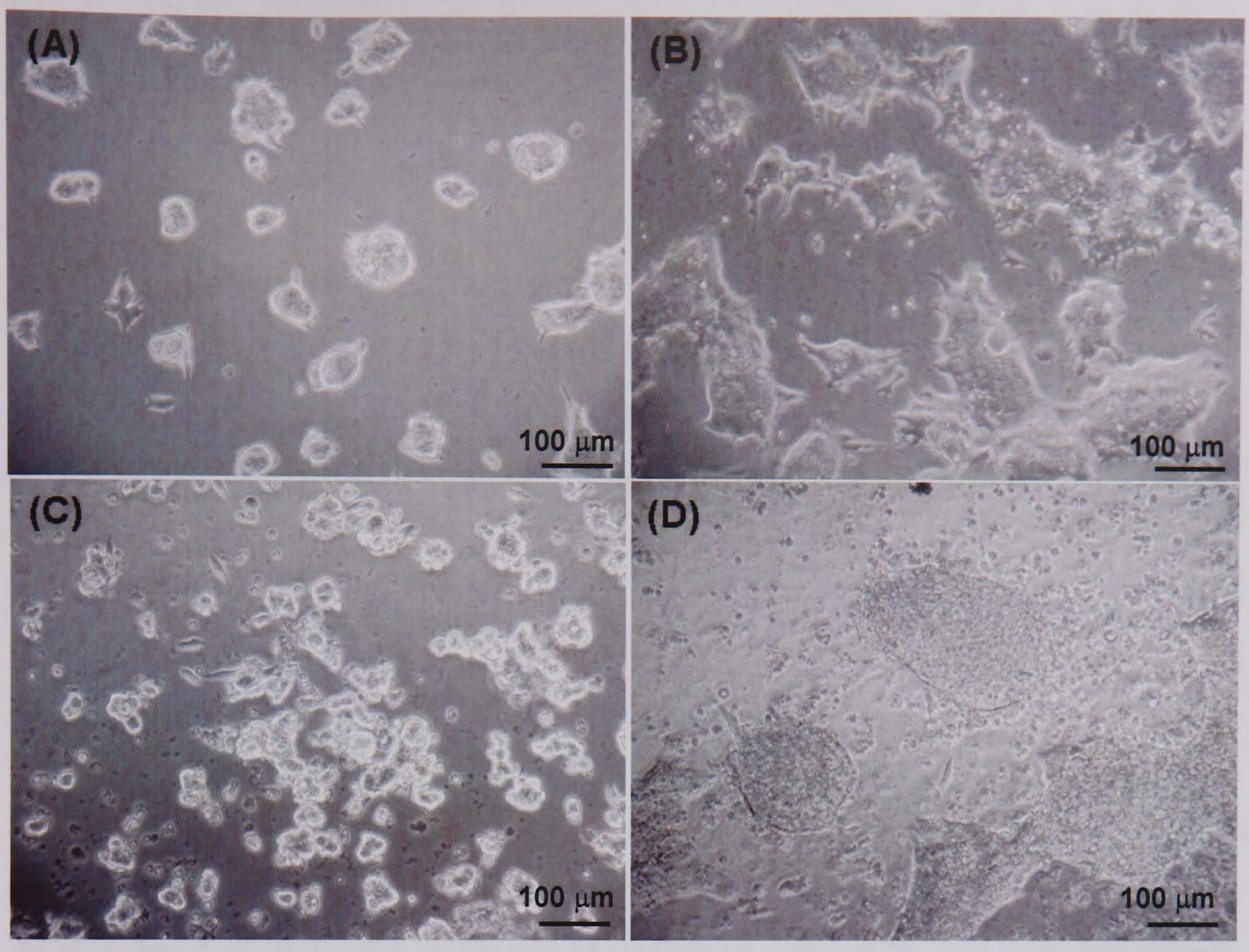
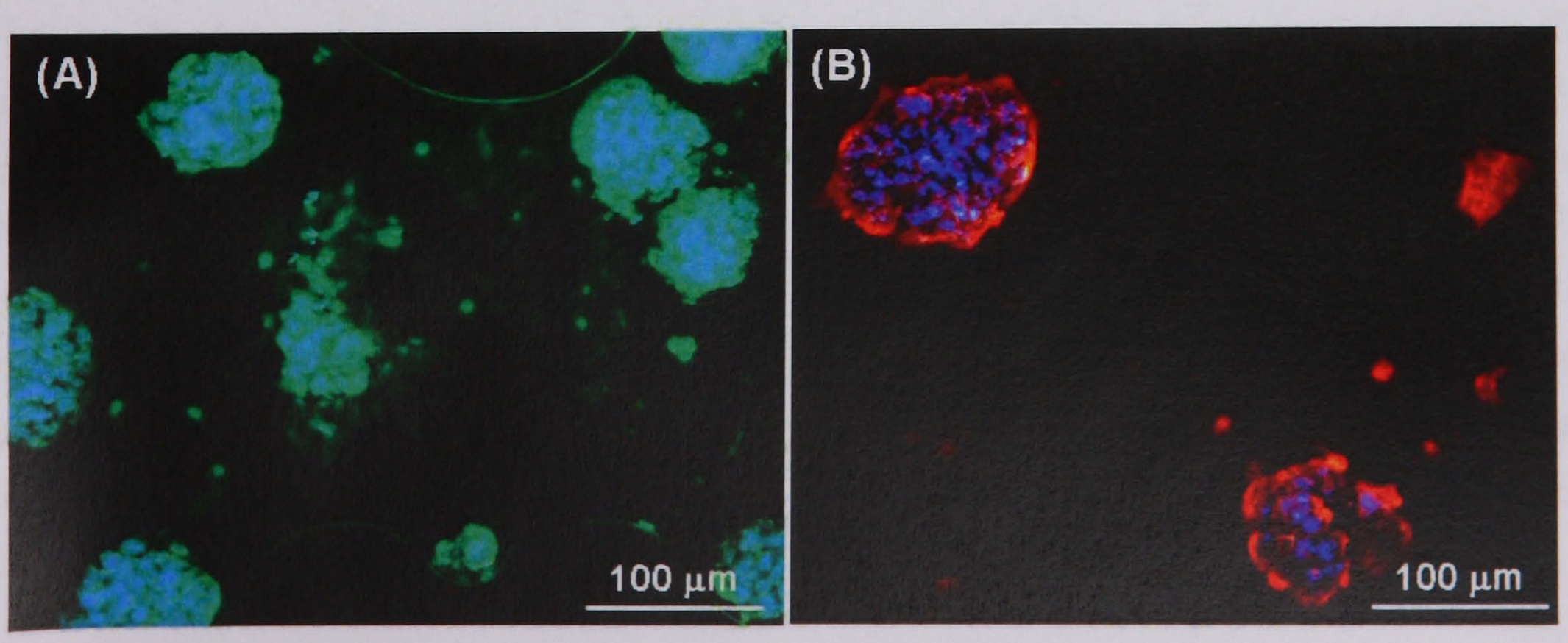


Figure 22. Morphological observation of mESCs in various culture conditions: (A) normal mESC (B) CM-mESC: HepG2 conditioned medium treated mESC. (C) CM-mESC-rr: mESCs were replated and cultured in mESC maintenance medium following HepG2 conditioned media treatment for 3 days. (D) CM-mESC-rd: mESCs were cultured in mESC maintenance media following HepG2 conditioned media treatment for 3 days.



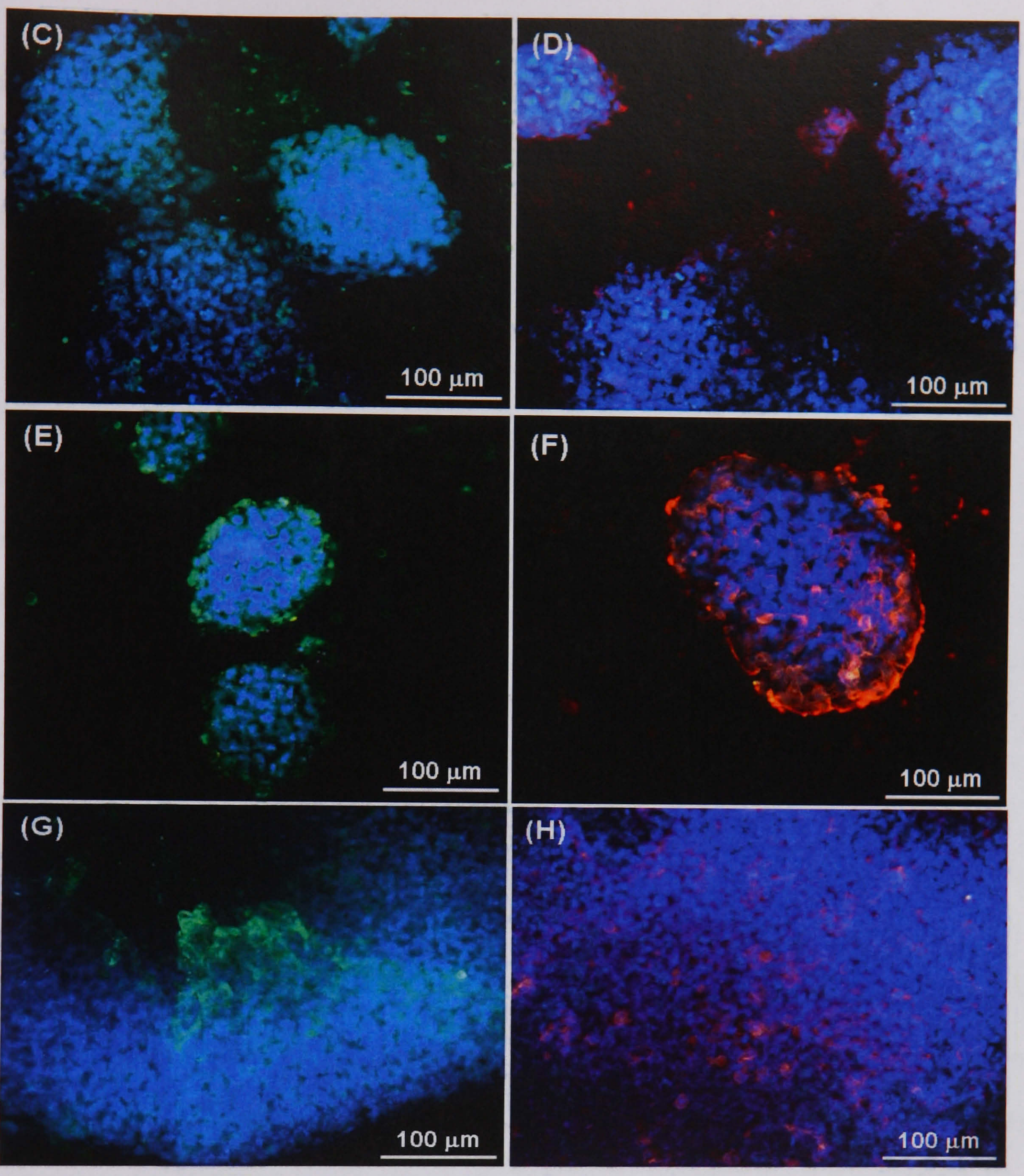


Figure 23. Immunostaining: (A) and (B): normal mESCs at day 3 expressing E-cadherin (Green), CD9 (pink), and DAPI (nuclear staining, blue). (C) and (D): CM-mESCs: HepG2 conditioned medium-treated mESC after 3 days of culture expressing E-cadherin (Green), CD9 (pink), and DAPI (nuclear staining, blue). (E) and (F): CM-mESC-rr: CM-mESCs were replated and cultured in mESC maintenance medium at day 3 expressing E-cadherin (Green), CD9 (pink), and DAPI (nuclear staining, blue). (G) and (H): CM-mESC-rd: CM-mESCs were cultured in mESC maintenance medium without replating at day 3 expressing E-cadherin (Green), CD9 (pink), and DAPI (nuclear staining, blue).

This reversible differentiation or dedifferentiation was further characterised by the expression of the E-cadherin and CD9 pluripotency markers. Consistent with previous data, mESCs showed well developed CD9 and E-cadherin molecular expression with typical colonies at day 3 (Figure 23 A&B). In contrast, CM-mESCs did not express expression (or faintly expressed) E-cadherin and CD9 at day 3 of culture (Figure 23 C&D). However, when the CM-mESCs were replated and cultured in mESC maintenance medium, the strong expression of CD9 and E-cadherin was detected, similar to the undifferentiated mESCs (Figure 23 E&F). However, when CM-mESCs were cultured in mESC maintenance medium without replating, the partial expression of CD9 and E-cadherin was detected in the colonies (Figure 23 G&H).

3.5. Discussion

mESCs are permanent cell lines that can be maintained indefinitely in the undifferentiated state in the presence of LIF while remaining pluripotent. Upon withdrawal of LIF and/or feeder support, mESCs start to differentiate spontaneously [Eldor JI 2000]. This unique property of ESCs has allowed studying differentiation in early development, understanding the underlying molecular mechanisms that control cell growth and differentiation *in vitro,* and for further applications to regenerative medicine and tissue engineering. However, standardisation is critical and it is essential to maintain the undifferentiation stage and self-renewal activity of ESCs while maintaining pluripotency and to develop defined culture conditions for specific differentiation into homogenous populations. Whether the ESCs undergo self-renewal or differentiation is likely to depend on

the state of the cells - stemness is maintained by suppressing lineage commitment. Assessment of the conserved, self-renewal-related transcription factors, such as Oct4, CD9, E-cadherin and ALPase is important in evaluating the quality of the starting mESC material. Our results illustrated that undifferentiated mESCs highly expressed Oct4, CD 9 and E-cadherin, and ALPase with typical three dimensional colony formation, which is in agreement with literature data [Niwa H 2000, Oka M 2002, Bloor DJ 2002, Dang SM 2004]. Hence, our results confirm that mESCs in expansion remained undifferentiated without losing their pluripotency.

Currently, the most accepted method to induce early differentiation is EB formation, since *in vitro* EB formation resembles early differentiation during embryogenesis [Leahy A 1999]. Specifically, osteogenic differentiation of mESCs has been demonstrated following spontaneously formation of EBs [Buttery LD 2001]. Recently, an alternative method of inducing mesoderm progenitors has been proposed that utilises conditioned media [Rathjen J 1999, Lake J 2003, Calhoun JD 2004, Mummery C 2000]. Several examples of the successful application of conditioned media for directing ESC differentiation exist in the literature. For instance, the use of conditioned medium from the visceral endoderm-like cell line, END-2, resulted in enhanced cardiogenic differentiation, when the ESCs were cultured in the conditioned medium and allowed to form EBs [Mummery C 2000]. In another approach, Rathjen and colleagues induced early differentiation of mESCs into an apparently homogenous cell population with a high capacity of forming mesoderm in EBS by treatment with conditioned medium derived from human hepatocellular carcinoma cell line, HepG2, which resulted in an increase in the number of beating colonies [Rathjen J 1999]. Rathjen's results showed that the HepG2 conditioned medium-treated mESCs can generate mesoderm in EBs more rapidly, almost two or three times faster than normal

mESC-derived EBs [Rathjen J 1999], which is agreement with our results. Our results on mesoderm stimulation were in agreement with Rathjen's. However, the full characterisation of the early differentiated cell population generated using the HepG2 condition medium, whether it is primitive ectoderm- or primitive streak/nascent mesoderm-like cells [Rathjen J 1999, Calhoun JD], is still pending.

Upon treatment of mESCs with HepG2 conditioned medium, enhanced cell adhesion and proliferation activity along with a flattened morphology and decreased expression of Oct4, E-cadherin, and ALPase were observed in comparison with untreated mESCs. During ESC colony formation, cell-cell adhesion via E-cadherin plays a key role in undifferentiated ESC colony formation [Bloor DJ 2002, Dang SM 2004]. Furthermore, E-cadherin expression by ESCs is down-regulated as the cells differentiate [Dang SM 2004]. These reports are in agreement with our results of the CM-mESCs with their flattened morphology and down-regulated E-cadherin, suggesting that certain factors produced by the HepG2 cell line influence cell adhesion and affect cell differentiation. Furthermore, the EB formation capacity of the CM-ESCs was also influenced, which can be attributed to the down-regulation of E-cadherin, plays a key role in cell aggregation during EB formation and differentiation [Dang SM 2004]. This also is in agreement with the fact that reduced initial endodermal layer formation in EBs gives rise to EB disorganization, since it has been demonstrated that disruption of endoderm formation leads to EB disorganization. According to Rathjen's research, HepG2 conditioned medium-treated ESCs have lost ability to form visceral endoderm during EB formation and are just restricted to form parietal endoderm [Rathjen J 1999]. However, these finding require further investigation.

Visceral endoderm plays a critical role in establishing anterior-posterior polarity in the mouse embryo and the primitive streak followed by mesoderm

formation [Lu CC 2001]. Recently, cell lines, with visceral endoderm functionally, have been used to induce mesodermal lineage differentiation [Rathjen J 1999, Lake J 2003, Mummery C 2000]. However, full characterisation of the cell population produced by treatment with the conditioned medium remains unresolved with two different pathways of early ESC differentiation being suggested. Rathjen's group showed that conditioned medium induced FGF 5 gene up-regulation and Rex-1 gene down-regulation, similar to the gene expression pattern of primitive ectoderm, while retaining the marker of pluripotency, Oct-4 [Rathjen J 1999]. In contrast, Calhoun presented evidence that treatment of hESCs with HepG2-conditioned medium resulted in up-regulation of TDGF1 (cripto), a gene essential for primitive streak and mesoderm formation in mouse embryos and a key component of the TGF-β1/Nodal signalling pathway. Consequently, their work suggested differentiation into primitive streak stage cells as further evidenced by DNA micro-array and real time RT-PCR analyses. Our results are in agreement with the primitive streak/nascent mesoderm differentiation pathway due to the up-regulation of Nodal and Cripto expression, which are key genes regulating primitive streak or nascent mesoderm formation [Calhoun JD]. The brachyury and goosecoid expression marked up-regulation observed further supports the primitive streak/nascent mesoderm pathway since during early development brachyury expression is restricted to the primitive streak and nascent mesoderm in the region that will define the posterior part of the embryo [Herrmann BG 1991]. It has been well documented that the early primitive streak is the origin of the migrating cells that form the extraembryonic mesoderm, where the epithelium-mesenchyme transition is temporally associated with the up-regulation of brachyury [Kispert A 1994]. In addition, mesenchyme differentiation is marked by the down-regulation of Oct3/4 [Flechon JE 2004] and expression of E-cadherin

[Burdsal CA 1993], which is in agreement with our results showing the temporal up-regulation of brachyury, goosecoid, nodal, and cripto expression and partial down-regulation of Oct4 and E-cadherin expression.

The differentiation of the undifferentiated mESCs into primitive streak/nascent mesoderm cell population following treatment with the HepG2 conditioned medium was reversible when the CM-mESCs were replated and cultured in ESC maintenance medium. These observations are supported by Rathjen's work demonstrating reversible differentiation of early differentiated mESCs into undifferentiated mESCs [Rathjen J 1999]. Furthermore, others have reported that reverse pathway from early mesoderm-specified progenitors to undifferentiated ESCs is regulated by Nanog expression [Suzuki A, 2006]. However, to date, the precise mechanism has not been fully elucidated.

3.6. Conclusion

We have demonstrated that the conditioned medium from the human hepatocarcinoma cell line HepG2 induced transition of mESCs a specific cell type with primitive streak/nascent mesoderm profile resulting in enhanced mesoderm formation during EB formation. Hence, this strategy for generating a specific cell population with high capacity of mesoderm formation could prove useful in skeletal tissue engineering application due to the potent cell source it produces. However, from a clinical application perspective, it requires the identification of the active factors within the conditioned medium and the formulation of a defined medium.

CHAPER IV

IN VITRO OSTEOGENIC AND CHONDROGENIC DIFFERENTIATION OF MURINE EMBRYONIC STEM CELLS USING EB FORMATION

4.1. Introduction: Current Approaches for the *In Vitro* EB-Mediated Osteogenic and Chondrogenic Differentiation of Embryonic Stem Cells

The vast majority of the current methodologies for *in vitro* osteogenic and chondrogenic differentiation rely on EB formation, which results in the spontaneous formation of the precursor germ layers as a prerequisite for terminal differentiation towards the osteogenic and chondrogenic lineages (Figure 24).

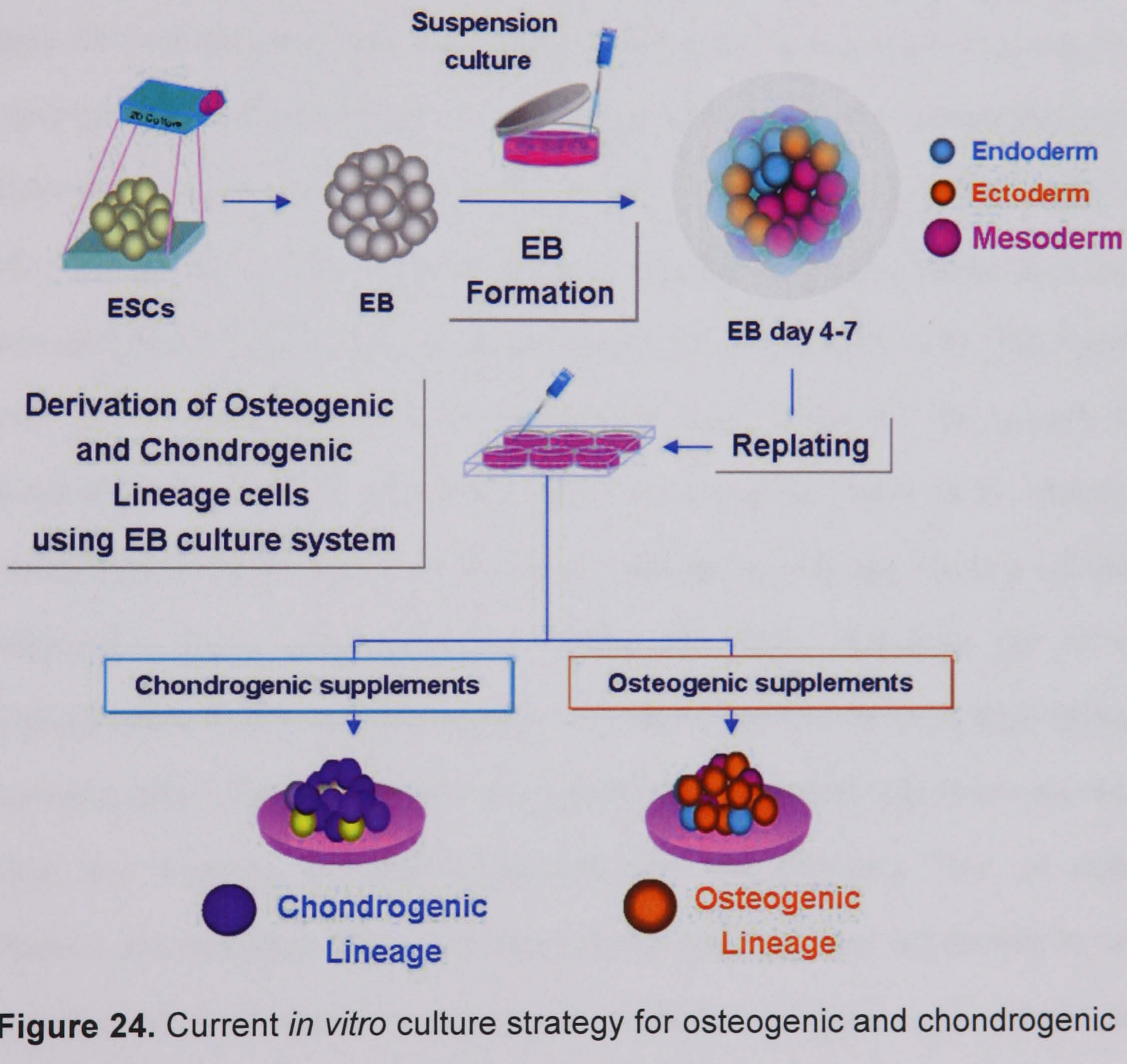


Figure 24. Current *in vitro* culture strategy for osteogenic and chondrogenic differentiation through EB formation.

A number of molecules have been applied in *in vitro* skeletal lineage differentiation to control mesodermal cell fates towards the terminal differentiation of ESCs into the desired specific cell lineage [Tanaka H 2004, Buttery LD 2001,

Mummery C 2002, Kawaguchi J 2005]. However, despite the progress made and the increased understanding of the biological mechanisms of growth factors or other supplements on ESC differentiation, the challenge remains in developing scalable and clinically suitable processes for the therapeutic application of ESCs in skeletal tissue engineering - mainly due to the much higher degree of plasticity possessed by ESCs compared with adult stem cells.

Currently, the vast majority of protocols for *in vitro* osteogenesis of ESCs employ EB formation for around 5 days in suspension followed by replating of the EB derived cells onto tissue culture dishes and differentiation to osteoblasts by the addition of osteogenic supplements [Kawaguchi J 2005, Woll NL 2006, Bielby RC 2005]. Specifically, it has been shown that addition of supplements such as β-glycerophosphate, ascorbic acid, dexamethasone, retinoic acid, and 1,25-hydroxy vitamin D3, factors that have all previously been used for the growth and differentiation of primary osteoblasts and mesenchymal stem cells, results in increased differentiation of ESCs along the osteogenic pathway [Buttery LD 2001, Kawaguchi J 2005, Woll NL 2006, Bielby RC 2005]. Similarly, for *in vitro* chondrogenesis, ESCs are allowed to form EBs for approximately 5 days followed by terminal differentiation into chondrocytes in three different culture environments through the addition of various chondrogenic supplements. One of culture methods is micro mass culture technique, which requires high cell density in order to form the cell condensation necessary for initial chondrogenesis [Tanaka H 2004, Nakayama N 2003]. Another technique is the pellet culture method, where cell aggregation for cell condensation is achieved by placement in conical tubes [Nakayama N 2003]. The final method is to plate whole EBs in tissue culture plates (EB plating method) [Kawaguchi J 2005, Kramer J 2005] and induce chondrogenesis by replacing the EB formation medium with chondrogenic media.

The chondrogenic supplements most commonly employed include BMP-2 and BMP-4 [Kramer J 2000], TGF-β3 [Kawaguchi J 2005], and dexamethasone [Tanaka H 2004]. Specifically, it has been reported that BMP-2 and BMP-4 promote chondrogenic differentiation using the direct EB plating culture method when added during day 3–5 of EB differentiation [Kramer J 2000]. Others have shown that retinoic acid treatment of EBs (to primarily induce mesoderm formation) followed by addition of TGF-β3 was sufficient to induce chondrogenesis from ESCs [Kawaguchi J 2005]. Furthermore, macroscopic cartilage formation has been demonstrated from EB cultures derived from fluorescence activated cell sorting (FACS) sorted-mesodermal progenitor cells by supplying a cocktail of IGF-I, TGF-β3, BMP-4 and platelet derived growth factor-BB (PDGF-BB) [Nakayama N 2003].

Therefore, for *in vitro* osteogenesis and chondrogenesis, the majority of approaches utilize the EB culture system where undifferentiated ESCs are allowed to form EBs for approximately 5 days followed by terminal osteogenic and chondrogenic differentiation using various supplements. However, EB based culture methods suffer certain disadvantages, mainly because controlling the spontaneous differentiation during EB formation is difficult – the precise mechanisms have not yet been identified – resulting in limited intact mesoderm in EBs and, consequently, a low yield for terminal differentiation. Furthermore, once mesoderm is formed, osteogenic and chondrogenic differentiation is in competition (or possibly even suppressed) by spontaneous cardiomyocyte differentiation. Hence, the need for novel methods that control and enhance osteogenic and chondrogenic differentiation more efficiently is enormous.

4.2. Objectives

The focus of this study was the investigation and development of an *in vitro* protocol for controlling and enhancing osteogenic and chondrogenic differentiation from mESC-derived primitive streak/nascent mesoderm-like cells by modulating the culture conditions and process, specifically the EB formation time.

4.3. Experimental Plan

Previously, we have demonstrated that HepG2 conditioned medium induced early differentiation of mESCs to a specific cell type with a gene expression similar to primitive streak/nascent mesoderm transient-stage cells, which showed an elevated expression of primitive streak/nascent mesoderm marker. Herein, we address whether the mESC-derived primitive streak/nascent mesoderm stage cells are also capable of efficiently differentiating into the osteogenic lineages. Specifically, the dissociated CM-mESCs derived-EB cells from different EB formation time points (day 1, 3 and 5) were subjected to osteogenic or chondrogenic supplements such as β-glycerophosphate, ascorbic acid and dexamethasone (osteogenic) or ascorbic acid, dexamethasone and TGFβ1 (chondrogenic). As the control group, the dissociated untreated ESC derived-EB cells day 5 of EB formation were used. Since during osteogenic and chondrogenic induction, spontaneous cardiogenic differentiation of mESCs can be detected unexpectedly with beating colonies present, spontaneous cardiogenic differentiation was also evaluated in this study. Therefore, cardiogenic/osteogenic/chondrogenic differentiation was investigated using

beating colony formation assay, bone nodule formation assay, cartilage nodule formation assay, immunocytochemical characterization, RT-PCR, expression of specific ECM proteins, and lineage specific enzyme activity evaluation, as described in CHAPTER II. In brief, the overall experimental plan is illustrated in Figure 25.

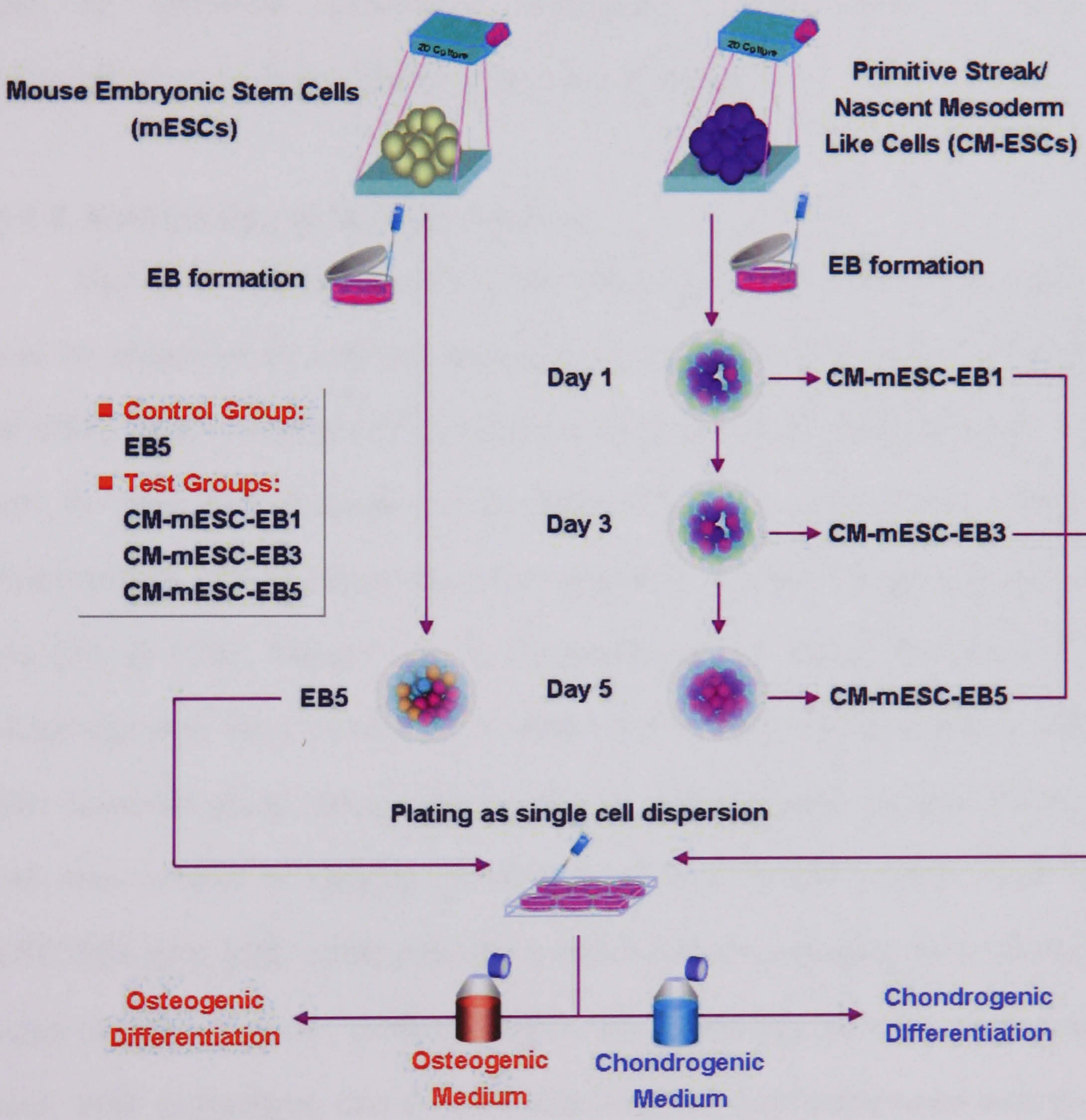


Figure 25. Schematic diagram of experimental process for EB-mediated osteogenic and chondrogenic differentiation of mESCs

4.4. Results

4.4.1. *In vitro* EB-mediated cardiogenic differentiation

The differentiation and maturation of mESC-derived cardiomyocytes as influenced by the use of HepG2 conditioned medium and EB formation time in order to suppress selectively cardiogenic differentiation in favour of osteogenic/chondrogenic differentiation was evaluated.

4.4.1.1. Morphology of beating colonies

During osteogenic/chondrogenic differentiation of mESCs, beating colonies could be observed in both the experimental and control groups (CM-mESC-EB5 and EB5), which confirmed the spontaneous cardiogenic differentiation of mESCs even in specified osteogenic/chondrogenic culture conditions. Spontaneous cardiomyocyte differentiation has been observed in both human and murine ESC lines [Xu C 2002, Kehat I 2002, Doevendans PA 2000, Boheler KR 2002]. Cardiomyocytes were readily identifiable due to their spontaneous contractions within days following plating. With continued differentiation (longer EB formation time), the number of beating foci increased and certain groups, such as CM-mESC-EB5 and EB5, could possibly contain localized beating cells. During early stages of differentiation, cardiomyocytes within beating colonies were small and round. With maturation, some of the ESC-derived cardiomyocytes expressed an elongated shape and beating cells were primarily mononucleated and rod-shaped with tight cell-cell contact (as shown in Figure 26), consistent with those observed in cardiomyocytes developing in the heart [Westfall MV 1997].

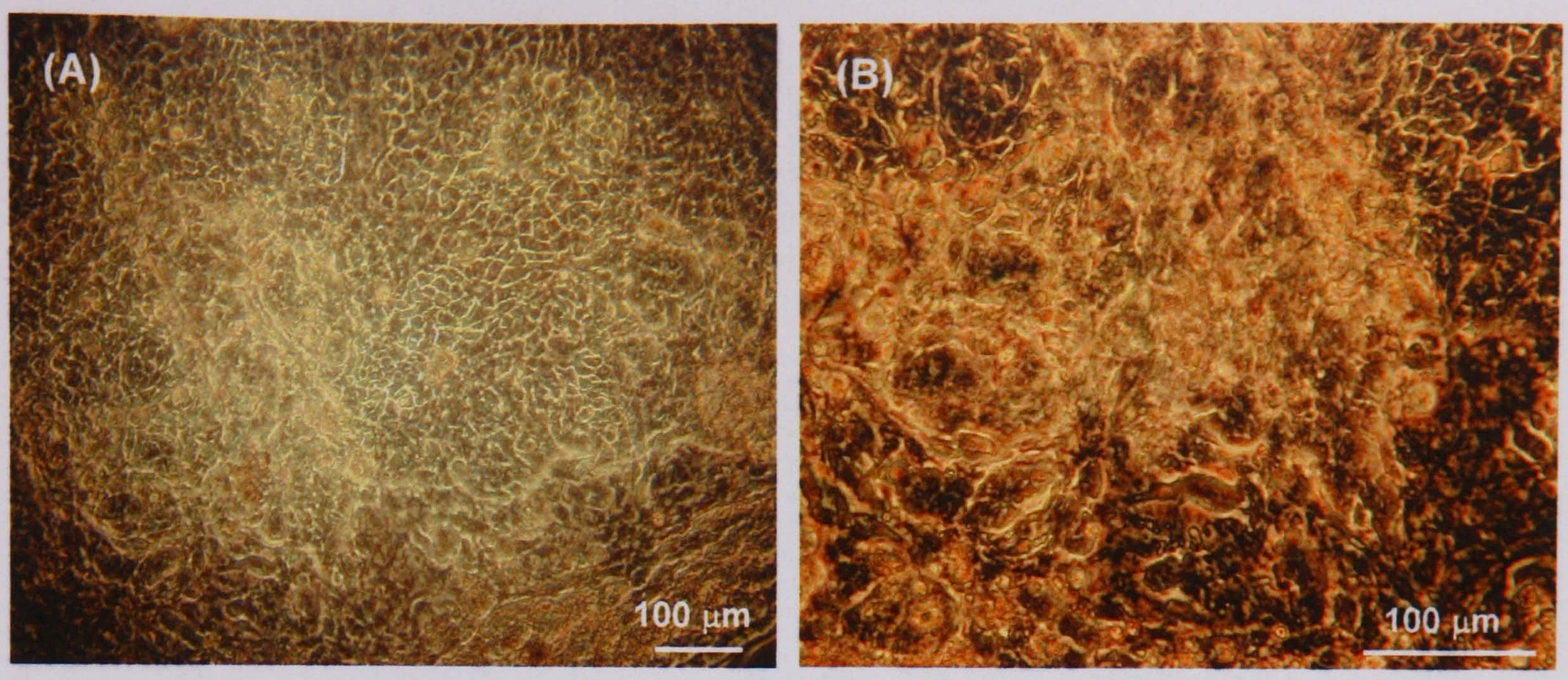


Figure 26. Morphology of beating colony. (A) and (B) Beating colonies after 16 days of culture.

4.4.1.2. Beating colony formation

In this study, mESCs and HepG2 conditioned medium-treated mESCs (CM-mESCs) were allowed to form EBs for 1, 3 or 5 days in EB formation medium (a MEM containing 15% FBS) followed by EB dissociation and subsequent culture in osteogenic or chondrogenic media for an additional 21 days. As shown in figure 27, enhanced mesoderm formation through the use of HepG2 conditioned medium resulted in a 3-4 fold increase ($P<0.05$) in the number of beating colonies in CM-mESC-EB5 as opposed to the EB5 control group for all culture times, where the number of beating colonies were 16.3 ± 5.1, 38.5 ± 5.8, 27.5 ± 10.2 colonies/well in CM-mESC-EB5 and 5.5 ± 3.1, 8.8 ± 3.0, 8.8 ± 4.6 colonies/well in EB5 at day 11, 16 and 21. In contrast, reducing the EB formation time resulted in the absence of beating colonies. Specifically, no beating colonies were observed for the CM-mESC-EB1 group as well as the CM-mESC-EB3 group at 21 days of culture (Figure 27).

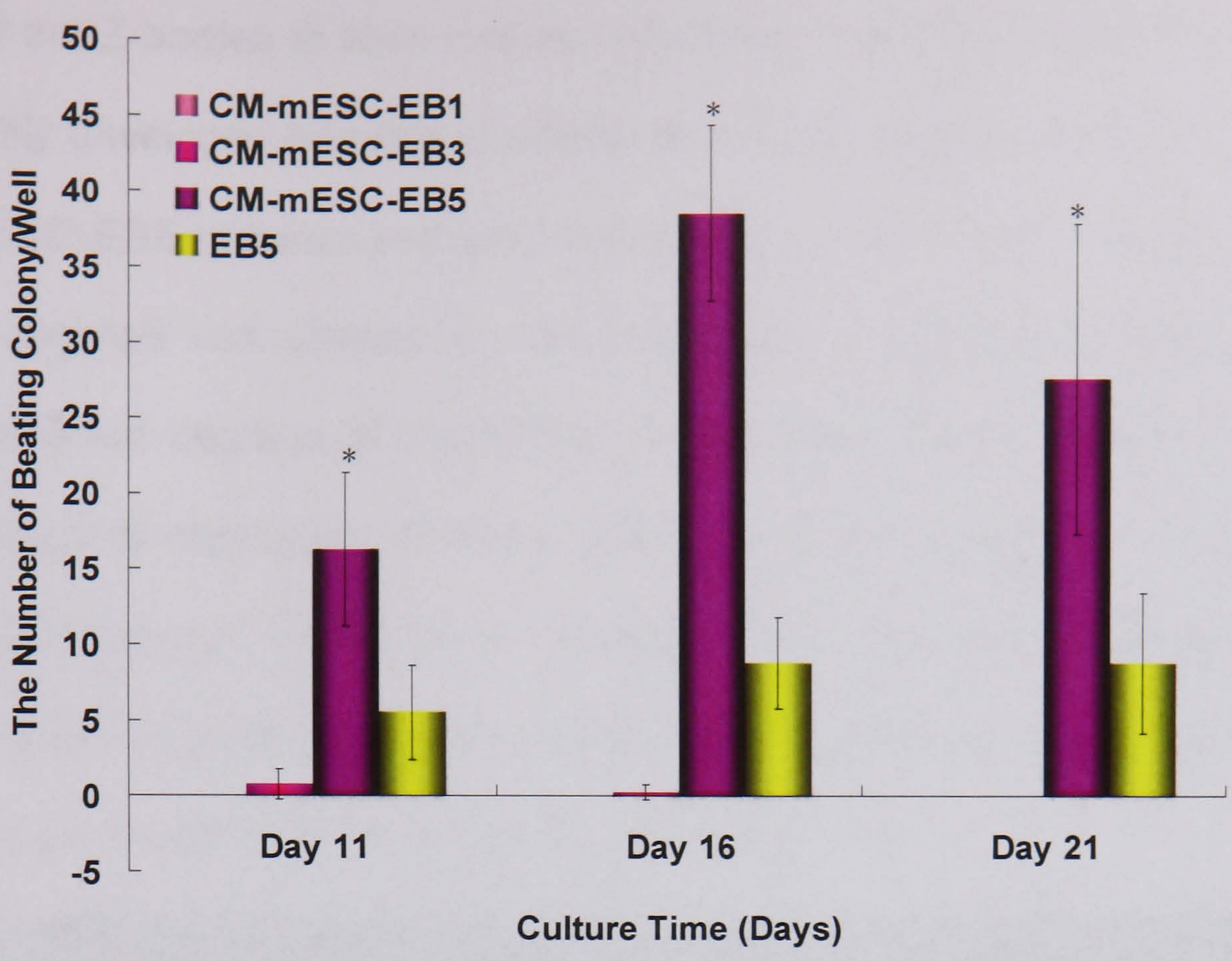


Figure 27. Effect of EB formation time on beating colony formation. Control group (EB5) represents mESCs maintained in conventional maintenance medium then allowed to form EBs for 5 days and then directed to the spontaneous cardiogenic differentiation for 21 days. The experimental groups were mESCs treated for 3 or 4 days with 50% HepG2 conditioned media followed by 1-day (CM-mESC-EB1), 3-day (CM-mESC-EB3), or 5-day (CM-mESC-EB5) EB formation period, and then directed to the spontaneous cardiogenic differentiation for 21 days. Data are shown as mean number of beating colonies ± SD (n = 4; *$p < 0.05$ compared to EB 5).

4.4.1.3. Immuno-staining for cardiogenic differentiation

One of the earliest steps in cardiomyogenesis is the assembly of contractile proteins into organized structures capable of contraction, which requires the polymerization and assembly of several different proteins into three types of filaments that interact with one another and become organized into sarcomeric units that comprise the myofibrils [Du A 2003]. The formation of a myofibril involves the precise ordering of multiple subunits into a linear array of sarcomeres. Myofibril formation begins at the spreading edges of the cardiomyocytes with the formation of premyofibrils that subsequently fuse at the

level of the Z-bodies to form mature myofibrils [Dabiri GA 1997]. Figure 28 shows the highly developed bundles of myofibrils and sarcomeres in cardiomyocytes from CM-mESC-EB5 cultures and also sarcomeric α-actinin and tropomyosin staining with elongated rod shapes in cardiomyocytes. Adjacent cardiomyocytes often show different degrees of myofibrillar organization. Some myofibrils were sparse and irregularly organized, whereas others contained parallel bundles of myofibrils. During cardiogenic differentiation stages, densely packed well organized bundles of myofibrils could be observed, and the sarcomeres had clearly defined Z bands, which could be detected at a high magnification.

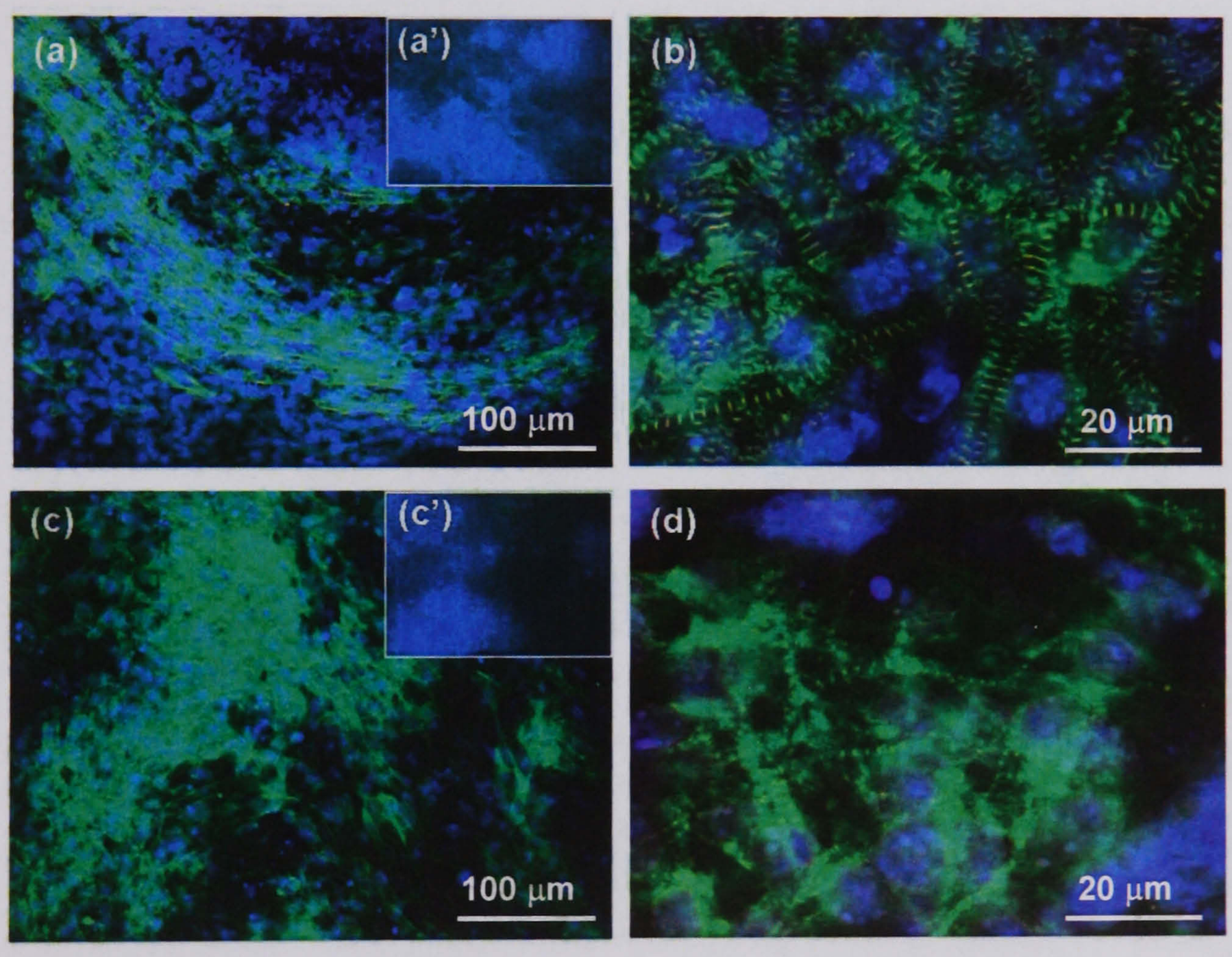


Figure 28. Immunocytochemical staining for sarcomeric α-actinin and tropomyosin in the CM-treated mESCs. (a) and (b): Sarcomeric α-actinin expression (green) and nuclear staining (DAPI; blue) at day 16 of culture. (c) and (d): Tropomyosin expression (green) and nuclear staining (DAPI; blue) at day 16 of culture. The insets (a') and (c') show negative controls for non-specific binding of the primary antibodies.

4.4.1.4. Cardiogenic gene expression

A murine Nkx-2.5 homeobox gene was identified as one of the important factors in the activation of cardiac α-actin and myosin heavy chain gene in cardiogenic differentiation [Chen CY 1996]. In mouse embryos, Nkx-2.5 transcripts were localized to early cardiac cell progenitors, prior to cardiogenic differentiation and continued to be expressed in cardiac myocytes throughout development [Lints TJ 1993]. Herein, at gene expression level, cardiogenic differentiation was characterised by evaluating the expression of Nkx-2.5 mRNA. RT-PCR analysis confirmed the high expression of transcription factor Nkx2.5 at day 11 of culture in the CM-mESC-EB5 and EB5 groups (Figure 29). In contrast, in CM-mESC-EB1 and CM-mESC-EB3 NKx2.5 expression was extremely weak. These results are in agreement with the beating colony assay and immunocytochemistry results demonstrating the correlation between cardiomyocyte beating colonies and cardiomyocyte marker and gene expression.

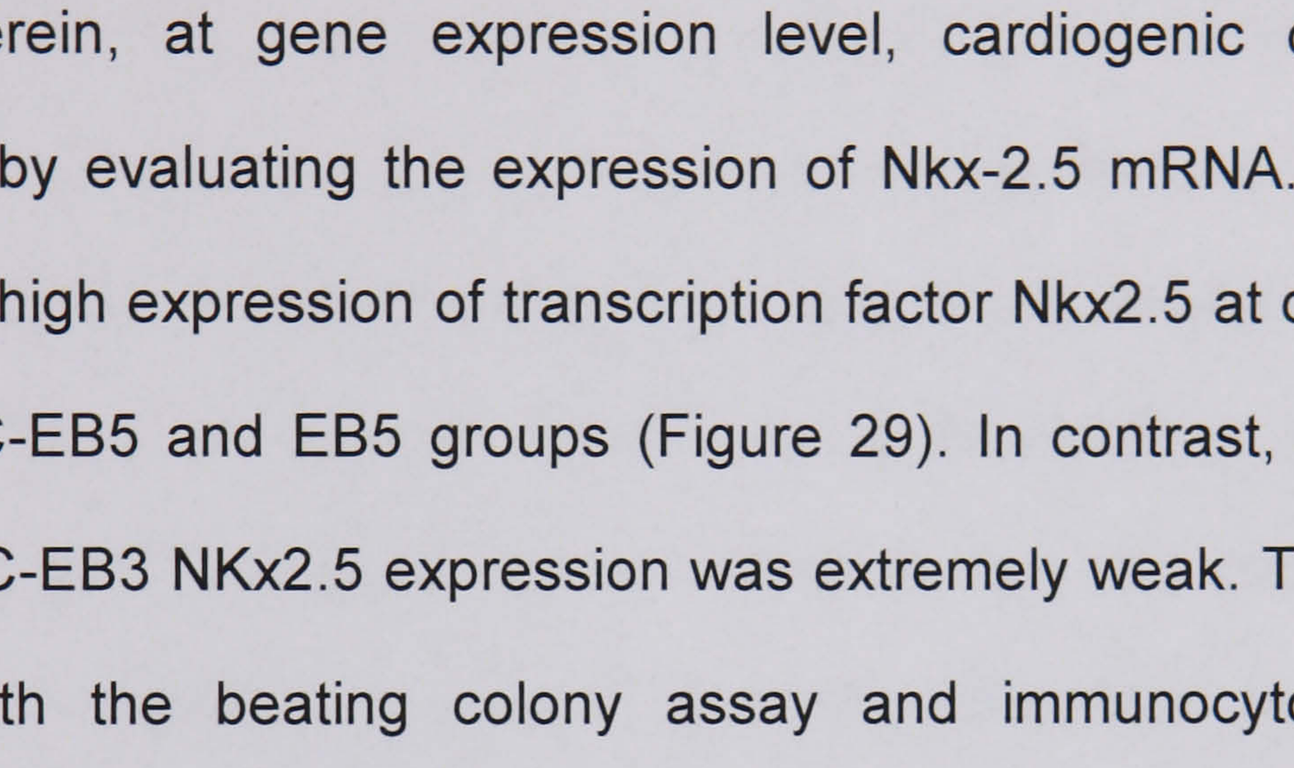


Figure 29. RT-PCR analysis of cardiogenic (Nkx-2.5) gene expression at day 11 of culture. GAPDH gene expression was used at the housekeeping control Lane M: 100 bp DNA ladder; Lane 1: CM-mESC-EB 1; Lane 2: CM-mESC-EB 3; Lane 3: CM-mESC-EB 5; Lane 4: EB 5.

4.4.2. *In vitro* EB-mediated osteogenic differentiation

In this study, *in vitro* osteogenic differentiation was characterised by

morphological observation, bone nodule formation assay, alkaline phosphatase activity assay immunocytochemical staining and RT-PCR.

4.4.2.1. Morphology of mineralised bone nodules

It has been well documented that mineralized bone nodules form when cells are grown in the presence of ascorbic acid and β-glycerophosphate [Tenenbaum HC 1982], and formation of mineralized nodules is enhanced by dexamethasone [Buttery LD 2001]. The bone nodule formation assay permits the specific assessment of bone-forming cells and a relative measure [Tenenbaum HC 1982]. In this study, mineralised nodules could be easily detected as very dark spots using a light microscope in all culture groups, indicating the osteogenic differentiation of mESCs. As shown in figure 30, mineralised bone nodules usually formed at the centre of cell colonies with various intensities.

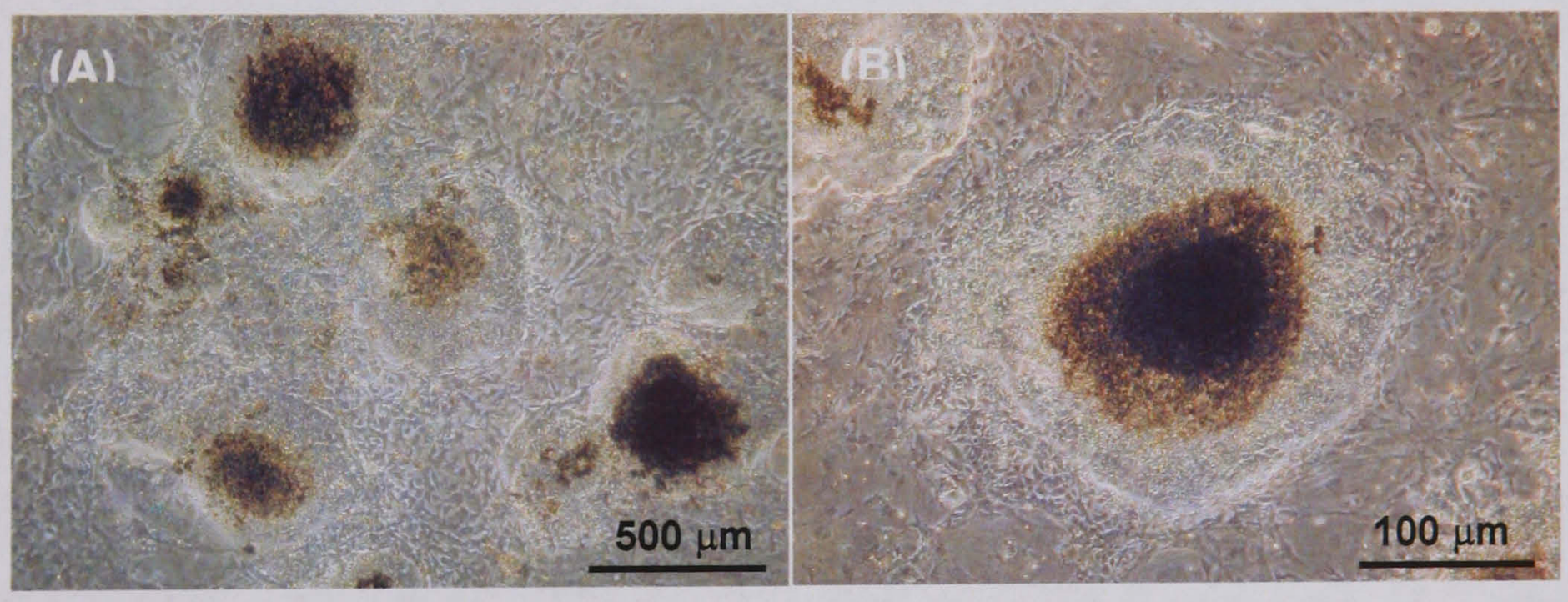


Figure 30. Morphology of mineralised bone nodule. (A) and (B): Mineralised bone nodules after 21 days of culture. Under light microscope.

4.4.2.2. Bone nodule formation

Osteogenic differentiation was assessed by staining with Alizarin Red in order to visualize mineralization (Figure 31). Quantification of mineralization was achieved by counting the mineralised bone nodules only if they were fluorescent

when exposed to UV light (excitation at 530-560 nm and emission at 580 nm), as shown in figure 32. This was done in order to exclude non-specific staining of cell aggregates, such as alizarin red S stained cell clusters formed by beating colonies or other cell types [Midura RJ 2004, Chang YL 2000]. Our results show that, with differentiation and maturation, the number of stained bone nodules increased in the conditioned medium-treated groups such as CM-mESC-EB1 and CM-mESC-EB3, and the size of bone nodules also increased in accordance with culture time and differentiation.

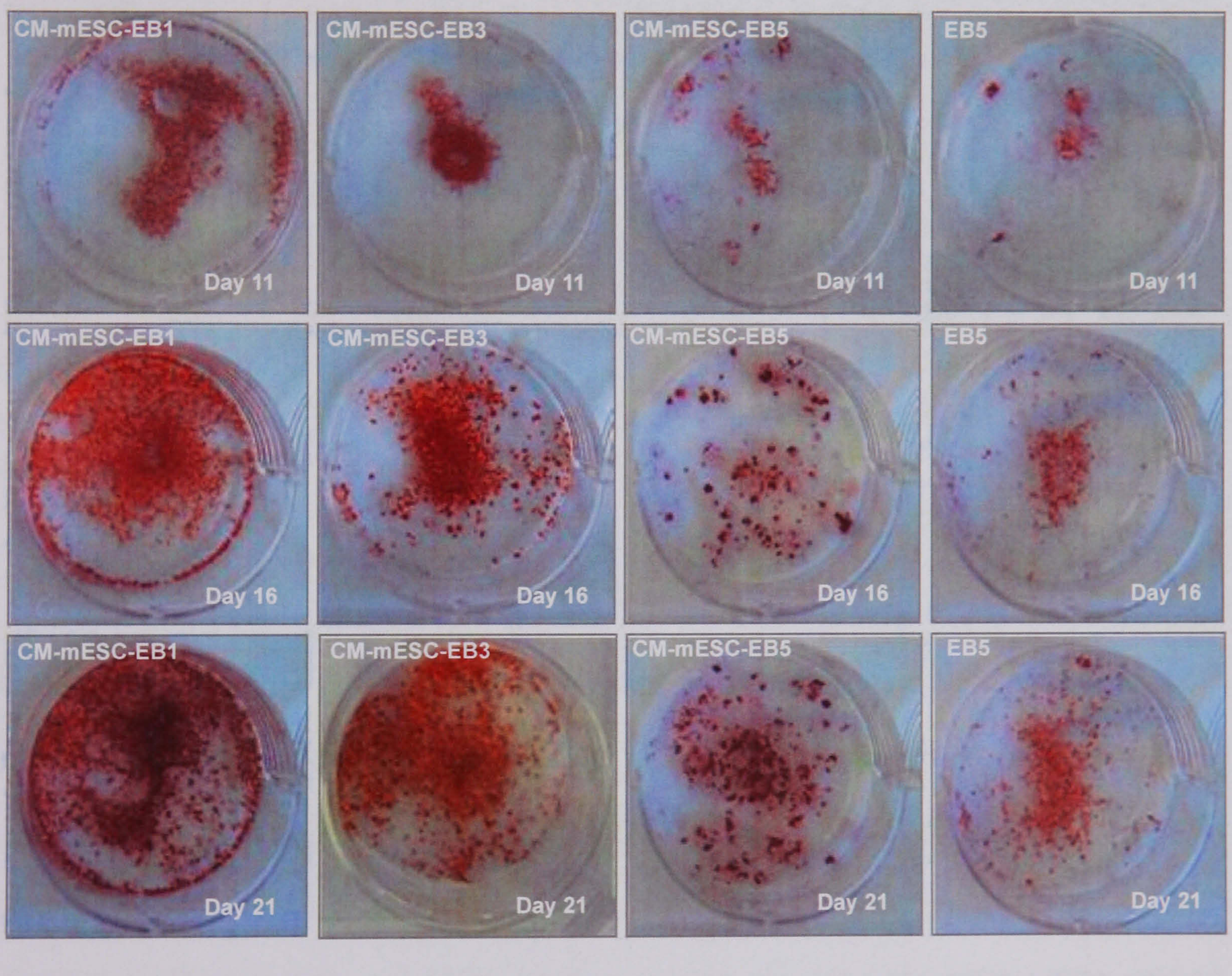
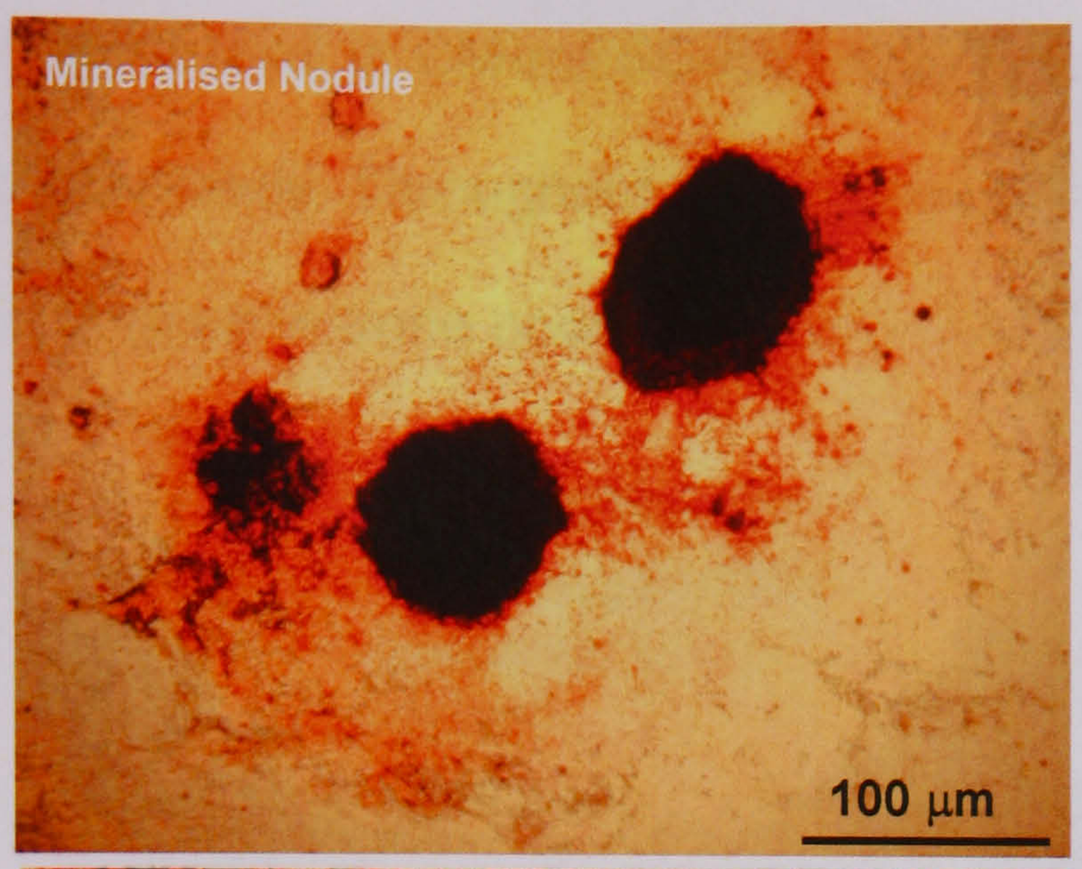
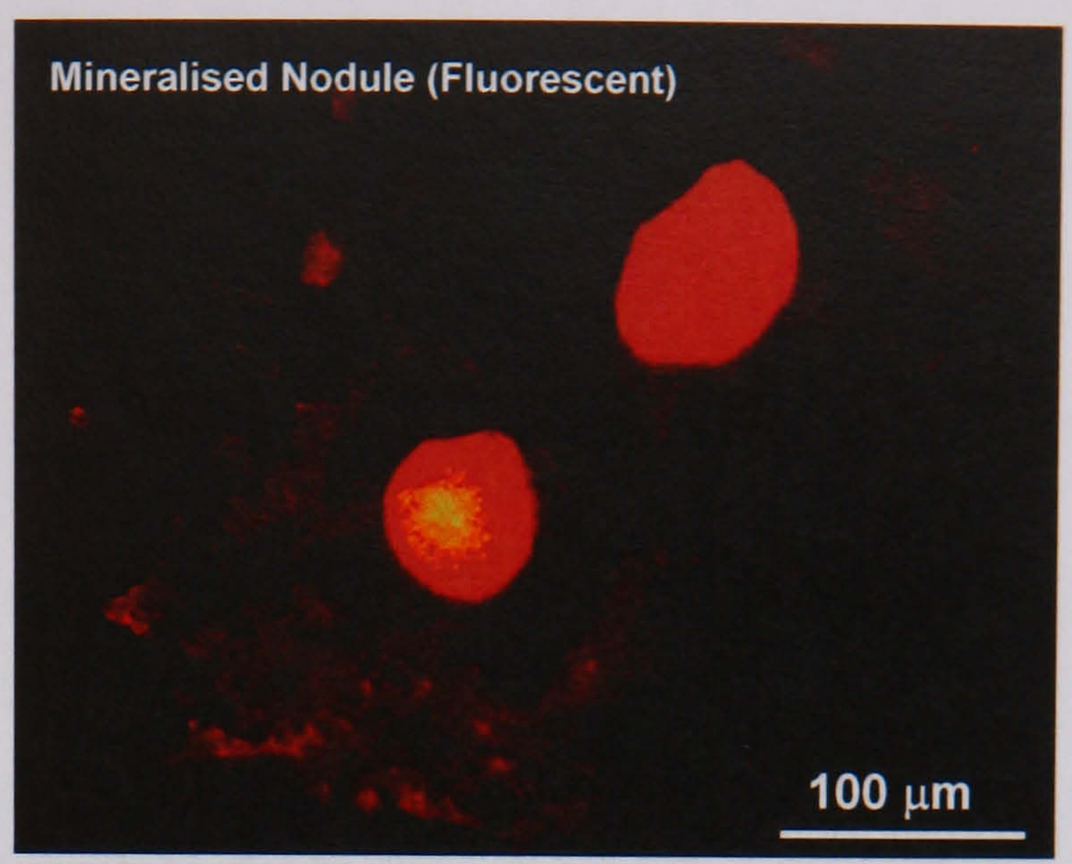
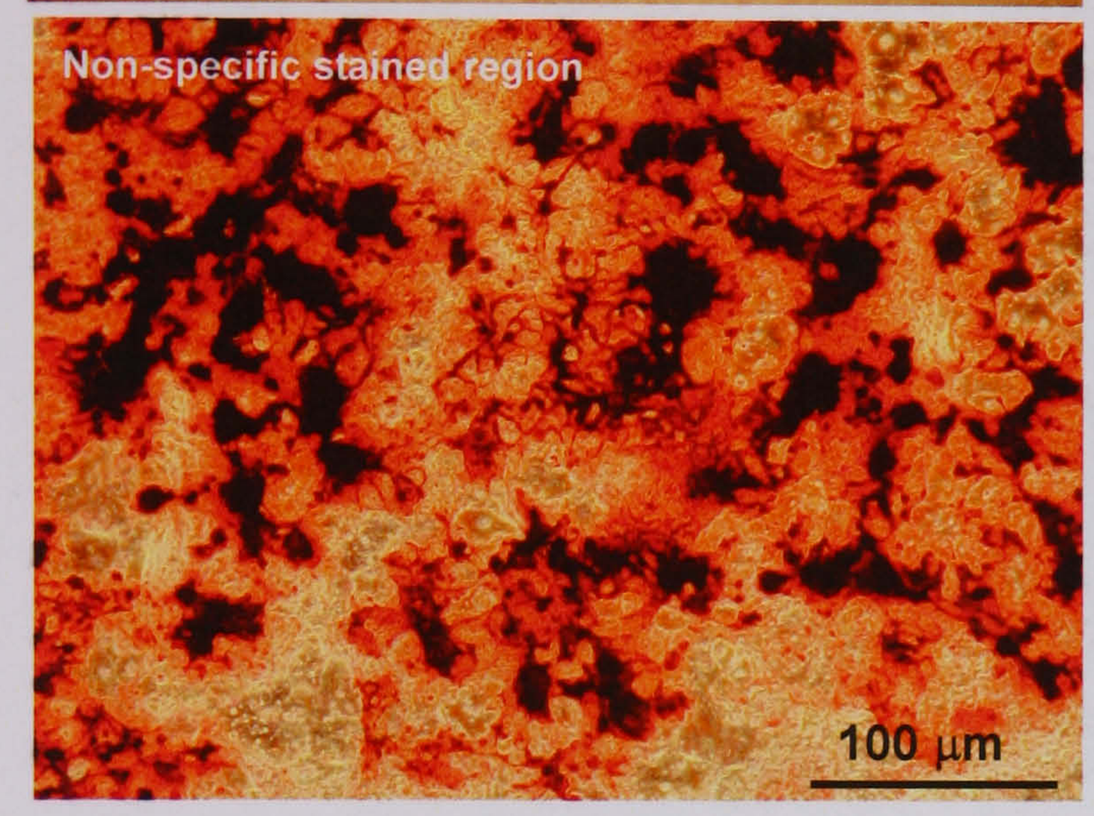


Figure 31. Alizarin red S stained bone nodules in a light microscope. Control group (EB5) represents mESCs maintained in conventional maintenance medium then allowed to form EBs for 5 days and then directed to osteogenic differentiation for 21 days. The experimental groups were mESCs treated for 3 or 4 days with 50% HepG2 conditioned media followed by 1-day (CM-mESC-EB1), 3-day (CM-mESC-EB3), or 5-day (CM-mESC-EB5) EB formation period, and then directed to osteogenic differentiation for 21 days.







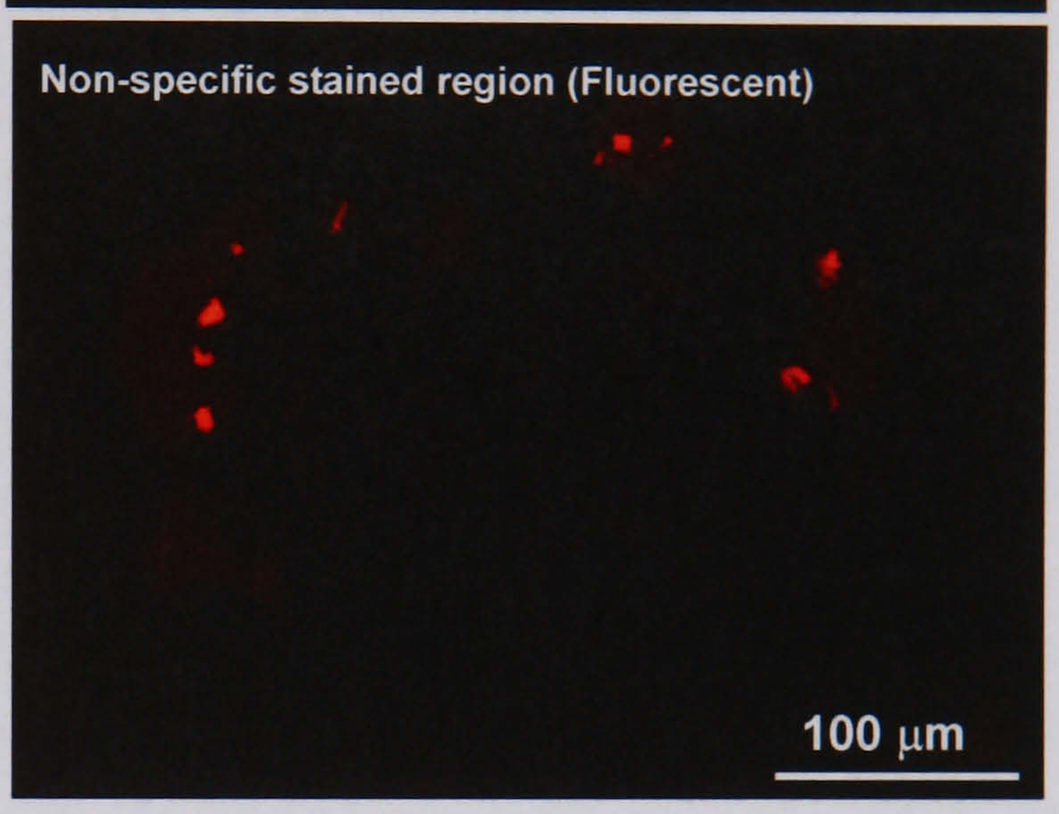


Figure 32. Alizarin red S stained bone nodules under UV light. Mineralised nodules shows red/orange fluorescence and non-specific stained area does not show fluorescence.

As shown in figure 33, a significantly higher number ($P<0.05$) of stained bone nodules was achieved by reducing the time the mESCs treated with conditioned medium were allowed to form EBs. Specifically, at days 11 and 16 of culture a 10-fold increase in the number of bone nodules formed in the CM-mESC-EB1 cultures as compared to the control EB5 group, where the number of bone nodules were 330 ± 59 and 563 ± 70 bone nodules/well in CM-mESC-EB1 and 18 ± 6 and 64 ± 7 bone nodules/well in EB5 at day 11 and 16, respectively. Subsequently, at day 21 an approximately 5-fold increase in the number of bone nodules formed by the CM-mESC-EB1 group as opposed to the control EB5 group was observed, where the number of bone nodules were 694 ± 61 bone

nodules/well in CM-mESC-EB1 and 192 ± 11 bone nodules/well in EB5 at day 21, respectively. Throughout the culture period, the CM-mESC-EB5 group showed no difference in bone nodule formation compared to the EB5 group.

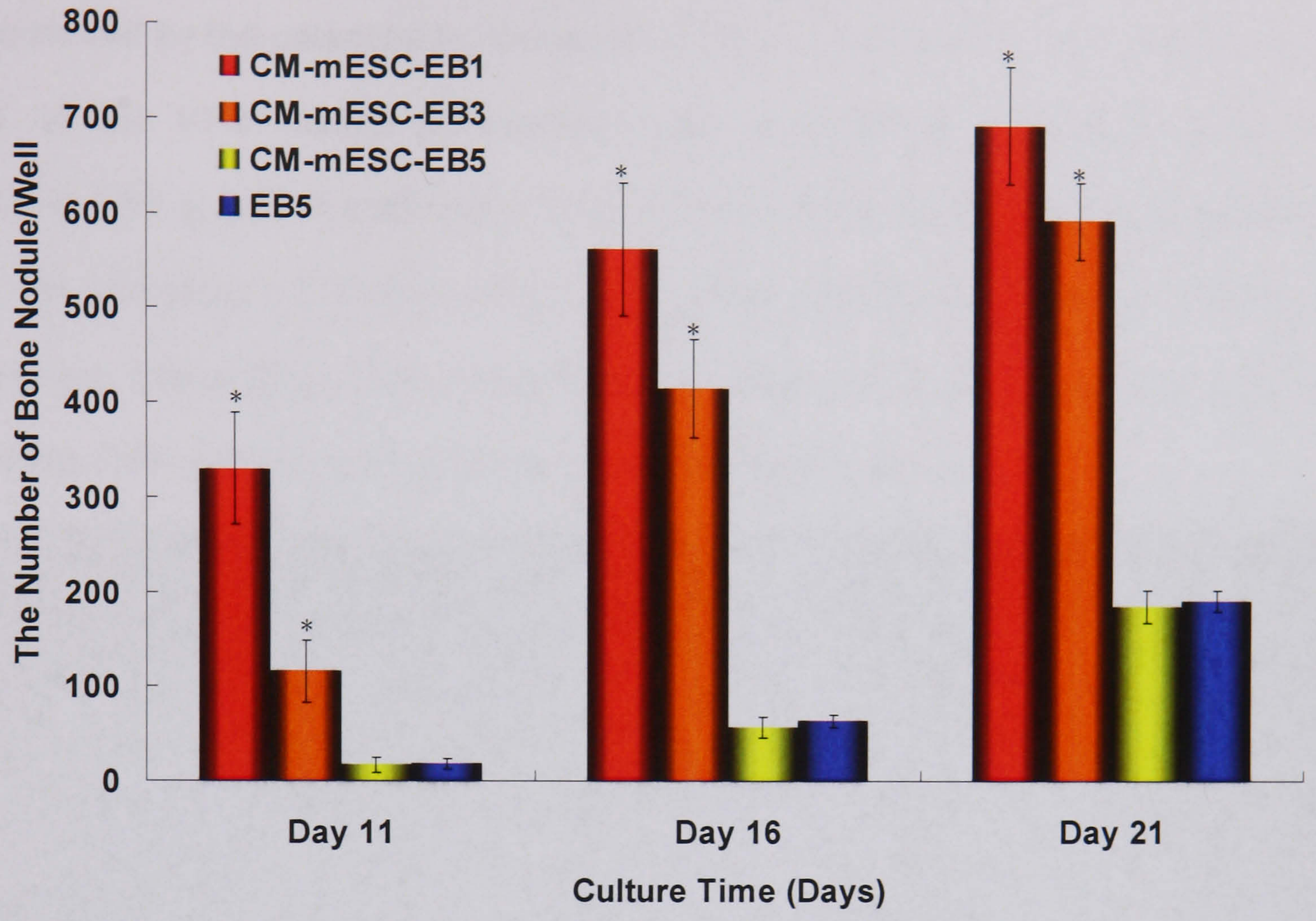


Figure 33. Bone nodule formation. Control group (EB5) represents mESCs maintained in conventional maintenance medium then allowed to form EBs for 5 days and then directed to osteogenic differentiation for 21 days. The experimental groups were mESCs treated for 3 or 4 days with 50% HepG2 conditioned media followed by 1-day (CM-mESC-EB1), 3-day (CM-mESC-EB3), or 5-day (CM-mESC-EB5) EB formation period, and then directed to osteogenic differentiation for 21 days. Data are shown as mean number of bone nodules ± SD (n = 4; *p < 0.05 compared to EB 5).

4.4.2.3. Immuno-staining for osteogenic differentiation

Osteoblast differentiation is controlled by the extracellular environment. One aspect of this environment is cell to cell interaction, which is particularly mediated by cadherins. Cadherin-mediated cell to cell adhesion is essential for the development and survival of multi-cellular tissues. In osteoblasts, the expression

of N-cadherin, cadherin-11, R-cadherin, and an isoform of K-cadherin has been reported [Mbalaviele G1998, Cheng SL 1998, Kawaguchi J 2001]. In osteoblast differentiation, cadherin-11 (also called as OB-cadherin), is constitutively expressed by the osteoblastic lineage [Kii I 2004]. In this study, as shown by figure 34, at day 16 of culture OB-cadherin was very strongly expressed in the CM-mESC-EB1 group. In particular, OB-cadherin immunostaining was well developed in the periphery of neighbouring cells, which maintained cuboidal shapes. In contrast, OB-cadherin-immunoreactive cells could hardly be observed in the CM-mESC-EB5 and EB5 groups at day 16 of osteogenic culture.

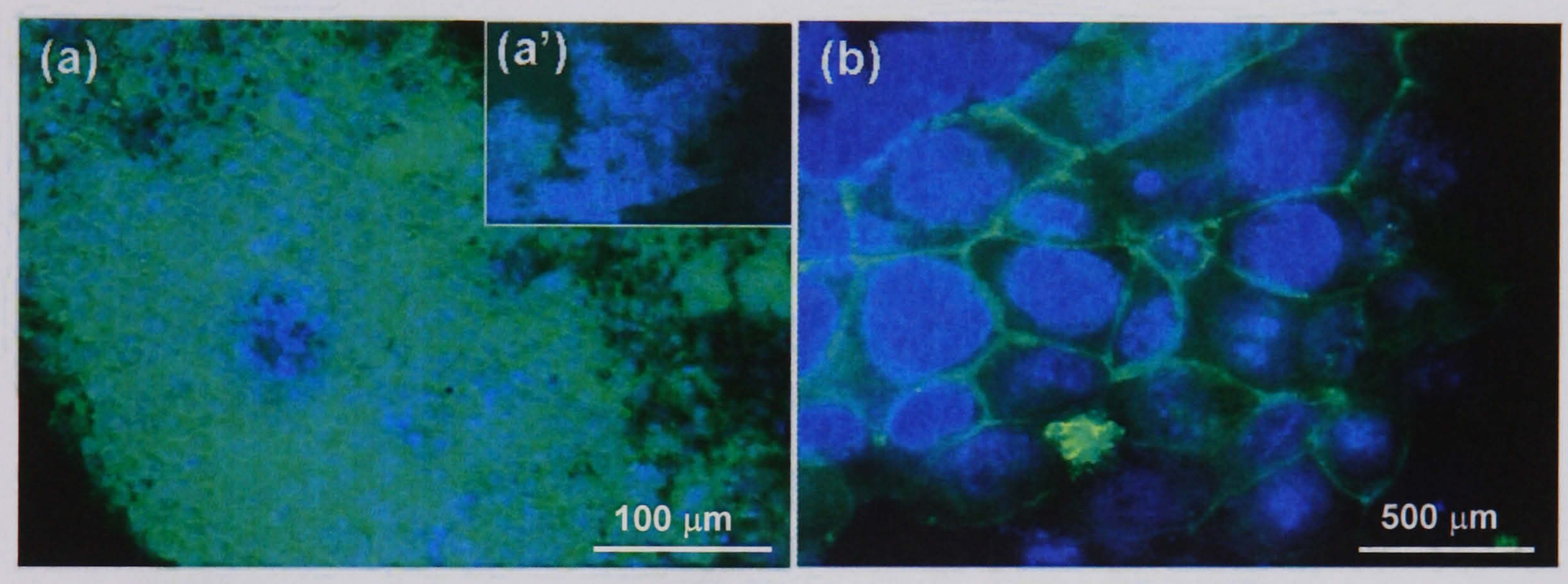


Figure 34. Immunocytochemical staining for OB-cadherin in CM-treated mESC-derived cultures. Expression of OB-cadherin (green) and nuclear staining (DAPI; blue) at day 16 of culture in the CM-mESC-EB1-derived osteogenic cells. Inset (a') shows negative control for non-specific binding of the primary antibody.

4.4.2.4. Alkaline phosphatase activity

Alkaline phosphatases (orthophosphoric-monoester phosphohydrolase, alkaline optimum, EC 3.1.3.1.) are cell surface glycoproteins that hydrolyze a variety of monophosphate esters. The bone isoenzyme has long been thought to play a role in the mineralization of bone [Wuthier RE 1985] and is widely used as a marker of mineralization and as a marker of the osteoblast phenotype. As shown in figure 35, alkaline phosphatase activity was enhanced 3-fold ($P<0.05$) in the

CM-mESC-EB1 and 2-fold in the CM-mESC-EB3 group in comparison with the control EB5 group at day 11 of the osteogenic culture - 377.7 ± 32.0 PNPμM/min/mg in the CM-mESC-EB1, 209.3 ± 22.8 PNPμM/min/mg in the CM-mESC-EB3, and 116.3 ± 16.5 PNPμM/min/mg in the EB5, respectively. No statistical difference in enzyme activity was observed between the CM-mESC-EB5 and EB5 groups. Furthermore, enzyme activity showed a time-dependent behaviour with a marked increase at day 11 and then a decrease to background levels from day 16 onwards. This temporal increase of alkaline phosphatase activity in CM-mESC-EB1 and CM-mESC-EB3 correlates with the increased bone nodule formation.

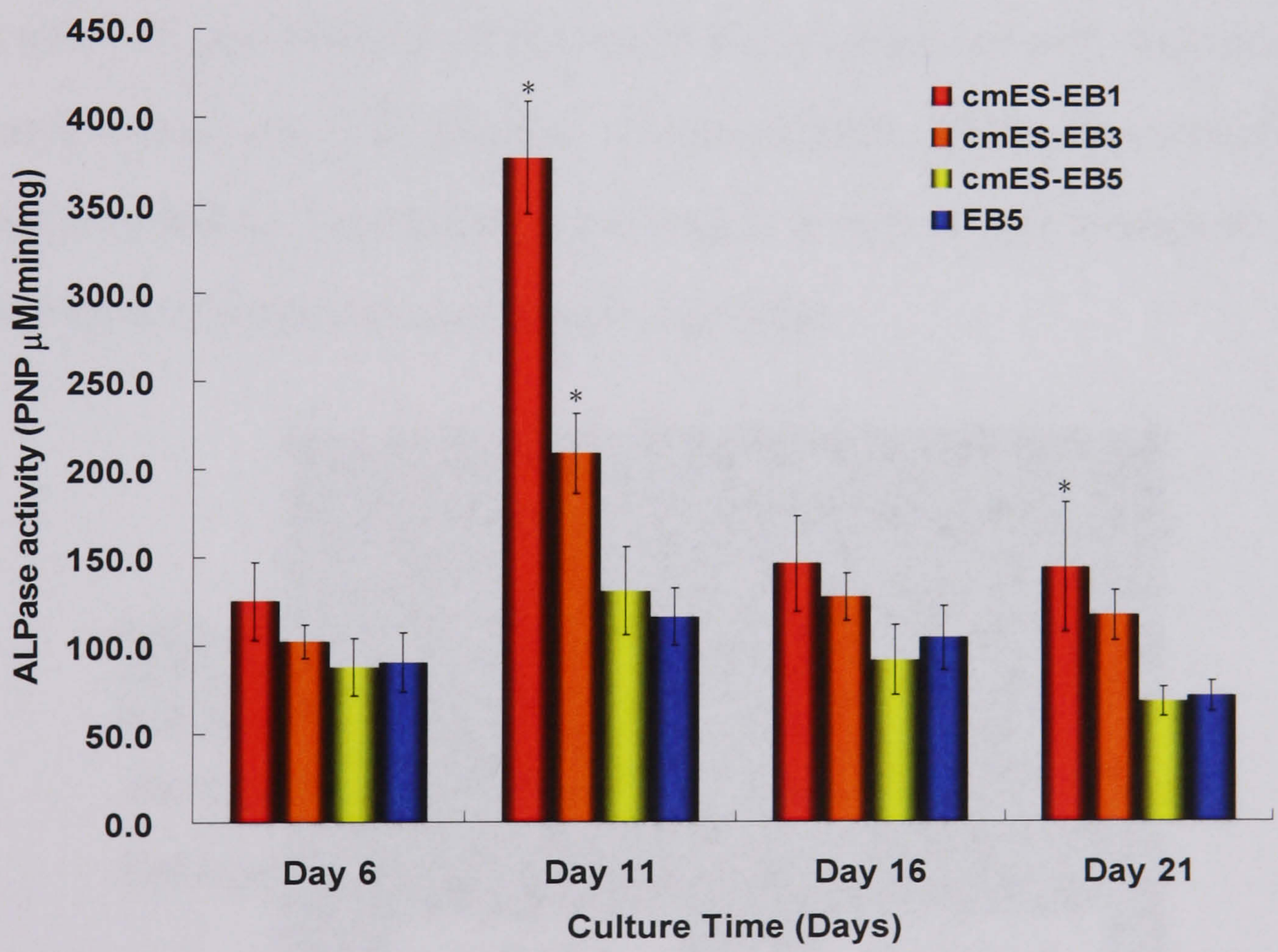


Figure 35. Alkaline phosphatase activity. Control group (EB5) represents mESCs maintained in conventional maintenance medium then allowed to form EBs for 5 days and then directed to osteogenic differentiation for 21 days. The experimental groups were mESCs treated for 3 or 4 days with 50% HepG2 conditioned media followed by 1-day (CM-mESC-EB1), 3-day (CM-mESC-EB3), or 5-day (CM-mESC-EB5) EB formation period, and then directed to osteogenic differentiation for 21 days. Data are shown as mean enzyme activity ± SD (n = 6; *$p < 0.05$ compared to EB 5).

4.4.2.5. Osteogenic gene expression

It is well established that core binding factor Cbfa1/Runx2 is an essential transcription factor required for osteoblast recruitment and differentiation, and bone formation [Banerjee C 2001]. In this study characterisation of osteogenic differentiation was performed by examining expression of Cbfa 1/Runx 2 using RT-PCR after 11 days of culture, at which point the highest expression of bone nodules was observed. As shown in figure 36, bands for Cbfa 1/Runx 2 were present in the CM-mESC-EB1 and CM-mESC-EB3 groups. In contrast, the CM-mESC-EB5 and EB5 groups showed extremely weak (almost non-existent) expression of Cbfa1/Runx2. These results are in agreement with the bone nodule formation assay and OB cadherin immunostaining results demonstrating the correlation between mineralised bone nodule formation and osteogenic marker expression and osteoblast related gene expression.

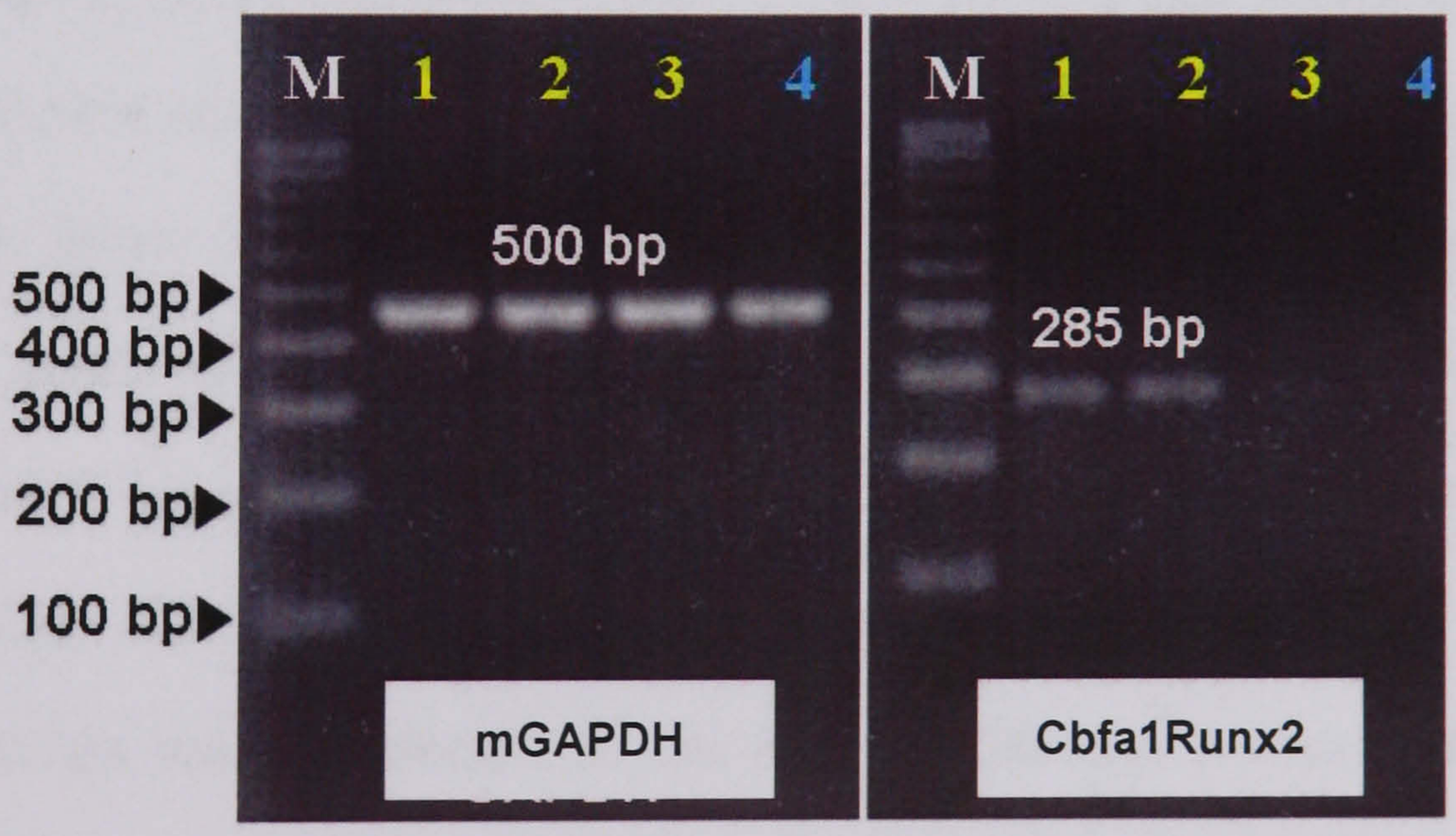


Figure 36. RT-PCR analysis of osteogenic (Cbfa1/Runx2) gene expression at day 11 of culture. GAPDH gene expression was used at the housekeeping control Lane M: 100 bp DNA ladder; Lane 1: CM-mESC-EB 1; Lane 2: c CM-mESC-EB 3; Lane 3: CM-mESC-EB 5; Lane 4: EB 5.

4.4.3. *In vitro* EB-mediated chondrogenic differentiation

The changes associated with the *in vitro* chondrogenic capacity of mESC as influenced by the use of HepG2 conditioned medium and EB formation time were studied. *In vitro* chondrogenic differentiation was characterised by morphological observation, cartilage nodule formation assay, GAG assay immunocytochemical staining and RT-PCR.

4.4.3.1. Morphology of cartilage nodule

Chondrogenic differentiation is triggered in pre-cartilage condensations and ultimately cartilage forms. In micromass cultures, dissociated cells with chondrogenic capacity interact to first form small aggregates, then bigger clusters and finally cartilage nodules [Lee YS 1998]. Such micromass cultures [Lee YS 1998, Ahrens 1977, Daniels 1996], have been an excellent model for analyzing the mechanisms of chondrogenesis. It has been also well documented that synthetic dexamethasone (DEX) increased the number of cartilage nodules formed in a dose-dependent manner [Grigoriadis AE 1998]. In addition, treatment with insulin-like growth factor-1 (IGF-I) also produced cell clustering and cartilage nodule formation, which are indicative of chondrogenesis with an increase in type II collagen and aggrecan mRNA that was time- and concentration-dependent [Mierisch CM 2002]. In this study, the dissociated EB cells from different EB formation times were subjected to the high cell density micromass culture with chondrogenic supplements such as dexamethasone, ascorbic acid and IGF-I. Distinct cartilage nodule like structures could be observed in all cultures, albeit with different frequency (Figure 37). Specifically, the nodules exhibited a distinct structure comprising of round-shaped cells separated by extracellular matrix surrounded by a circular arranged fibrillar matrix that was easily detected by light

microscopy, which is in agreement with the reported typical structure of ESC-derived chondrocytes [Kramer J 2000]. Positive staining of the nodules with alcian blue indicated cartilage-like extracellular matrix accumulation. In the cartilage nodules, most of cells showed round shape with tight contact between cells, and peripheral space of cells stained positive for GAG, as indicated by the alcian blue and neutral red staining (Figure 37).

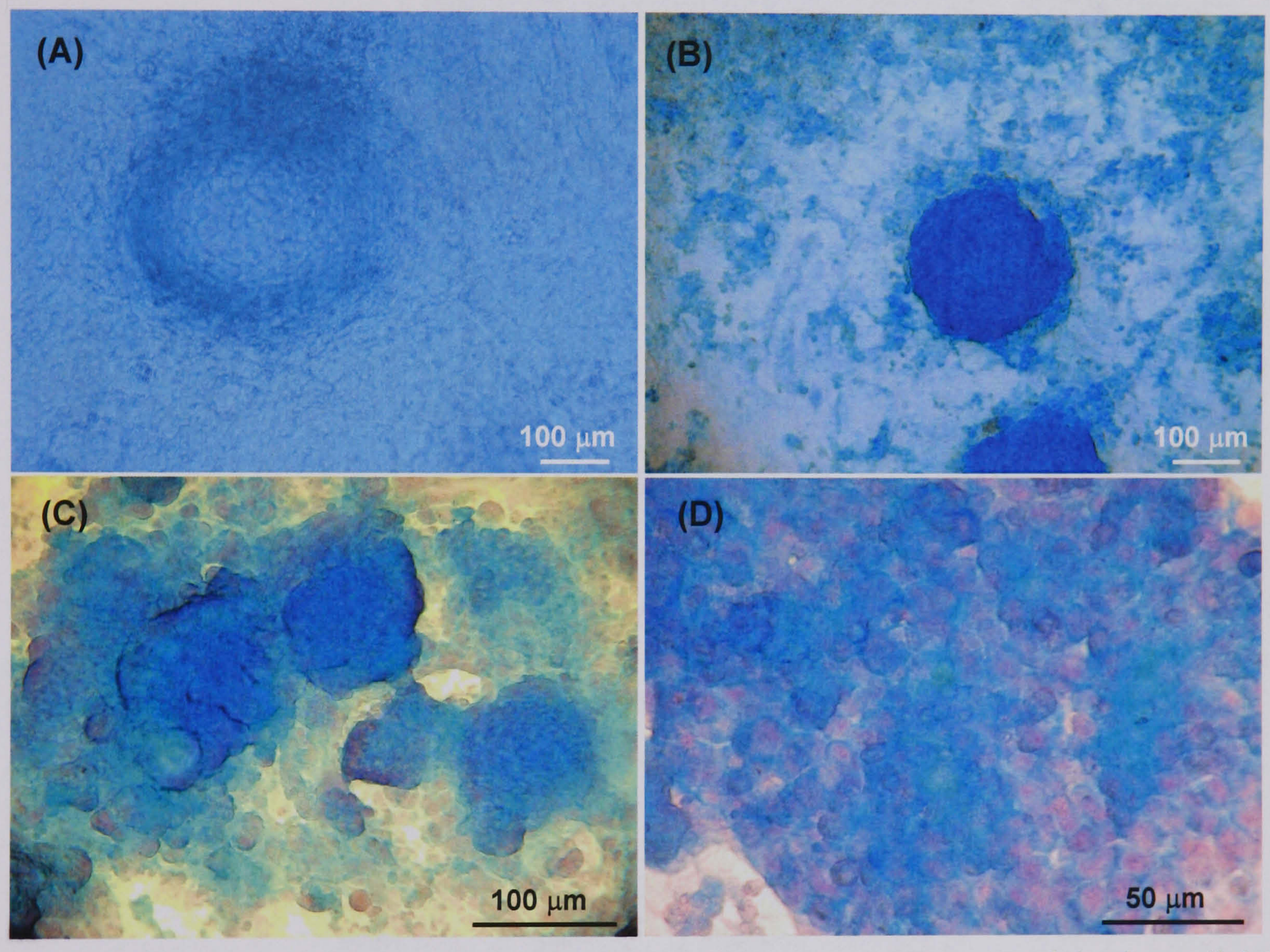


Figure 37. Morphology of cartilage nodules. (A): cartilage nodule in a light microscope. (B): Alcian blue stained bone nodules in a light microscope. (C): Double stained cartilage nodule with Alcian blue and Neutral Red. (D): Highly magnified feature of double stained cartilage nodule.

4.4.3.2. Cartilage nodule formation

Following morphological observation and alcian blue staining of the cartilage nodules, the extent (area) of the stained nodules was quantified. Specifically, the size of the alcian blue stained portions (dark blue) of cartilage

nodules was determined in relation to the total observed area. At day 15, CM-mESC-EB1 showed a 2.5 fold higher relative stained areas than other test groups; the other test groups showed no significant difference in the alcian blue stained area (25.70 ± 4.55 % in the CM-mESC-EB1, 10.61 ± 6.67% in the CM-mESC-EB3, 8.60 ± 5.36 % in the CM-mESC-EB5 and 8.47 ± 2.56% in the EB5, respectively).

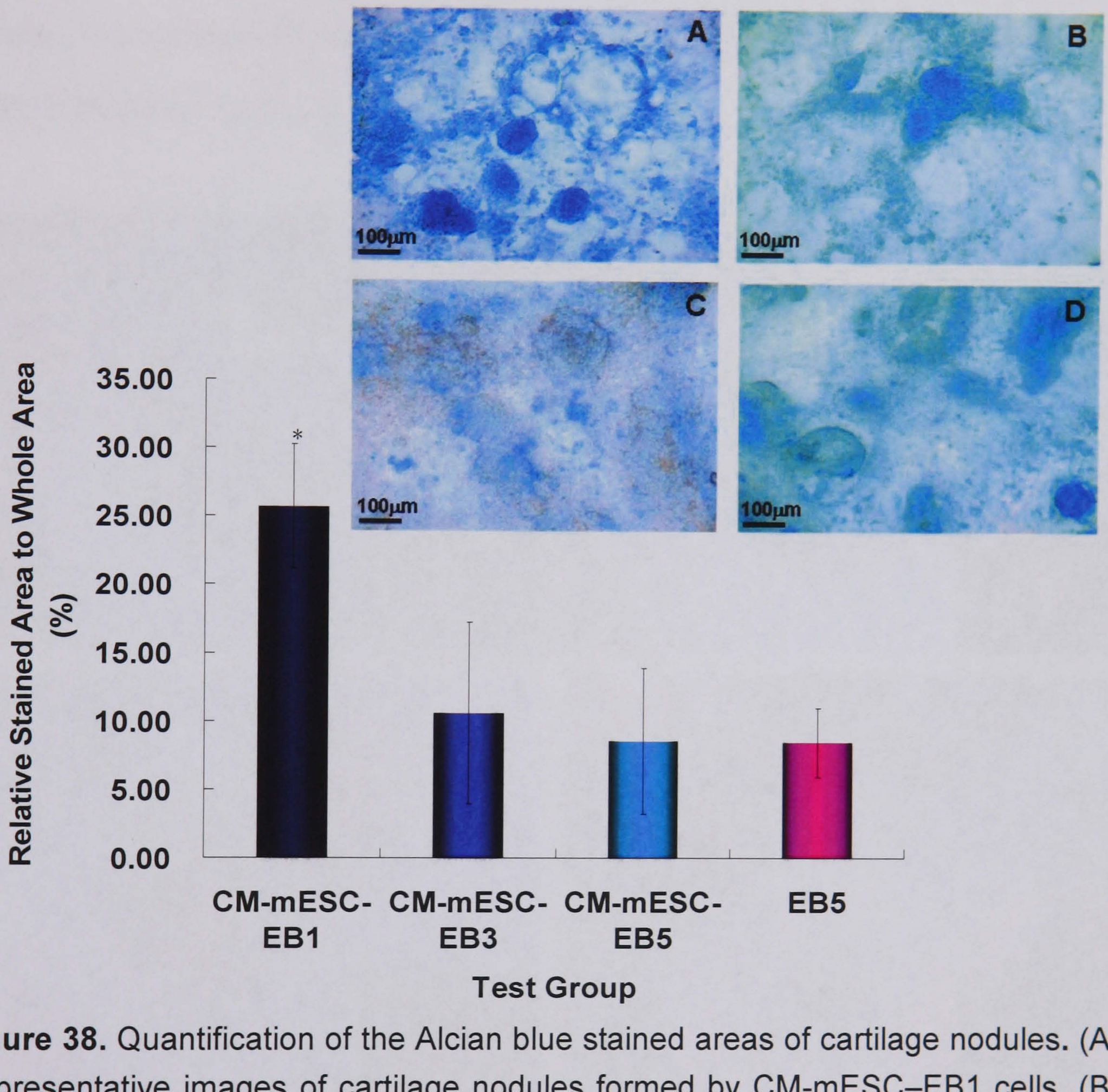


Figure 38. Quantification of the Alcian blue stained areas of cartilage nodules. (A): Representative images of cartilage nodules formed by CM-mESC–EB1 cells. (B): Representative images of cartilage nodules formed by CM-mESC-EB3. (C): Representative images of cartilage nodules formed by CM-mESC-EB5. (D): Representative images of cartilage nodules formed by EB5. Data shown as mean relative stained area ± SD (n=4, * $P<0.005$ compared to EB5).

In addition, to determine whether Alcian blue staining was due to the cartilage nodules or other cell aggregates, such as bone nodules, a dual staining

with Alcian blue and Alrizarin red-S was performed. As shown in figure 39, the dark blue stained region, which was considered as cartilage nodules and frequently found in the CM-mESC-EB1 group, was not stained by Alizarin red S, confirming that these strongly-stained areas were derived from cartilage nodule. In contrast, some light blue stained nodules, which could be found in the other test groups, showed mineralised calcium deposit as indicated by the presence of fluorescence from Alizarin red S staining.

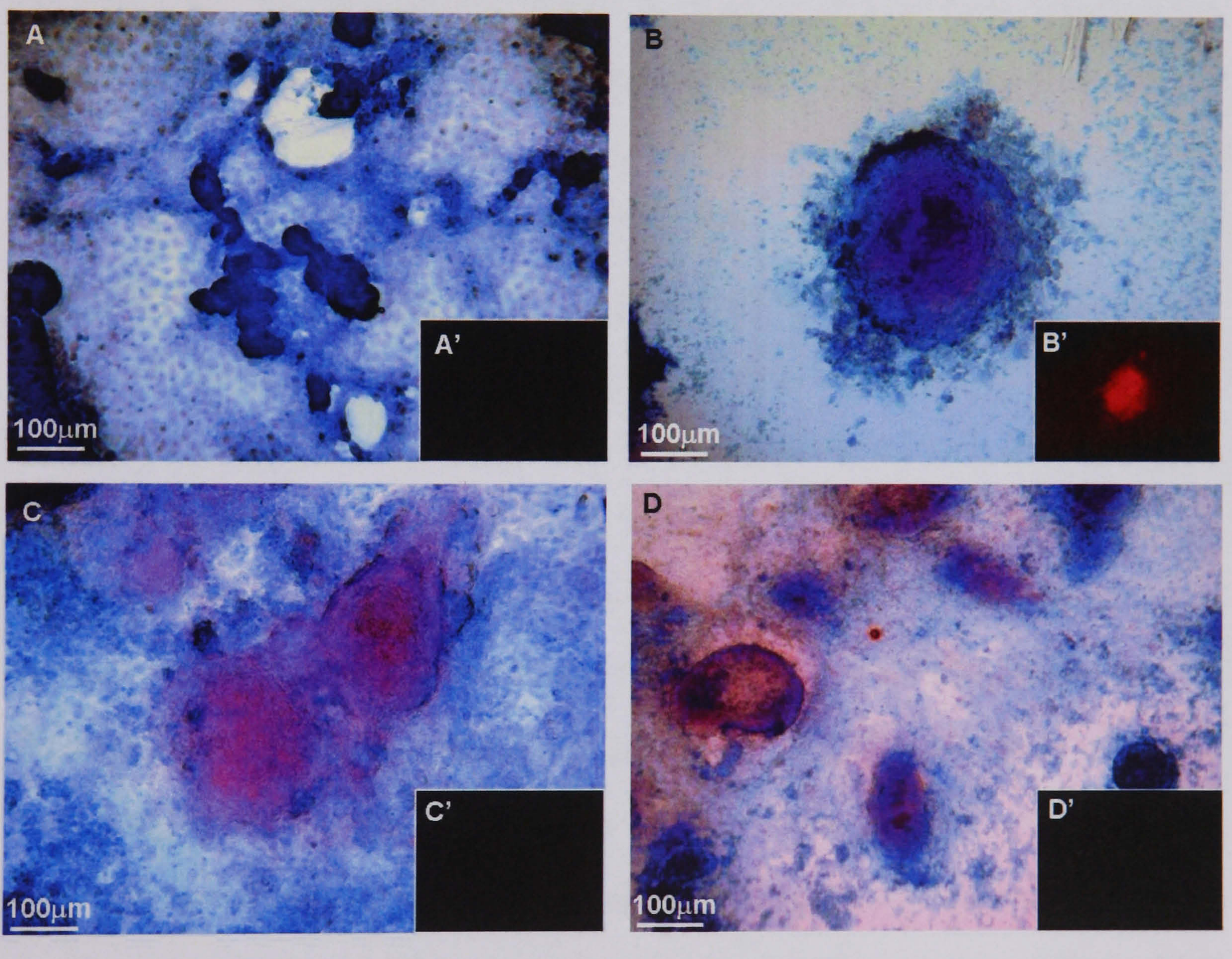


Figure 39. Alcian blue and Alizarin red-S double staining. (A) Representative image of well stained cartilage nodules of CM-mESC -EB1. (A') High power image of nodules and confirmation of mineralization by UV fluorescence (inset). (B) Representative images of mineralised nodules in CM-mESC -EB3. (B') High power image of minerlaised nodules by UV fluorescence (inset). (C) Representative image of other cell colonies in CM-mESC-EB5. (C') High power image of minerlaised nodules by UV fluorescence (inset). (D) Representative images of

other cell colonies in EB5. (D') High power image of minerlaised nodules by UV fluorescence (inset).

4.4.3.3. Glycosaminoglycan (GAG) synthesis

Cartilage is particularly rich in specialised extracellular matrix, with matrix making up 90% of the dry weight of the tissue [Poole AR 2001]. ECM has dense collagen and proteoglycan networks that determine mechanical and functional properties of the tissue [Poole AR 2001, Knudson CB 2001]. ECM molecules in cartilage cooperate with growth factors to regulate chondrogenic differentiation and cartilage development. Proteoglycan interactions with collagen fibrils and growth factors have been implicated in the regulation of ECM assembly and growth factor functions [Knudson CB 2001]. The major components of proteoglycans are glycosaminoglycans, which are involved in cell-cell and cell-matrix interactions during chondrogenic differentiation [Maleski MP 1996]. In this study, the analysis of alcian blue staining was accompanied by measuring the sulfated GAG content produced by chondrogenic cells using DMMB assay method. As shown in figure 40, the relative matrix sulfated GAG amount in the CM-mESC-EB1 group was detected at a much higher level (2 fold to 2.5 fold) throughout the culture period - increasing at day 5 and 10 and then slightly decreasing at day 15. The CM-mESC-EB3 group showed the distinct temporal increase of GAG content at day 5 followed by rapid decrease during the subsequent culture time. In contrast, the CM-mESC-EB5 and EB5 groups showed a relatively constant sulfated GAG production at relatively low levels throughout the culture period, which was not significantly different. The higher content of sulfated GAG in the CM-mESC-EB1 group is in agreement with the high alcian blue stained area observed.

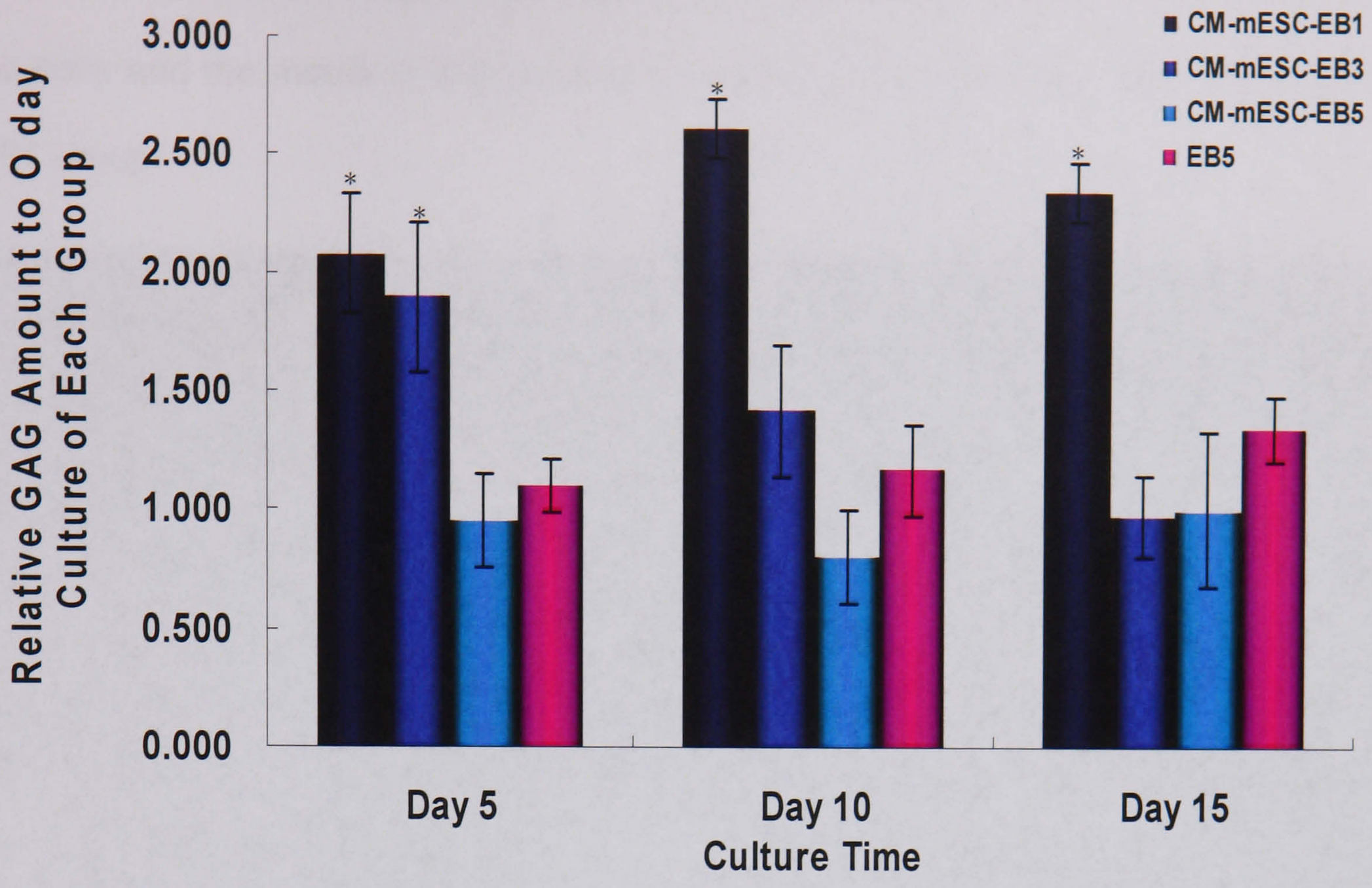


Figure 40. Quantification of relative matrix sulfated GAG amount produced by culture. The experimental and control groups are as follows: The experimental groups were mESC treated for 4 days with 50% HepG2 conditioned media (CM-mESC) followed by 1-day (CM-mESC-EB1), 3-day (CM-mESC-EB3), or 5-day (CM-mESC-EB5) EB formation period. Finally, CM-mESC-EB cultures were directed to the chondrogenic lineage for 15 days, similar to the control group, using chondrogenic medium. Control group represents mESCs maintained for 3 days in conventional maintenance medium then allowed to form EBs for 5 days (EB5) and then directed to the chondrogenic lineage for 15 days using the chondrogenic medium. Data shown as mean relative GAG content at each culture time to GAG content at 0 day culture of each test group ± SD (n=6 * $p<0.005$ compared to EB5).

4.4.3.4. Immuno-staining for chondrogenic differentiation

One of the distinct ECM proteins in cartilaginous matrix is type II collagen, which plays an important role in modulating the mechanical and structural properties of cartilage; type II collagen interacts with the minor collagens IX and XI to form heterotypic fibrils [Poole AR 2001]. As shown in figure 41, at day 15 of

culture, small islands of type II collagen matrix (green stain) were observed in both the cells and the matrix in the peripheral space around the cells in the CM-mESC-EB1 group.

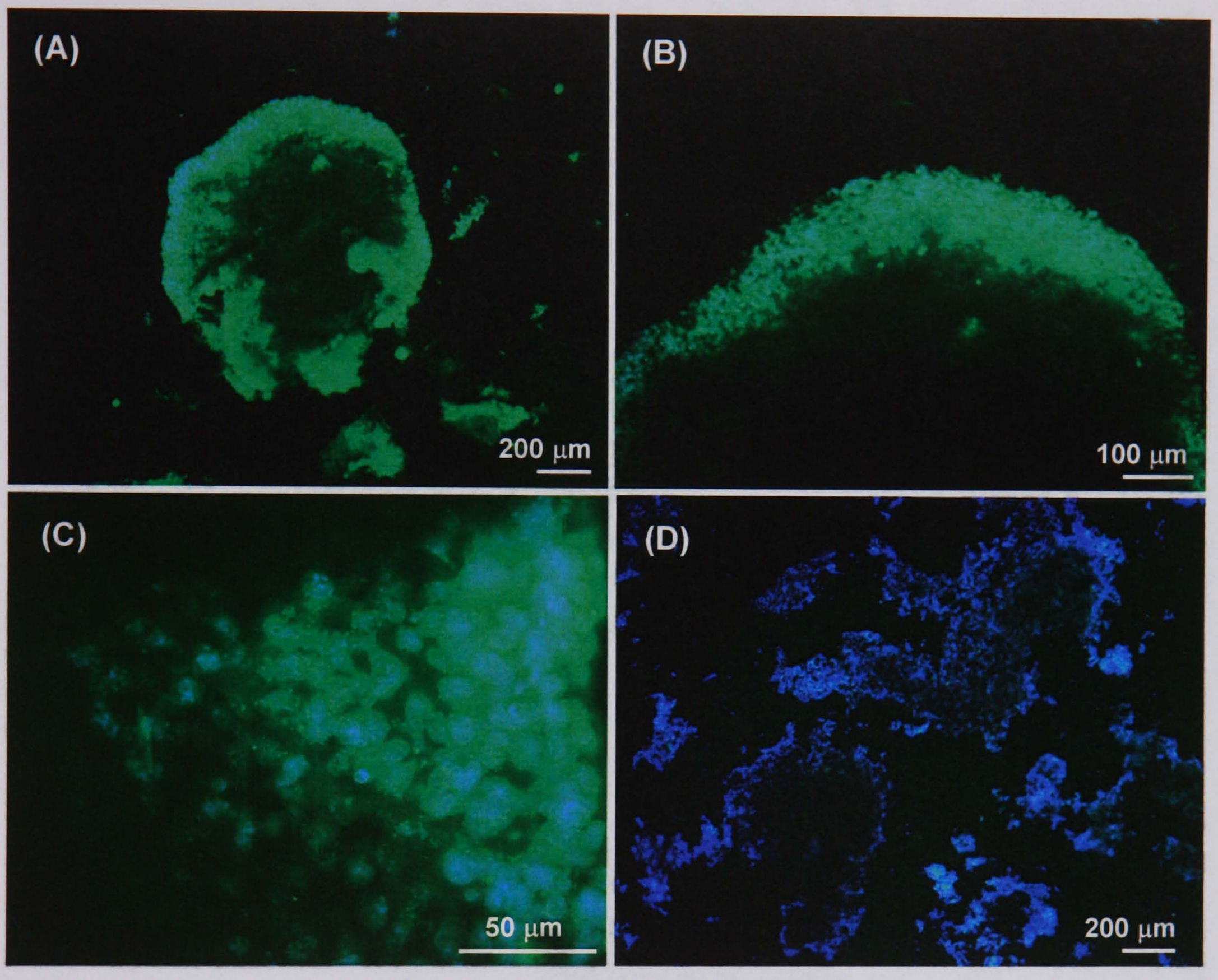


Figure 41. Immunostaining of cartilage nodules with type II collagen antibody. (A), (B) and (C) cartilage nodules after 15 day of culture with the use of anti type II collagen (Green) and DAPI (nuclear staining, blue); X 40, X 100, and X 400 magnification. (D) Negative staining with the use of anti type II collagen antibodies and DAPI.

4.4.3.5. Chondrogenic gene expression

The genotypic profiling of the chondrogenic markers using RT-PCR at different culture time points is shown in figure 42. Type II collagen can be expressed in two forms by alternative splicing; the pre-chondrogenic splice variant

(collagen IIA) and the adult splice variant (collagen IIB) [Sandell LJ 1991]. Type II collagen RNA expression for both variants was observed at substantial levels in the CM-treated mESCs with reduced EB formation time (CM-mESC-EB1). In particular, expression of the adult variant (collagen IIB) was prominent and constant during chondrogenic differentiation in CM-mESC-EB1. Consistent with type II collagen RNA expression, we observed that aggrecan expression, one of the major structural components of cartilage [Watanabe H 1998], was constant in the CM-mESC-EB1 group throughout the culture time. Finally, Sox-9 expression, a major transcription factor controlling chondrogenic differentiation [Kulyk KM 2000], appeared to be increasing with culture time during chondrogenic differentiation in the CM-mESC-EB1 group. In contrast, expression of type X collagen, a matrix protein expressed mainly in hypertrophic chondrocytes [Schmid TM 1985], was not detected in the CM-mESC-EB1 group.

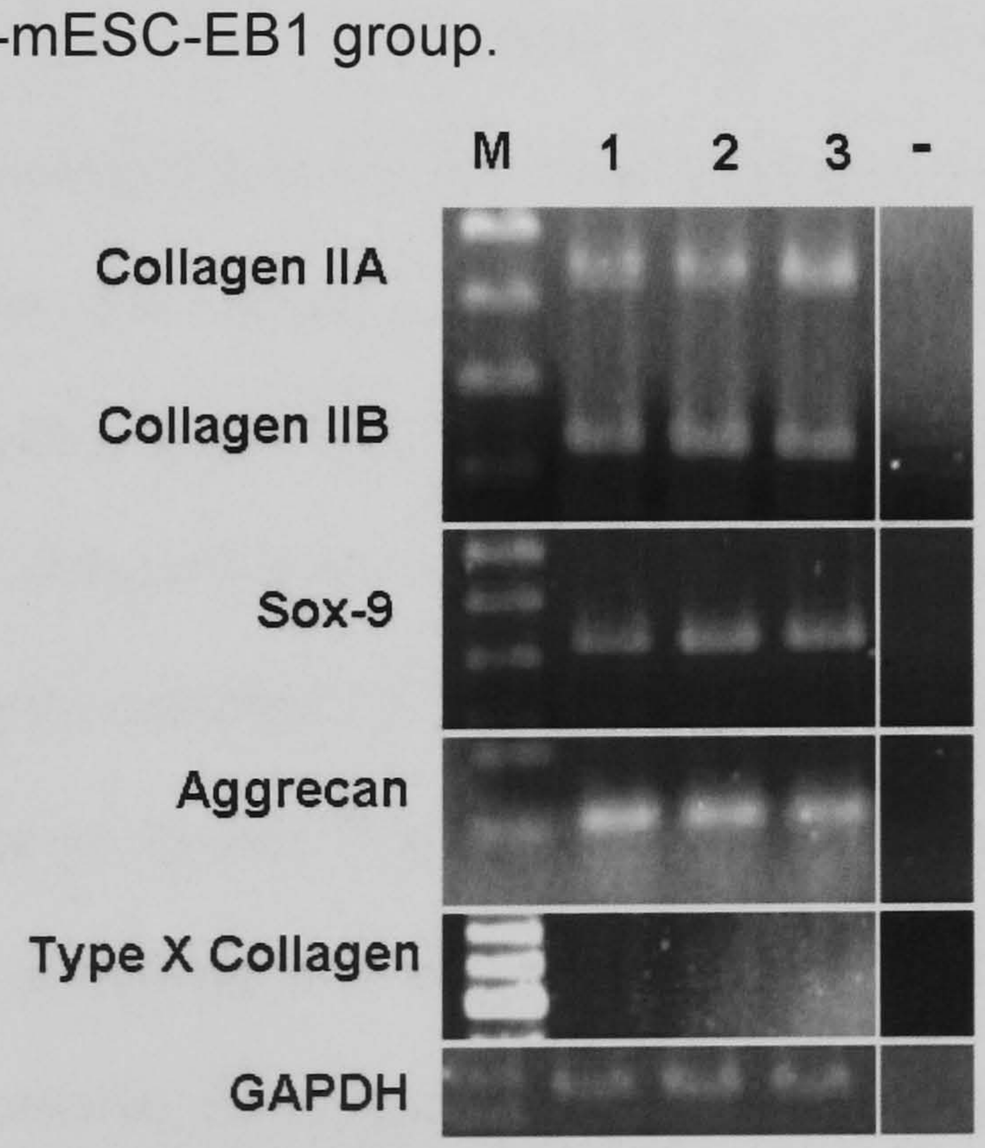


Figure 42. Molecular analysis (RT-PCR) of type II collagen, aggrecan, sox-9 and type X collagen gene expression with GAPDH control lanes. Lane M: EZ Load 100 bp Molecular Ruler. Lane 1, 2 and 3: CM-mESC -EB1 cells were cultured in chondrogenic media for 5, 10 and 15 days.

4.5. Discussion

ESC differentiation can be induced by removal of LIF and subsequent culture in suspension to generate the three germ layers, namely mesoderm, endoderm, and ectoderm, through the EB mediated spontaneous differentiation. This culture strategy has been generally accepted as the conventional way to induce further differentiation, including skeletal lineage differentiation such as cardiogenic, osteogenic and chondrogenic differentiation [Tanaka H 2004, Buttery LD 2001, Mummery C 2002, Kawaguchi J 2005]. However, this approach faces several limitations. First, the fact that all three germ layers are formed results in the competition of mesoderm formation with endoderm and ectoderm formation, thus limiting the available pool of cells and producing a heterogeneous cell population. Furthermore, once mesoderm is formed, osteogenic and chondrogenic differentiation is in competition (or even suppressed) by spontaneous cardiogenic differentiation within the intact mesoderm. Therefore, control of the desired differentiation, including at the EB formation process, is required for the enhanced and exclusive ESC differentiation to our desired specific cell type. In the previous chapter we have demonstrated that a specific cell population with high capacity to form mesoderm was generated from mESCs through HepG2-CM treatment. In this chapter, we have evaluated the osteogenic and chondrogenic differentiation as well as the spontaneous cardiogenic differentiation from this early differentiated mESCs and established a novel culture protocol to control specific differentiation.

During the early stages of embryogenesis, the mesoderm gives rise to cardioblasts, which subsequently differentiate into cardiomyocytes. Cardiogenic differentiation has been considered as a primary event in mesodermal differentiation [Arai A 1997]. It has been reported that EB formation reproduces

cardiomyocyte development and allows maturation from primitive precursor cells to highly specialized phenotypes of cardiac tissue. Within the developing EB, cardiomyocytes are located between the epithelial layer and the basal layer of mesenchymal cells [Leahy A 1999]. Cardiomyocytes are readily identifiable due to their spontaneous contraction within 1 to 4 days after plating. With continued differentiation, the number of spontaneously beating foci increases and all the EBs may contain localized beating cells [Zhou X 2003]. In this chapter, we achieved enhanced spontaneous cardiogenic differentiation of mESCs by extending the CM-mESC-derived EB formation period to 5 day (CM-mESC-EB5) without the addition of any strong cardiogenic stimulators. Specifically, at day 16 of culture there was a 4-fold increase in the number of beating colonies in the long EB-formation, CM-mESC-EB5 group generating approximately 1.7, 4.0 and 2.9 beating colonies/cm^2 at day 11, 16 and 21 of culture, respectively, as compared to the control EB5 group. In comparison, cardiomyocyte differentiation of mESCs enhanced by gene mutation after 13 days of culture by plating individual 5 day-EBs, generated approximately 3.4 beating colonies/cm^2 [Zhou X 2003]. This controlled and enhanced cardiogenic differentiation was further characterised by cardiogenic gene, Nkx-2.5, expression and molecular, sarcomeric α-actinin and tropomysin, expression. Murine Nkx-2.5 is predominantly expressed in the heart and in cardiac progenitor cells at the early developmental stage and it is widely used as one of the earliest markers of the precardiac cells [Mummery C 2002]. It has been reported that during the early stages of differentiation, cardiomyocytes within EBs are typically small and round and that the nascent myofibrils are sparse and irregularly organized or lacking, whereas others contain parallel bundles of myofibrils that show evidence of Z bands [Dabiri G 1997]. With maturation, ESC-derived cardiomyocytes become elongated with well-developed myofibrils and

sarcomeres. Herein, Nkx-2.5 gene expression as well as molecular expression of sarcomeric α-actinin and tropomysin were detected in the CM-mESC-EB5 and control EB5 groups, but not detected in both CM-mESC-EB1 and CM-mESC-EB3 groups. These results suggest that cardiogenic differentiation can be enhanced by increased mesoderm formation from the primitive streak/nascent mesoderm-like cell population and is dependent on EB formation period.

Whereas increasing the EB formation time resulted in enhanced cardiomyocyte differentiation, the extended EB formation groups, namely CM-mESC-EB5 and EB5, showed no significant difference and enhancement in bone nodule formation, ALPase activity, or Cbfa1 expression. In contrast, reducing the EB formation time resulted in significant enhancement of osteogenic differentiation in the CM-mESC-EB1, mainly, and CM-mESC-EB3 groups. The bone nodule formation assay indicated that the highest bone formation was obtained in the CM-mESC-EB1 group, where the CM-mESCs were allowed only one day of EB formation, generating 34 ± 6, 59 ± 7 and 72 ± 6 bone nodules/cm^2 at day 11, 16 and 21 of culture, respectively. A comparison with literature data shows that induction of osteogenic precursor cells from foetal tissue produced approximately 8 bone nodules/cm^2 after 19 days of culture through supplementation with ascorbic acid and glycerophosphate [Zur Nieden NI 2003]. Despite the difficulty in comparing directly with literature data, our results certainly suggest that our methodology offers improved osteogenic differentiation in terms of culture time and yield. Several *in vitro* studies for osteogenic differentiation have demonstrated that the process of osteoblast differentiation is divided into three temporal phases: proliferation, maturation/matrix synthesis, and mineralization [Abe Y 2000]. We evaluated osteogenic differentiation by assessing OB cadherin expression, Cbaf-1 expression, and the ALPase assay. OB cadherin is highly expressed in

osteoblastic cell lines and during mesenchymal cell differentiation including the osteoblastic lineage [Lecanda F 2000, Luegmayr E 2000]. OB cadherin staining was well developed in the periphery of neighbouring cells, which maintained cuboidal shapes. These results were in agreement with the bone nodule assay results. Specifically, OB cadherin was expressed only in the CM-mESC-EB1 and CM-mESC-EB3 groups at day 11 of culture, whereas it was scarcely detected in the CM-mESC-EB5 and EB5 groups. This corresponds perfectly with the bone nodule count observed for these groups. Furthermore, expression of Cbfa1 confirmed the above mentioned results. The core binding factor (Cbfa1; also known as runt related transcription factor (Runx2)) is a member of the runt homology domain family of transcription factors essential for osteoblast differentiation and bone formation and is expressed in all osteoblasts. The Cbfa1 protein has been reported to bind to the promoters of several genes that are expressed predominantly in osteoblasts and has been shown to increase the expression of osteocalcin, osteopontin, and type I collagen genes and induce ALP expression [Banerjee C 2001]. Cbfa1 expression was only observed in the CM-mESC-EB1 and CM-mESC-EB3 groups and was hardly detected in the CM-mESC-EB5 and EB5 groups at day 11, signifying the consistency of our results in terms of osteogenic differentiation. Finally, we also evaluated the ALPase activity, a key enzyme in osteogenic differentiation. Alkaline phosphatase (ALPase) belongs to a family of proteins that are anchored to the plasma membrane via a glycosyl-phosphatidinositol linkage [Wuthier RE 1985]. ALPase is widely used as a marker for the osteoblast phenotype, not least because of the simplicity with which it can be assessed. Osteoblasts express the tissue-non specific form of the enzyme. High levels of ALPase are seen in both pre-osteoblasts and osteoblasts *in vivo* and in differentiating osteoblasts *in vitro*. The biological function of ALPase

is still unknown except for a role in bone mineralization. Our results indicate that the CM-mESC-EB1 group, which has consistently showed the most enhanced osteogenic differentiation, had a 3-fold increase in ALPase activity as compared to the background levels of the other groups. This is consistent with the full gamut of our results and the transient nature of osteogenic differentiation *in vitro*.

In the parallel study to the osteogenic differentiation, chondrogenic capacity of the CM-mESCs was evaluated. Recently, many attempts have been made to induce in vitro differentiation of ESCs into the chondrogenic lineage. Kramer et al. have reported in 2000 that BMP-2 and BMP-4 directs ESCs to the chondrogenic fate when added during day 3–5 of EB differentiation [Kramer J 2000]. Those chondrocytes isolated from the EBs possess a certain plasticity to undergo hypertrophy and calcify [Kramer J 2000]. In contrast, others have shown that skeletal lineage differentiation of ESCs is highly dependent on the type of growth factor or supplement, and indicated that BMP-4 acted predominantly to promote osteogenic differentiation and retinoic acid treatment of EBs followed by TGF-β3 treatment of outgrowths was sufficient to induce chondrogenesis from ESCs [Kawaguchi J 2005]. In another report, chondrogenesis was enhanced by the addition of dexamethasone in intact EB cultures [Tanaka H 2004]. In a different approach, it has been reported that mesodermal progenitor cells, identified as PDGFRα$^+$ and/or foetal liver kinase-1 (flk)$^+$ cells, were isolated from ESCs using FACS sorting, whereby macroscopic cartilage formation was achieved in EB cultures by supplying various growth factors such as IGF-I, TGF-β3, BMP-4 and PDGF [Nakayama N 2003]. In conclusion, the vast majority of methods for the derivation of the chondrogenic lineage from ESCs are based on EB culture system. To our knowledge, this is the first report demonstrating the derivation of chondrogenic cells from mESCs using enhanced mesoderm progeny and a single

cell unit culture system producing macroscopic cartilage formation.

In this chapter, we demonstrate the derivation of chondrocytes from mESCs. Specifically, the presence of matrix components produced by chondrogenic cells was confirmed by the Alcian blue staining. In particular, the extent of Alcian blue staining was higher in the CM-mESC-EB1 group, which was allowed only 1 day of EB formation, consistent with the higher levels of GAG content proved by DMMB assay. These CM-mESCs derived chondrocytes organized cartilage-like nodules in two dimensional cultures showing intensive staining for GAG and type II collagen expression. In addition, an Alcian blue and Alizarin red S double staining confirmed that the cartilage-like nodules in the CM-mESC-EB1 could be attributed to the chondrocytes derived, which was in contrast to the results obtained from the other groups, including the control group, where multiple lineage differentiation, including cardiogenic differentiation, was occurring. Beating colonies could be easily detected in all experimental groups except the CM-mESC-EB1 in accordance with the results obtained from our osteogenic differentiation. The RT-PCR results confirmed the enhanced chondrogenic obtained in the CM-mESC-EB1 group with the expression of genes characteristic for chondrogenic differentiation such as type II collagen [Sandell LJ 1991], aggrecan [Watanabe H 1998], and sox-9 [Kulyk KM 2000] throughout whole culture period. It has been well established that the pre-chondrogenic splice variant (collagen IIA) and adult splice variant (collagen IIB) are differentially regulated according to the differentiation stage of chondrogenic cells and that collagen IIA is usually upregulated in the initial stage of chondrogenic differentiation and collagen IIB is expressed highly in maturation stage of chondrogenic cells [Sandell LJ 1991, Hegert C 2002]. However, in our study, the mRNA levels of collagen IIA and IIB were similar in CM-mESC-EB1 group

throughout the culture period. A possible explanation for these results is that a heterogeneous population with different maturation stages in the CM-mESC-EB1 group was produced. This clearly necessitates further investigation in order to achieve the production of the required homogenous population at the same maturation stage for any future clinical applications. Therefore, our results clearly indicate that increasing the EB formation time results in enhanced cardiogenic differentiation and reducing the EB formation time results in significant enhancement of osteogenic/chondrogenic differentiation.

4.6. Conclusion

In conclusion, controlling the EB formation period of the mESCs treated with the conditioned medium resulted in the preferential stimulation of cardiogenic, osteogenic or chondrogenic differentiation, respectively. Reducing the EB formation time to 1 day resulted in the enhanced osteogenic or chondrogenic differentiation, which was superior to the conventional EB formation process. This could provide the basis for a new approach for the up-regulation of specific mesodermal differentiation pathways for ESCs that could have applications in bone and cartilage tissue engineering.

CHAPER V

IN VITRO DIRECT OSTEOGENIC AND CHONDROGENIC DIFFERENTIATION OF MURINE EMBRYONIC STEM CELLS WITHOUT EB FORMATION PROCESS

5.1. Introduction

In vitro differentiation of ESCs can eventually lead to clinical applications by generating large quantity of the desired cells or tissues suitable for bone and cartilage defects. Many proposed applications of ESCs for skeletal tissue regeneration, such as bone and cartilage regeneration, are predicated on the assumption that it will be possible to obtain pure populations of differentiated cells, such as osteoblasts and chondrocytes from ESCs. To obtain physiologically functional specific lineage cells from ESCs that are suitable for transplantation, controlled differentiation procedures must be implemented.

Table 8: Current approaches for *in vitro* EB mediated osteogenesis and chondrogenesis

OSTEOGENESIS	CELL	CULTURE STRATEGY
Buttery *et al* 2001	mESC (E14)	EB formation (5 days) → trypsinisation → 2D culture
Kawaguchi *et al* 2005	mESC (E14)	EB formation (5 days) → Direct EB plating and culture
Bielby *et al* 2005	mESC (E14)	EB formation (5 days) → trypsinisation → 2D culture
Garreta *et al* 2006	mESC (R1)	EB formation (8 days) → trypsinisation → 2D culture and 3D culture
Cao *et al* 2005	hESC (H9)	EB formation (4-5 days) → Direct EB plating and culture
CHONDROGENESIS	**CELL**	**CULTURE STRATEGY**
Kawaguchi *et al* 2005	mESC (E14)	EB formation (5 days) → Direct EB plating and culture
Kramer *et al* 2000 & 2005	mESC (D3)	EB formation (5 days) → Direct EB plating and culture
Nakayama *et al* 2003	mESC (E14)	EB formation (3-5 days) → trypsinisation → Micromass 2D culture, Pellet culture
Tanaka *et al* 2004	mESC (E14)	EB formation (5 days) → Prolonged EB culture in hydrogel or → trypsinisation → Micromass 2D culture,
Hwang *et al* 2006 (1)	mESC (D3)	EB formation (5 days) → Prolonged EB culture in hydrogel or→ Direct EB plating and culture

A range of approaches have been developed to achieve this. For *in vitro* osteogenic and chondrogenic differentiation, the most widely used protocol for the induction of spontaneous differentiation is that of embryoid body (EB) formation for the early differentiation of ESCs to form mesoderm or mesoderm progenitors, along with the two other germ layers. This spontaneously formed mesoderm provides potent pool of progenitors for following further osteogenic and chondrogenic lineage differentiation [Tanaka H 2004, Buttery LD 2001, Kawaguchi J 2005, Bielby RC 2005, Nakayama N 2003, Kramer J 2005, Cao T 2005, Hwang NS 2006(1)]. The EBs are typically replated in monolayer cultures, after around 5 days of EB formation followed by terminal differentiation.

Under the suspension culture system for EB formation, early differentiation of ESCs in EBs is processed in two phases. Within the first 2–4 days of EB formation, ESC aggregates give rise to simple EBs containing an outer layer of endodermal cells, then these cells begin to synthesize extracellular matrix molecules, such as laminin, and a complete basement membrane is laid down between the primitive endoderm cells and the remaining undifferentiated ESCs within EB. Shortly afterwards, the ESCs within the EB start to differentiate to epiblast cells and, subsequently, around day 4 some of the epiblast cells that are aligned against the basement membrane polarize to form a columnar epithelium, while the inner cells of simple EBs undergo the process of programmed cell death to form cystic EBs with the formation of a central cavity formed by apoptosis and differentiation of a columnar epithelium with a basal lamina, a process called cavitation. Cavitation becomes evident when the resultant cellular debris is phagocytosed by the cells of the epiblast derived epithelium [Coucouvanis E 1995, Li S 2002] (Figure 43). This cavitation by programmed cell death is an inevitable, spontaneous process, making control of cell death within the EBs very difficult,

thus resulting in loss of available cells for terminal differentiation.

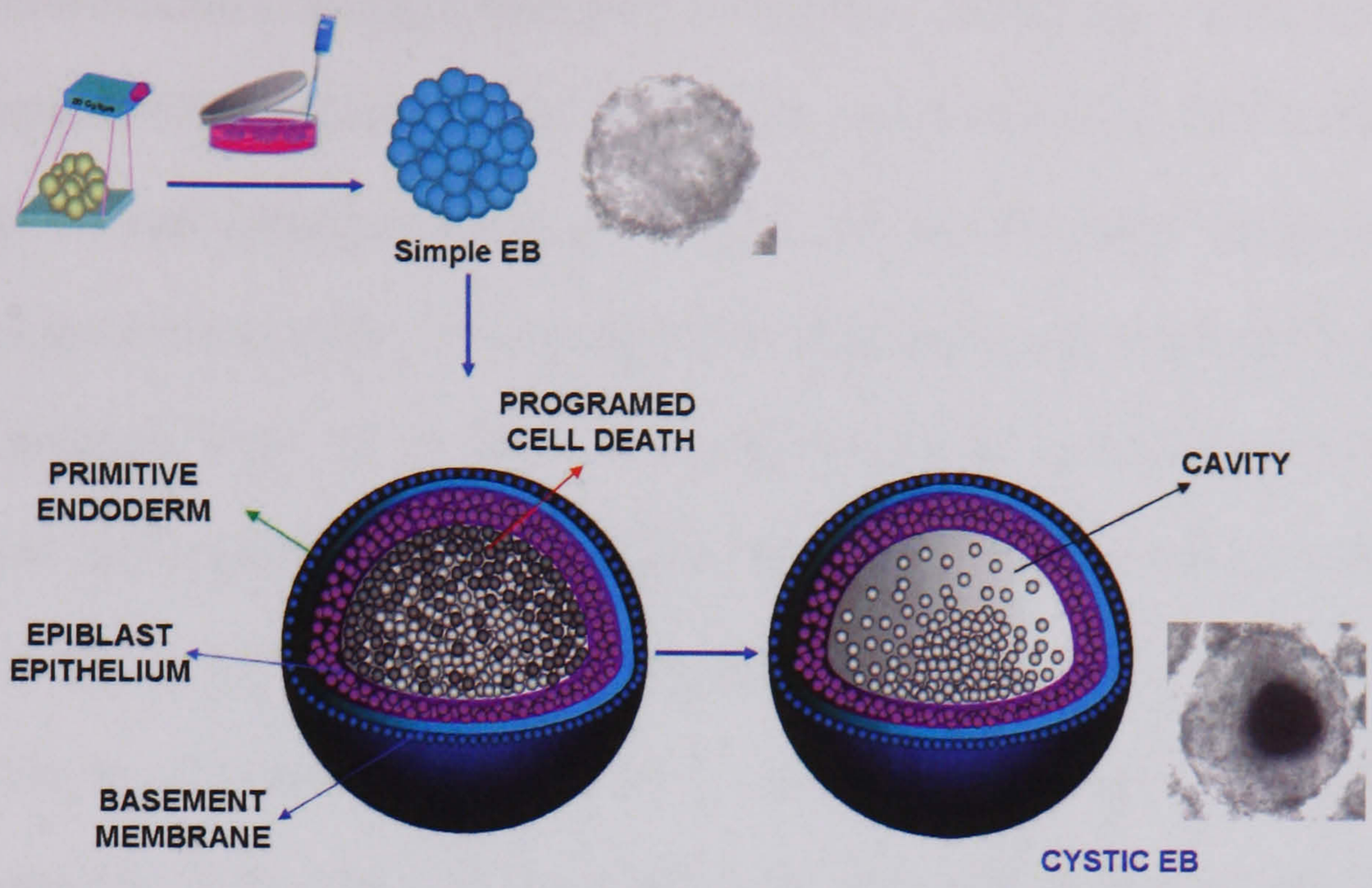


Figure 43. Schematic illustration of cystic EB formation.

Furthermore, despite the tremendous amount of research on ESC differentiation by employing EB formation, limited knowledge exists concerning the culture conditions and requirements of EB culture and the differentiation mechanism(s) and cellular interactions occurring during EB formation. Thus, little is known about the process guiding the development of the three germ layers and the specific lineage of cells within the EBs [Khoo MLM 2005].

Recently, attempts have been made to induce specific lineage differentiation of ESCs directly by completely bypassing the EB formation process. Lee et al reported the screening of 880 compounds for their capability to induce cardiogenic differentiation efficiently using established ESC clones that expressed EGFP under the transcriptional control of a cardiac specific promoter, α-MHC promoter, and a compound, ascorbic acid, markedly increased the differentiation of ESCs into cardiac myocytes directly in 2D culture without EB formation process [Takahashi T 2003]. In addition, in their study, it was reported that monolayer

culture of ESCs without EB formation reduced background differentiation, other lineage differentiation, and enabled high-throughput screening [Takahashi T 2003]. For osteogenic differentiation of ESCs, Langer and colleagues demonstrated ESC differentiation into osteogenic lineage without the EB formation step showed a 7-fold increase in the number of osteogenic lineage cells and the spontaneous bone nodule formation after 10-12 days in the presence of an osteogenic medium in comparison with osteogenic differentiation through 5 days of EB formation. When the ESCs were allowed to form EBs and the EBs were replated following dissociation, bone nodules formed after 4 weeks of culture only in the presence of dexamethasone. This research suggests that ESC differentiation into osteogenic lineage cells without an EB step can be used to derive large quantities of functional osteogenic cells for bone tissue engineering [Karp JM 2006]. From the literature, it is evident that the need of novel method to control and enhance lineage specific differentiation more efficiently is required, and increasing the efficiency of deriving specific lineage cells from ESCs would likely require better control over the cell microenvironment.

5.2. Objectives

The aim of this chapter is the development of a efficient culture process/system for directing and enhancing direct lineage-specific differentiation of mESCs into osteogenic/chondrogenic lineages which consists of two culture phases: a) mESCs differentiation into primitive streak/nascent mesoderm-like cells through the use of HepG2 conditioned medium in order to acquire potent cell source and b) terminal osteogenic/chondrogenic differentiation in osteogenic/chondrogenic culture media directly from the primitive streak/nascent

mesoderm-like cell population without the EB formation process.

5.3. Experimental Process

Previously we have shown that mESCs differentiate into primitive streak/nascent mesoderm like cells by the treatment of HepG2 conditioned medium (Chapter III) and that this cell population showed enhanced *in vitro* osteogenic or chondrogenic differentiation through the modulation of EB formation period (Chapter IV). In this chapter, direct *in vitro* osteogenesis or chondrogenesis of mESCs was achieved by removing EB formation process resulting in a novel culture strategy that is more efficient, controlled, reproducible, and amenable to automation for application to skeletal tissue engineering. Specifically, mESCs were plated on tissue culture plates and cultured in 50:50 HepG2 conditioned medium for 3 days in order to induce early differentiation into a primitive streak/nascent mesoderm like cell population, followed by terminal differentiation into osteogenic or chondrogenic lineages by simply replacing the conditioned medium with osteogenic or chondrogenic media containing the appropriate supplements such as β-glycerophosphate, ascorbic acid and dexamethasone (osteogenesis) or ascorbic acid, dexamethasone and TGFβ1 (chondrogenesis). Thus direct osteogenic or chondrogenic differentiation without EB formation was assessed using various techniques such as, characterisation of mineralised bone nodules, bone nodule formation assay, alkaline phosphatase expression, cartilage nodule formation assay, immunocytochemical characterisation, RT-PCR, and other specific ECM and lineage specific enzyme activity evaluation, which detailed explanation was described at CHAPTER II. The overall experimental process was illustrated in figure 44.

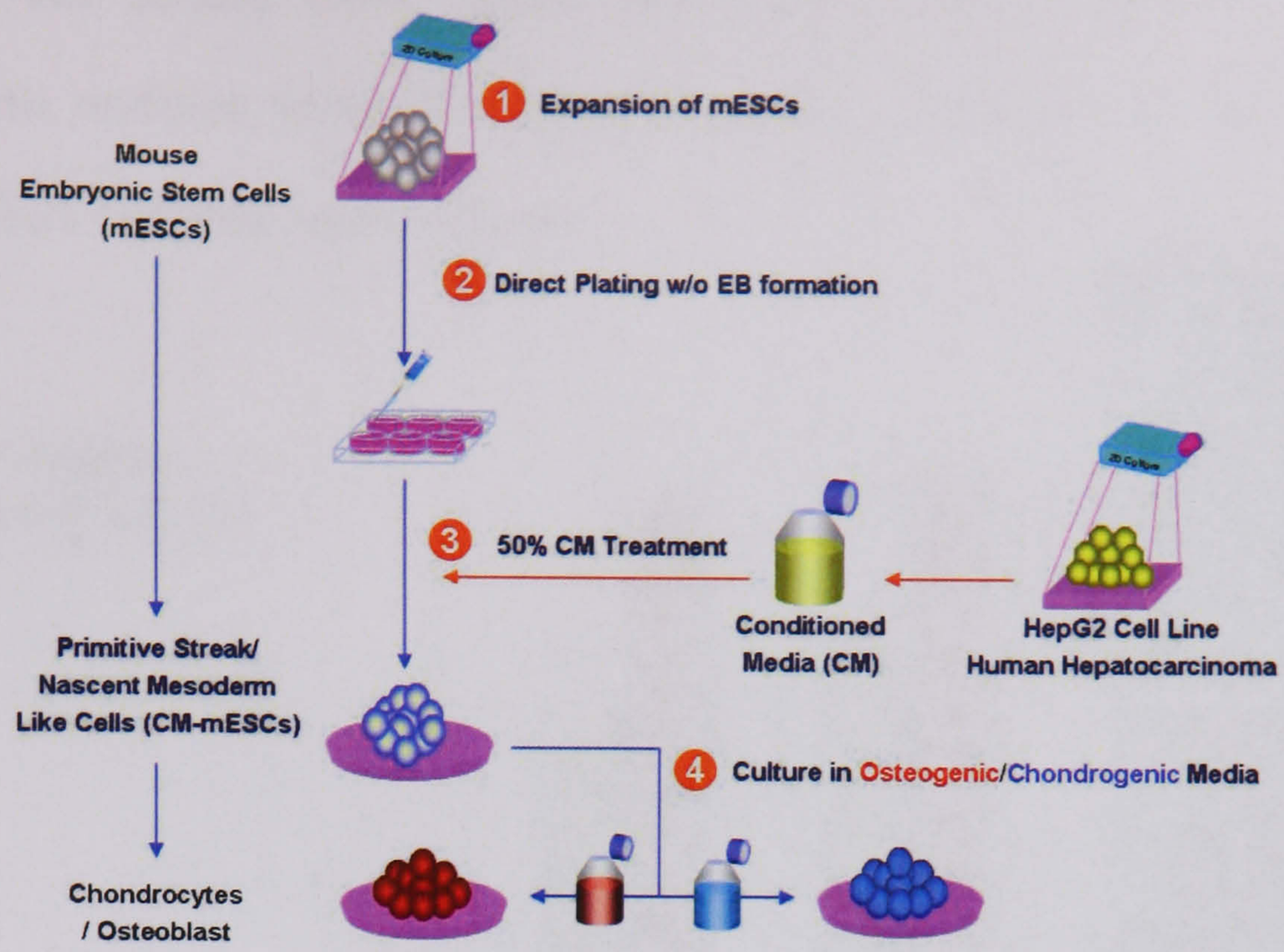


Figure 44. Schematic illustration of direct *in vitro* osteogenesis and chondrogenesis without EB formation process

5.4. Results

5.4.1. Direct osteogenic differentiation

5.4.1.1. Bone nodule formation and quantification

Bone development *in vitro* is routinely assessed via the formation of bone nodules [Sottile V 2003, Woll NL 2006, Zur Nieden NI 2003, Buttery LD 2001, Bielby RC 2005]. The bone nodule formation assay was performed using specific Alizarin red S (ARS) staining and the quantification of extracted ARS from stained bone nodules using the cetylpyridinium chloride (CPC) extraction method [Gregory CA 2004]. As shown in figure 45, the stained area increased with culture time as differentiation progressed; distinct mineralisation was induced from day 11 of osteogenic culture in both groups with the conditioned medium-treated mESCs (CM-mESCs) showing enhanced mineralization than the control mESCs

throughout the culture time. Specifically, approximately 50% increase in the stained bone nodules formed in the CM-mESCs cultures as compared to the control mESCs cultures was obtained.

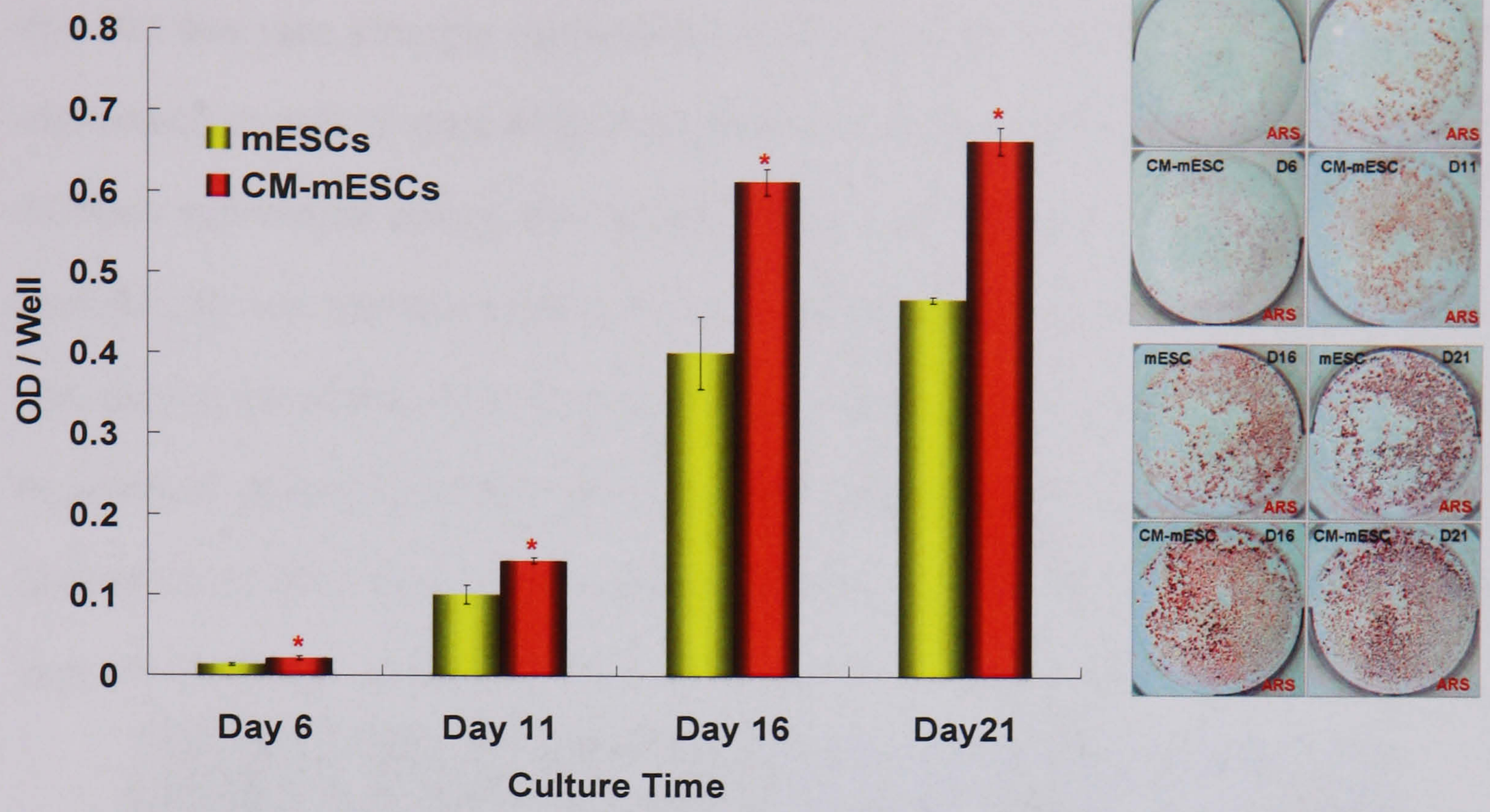


Figure 45. Alizarin red S quantification for evaluating bone nodule formation. mESCs: non-treated normal mESCs. CM-mESCs: HepG2 conditioned media treated mESCs Data are shown as mean OD ± SD (n = 6; *$p < 0.05$ compared to mESCs).

5.4.1.2. Characterisation of mineralised bone nodule

It has been well demonstrated that ascorbic acid is necessary for formation of the collagenous matrix and β-glycerophosphate for subsequent mineralisation, which is mainly cell mediated through alkaline phosphatase activity expressed by osteogenic cells [Bellows CG 1991, Bellows CG 1986]. In addition, phosphate ions are required for mineralisation *in vitro* with β-glycerophosphate being the source [Binderman I 1979]. However, spontaneous non-specific mineral precipitation, which may not be cell-mediated, may be generated from the culture medium's phosphate and calcium content. Herein, in order to evaluate whether bone nodule formation was cell-mediated or was non-specific mineral precipitation, the

mineralised nodules were characterised by ALPase expression and alizarin red S staining. Under light microscopy, dark irregular shaped mineral deposition could be easily detected mainly at the central space in cell aggregations (Figure 46A), and ALPase was strongly expressed only around the mineral deposits with slight expression in cells (Figure 46B). Accompanied with morphological observation and ALPase expression assay, the calcium deposit on mineralised bone nodules was stained calcium specific alizarin red S, and figure 46C shows a strongly stained red spot on mineralize nodules with slightly stained region around mineral deposits. In addition, when the alizarin red S-stained area was exposed to filtered UV light (excitation at 530-560 nm and emission at 580 nm), the detection of fluorescence was confined only on mineral deposits, as shown in figure 46D.

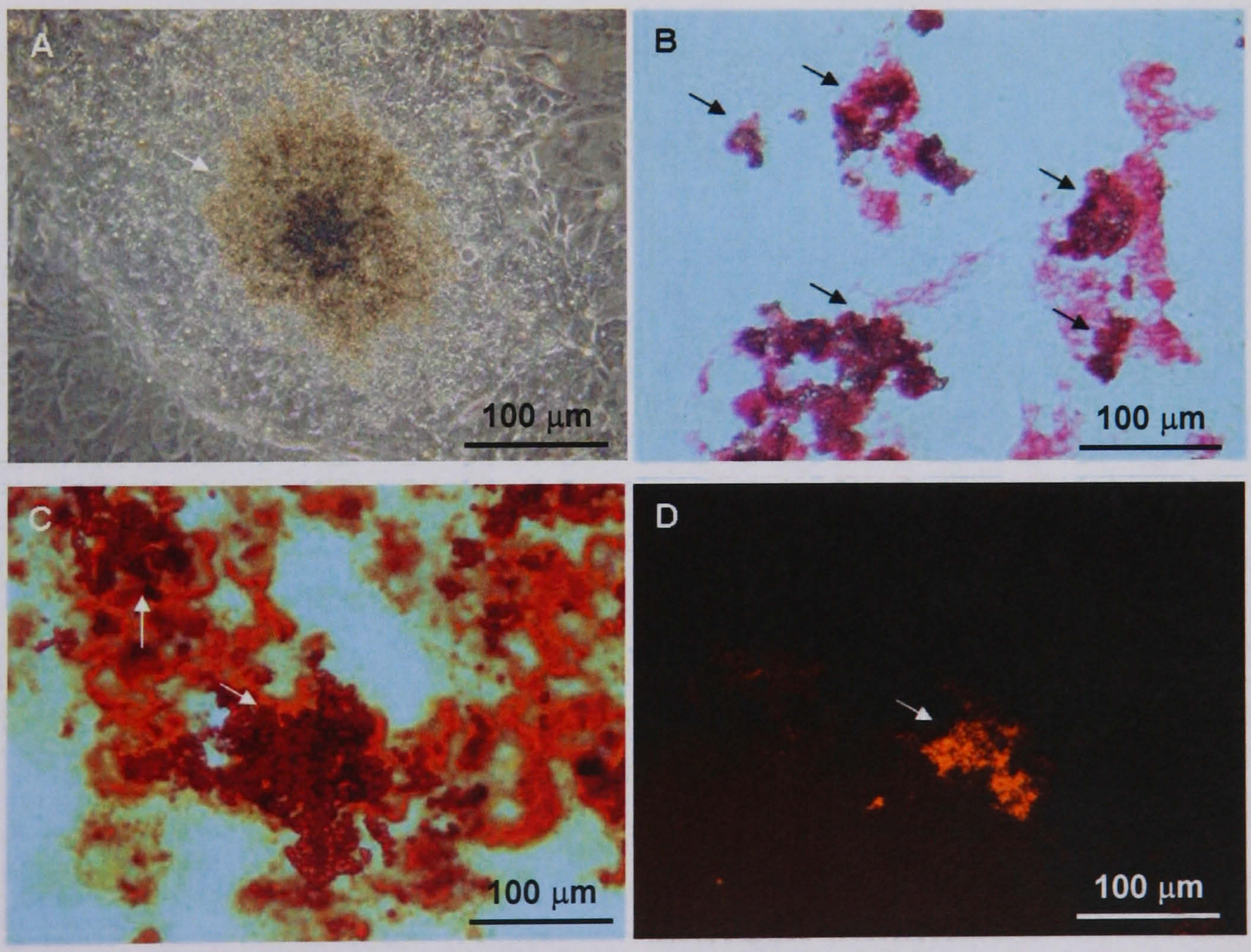
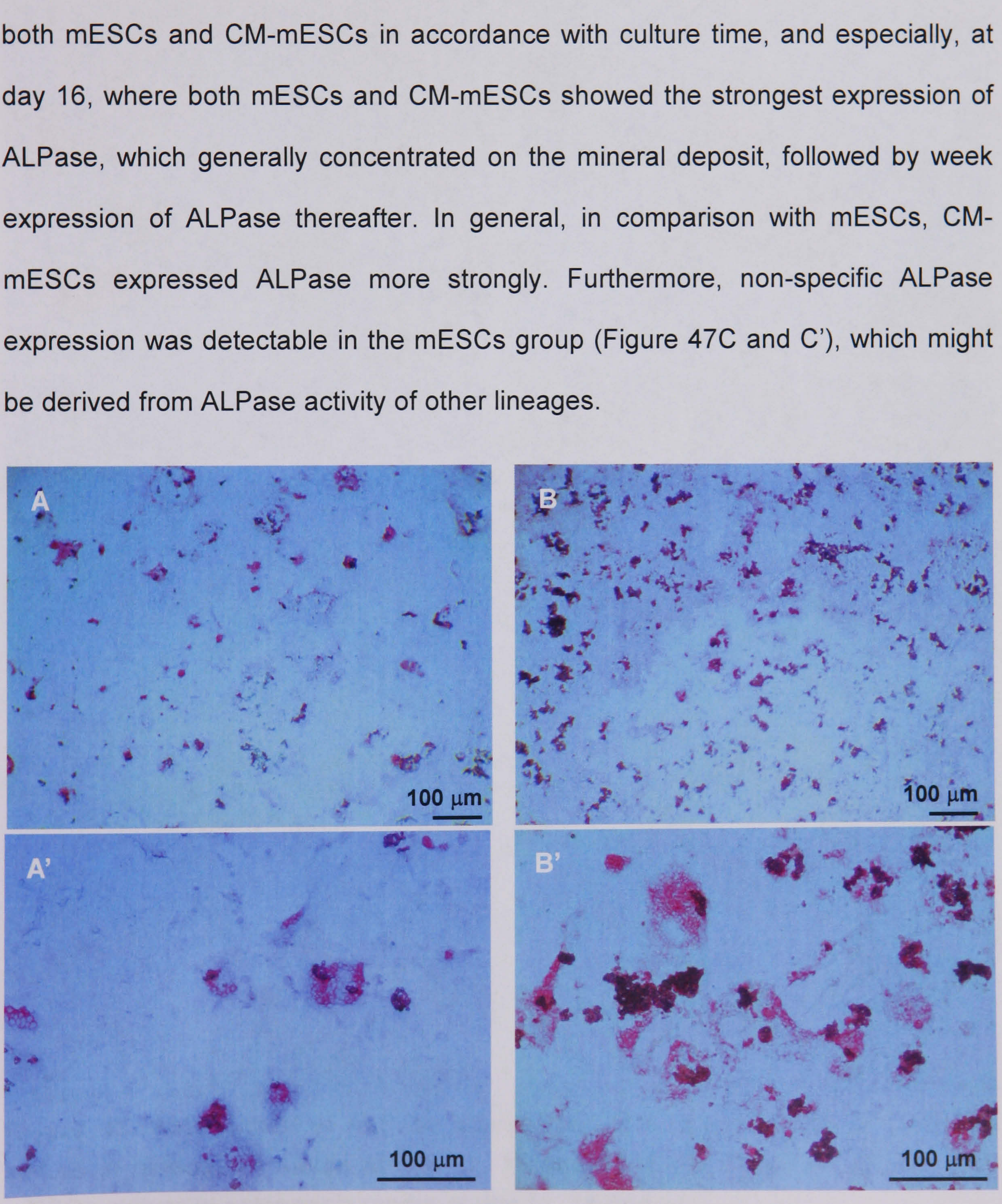


Figure 46. Characterisation of mineralised bone nodules; (A) Morphology of bone nodule under light microscopy. (B) ALPase expression on bone nodules. (C) Alizarin red S stained bone nodules under light microscopy. (D) Alizarin red S stained bone nodules showing fluorescence. Arrow indicates mineral deposits.

5.4.1.3. ALPase expression and activity quantification

In order to characterize the osteogenic differentiation stage of the control mESCs and experimental CM-mESCs in osteogenic medium, expression and time-course analysis of ALPase activity, which is widely used as a marker of mineralization and as a marker of the osteoblast phenotype, was evaluated. As show in figure 47, the gradual increase of ALPase expression was detected in both mESCs and CM-mESCs in accordance with culture time, and especially, at day 16, where both mESCs and CM-mESCs showed the strongest expression of ALPase, which generally concentrated on the mineral deposit, followed by week expression of ALPase thereafter. In general, in comparison with mESCs, CM-mESCs expressed ALPase more strongly. Furthermore, non-specific ALPase expression was detectable in the mESCs group (Figure 47C and C'), which might be derived from ALPase activity of other lineages.



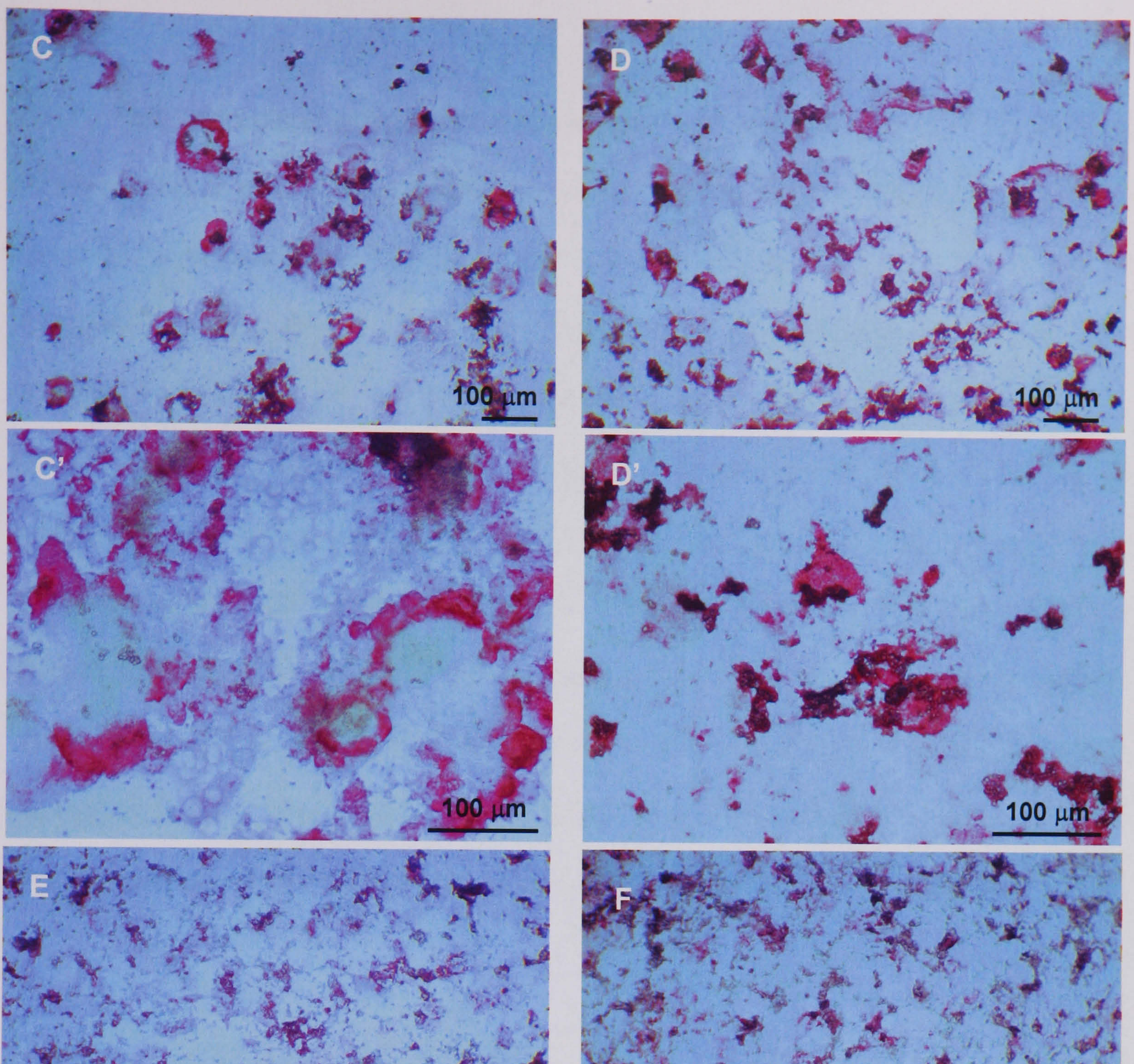


Figure 47. Assessment of ALPase expression. A, C, E and A', C', E' ; mESCs culture in osteogenic media at day 11, 16 and 21. B, D, F and B', D', F' ; CM-mESCs culture in osteogenic media at day 11, 16 and 21.

The expression of ALPase was supported by the quantification of ALPase activity using a colorimetric assay. As shown in figure 48, CM-mESCs showed relatively lower level of ALPase activity in comparison with mESCs at day 0 prior to osteogenic differentiation. Following osteogenic differentiation, consistent with ALPase expression, enzyme activity showed a time-dependent behaviour with a marked increase at day 16 and then a decrease to background levels from day 21 onwards in both mESCs and CM-mESC culture in osteogenic medium. Specifically, ALPase activity was enhanced around 1.6-fold ($P<0.05$) in the CM-mESC in comparison with the control mESC group at day 16 of the osteogenic culture, which were 485.3 ± 43.6 PNPμM/min/mg in the CM-mESC and 320.2 ± 24.9 PNPμM/min/mg in the mESC. This temporal increase of ALPase activity in both CM-mESC and mESC correlates with the increased bone nodule formation.

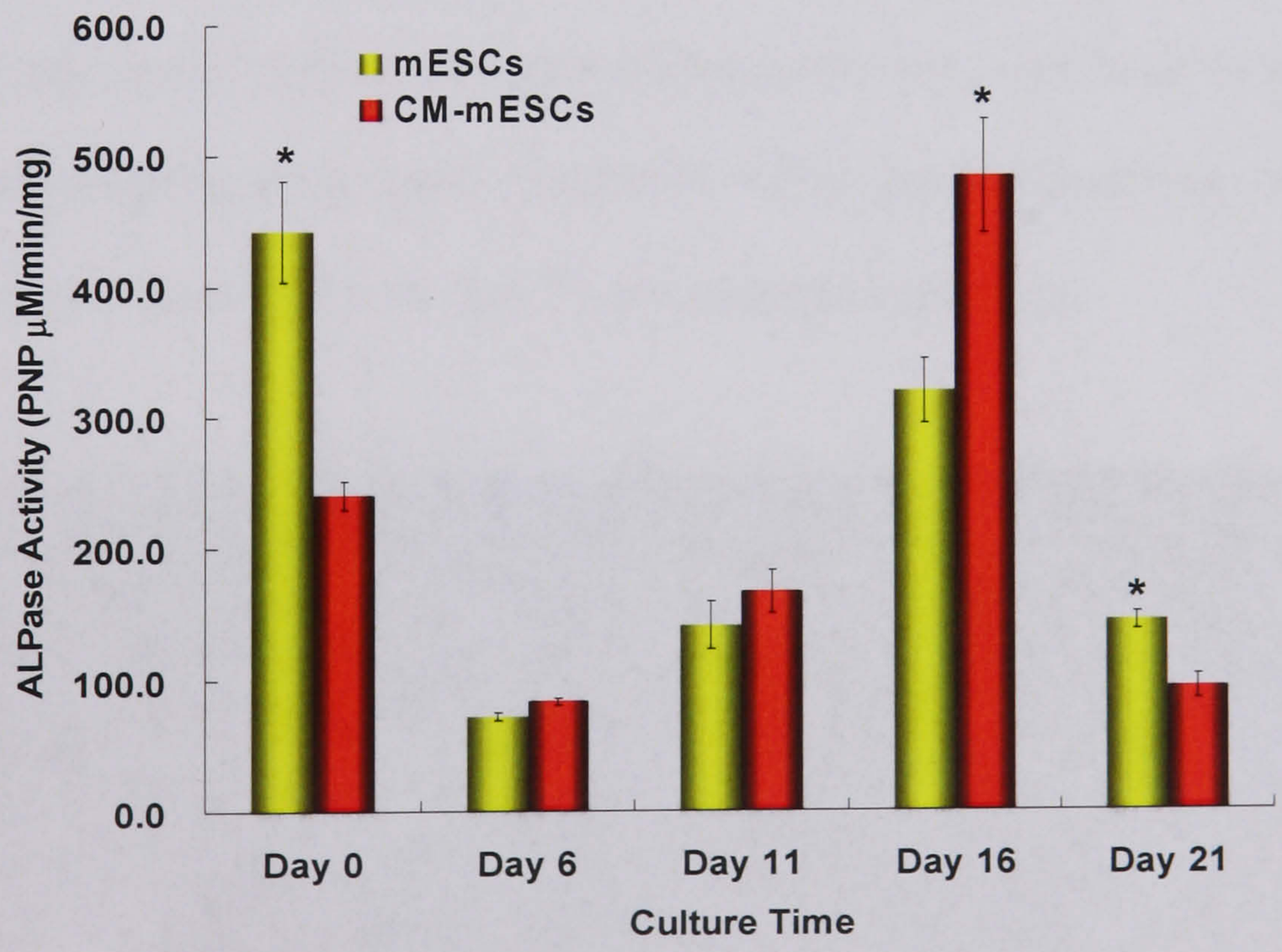


Figure 48. Colorimetric assay for assessing ALPase activity. mESCs; non-treated normal mESCs. CM-mESCs; HepG2 conditioned media treated mESCs. Data are shown as mean enzyme activity ± SD (n = 6; *$p < 0.05$ compared to mESCs).

5.4.1.4. Immuno-staining for osteogenic differentiation

Osteoblast differentiation is controlled by the extracellular environment. The principal role of osteoblasts in bone formation is to secrete the matrix framework upon which bone is built by actively synthesizing many proteins during their developmental and maturation stages. This matrix framework is mainly composed of densely packed type I collagen fibrils infiltrated by hydroxyapatite (HA) crystals and small amounts of distinctive non-collagenous proteins, such as osteopontin. Osteopontin (OPN) is a highly phosphorylated sialoprotein that is a prominent component of the mineralized extracellular matrices of bones [Sodek J 2000]. In osteoblast differentiation, type I collagen and OPN are constitutively and regularly expressed [Zhu JX 2001, Chen Y 1992, Zhou HY 1995]. Herein, osteogenic differentiation was further characterized by assessing type I collagen and OPN expression. As shown in figure 49, at day 21 of culture type I collagen and OPN were very strongly expressed in the CM-mESCs cultured in osteogenic medium. In particular, type I collagen immunostaining was well developed in the periphery of neighbouring cells. Similarly, OPN immunoreactive cells could be observed in the CM-mESCs at day 21 of osteogenic culture.

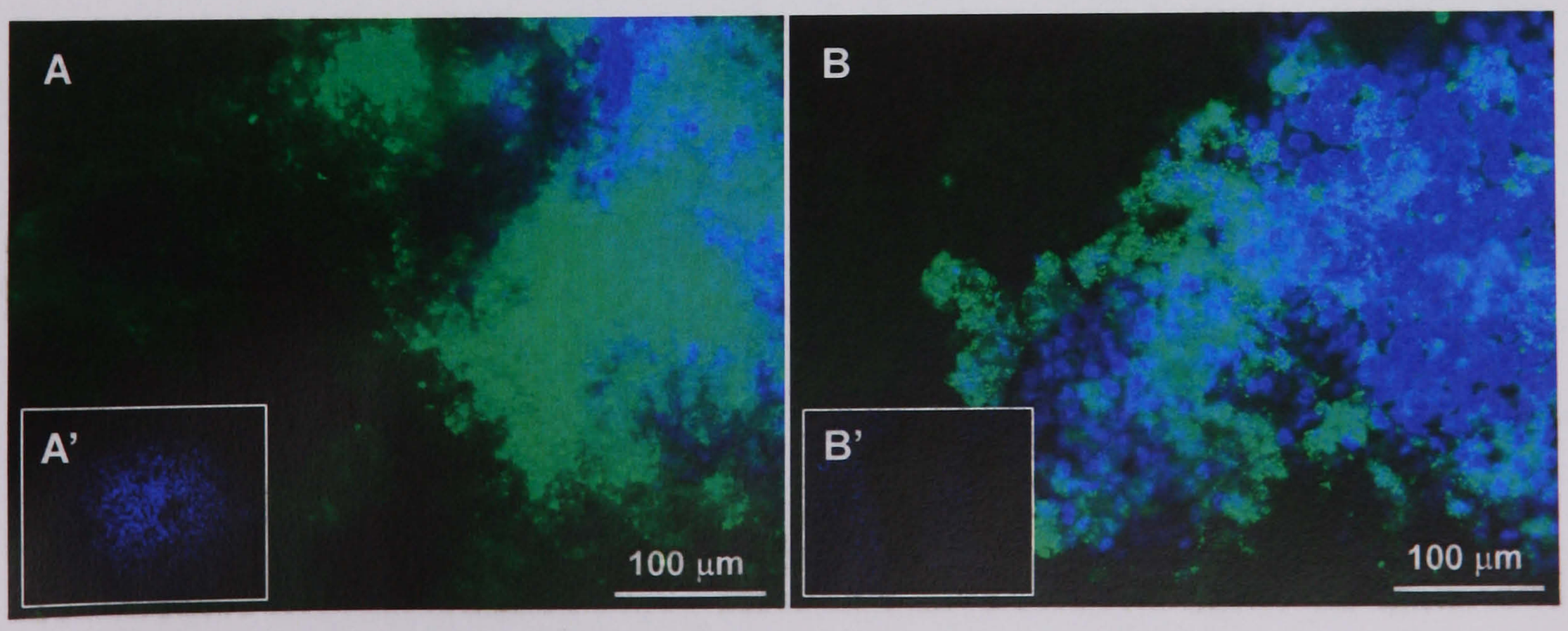


Figure 49. Immunocytochemical staining for type I collagen and osteopontin

(OPN) in CM-treated mESC-derived cultures. (A) Expression of type I collagen (green) and nuclear staining (DAPI; blue) at day 21 of culture in the cmES-EB1-derived osteogenic cells. (B) Expression of osteopontin (OPN) (green) and nuclear staining (DAPI; blue) at day 21 of culture in the cmES-EB1-derived osteogenic cells. Inset (A') and (B') shows negative control for non-specific binding of the primary antibody.

5.4.1.5. Osteogenic gene expression

It is well known that core binding factor Cbfa1/Runx2 is an essential transcription factor required for osteoblast recruitment and differentiation and bone formation [Banerjee C 2001] and that Osterix is a bone-related transcription factor that controls both growth and differentiation in osteoblasts and osteogenic differentiation of ESCs [Nakashima K 2002, Guanping T 2004]. In addition, the osteocalcin gene encodes an osteoblast-specific protein that is induced with the onset of mineralization at late stages of differentiation [Viereck V 2002]. Herein, the direct osteogenic differentiation of mESCs without EB formation was evaluated at the genetic level by examining the expression of osteocalcin, Cbfa1/Runx2 and osterix using RT-PCR. As shown in figure 50, gene expression confirmed osteogenic differentiation for both mESCs and CM-mESCs derived osteoblasts. Specifically, Cbfa1/Runx2 expression was constant throughout the culture period for both groups, yet a relatively stronger expression of osteocalcin and osterix was observed in the CM-mESCs in comparison to the mESCs. These results are in agreement with the bone nodule formation assay, mineralised nodule characterisation and type I collagen and osteopontin immunostaining results demonstrating the correlation between mineralised bone nodule formation and osteogenic marker expression and osteoblast related gene expression.

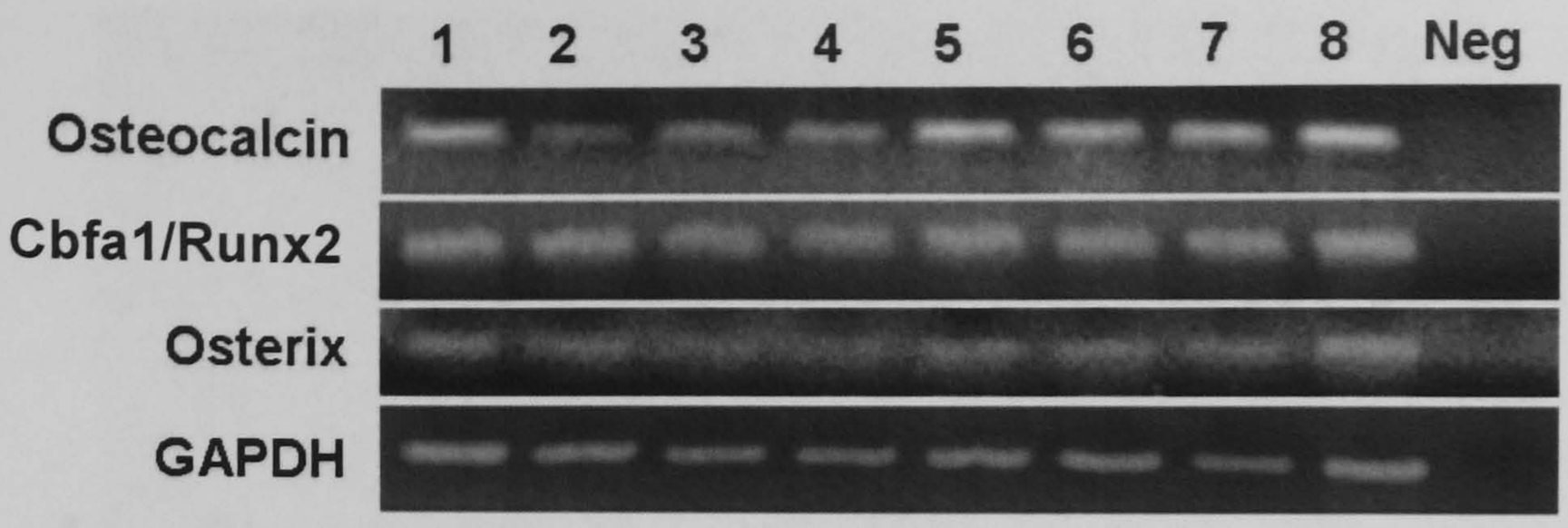


Figure 50. RT-PCR analysis of osteogenic gene expression. GAPDH gene expression was used at the housekeeping control. Lane 1 – 4: osteogenic culture of mESCs for 6, 11, 16 and 21 days. Lane 5 – 8: osteogenic culture of CM-mESCs for 6, 11, 16 and 21 days.

5.4.2. Direct chondrogenic differentiation

5.4.2.1. Morphological evaluation

Herein, the control, mESCs, and experimental, Cm-mESCs, groups were subjected to the high cell density micromass culture with chondrogenic supplements, such as dexamethasone, ascorbic acid and TGF-β1 without EB formation. Distinct cartilage nodule-like structures could be observed in with different frequency in both the CM-mESCs and mESC groups, where cells formed three-dimensional round shaped aggregates, as seen in figure 51A and B; the frequency being higher in the CM-mESC group. Following 15 days of chondrogenic differentiation, cartilage nodules containing round-shaped chondrocytes were observed with the nodules exhibiting a distinct structure comprising of round-shaped cells separated by extracellular matrix surrounded by a circular arranged fibrillar matrix that was easily detected by light microscopy. However, in the control mESC cultures, different morphologies could be detected easily which might indicate other lineage differentiation (Figure 51 C and D).

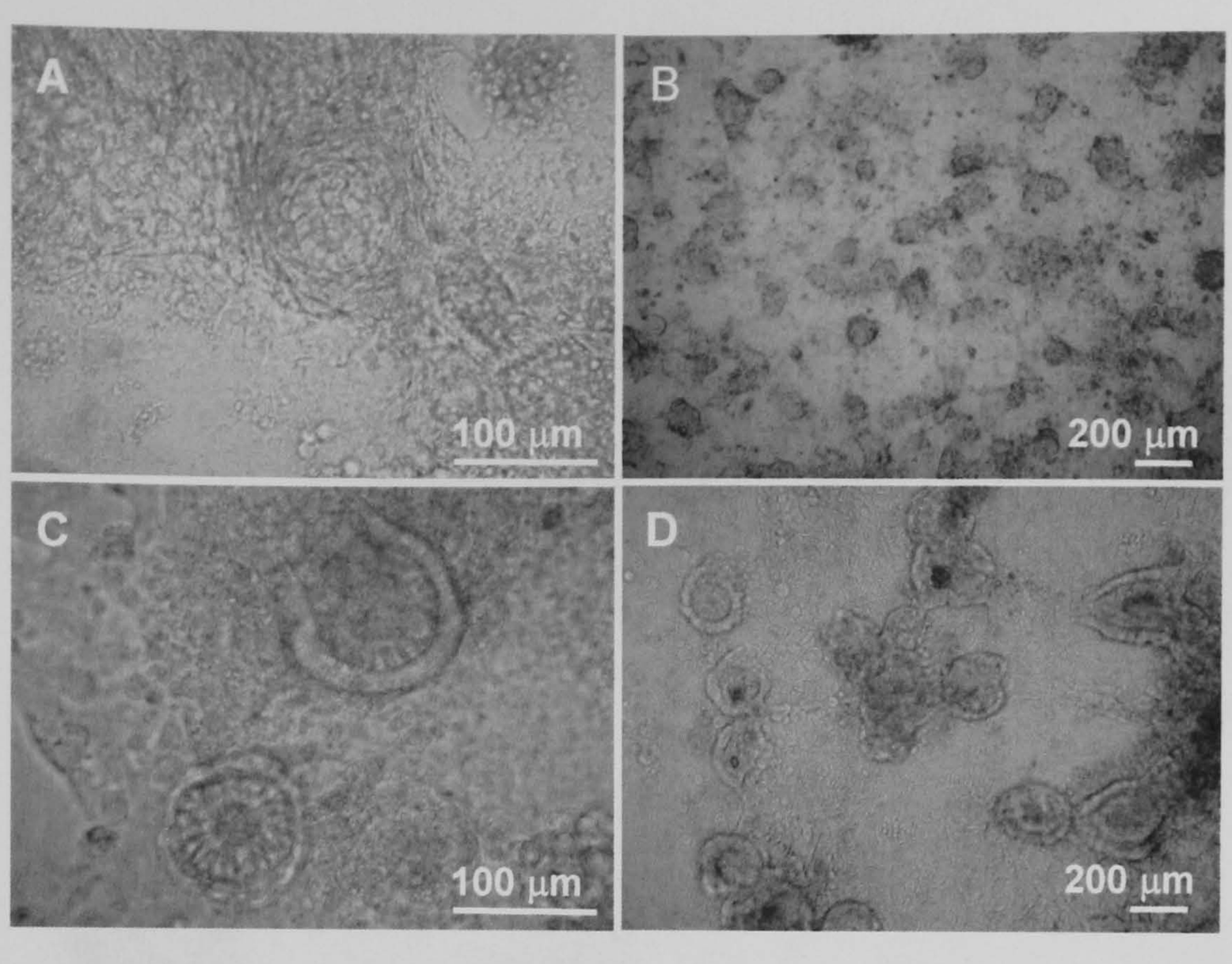


Figure 51. Morphology of cartilage nodules and other cell lineages. (A) and (B): cartilage nodule. (C) and (D): Other cell lineages found in mESC group.

5.4.2.2. Cartilage nodule formation

When mESCs and CM-mESCs were cultured in chondrogenic conditions in the absence of EB formation, local condensation occurred in monolayer cultures and the condensed cells gradually formed cartilage nodules. These cartilage nodules could be easily detected by GAG specific staining, such as alcian blue staining. Following 15 days of chondrogenic differentiation, the cartilage nodules exhibited a distinct structure comprising of round-shaped chondrocytes separated by extracellular matrix (ECM) surrounded by a circular arranged fibrillar matrix [Maleski MP 1996], and positive staining of the nodules with Alcian blue, indicative of cartilage-like extracellular matrix accumulation. Our results indicated that the CM-mESCs resulted in enhanced chondrogenesis, as shown in figure 52. Specifically, an 1.8-fold increase ($P < 0.05$) in the stained areas was obtained in the CM-mESCs compared with the control group of untreated mESCs, with 31.89 $\pm$ 2.50 % of stained area in the CM-mESC group and 17.89 $\pm$ 2.22 % of stained

area in the mESC group, respectively.

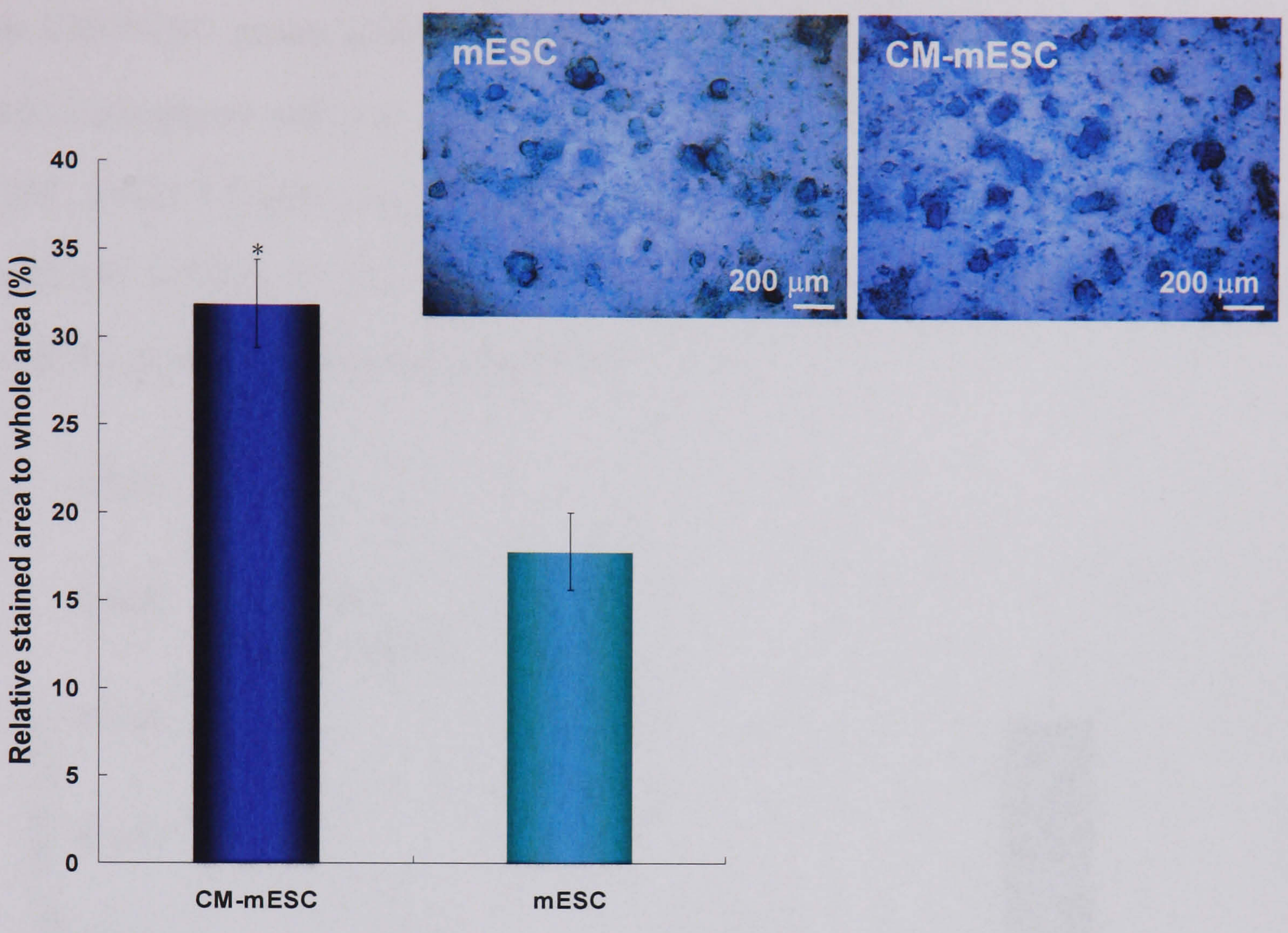


Figure 52. Quantification of the Alcian blue stained areas of cartilage nodules. mESC: non-treated normal mESCs. CM-mESC: HepG2 conditioned media treated mESCs. Data shown as mean relative stained area ± SD (n=4, * $P<0.05$ compared to mESCs).

5.4.2.3. Extracellular Matrix Synthesis

Cartilage tissues consist of sparsely embedded chondrocytes in a specialized ECM. ECM has dense collagen and GAG networks that determine mechanical and functional properties of the tissue [Poole 2001]. Furthermore, both pre-cartilage condensation and cartilage nodule formation are regulated influenced by extracellular matrix components, such as GAG and collagen [Poole AR 2001. Knudson CB 2001]. For the functional evaluation of chondrogenic differentiation, GAG and collagen synthesis were quantified. Our results showed that GAG and

collagen synthesis in the CM-mESC group was much higher than the control mESC group as culture time progressed. Specifically, GAG content produced in the CM-mESC group showed around an 2-fold increase throughout the culture period compared with the control group of mESC, with 0.304 ± 0.052, 0.306 ± 0.057, 0.503 ± 0.099 μg/μg of DNA at day 5, 10 and 15 in the CM-mESC group and 0.147 ± 0.019, 0.106 ± 0.041, 0.266 ± 0.084 μg/μg of DNA at day 5, 10 and 15 in mESC group, respectively (Figure 53).

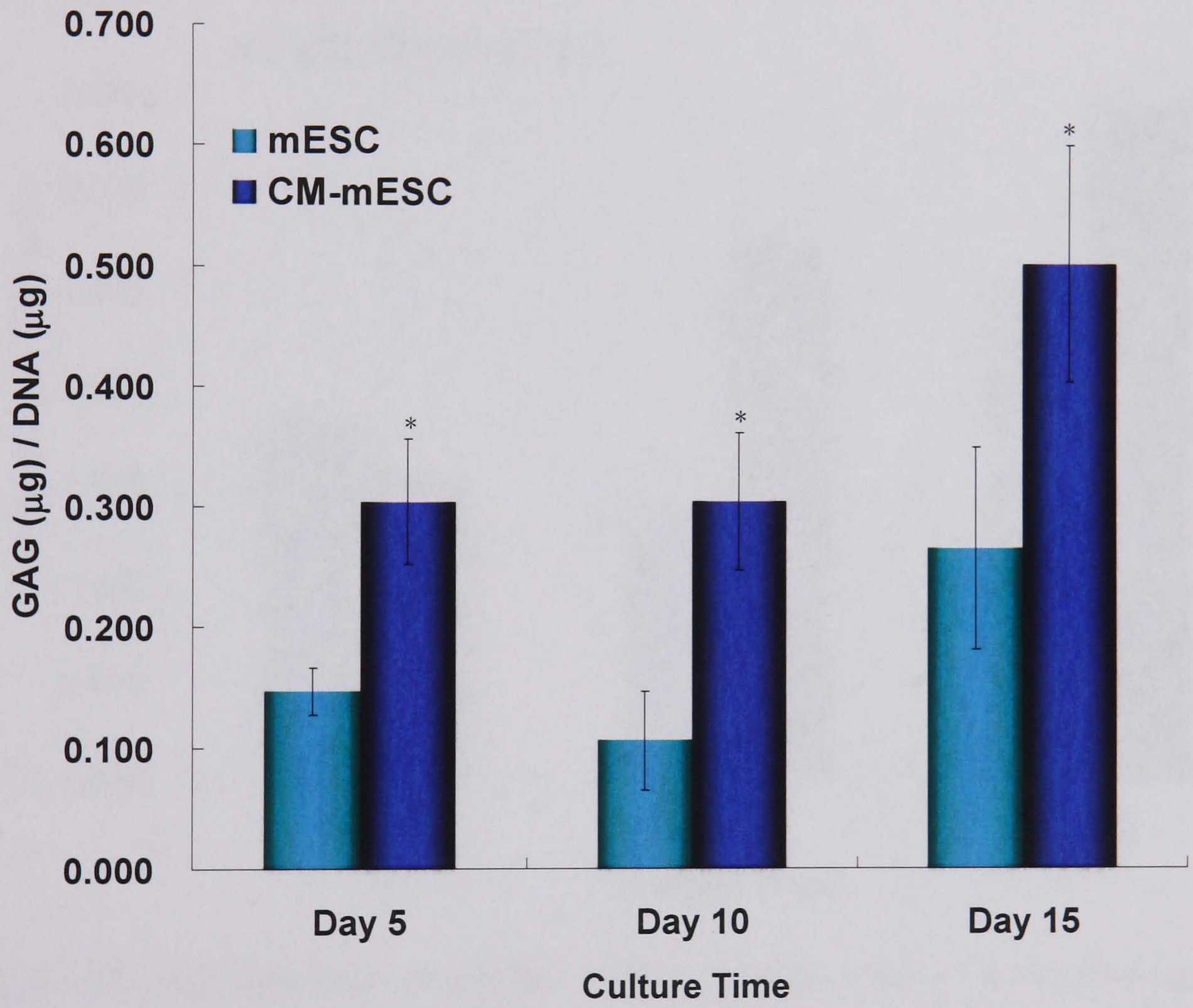


Figure 53. Quantification of relative matrix sulfated GAG amount produced by culture. mESC: non-treated normal mESCs. CM-mESC: HepG2 conditioned media treated mESCs. Data shown as mean relative GAG content at each culture time to GAG content at 0 day culture of each test group ± SD (n=6 * $p<0.05$ compared to mESCs).

For collagen synthesis, at day 5 of culture, there was no significant

difference between the CM-mESC and mESC groups. However, collagen content in CM-mESC group showed 1.9- and 1.4-fold increase at day 10 and 15 of culture in comparison with the mESC group, with 1.545 ± 0.106, 2.746 ± 0.541, 3.463 ± 0.194 μg/μg of DNA at day 5, 10 and 15 in the CM-mESC group and 1.816 ± 0.094, 1.403 ± 0.142, 2.494 ± 0.329 μg/μg of DNA at day 5, 10 and 15 in the mESC group, respectively (Figure 54).

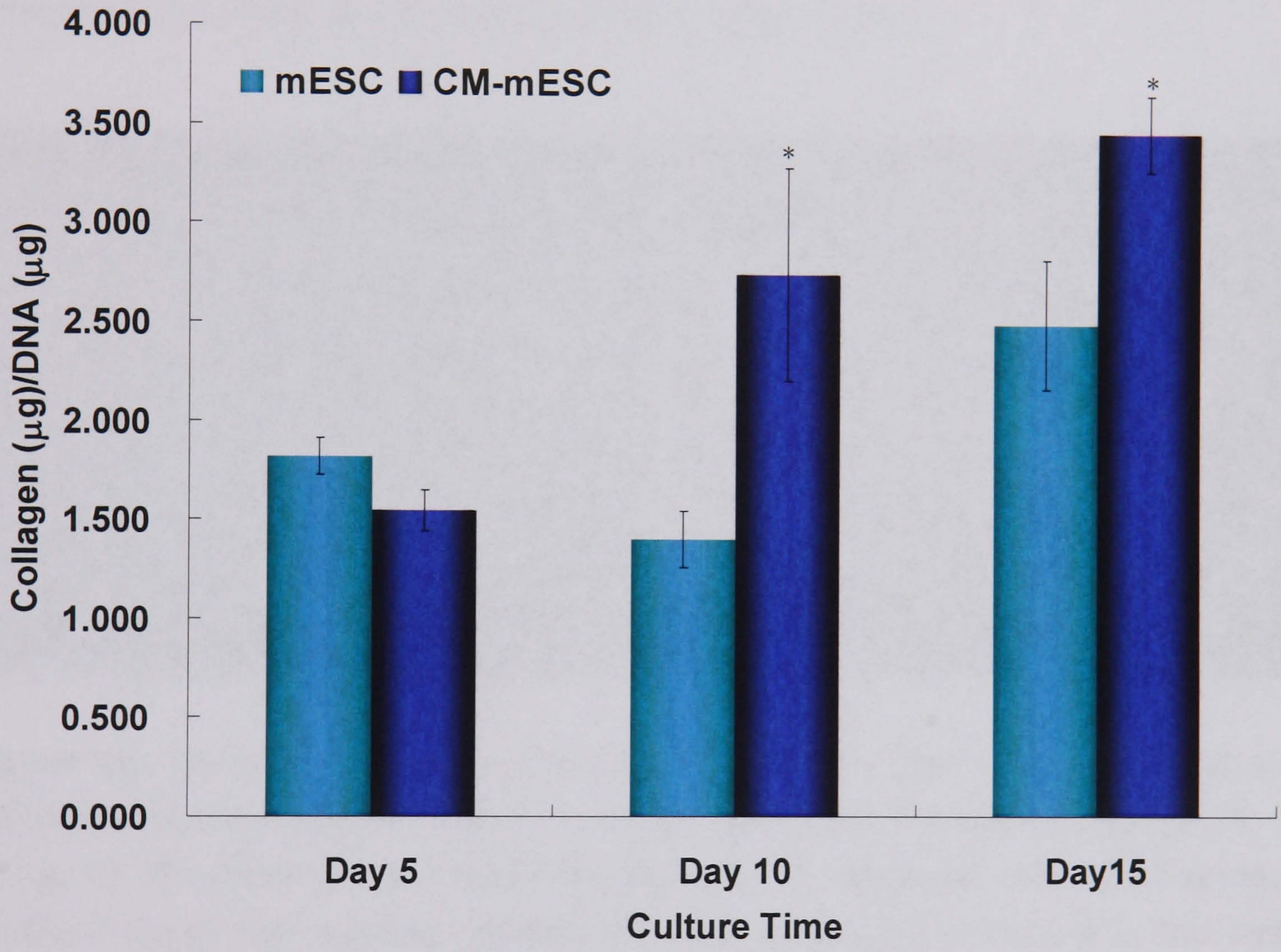


Figure 54. Quantification of relative matrix collagen amount produced by culture. mESC: non-treated normal mESCs. CM-mESC: HepG2 conditioned media treated mESCs. Data shown as mean relative collagen content at each culture time to GAG content at 0 day culture of each test group ± SD (n=6 * p<0. 05 compared to mESCs).

5.4.2.4. Immuno-staining for chondrogenic differentiation

One of the most important transcription factors that is expressed during

early chondrogenesis is the high-mobility group (HMG) box protein Sox-9 [Kulyk KM; 2000]. In addition, one of the distinct ECM in the cartilaginous matrix is type II collagen which plays an important role in modulating the mechanical and structural properties of cartilage [Poole AR; 2001]. As shown in figure 55A, at day 15 of culture, small islands of type II collagen matrix protein (green stain) were observed in both the control and experimental groups. In addition, Sox-9 was observed distinctly in a central region of the cells within cartilage nodules, which were easily confirmed by nuclear counterstaining with PI (Figure 55B).

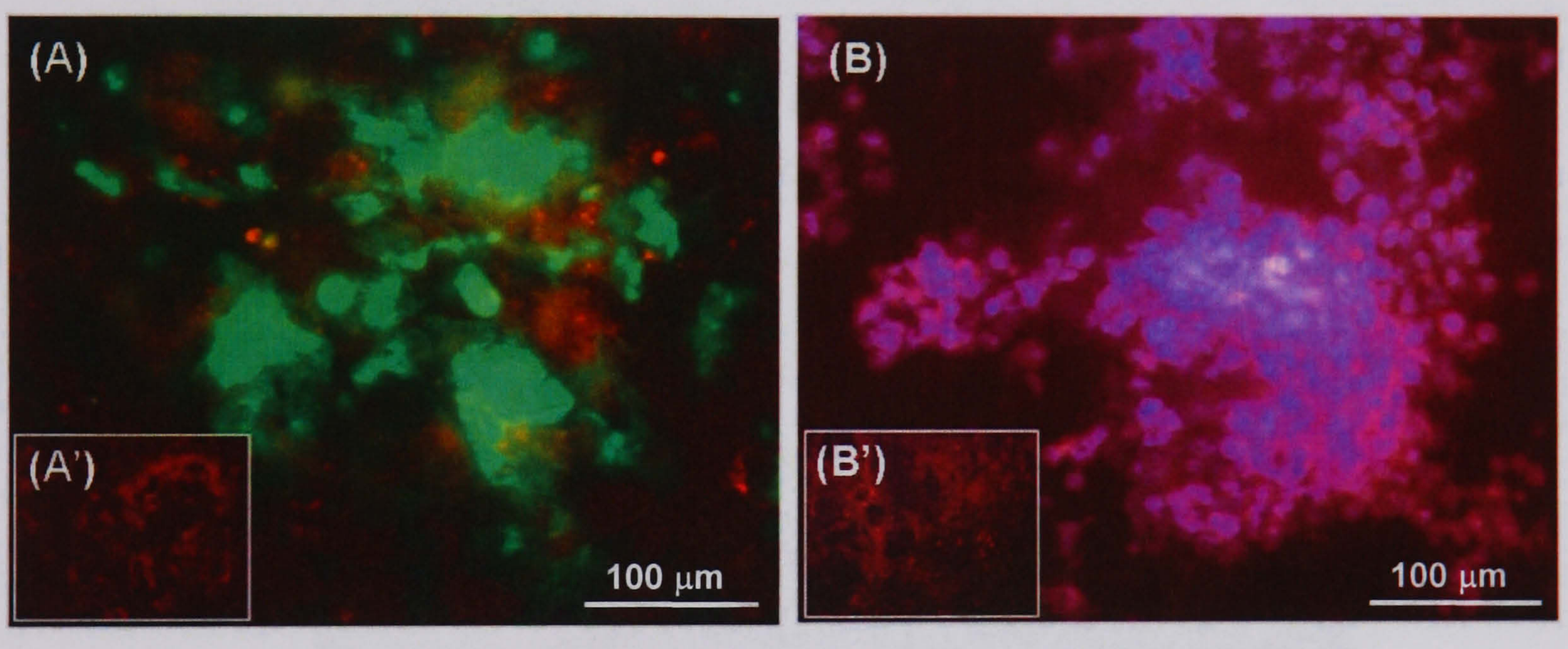


Figure 55. Immunostaining of cartilage nodules with type II collagen and sox-9 antibody. (A) Expression of type II collagen (green) and nuclear staining (PI; red) at day 15 of culture in the cmES-EB1-derived chondrogenic cells. (B) Expression of Sox-9 (blue) and nuclear staining (PI; red) at day 21 of culture in the cmES-EB1-derived chondrogenic cells. Inset (A') and (B') shows negative control for non-specific binding of the primary antibody.

5.4.2.5. Chondrogenic gene expression

The genotypic profiling of chondrogenic markers in this study using RT-PCR at different culture time points is shown in figure 56. Upon chondrogenic differentiation, type II collagen, aggrecan and link protein transcript, which are major structural component of cartilage [Sandell LJ 1991, Watanabe H 1998,

Rodriguez E 2005, Neame PJ 1994], were readily detectable from day 5 of culture in both culture groups, and type II collagen mRNA expression was upregulated substantially higher at day 10 of chondrogenic culture in the CM-mESCs group and at day 15 of culture in the mESCs group, respectively. Furthermore, Sox-9 mRNA expression, a major transcription factor controlling chondrogenic differentiation [Kulyk KM 2000], became detectable at day 5 of chondrogenic culture and appeared to be increasing with culture time during chondrogenic differentiation in both the mESCs and CM-mESC groups. Furthermore, Scleraxis, a basic helix-loop-helix (bHLH) transcription factor expressed in developing chondrogenic cell lineages during embryogenesis [Brown D 1999], was induced at day 5 of chondrogenic culture and expressed at constant levels in the CM-mESCs. In contrast, Scleraxis expression became detectable at low levels at day 15 of chondrogenic culture in the control mESCs group.

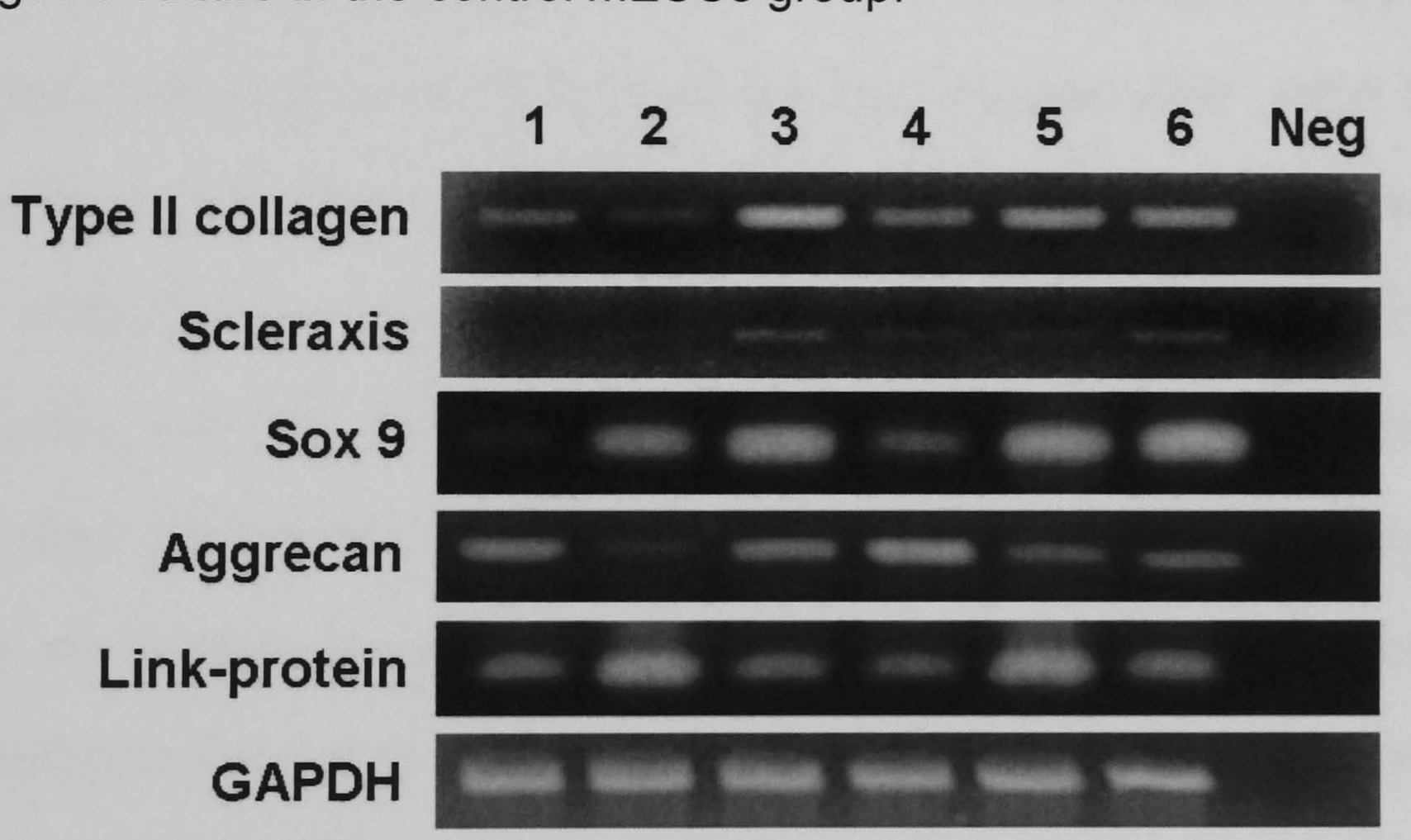


Figure 56. Molecular analysis (RT-PCR) of type II collagen, scleraxis, sox-9 aggrecan, and link-protein gene expression with GAPDH control lanes. Lane 1, 2 and 3: mESCs were cultured in chondrogenic media for 5, 10 and 15 days. Lane 4, 5 and 6: CM-mESCs were cultured in chondrogenic media for 5, 10 and 15 days.

5.5. Discussion

In Chapters III and IV, we demonstrated that mESCs were induced to differentiate into a cell population with high capacity for osteogenic or chondrogenic differentiation through stimulation with the HepG2 conditioned medium and modulation of the EB formation period. However, for future clinical applications of this culture strategy to bone and cartilage tissue engineering, reproducibility, control, and automation are imperatives that need to be considered. Hence, we have demonstrated herein the direct differentiation of ESCs into the desired cell types in the absence of EB formation although EB-mediated ESCs differentiation has been widely accepted by most researchers [Tanaka H 2004, Buttery LD 2001, Kawaguchi J 2005, Bielby RC 2005, Nakayama N 2003, Kramer J 2005, Cao T 2005, Hwang NS 2006 (1)]. One of limitations in EB-mediated differentiation strategy is the spontaneously induced cavitation within EBs. This cavitation by programmed cell death is an inevitable, spontaneous process, which is very difficult to control resulting in loss of available cells for terminal differentiation even in the specialized culture conditions for lineage specific differentiation [Coucouvanis E 1995, Li S 2002]. In addition, the spontaneous formation of all three germ layers within the EBs can result in reduced yield of differentiation to the cell type of interest and a heterogeneous population due to mostly unknown precise mechanism(s) of cellular interactions within the EBs [Khoo MLM 2005]. From those limitations, the need of novel culture strategy by bypassing EB formation process is evident, considering more efficient, simple and easy manageable bioprocesses for tissue engineering,

The assessment of functional osteogenic activity and quantification of the extent of mineralization were achieved by Alizarin red S staining. The increase in

the stained mineralised area with culture time was representative of normal osteogenesis. Furthermore, the enhanced osteogenesis in the CM-mESC group indicated that the HepG2 conditioned medium in the absence of EB formation produced superior results in both time and extent of differentiation that the standard protocol requiring EB formation. To discriminate between cell-mediated and non-specific mineral deposits, a calcium responsive alizarin red S stain was employed [Midura RJ 2004, Chang YL 2000] in addition to observance of fluorescence, indicating high density of calcium. In addition, alkaline phosphatase (ALPase) expression was clearly confined around mineral deposits. The ALPase has been thought to play a role in the mineralization of bone [Wuthier RE 1985] and as a marker of the osteoblast phenotype. Our results demonstrated that mineralization was cell-mediated in the experimental group (CM-mESCs), which is consistent with reports that cellular-derived mineral deposits are formed *in vitro* in the presence of β-glycerophosphate as an additional source of phosphate ions [Tenenbaum HC 1982, Chang YL 2000]. It has been well documented that ALPase attached covalently to the external surface of plasma membranes is involved in the mineralization of hard tissues [Togari A 1993] and that ALPase of osteoblastic cells is released into the medium during maturation. Hence, the temporal increase of ALPase activity observed in our results is consistent with the progress of mineralization [Yoshikawa M 1999]. The enzymatic hydrolysis activity of ALPase is necessary to initiate biological mineralization by hydrolyzing β-glycerophosphate and promoting mineralization [Sugawara Y 2002]. In accordance with the quantitative data of mineralised bone nodule formation, CM-mESCs showed relatively higher ALPase activity than mESCs, indicating the enhanced osteogenic activity. The relatively lower ALPase activity in CM-mESCs at day 0 represents their early differentiation stage due to treatment with the

HepG2 conditioned medium. It has been demonstrated that undifferentiated ESCs show a high level of expression ALPase which decreases following differentiation [Thomson JA 1998].

In addition to functional characterisation, osteogenic cells are known to express various specific markers that distinguish them from other cell types. In *in vitro* bone formation, the mineralised bone nodules consist of cuboidal osteoblasts embedded within the bone matrix [Malaval L 1999]. This bone matrix is mainly composed of dense packed type I collagen fibrils infiltrated with hydroxyapatite crystals and small amounts of bone specific proteins, such as osteopontin. Type I collagen is the most abundant protein of bone [Rossert J 2002] and is essential for bone growth and development. Furthermore, osteopontin is one of the major bone sialoproteins which is essential for the process of mineralisation [Sodek J 2000]. The expression of these molecules is controlled during osteogenic differentiation [Zhu JX 2001, Chen Y 1992, Zhou HY 1995]. Our results in the expression of type I collagen and osteopontin in the matrix of bone nodules were in accordance to literature data and was further verified by the gene expression profiles of specific genes. Cbfa1/Runx2, a transcription factor that is the earliest marker of osteogenesis, is expressed in early mesenchymal condensation [Ducy P 1997, Banerjee C 2001] and participates in mature osteoblast by controlling the expression of type I collagen and bone sialoproteins, such as osteocalcin and osteopontin [Ducy P 1997, Banerjee C 2001]. The early expression at day 5 of Cbfa1/Runx2 in our results was in accordance to the literature data and demonstrated the enhanced osteogenesis in the CM-mESC group over the control group. These results were further supported by the robust osteocalcin expression in CM-mESCs, which persisted to 21 days of culture in comparison with mESCs. In addition, osterix, an osteoblast-specific transcription factor required for the

differentiation of osteoprogenitors into mature osteoblasts [Nakashima K 2002, Guanping T 2004], was upregulated strongly at late culture stage in CM-mESCs, which is consistent with a report that osterix is upregulated several days later than Cbfa1/Runx2 developmentally [Woll NL 2006]. Finally, these results are in agreement with the bone nodule formation assay, mineralised nodule characterisation and type I collagen and osteopontin immunostaining results demonstrating the correlation between mineralised bone nodule formation and osteogenic marker expression and osteoblast related gene expression.

Direct chondrogenesis was also achieved without EB formation, as demonstrated by our data. The process of chondrogenesis occurs in stages beginning with the aggregation of chondroprogenitor from mesenchymal cells into precartilage condensations. The cells in the centre of the nodules remain spherical and are surrounded by an abundant cartilaginous extracellular matrix. The cells in the periphery of the nodules acquired a discoid morphology and are surrounded by a sparse extracellular matrix [Hall BK 2000, Tuan RS 2004, Kuettner KE 1982]. In our results, morphological cell condensations were apparent by day 5 of differentiation and distinct cartilaginous nodules could be observed by day 15 which further increased in number and size. Local condensation occurred in monolayer cultures, and round shaped chondrocyte was observed at the centre area of cartilage nodules; these nodules exhibited a distinct structure comprising of round-shaped cells separated by extracellular matrix surrounded by a circular arranged matrix that was easily detected by light microscopy. For the further characterisation of cartilage nodules to assess functional chondrogenic activity, cartilage nodules in chondrogenic culture were stained by GAG specific Alcian blue and the relative stained area were measured, cartilage nodules, after 15 days of chondrogenic culture, were easily detected by positive staining with Alcian blue,

indicative of cartilage-like extracellular matrix accumulation, and the HepG2 conditioned media-treated mESCs (CM-mESCs) resulted in enhanced chondrogenesis with a 1.8-fold increase in the stained areas in compared with the control group of untreated mESCs, suggesting that HepG2 conditioned media induced mESC early differentiation strategy generate a cell population with high capacity of mesodermal lineage differentiation. These accumulated extracelluar matrix are mainly composed of dense collagen and GAG networks that determine mechanical and functional properties of the cartilage tissue [Poole 2001]. In addition, both precartilage condensation and cartilage nodule formation are regulated by extracellular matrix components such as GAG and type II collagen [Poole AR 2001. Knudson CB 2001]. Under our chondrogenic condition, High GAG and collagen deposition was detected in highly condensed areas of cell growth in CM-mESCs cultures. GAG and collagen synthesis in CM-mESC group was much higher than mESC group in accordance with culture time. Specifically, GAG content produced in CM-mESC group showed around 2-fold increase for whole culture period compared with the control group of mESC. In collagen synthesis, at day 5 of culture, there was no significant difference in collagen content between CM-mESC and mESC, but collagen content in CM-mESC group showed 1.9- and 1.4-fold increase at day 10 and 15 of culture in comparison with mESC group. This finding was further validated by immunocytochemical analysis carried out on day 15 of differentiation. Chondrocyte marker proteins such as type II collagen, one of major macromolecules produced by chondrocyte [Poole AR 2001], and Sox-9, one of the most important transcription factors that are expressed during early chondrogenesis [Kulyk KM 2000], expression in cartilage nodules were evaluated. Type II collagen deposition in the cartilage nodules found predominately in both cells and the matrix synthesized by CM-mESCs, and

immunostaining for Sox-9 was easily detected in a central region of cells within cartilage nodules, indicating well defined chondrogenic differentiation.

Chondrogenic differentiation was also characterized by distinct cellular phenotypes, which could be identified by specific extracellular matrix and transcription factor gene expression profiles. Type II collagen, aggrecan and link protein are major structural components of cartilage [Sandell LJ 1991, Watanabe H 1998, Rodriguez E 2005, Neame PJ 1994] and matrix network composed of these macromolecules determines mechanical and functional properties of the tissue [Poole 2001]. In addition to chondrocyte specific extracellular matrix macromolecules, there are specific transcription factors controlling chondrogenic differentiation. Scleraxis, one of major transcription factor, is expressed in mesenchymal progenitors and during chondrogenesis [Brown D 1999], and Sox-9 is major transcription factor directing chondrogenic differentiation [Kulyk KM 2000]. The two transcription factors regulate the fate of cells that interact with each other during differentiation pathways. Recent research reported the presence of temporal and spatial association of scleraxis expression during embryonic development of mesenchymal precursor cells in close association with that of Sox-9 expression in chondrogenic cells in skeletal tissues [Asou Y 2002]. Upon chondrogenic differentiation, type II collagen, aggrecan and link protein transcription were induced from day 5 of culture. Especially, substantially upregulated type II collagen mRNA expression was observed in CM-mESCs group respectively. However, aggrecan and link protein transcripts were not expressed in constant level in both chondrogenic culture of CM-mESCs and mESCs, which might be due to heterogeneous cell population expressing them. Different from type II collagen which is expressed only in cartilaginous tissue, although aggrecan and link protein are distinct molecules found in cartilage tissue and expressed in

chondrogenic cell lineage, it was well known that aggrecan and link protein can be also expressed by other cell lineage and non-cartilaginous tissue [Carulli D 2007, Binette F 1994]. In the expression of chondrogenic transcription factor, there was also significant induction of Sox-9 and scleraxis genes in chondrogenic culture of CM-mESCs, and Sox-9 and scleraxis transcripts were upregulated as culture time passed. In contrast, even though Sox-9 expression in chondrogenic culture of mESCs showed similar pattern with CM-mESCs with relatively week intensity, mESCs showed relatively weak expression of scleraxis mRNA. Finally, gene expression analysis showed that direct chondrogenic differentiation was achieved under the culture condition with chondrogenic supplement from direct culture of mESCs without EB formation step, and was enhanced in chondrogenic culture of early differentiated mESCs (CM-mESCs) through preliminary treatment with HepG2 conditioned medium, showing the correlation between cartilage nodule formation, chondrogenic specific extracellular matrix production and chondrogenic marker expression.

5.6. Conclusion

The novel culture strategy for directing osteogenic and chondrogenic differentiation of mESCs described here is completely devoid of EB formation process, enabling *in vitro* direct osteogenesis and chondrogenesis. Removing the EB formation step resulted in the almost exclusive osteogenic and chondrogenic differentiation, which would be more efficient and easy than the conventional EB mediated differentiation culture method. In addition, osteogenic and chondrogenic differentiation could be enhanced by the use of early differentiated ESCs, which induced by HepG2 conditioned medium treatment. By taking advantage of the

ease of directing and enhancing *in vitro* osteogenic/chondrogenic differentiation, the ESCs osteogenic/chondrogenic differentiation culture described here would provide an efficient and easy culture strategy for applying to bone and cartilage tissue engineering in the context of macroscopic bone and cartilage formation. This culture system may lead to a better strategy for bone and cartilage repair and bone and cartilage tissue engineering.

CHAPER VI

BIOPROCESSING FOR THREE DIMENSIONAL BONE AND CARTILAGE TISSUE LIKE CONSTRUCT FORMATION USING ALGINATE ENCAPSULATED MURINE EMBRYONIC STEM CELLS AND HARV BIOREACTORS

6.1. Introduction

Recently, in the field of skeletal tissue engineering, osteogenic and chondrogenic construct has been fabricated by isolating various cell type including primary adult cells and bone marrow stem cells that are expanded in tissue culture flasks and cultured on or in various three dimensional scaffold which are made of natural or synthetic biomaterials in bench-scale [Suh H 2000, Suh H 2001, Ceuninck FD 2004, Hwang NS 2006(1)]. Specially, recent skeletal tissue engineering studies have shown the potential use of ES cells for bone and cartilage tissue regeneration in three dimensional scaffold systems with appropriate growth factors. Hwang NS et al reported that three dimensional scaffold culture system by encapsulating mESCs derived EBs with natural, synthetic and hybrid biomaterials such as poly(ethylene glycol (PEG))-based hydrogels, PEG hydrogel containing glucosamine, arginine-glycine-aspartate (RGD)-modified poly(ethylene glycol)-diacrylate (PEGDA) hydrogels and alginate based hydrogel provided suitable environment for chondrogenic differentiation resulting in three dimensional structure like neocartilage [Hwang NS 2006(1), Hwang NS 2006(2), Hwang NS 2006(3), Tanaka H 2004]. In other hands, in three dimensional osteogenic differentiation of ESCs, there has been only one tissue engineering based approaches in development of three dimensional bone like construct. The report demonstrated that mESCs derived EBs were encapsulated by self-assembling peptide, a synthetic nanofiber biomaterial made of commercially available peptides (RAD16-I peptide, BD PuraMatrix Peptide Hydrogel), and induced to differentiate into osteoblast like cells in a three dimensional culture system, which was proved by evaluating matrix mineralization, collagen I synthesis, ALPase activity, and expression of the osteoblast

transcription factor Runx2 [Garreta E 2006].

However, such culture process in static culture system has some drawbacks even though three dimensional scaffolds are used. It has been well known that mass transfer limitations involved during *in vitro* culturing of three dimensional constructs result in limited cell growth into the three dimensional construct [Ishaug-Riley SL 1998, Holy CE 2000]. In such static culture system, cell growth and tissue formation are usually confined on top of surface of scaffold resulting in poor penetration of cells and poor three dimensional tissue formation. For instance, it was reported that some cells (bone marrow stem cells) which were initially seeded at internal part of the three dimensional porous scaffolds could migrate by chemotaxis towards outer surface where nutrient concentration is higher. The remaining cells inside of scaffold showed decreased osteogenic differentiation and lower expression of osteogenic specific genes [Glowacki J 1998]. It has been well documented that transport of nutrients into the centre point of three dimensional scaffold mainly depends on diffusion, which can not satisfy the metabolic requirement of cells on three dimensional scaffolds for long culture period [Mueller SM 1999]. These results might be due to potential mass transfer limitations including external and internal mass transfer limitation with respect to the supply of oxygen and medium components. However, these mass transfer limitations can be reduced by the use of bioreactors.

Bioreactors become essential in tissue engineering, not only because they provide an *in vitro* culture system mimicking *in vivo* conditions for the growth of cells to form three dimensional tissue substitutes, but also because they enable systematic studies of the responses of living tissues to various mechanical and biochemical cues. In addition, bioreactors can drastically reduce the amount of space and handling steps involved and increase the volumes of tissue-engineered

product in comparison with *in vitro* the flasks based culture strategy which might provide a limit in their productivity due to limited cell expansion that can be supported by a given surface area for cell growth, and handling for culture maintenance makes the process labour intensive. In recent years, among various types of bioreactors, Rotating Wall Vessel (RWV) bioreactors such as High Aspect Ratio Vessel (HARV) bioreactor have been widely used in the culture of cells seeded on scaffolds or microcarriers or without scaffold in cartilage [Ohyabu Y 2006] and bone [Qiu QQ 1999, Botchwey EA 2001] tissue formation *in vitro*. The RWV bioreactor is designed to optimize to produce laminar flow and minimize the mechanical stresses on cell aggregates in culture by minimizing shear and turbulence, and is a device that creates a unique environment, while providing adequate nutrition and oxygenation, ideal for mammalian cell culture, that supports three dimensional tissue growth [Hammond TG 2001]. Oxygenation is provided by a permeable silicon rubber membrane through the stationary inner cylinder, allowing the passive exchange of gases to and from the medium, whereas the outer cylinder is impermeable and rotates at a controlled rate. The free falling of the microcarrier inside the bioreactor as a result of gravity can be balanced by the centrifugal forces due to the rotation of the outer-cylinder, thus establishing suspension culture environment for microcarrier [Pollack SR 2000, Hammond TG 2001]. (Figure 57)

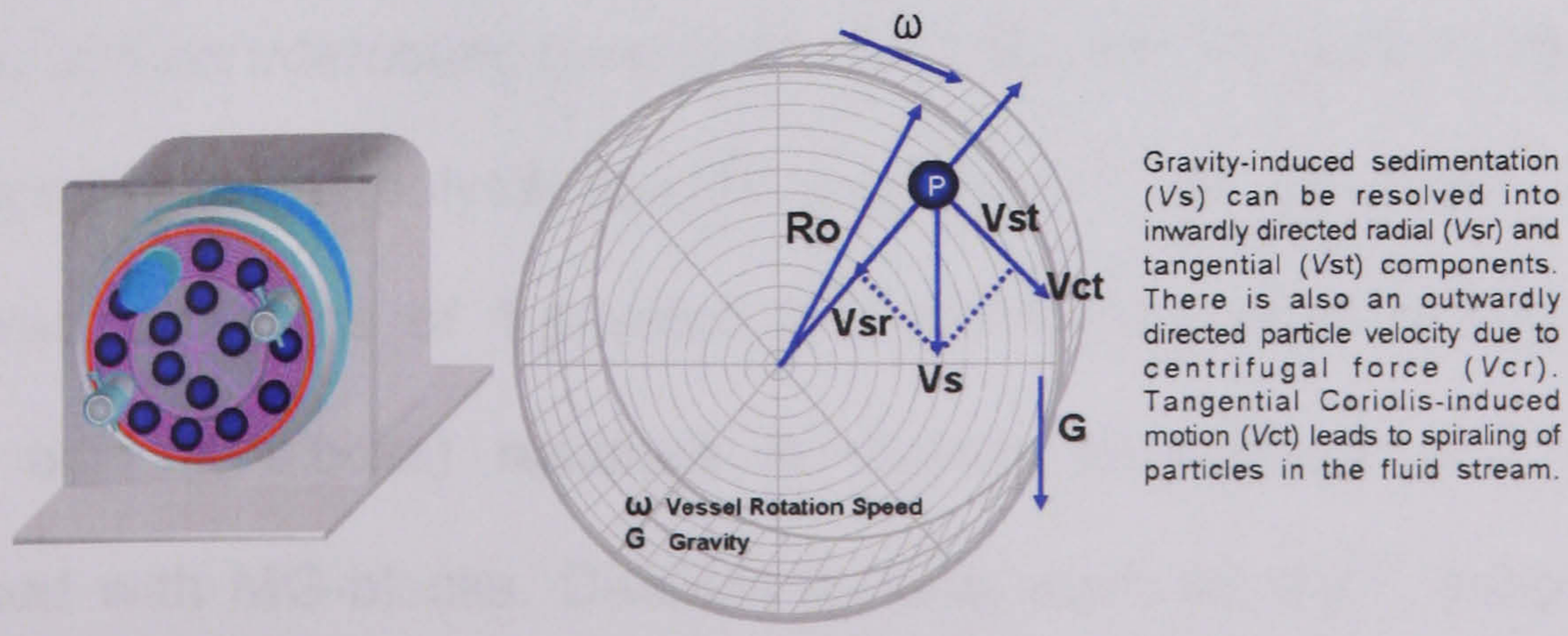


Figure 57. RWV bioreactor and influencing factor diagram for particle move.

Accompanied with bioreactor system, another important factor in three dimensional culture system could be the selection of microcarrier for cell growth and three dimensional tissue formation. In skeletal tissue engineering, various biomaterials such as natural or synthetic polymers and hydrogels have been used as supporting matrix for cell growth and differentiation [Suh H 2000, Suh H 2001, Ceuninck FD 2004]. In case of natural and synthetic polymers, porous scaffolds have been favoured by most of researchers for constructing three dimensional bone and cartilage like structure *in vitro*. However, porous structure and non-homogenous shape like cylindrical or disc type may give rise to very complex motion in bioreactors, which could be very difficult to model and evaluate the influence of mechanical stress to the scaffolds, resulting in poor consistency in data. Hence, hydrogels with spherical shape could be considered as another candidate, because their simple shape like sphere may make it easier relatively to expect their motion and the effect of environmental condition in bioreactors, and extensive studies have been processed about model and experimental validation of such particles motion in bioreactors to optimize suspension culture [Pollack SR 2000, Hammond TG 2001]. In various biomaterials forming hydrogel, alginate has been widely used for cell encapsulation, drug or growth factor delivery and tissue engineering [Ceuninck FD 2004, Masuda K 2003, Gu F 2004] due to its great biocompatibility (low undesirable immune response), significant mechanical resistance, and an interesting biodegradability [Becker TA 2000, King A 2001].

Alginate is a polysaccharide extracted from seaweed composed of homopolymeric regions of 1,4-linked b-D-mannuronic acid (M-blocks) and a-L-guluronic acid (G-blocks) residues in varying proportions and arrangements interspersed with MG-blocks. Divalent cations, such as Ca^{2+}, cooperatively bind between the G-blocks of adjacent alginates chains, creating ionic interchain

bridges and subsequent gelling of aqueous alginate solutions [Martinsen A 1989]. The constitution of alginate gel networks is a complex phenomenon. The different gel network structures have been well demonstrated by Bienaime et al [Bienaime C 2003]. The gel network of alginate bead is mainly composed of a superficial crust, a subsurface, cavities, shafts and shaft clusters, a medium gelled zone, and a weak gelled zone, which formed by the heterogeneous distribution of calcium inside the gel matrix (Figure 58). The gelation process are as follows; After formation of a superficial crust layer with the highest calcium and alginate concentration, which make the gel bead be tightened, the volume of gel bead is gradually reduced due to the tightening of the superficial crust by water expulsion, and then alginate molecules in the centre of the gel bead which still is not crosslinked with calcium ion gradually moved to the boundary space with high calcium content. Finally, during this cascade of reaction-diffusion processes, micro fractures, shafts and cavities are formed.

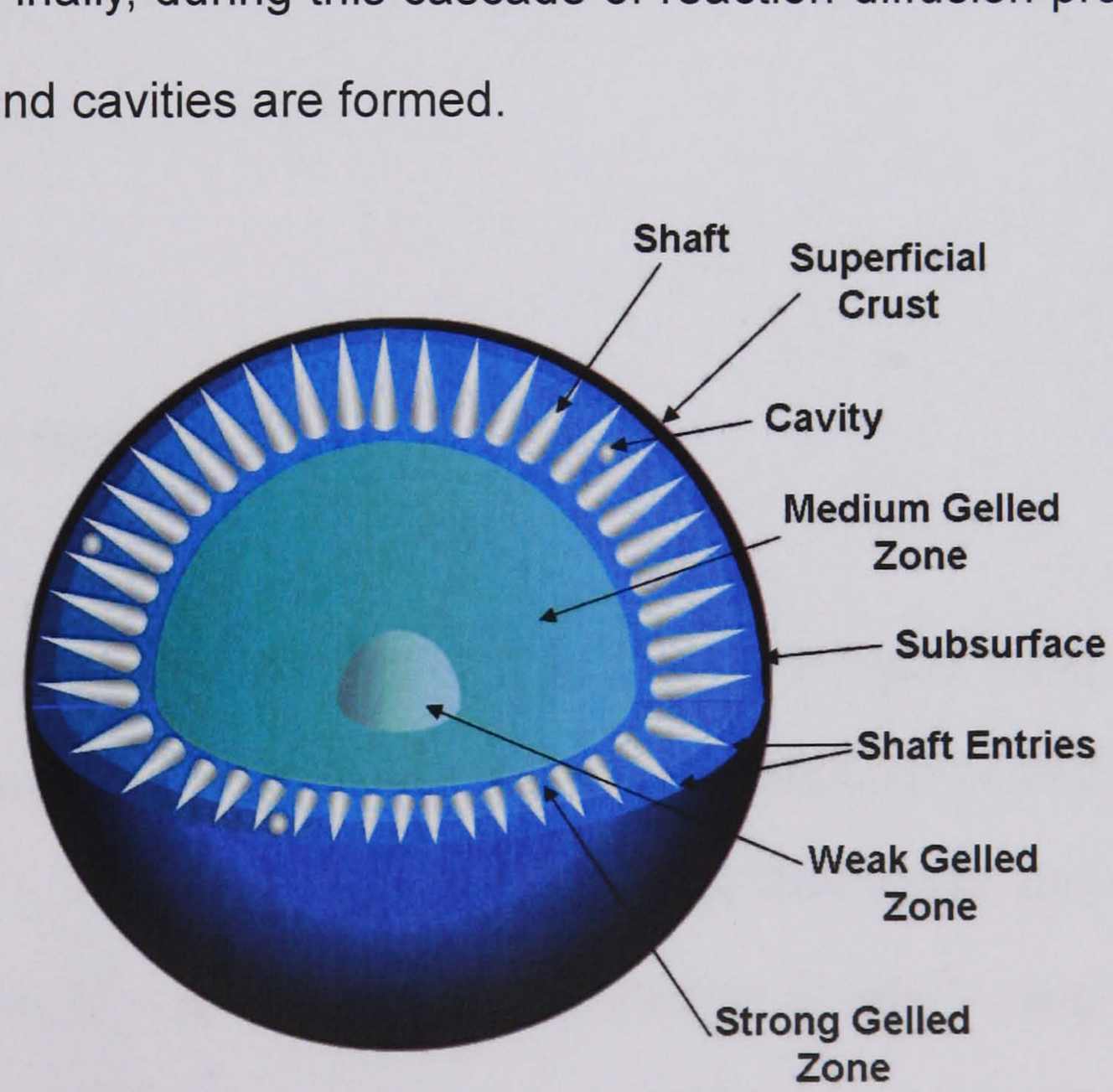


Figure 58. Schematic representation of the different gel network structures of a Ca-alginate hydrogel.

Such simple and reproducible gelation process and good biocompatibility makes alginate widely used as biomedical materials for various applications, and can provide suitable matrix for cell growth and function in three dimensional culture system using a bioreactor.

6.2. Objectives

The aim of this study was to develop single step culture process for direct osteogenic and chondrogenic differentiation of mESC, finally develop three dimensional bone and cartilage tissue like construct, using alginate encapsulation and HARV bioreactors and by applying previously established differentiation strategy, resulting in efficient and reproducible culture system for bone and cartilage tissue engineering applications.

6.3. Experimental Process

Finally, in this study, each previous culture strategies were integrated into single-step culture process using alginate encapsulation and HARV bioreactor for developing three dimensional bone and cartilage like tissue formation. mESCs were encapsulated with alginate solution including gelatin through reaction with calcium, and then placed in the vessel of HARV bioreactor. For first 3 days, encapsulated mESCs were cultured in 50% HepG2 conditioned media in order to induce early differentiation of mESCs into primitive streak/nascent mesoderm like cells, and then encapsulated cells were subjected to differentiate into osteogenic

and chondrogenic lineage cells by changing the conditioned media with osteogenic or chondrogenic media including osteogenic supplements such as β-glycerophosphate, ascorbic acid and dexamethasone or including chondrogenic supplements such as ascorbic acid, dexamethasone and TGF-β1. Finally, the single step 3D osteogenic and chondrogenic differentiation was investigated using various techniques; live/dead assay, morphological observation, histological staining, immunohistochemical staining, and RT-PCR, which detailed explanation was described at CHAPTER II. In brief, the overall experimental process was illustrated in figure 59.

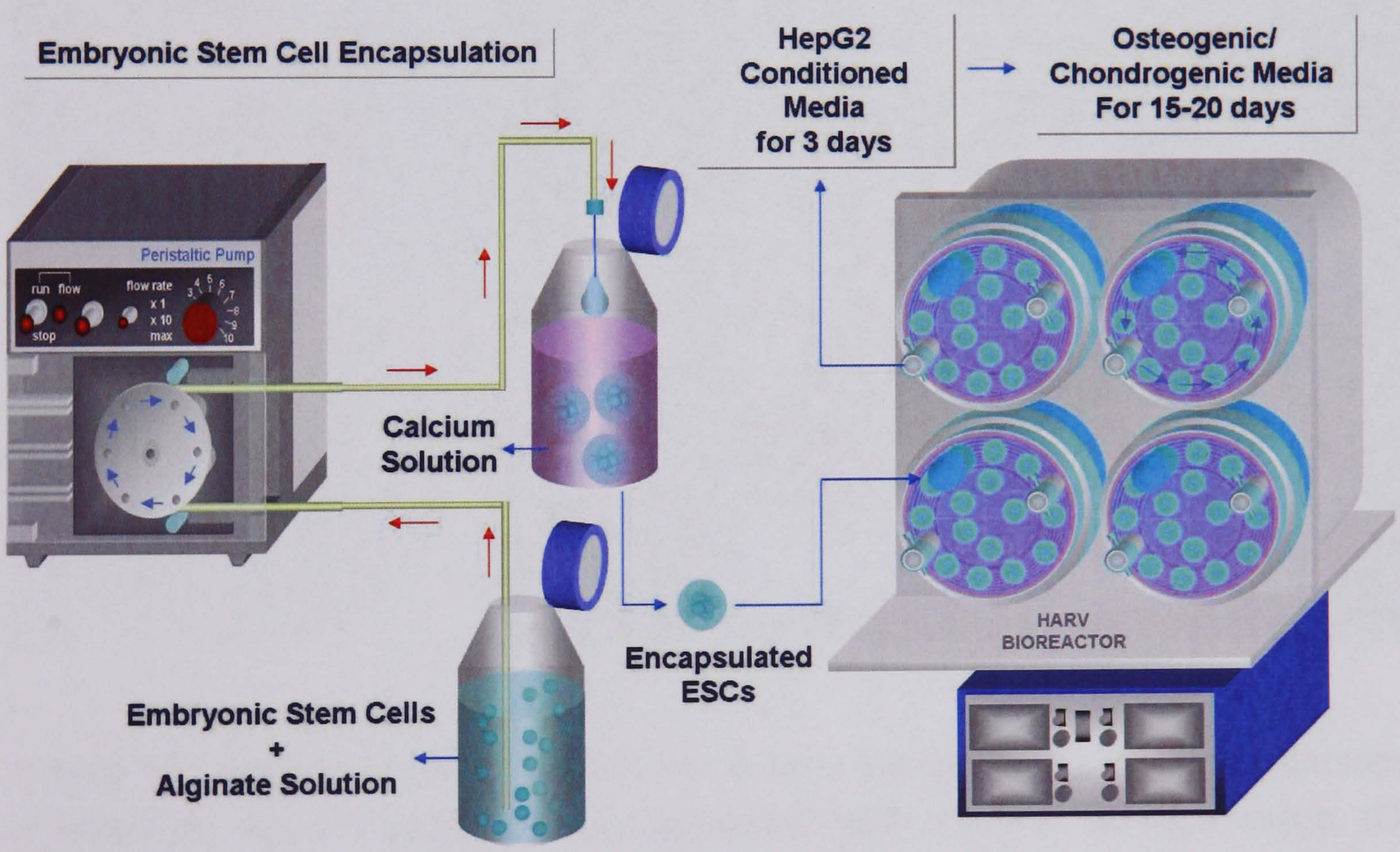


Figure 59. Experimental process for single step 3D osteogenesis and chondrogenesis in a HARV bioreactor

6.4. Results

6.4.1. Alginate beads and HARV bioreactor system

For the single step osteogenesis and chondrogenesis, mESCs were encapsulated by 1.1% alginate including 0.1% gelatin, and the cell + alginate beads were placed in 50 ml bioreactor vessels, and then these vessels were rotated at the speed of 25 rpm. The morphology and pictures of alginate beads and a HARV bioreactor system was shown in figure 60. Figure 60 portrays alginate beads encapsulating mESCs with approximate diameter from 2 mm to 2.5 mm.

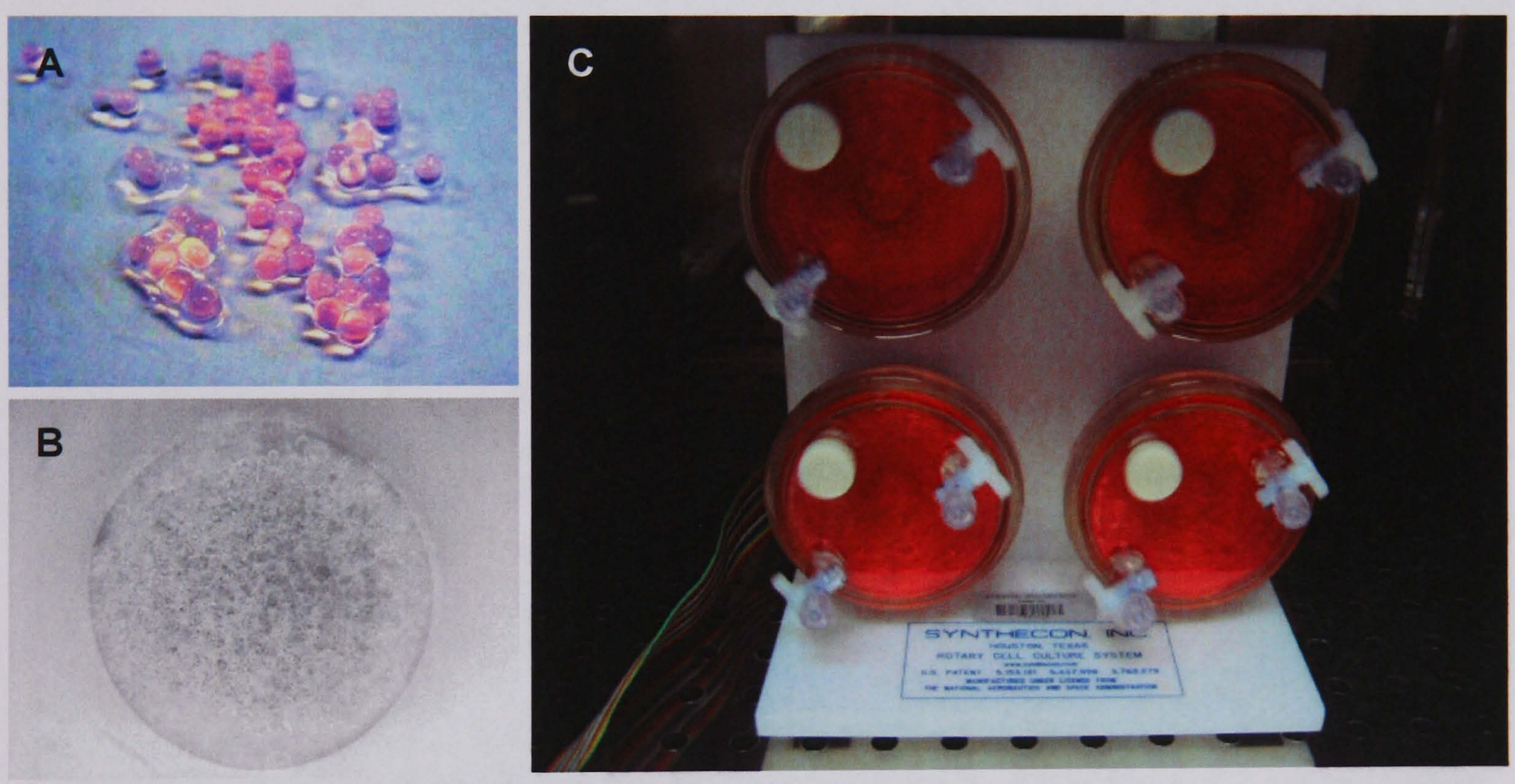
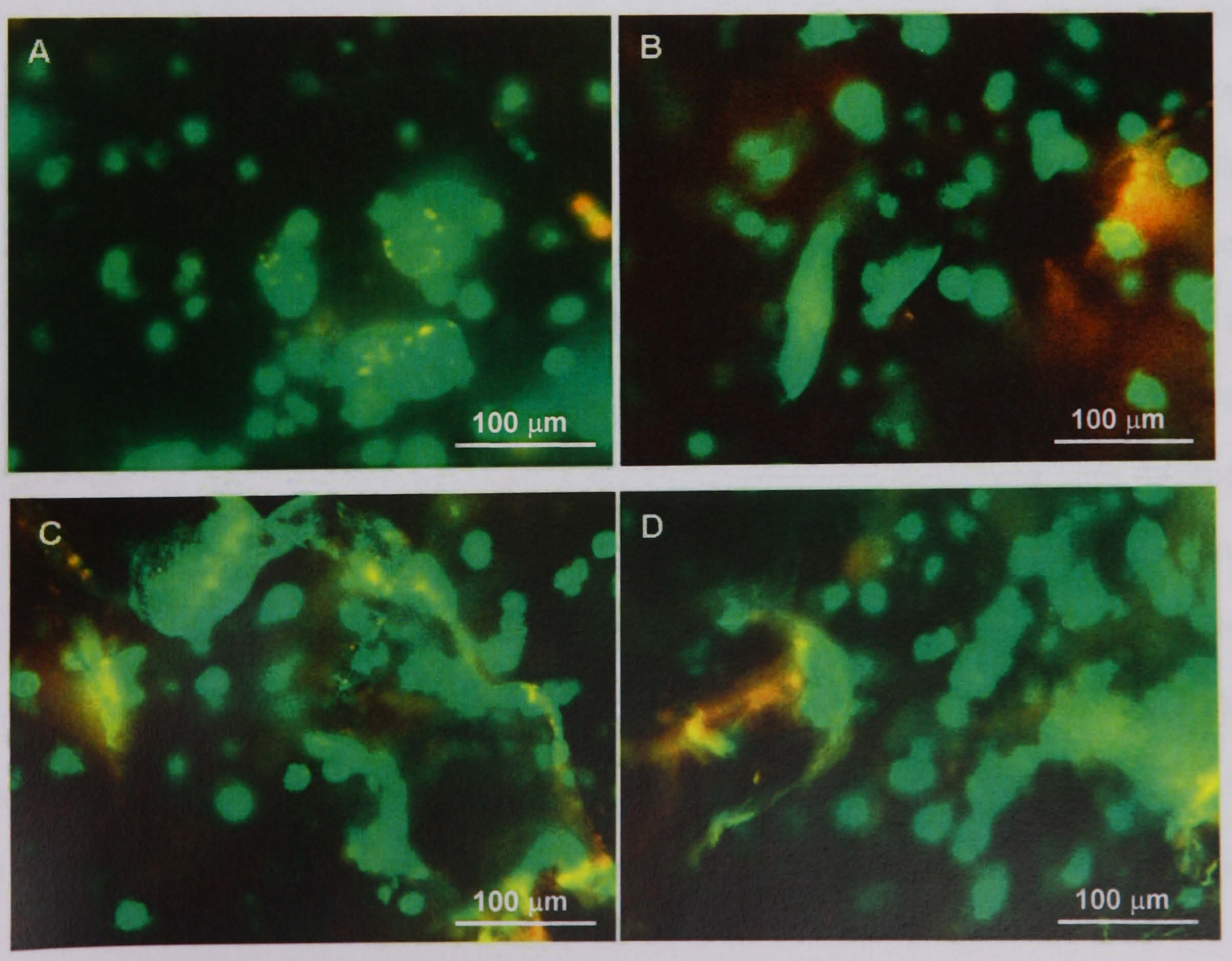


Figure 60. Alginate beads and HARV bioreactor system. (A) and (B) Morphology of spherical alginate beads and encapsulated mESCs within alginate beads. (C) HARV bioreactor equipped with four vessels containing around 500 alginate beads and media.

6.4.2. *In vitro* single step 3D osteogenesis in a HARV bioreactor

6.4.2.1. Observation of cell viability

Time course cell viability of CM-mESCs within alginate beads in 3D osteogenic culture was visualized using a two-colour fluorescence cell viability assay that is based on the simultaneous determination of live and dead cells that measure intracellular esterase activity and plasma membrane integrity. Calcein AM is cleaved by intracellular esterases to label live cells brightly with green fluorescence. Ethidium homodimer (EthD-1) enters cells that have lost plasma membrane integrity, producing bright red fluorescent labelling of dead cells. As shown in figure 61, at early stage of osteogenic culture, most of cells within alginate beads showed intensified green fluorescence indicating live cells with very few yellow or orange fluorescence, and as culture time passed, population of dead cells was gradually increase, but the size of cell aggregation with tissue like structure was also increased.



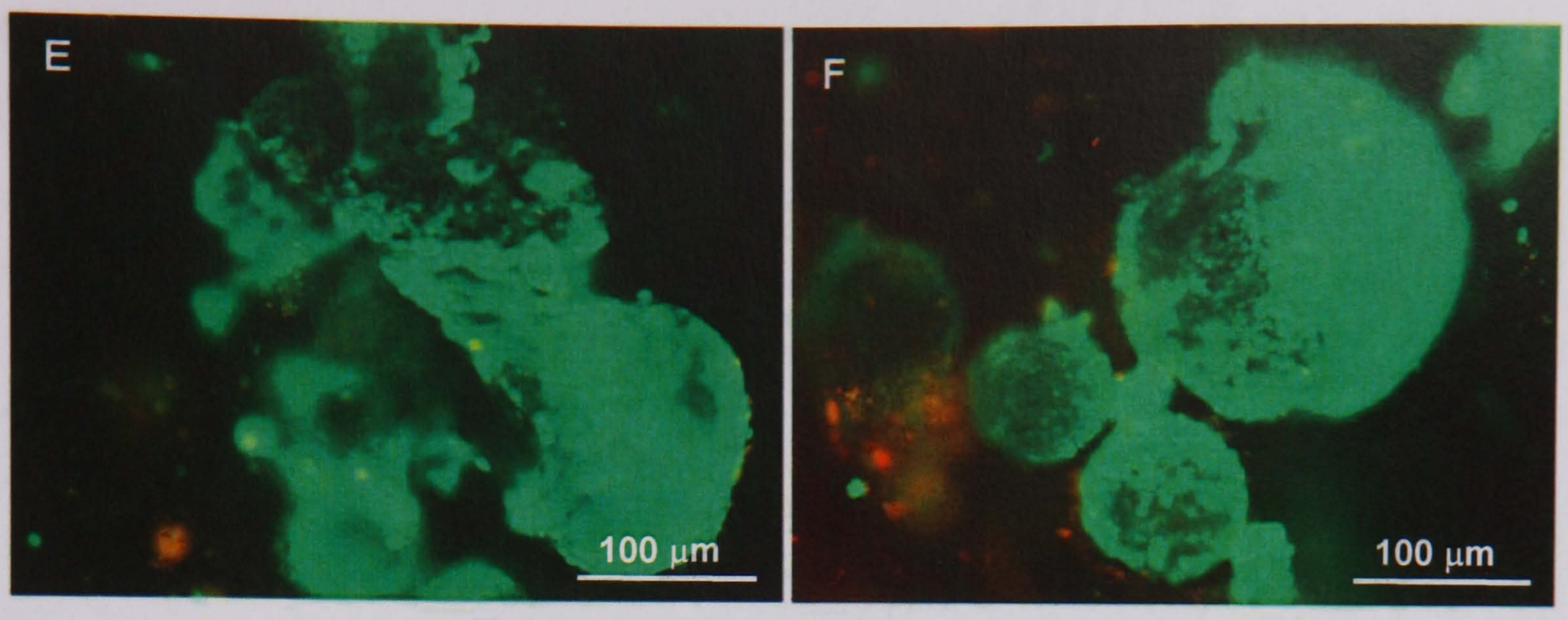


Figure 61. Live/dead assay and morphology of cells within alginate beads in 3D osteogenesis. A and B; CM-mESCs in alginate beads at day 0 of osteogenic culture in HARV bioreactor. C and D; CM-mESCs in alginate beads at day 11 of osteogenic culture in HARV bioreactor. E and F; CM-mESCs in alginate beads at day 16 of osteogenic culture in HARV bioreactor (X200 magnifications).

6.4.2.2. Bioprofiling

Following live and dead assay, in order to evaluate the growth kinetics of CM-mESCs within alginate beads indirectly, the consumption of nutrient in the osteogenic media in a HARV bioreactor was evaluated by measuring time-course concentration of glucose, lactate and ammonia, and by detecting pH of media during whole culture. In this study, the osteogenic media was refreshed every two days just after measuring the concentration of nutrients in cultured media using a bio-profiler. In pH kinetics, even though the fresh medium was supplied every two days, pH of Medium gradually decreased from 7.5 to 7.2 as culture time passed (Figure 62A). In glucose consumption kinetics, glucose concentration in medium was also reduced rapidly from 5.4 mM to around 0.15 mM even at day 2 of culture, followed by further reduction to 0 mM. In an opposite pattern with pH and glucose, ammonia and lactate concentration went up to 4.00 mM from 2.75 mM and up to 11.75 mM from 0 mM in medium, indicating ammonia and lactate production and

release though metabolism of cells within alginate beads into medium.

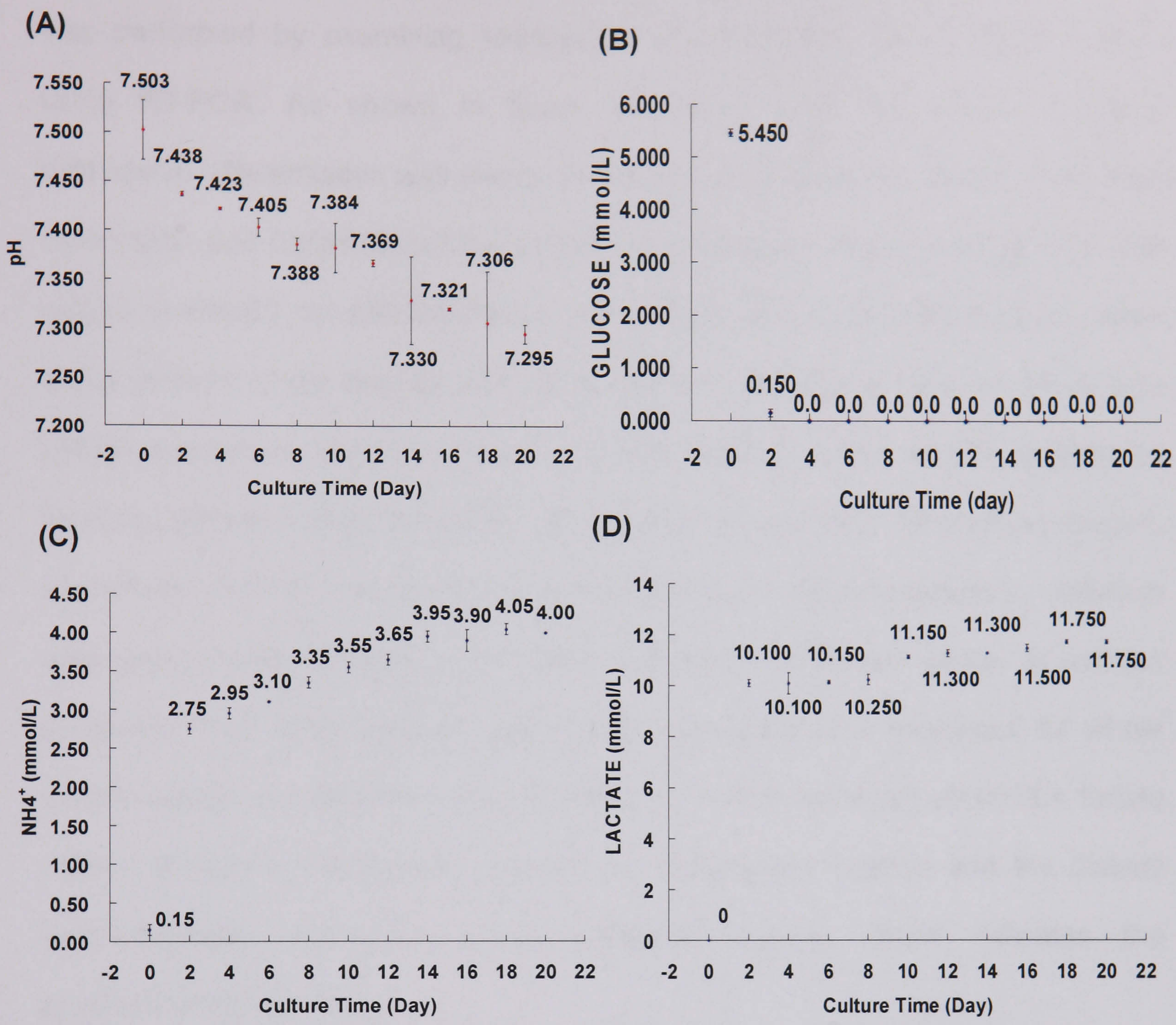


Figure 62. The change of pH, glucose, ammonia and lactate concentration in medium in accordance with culture time during 3D osteogenesis. (A) pH change, (B) Change of glucose concentration, (C) Change of ammonia concentration, (D) Change of lactate concentration.

6.4.2.3. Osteogenic gene expression

Following the evaluation of cell growth and metabolic activity in HARV bioreactor culture system, osteogenic differentiation was also characterized by distinct cellular phenotypes, such as a component of specific extracellular matrix and transcription factor gene expression profiles. In this study, direct osteogenic differentiation of mESCs by bypassing EB formation process was evaluated by

osteogenic gene expression level. Characterisation of osteogenic differentiation was performed by examining expression of osteocalcin, Cbfa1/Runx2, osterix using RT-PCR. As shown in figure 63, these gene expression indicating osteogenic differentiation was clearly detected in 3D osteogenic culture. Especially, osteocalcin and Cbfa1/Runx2 transcripts were induced to express in mESCs after culture in HepG2 conditioned medium for 3 days, and expressed at steady state levels through whole osteogenic culture period in osteogenic medium, but osterix mRNA expression was not detected in the culture under HepG2 conditioned medium. Different from the pattern of osteocalcin and Cbfa1/Runx2 expression, expression of osterix transcript was upregulated by 11 day of osteogenic culture in osteogenic media, followed by consistent expression for further culture. In addition, to confirm their differentiation stage, Oct4 expression was evaluated for whole culture period, showing the strong expression of Oct4 transcript of mESCs before culture in HepG2 conditioned medium and osteogenic medium and the distinct down-regulated expression over osteogenic culture, which indicates the progressive differentiation.

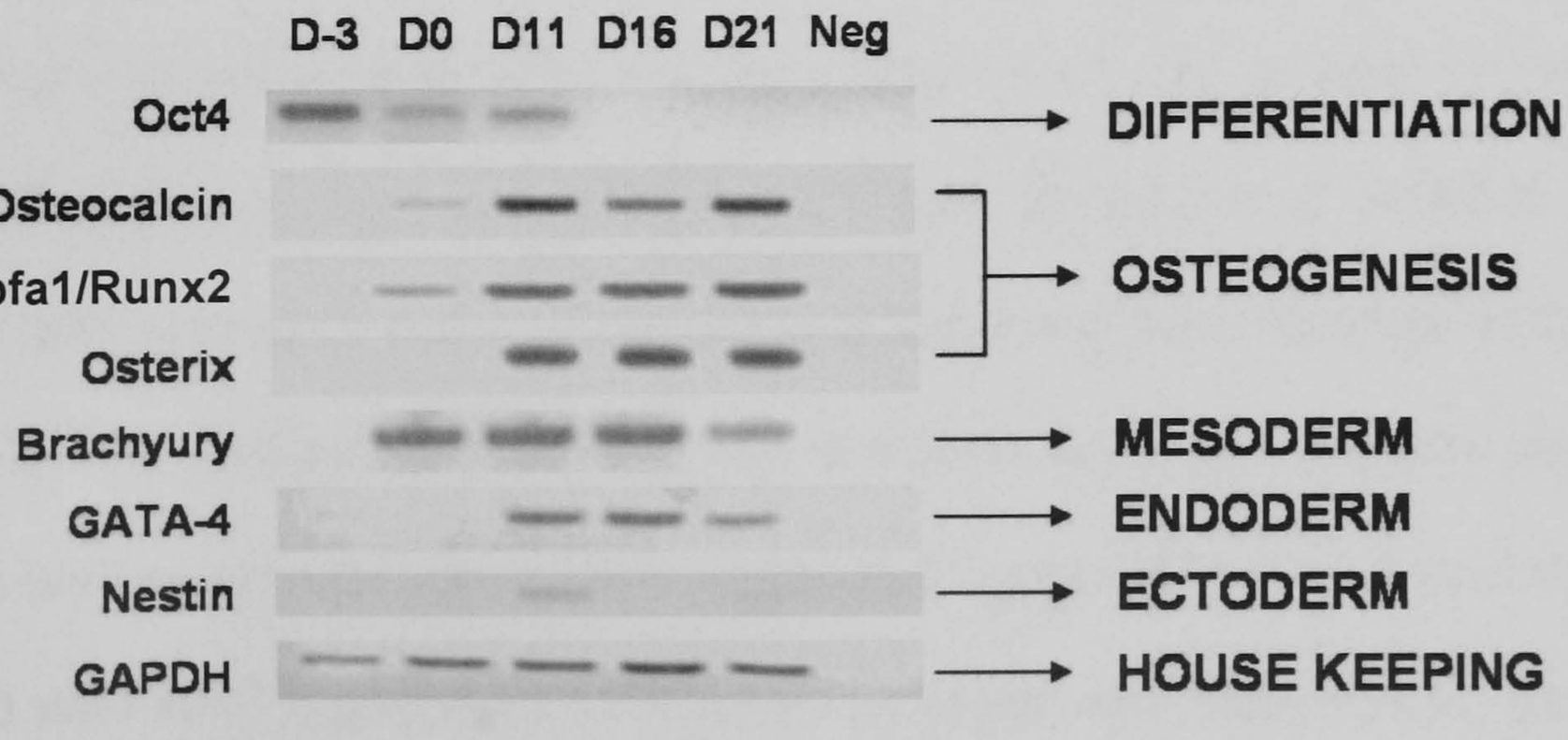
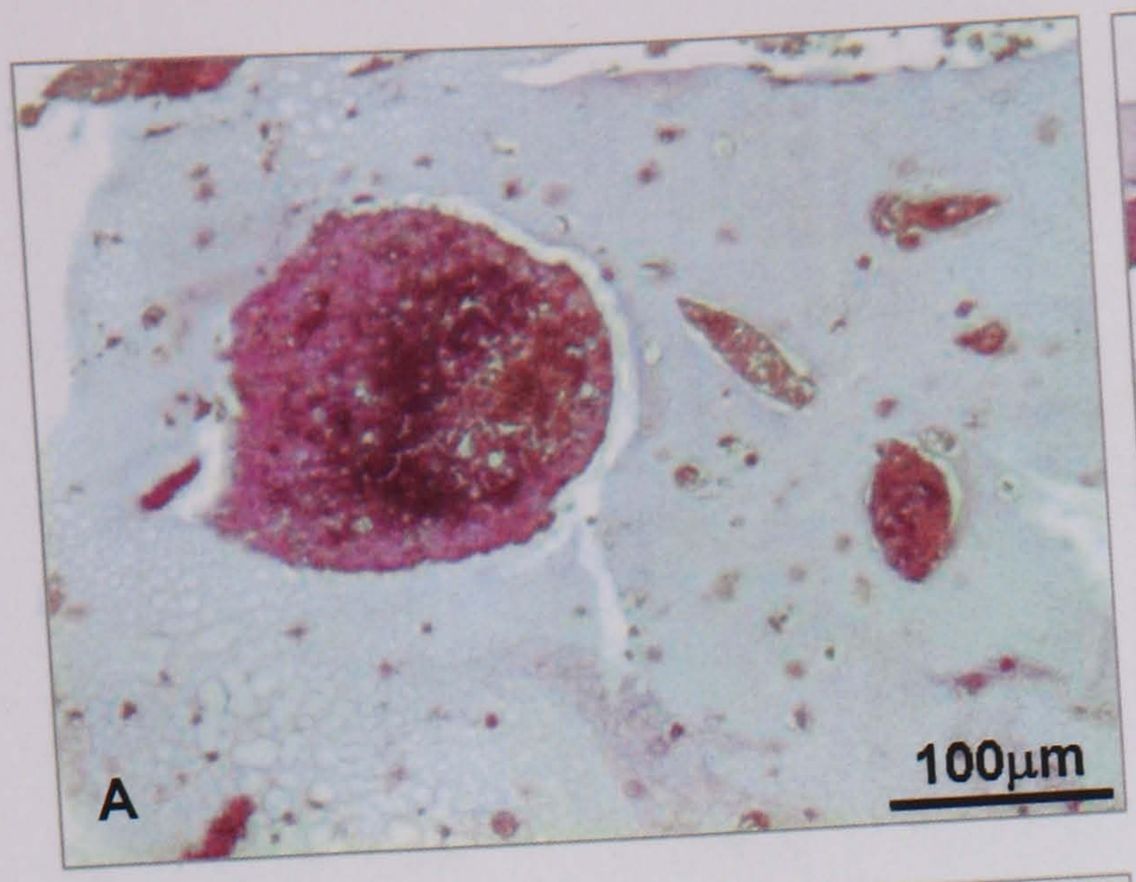
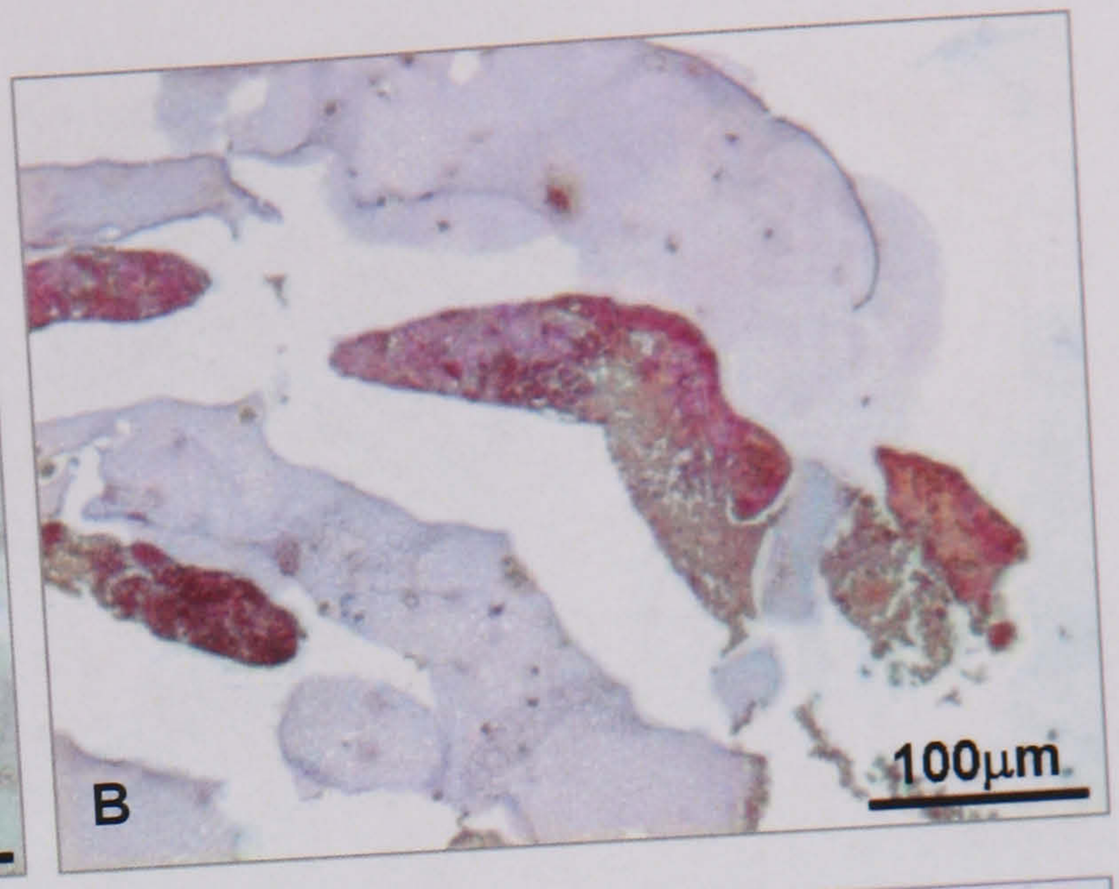


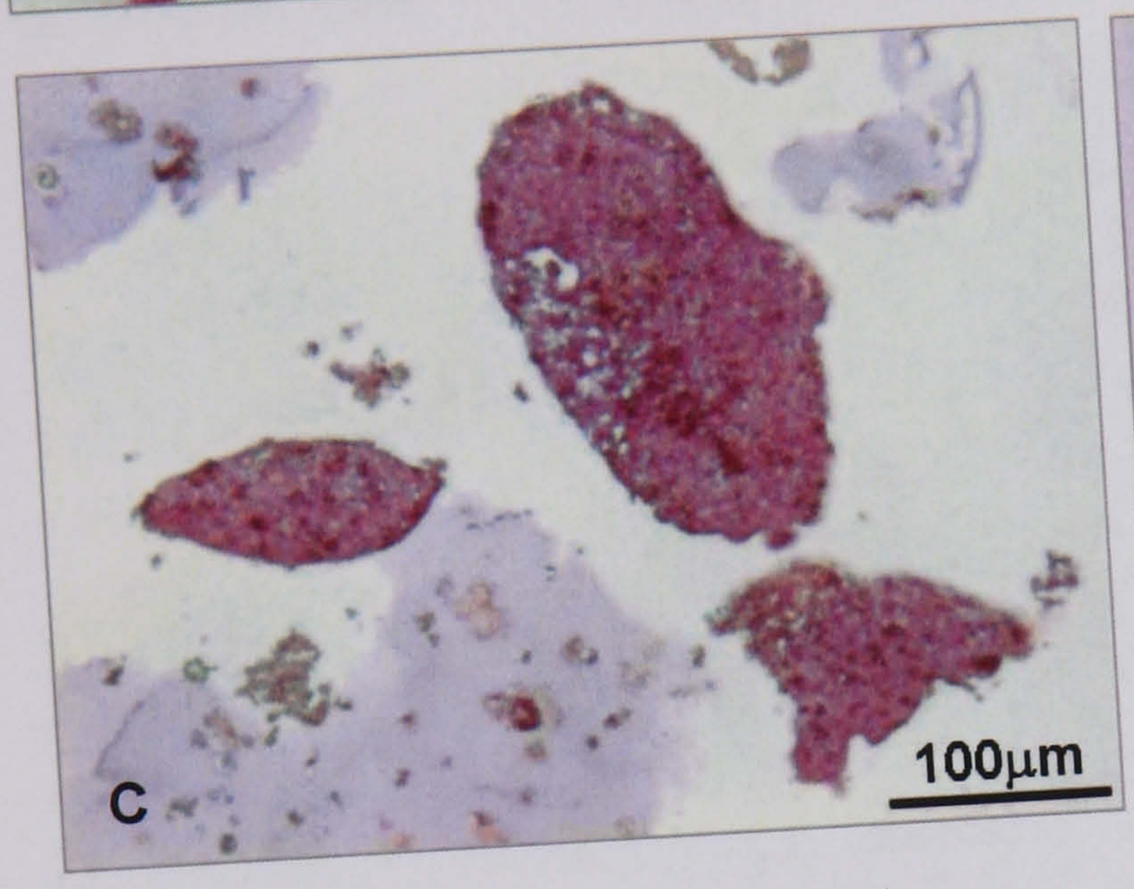
Figure 63. RT-PCR analysis of osteogenic gene expression in 3D osteogenesis.

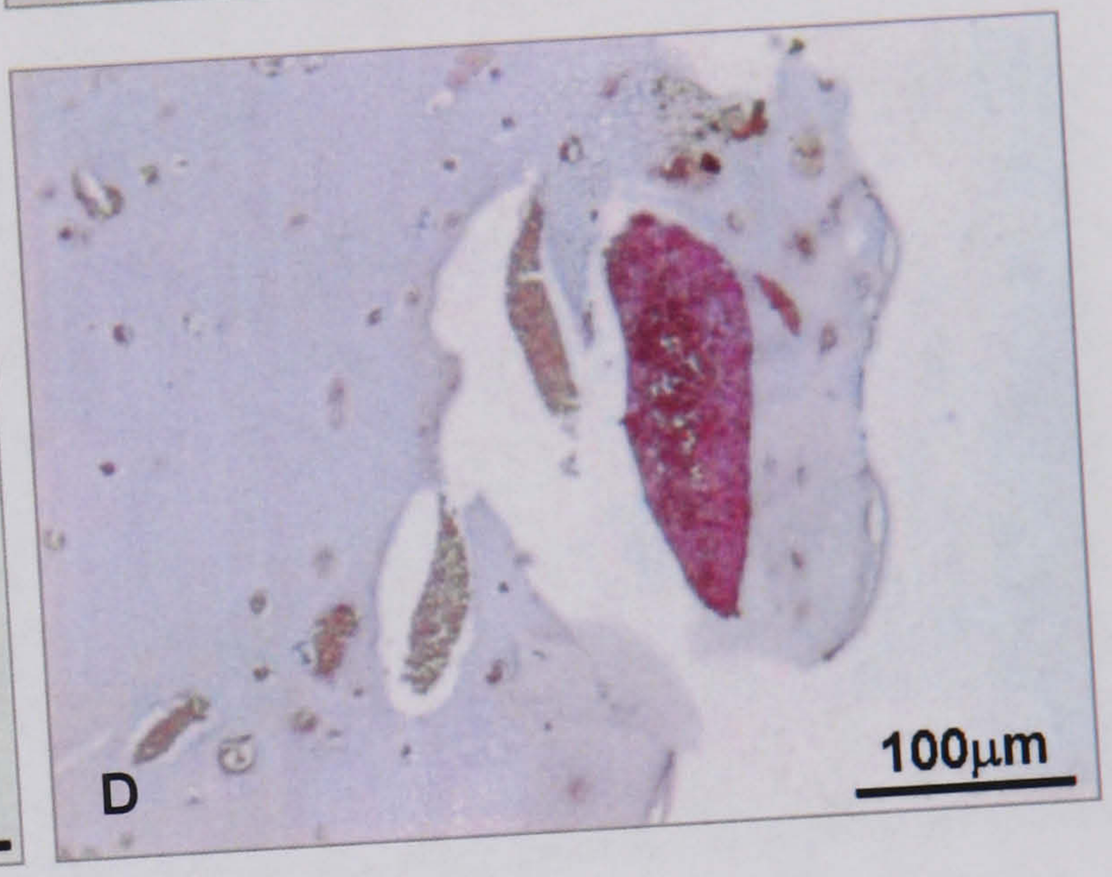
6.4.2.4. Staining and immuno-staining

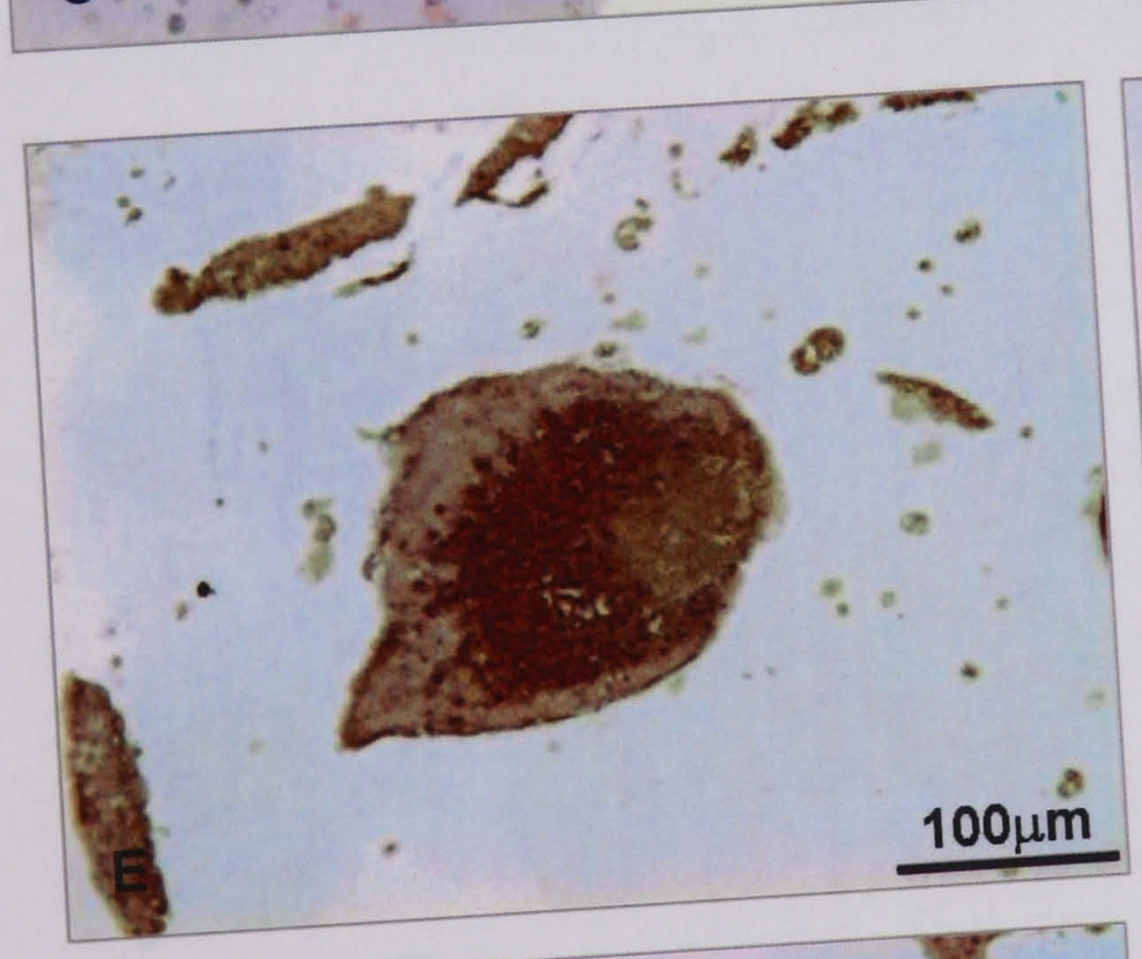
In our previous study, early differentiated mESCs (CM-mESCs) formed mineralised bone nodules *in vitro* in 2D culture system without EB formation process. Therefore, we addressed whether the CM-mESCs were also capable of forming mineralised bone nodule in 3D culture system using alginate beads and a HARV bioreactor. The encapsulated mESC were subjected to be cultured in HepG2 CM in order to induce early differentiation into specific cell population with high osteogenic capacity and then to differentiate directly into osteogenic lineage in replaced osteogenic medium in suspension culture system within bioreactor. The H&E staining showed well developed three dimensional tissue formation within alginate beads with size variation, which some of large tissues represents 200-300 μm in diameter or length, after 21 days of osteogenic culture (Figure 64 A-D). In addition, in order to confirm whether these tissues were mineralised bone tissue by osteogenic differentiation, Alizarin red S (ARS) staining was done for the characterisation of calcium deposit in tissues. ARS staining represents mineralised areas that stained dark-red with ARS, which became noticeable around centre region of tissues, indicating bone nodule-like mineralised matrix accumulation, and the other areas showed weak ARS staining (Figure 64 E-H). In addition, when the ARS-stained area was exposed to filtered UV light (excitation at 530-560 nm and emission at 580 nm), only mineralised area represented fluorescence as shown in figure 64 I-L. For further confirmation, the sections were stained with anti-type I collagen as well as an anti-osteocalcin antibody (Figure 64 M-T). Most of the areas that stained with ARS expressed both type I collagen and osteocalcin. Especially, type I collagen was expressed markedly at peripheral region around cells and tissues, and osteocalcin immuno-staining was also found at similar region with type I collagen with relatively weak intensity.


A
100μm

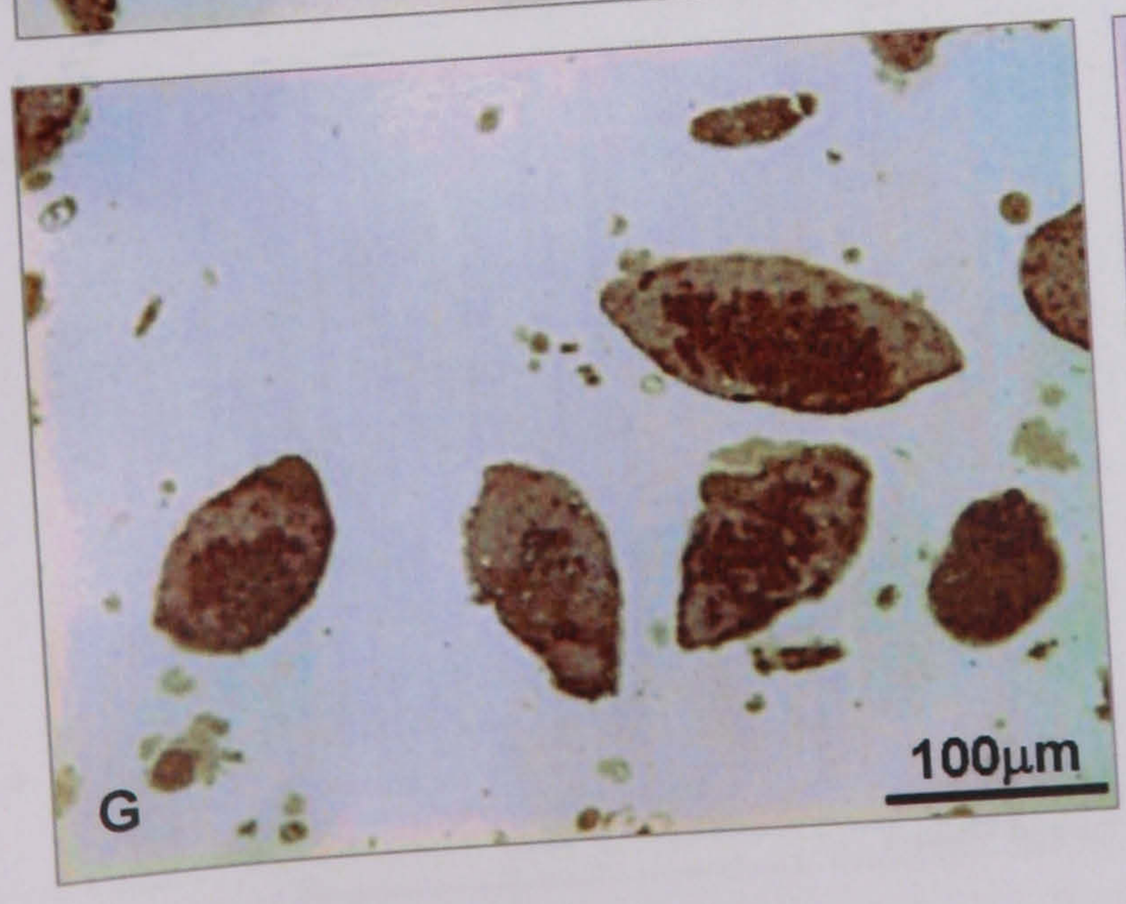

B
100μm

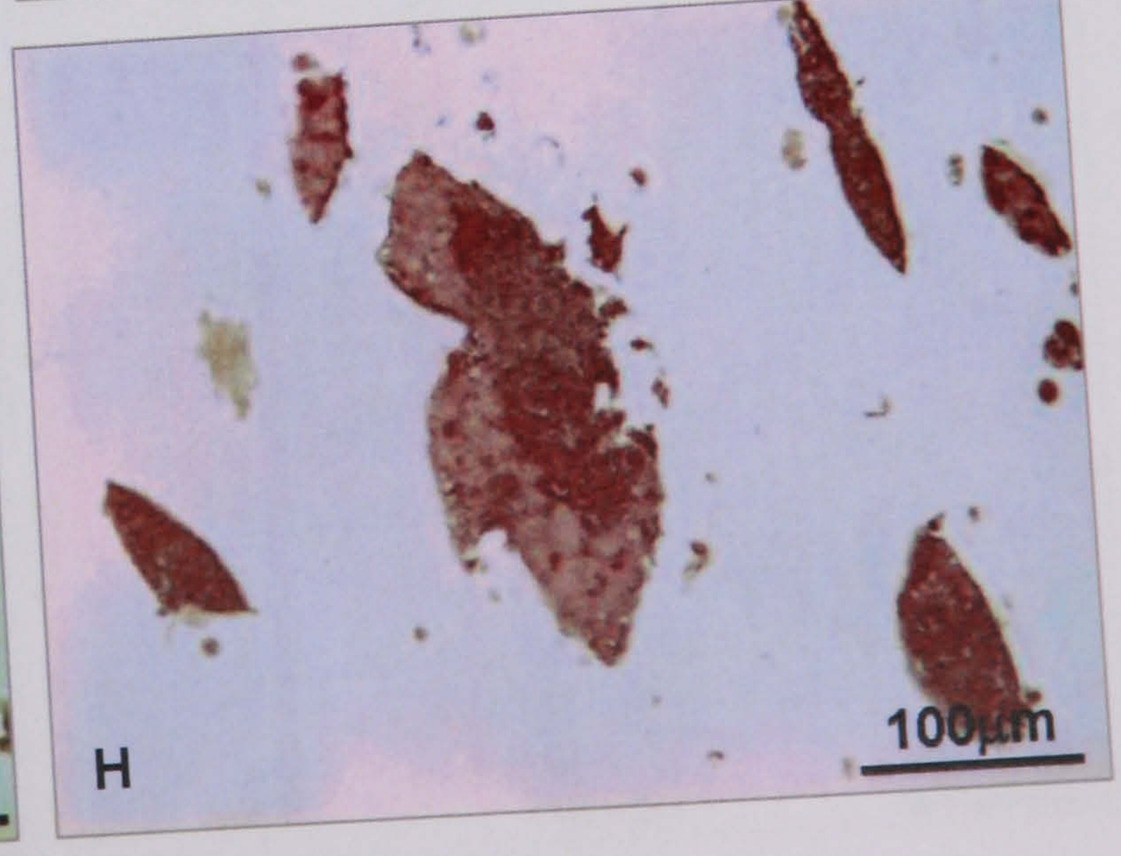

C
100μm

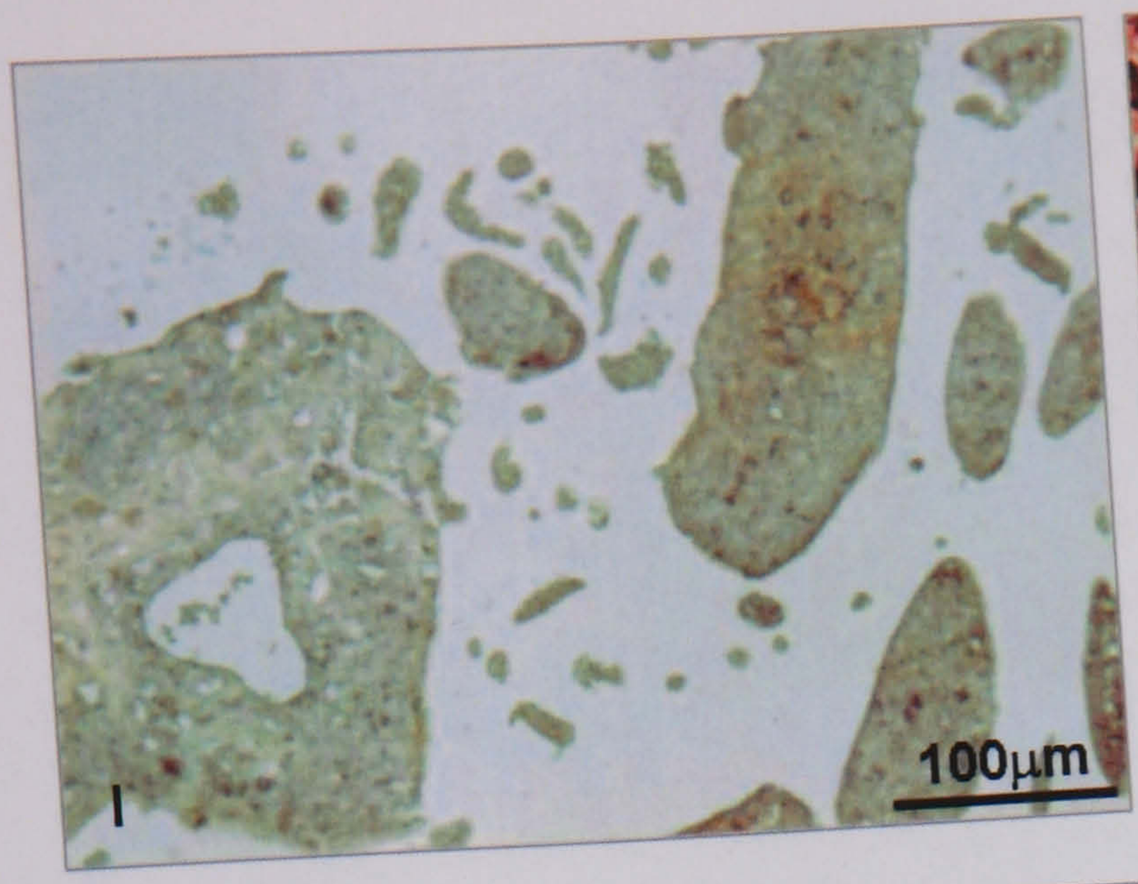

D
100μm

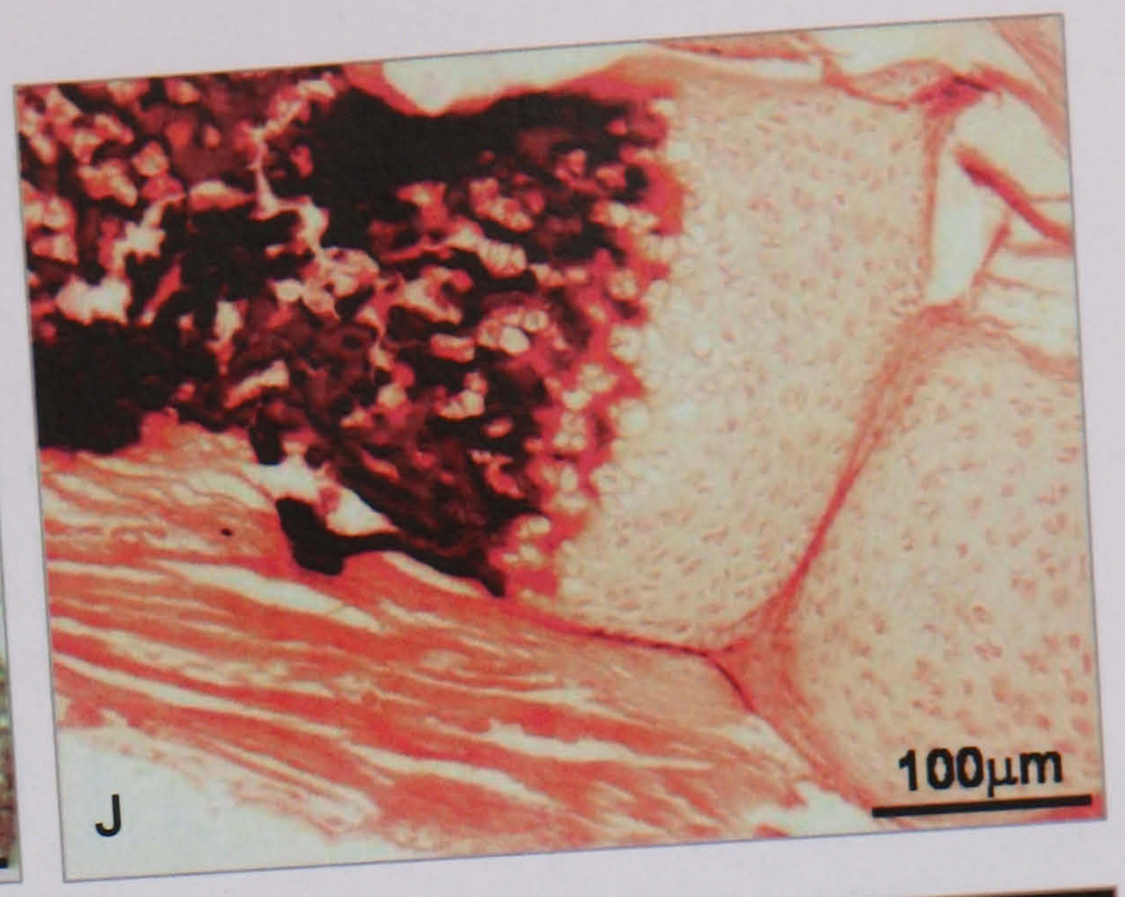

E
100μm

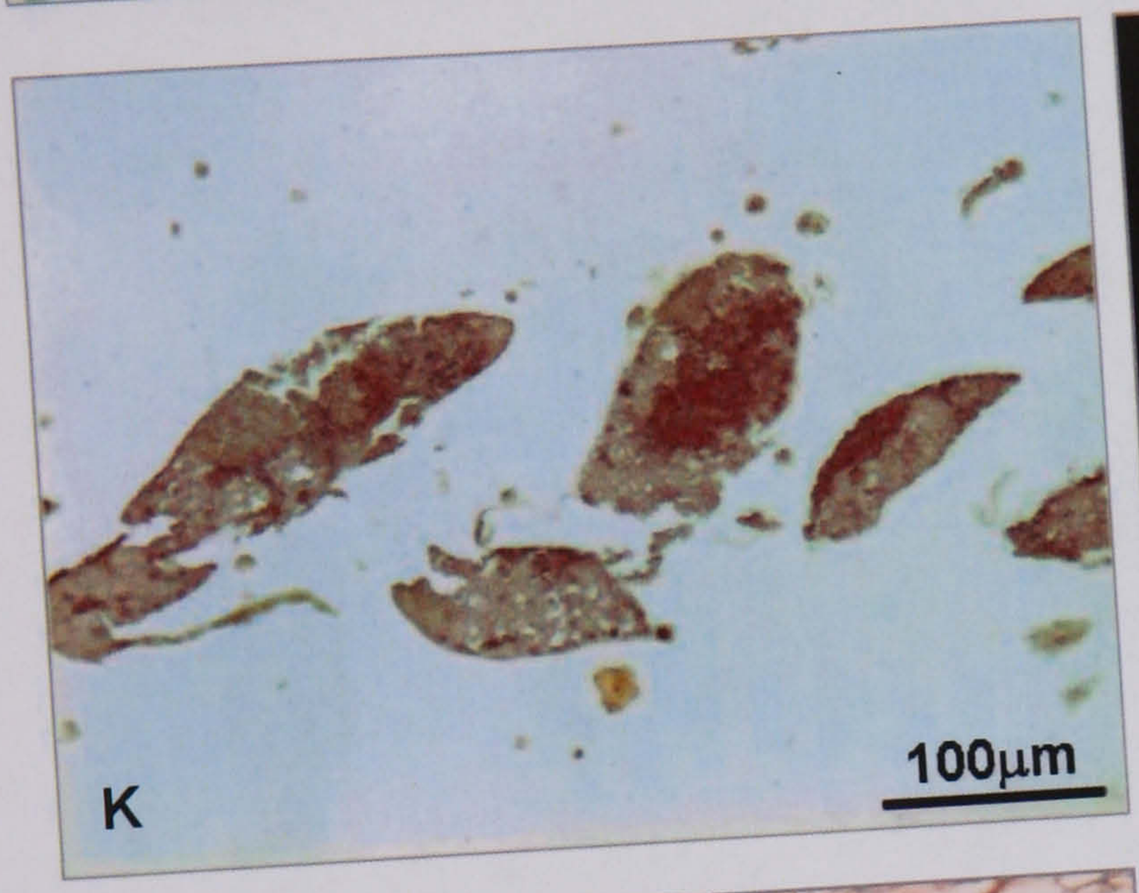

F
100μm

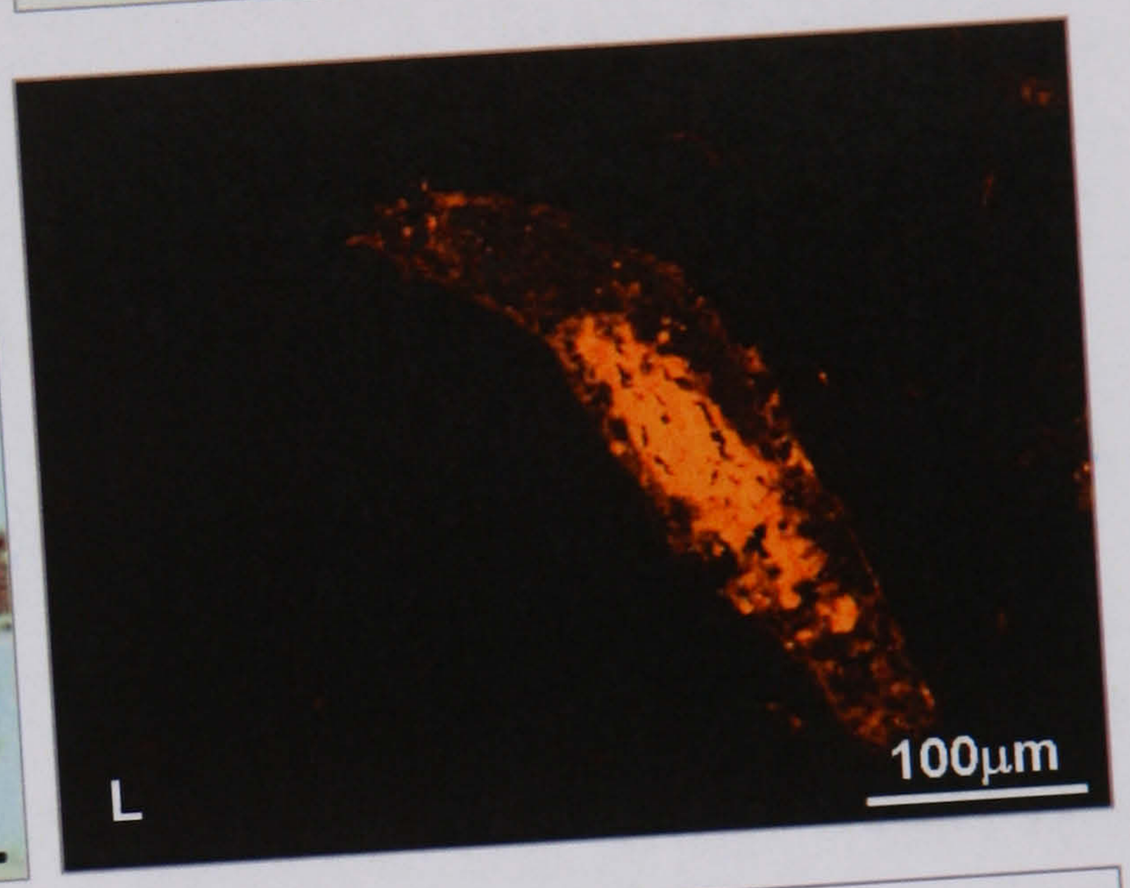

G
100μm

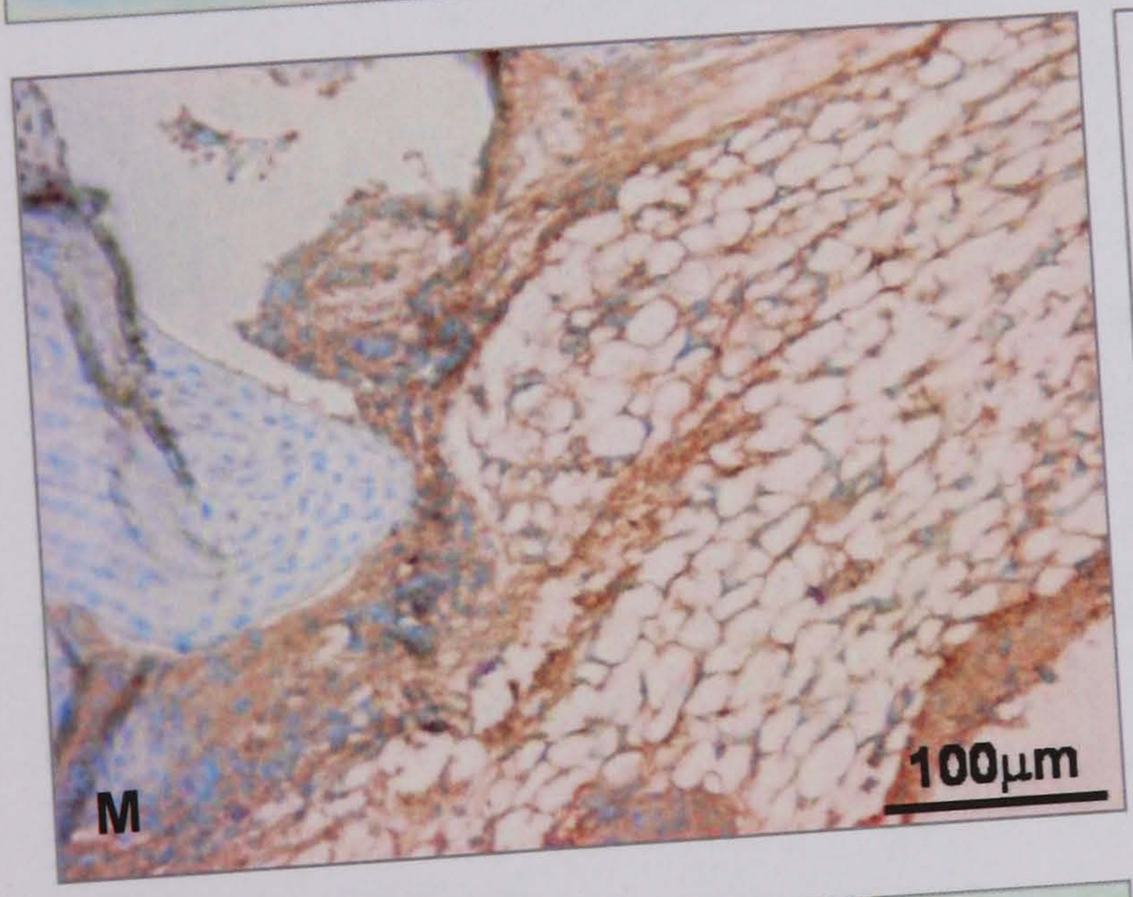

H
100μm

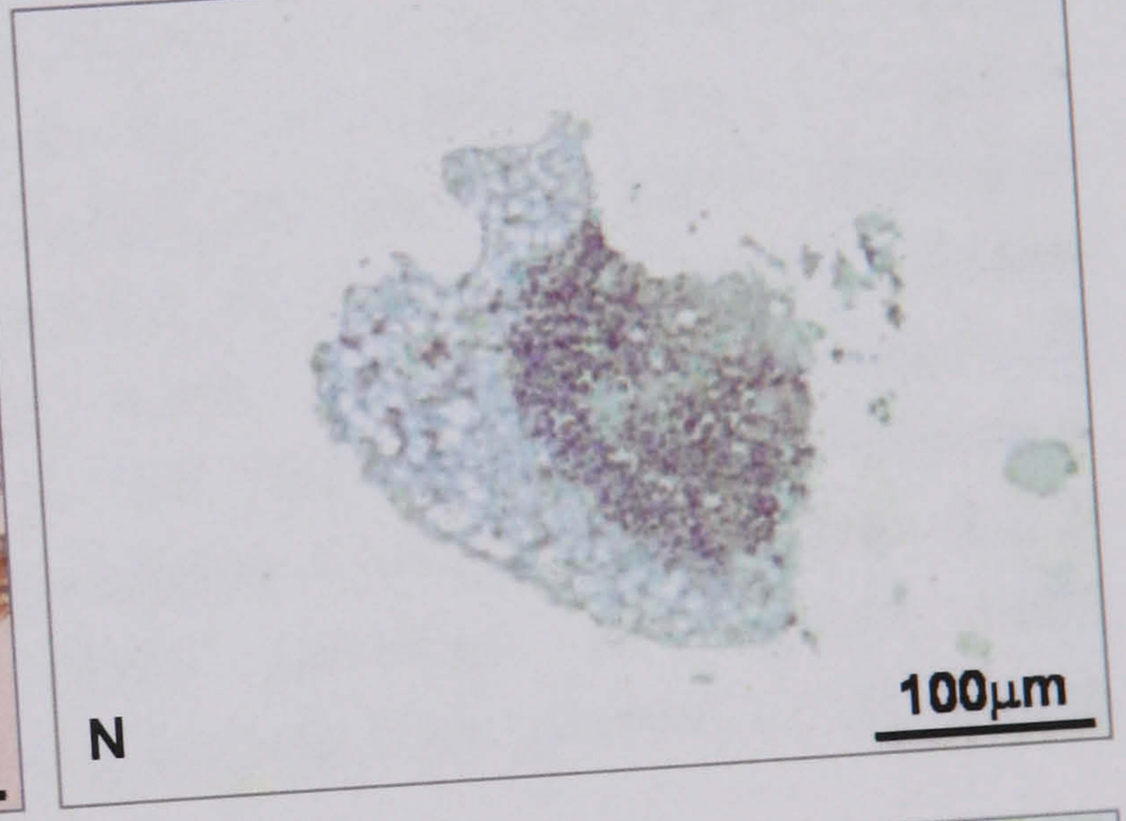

I
100μm

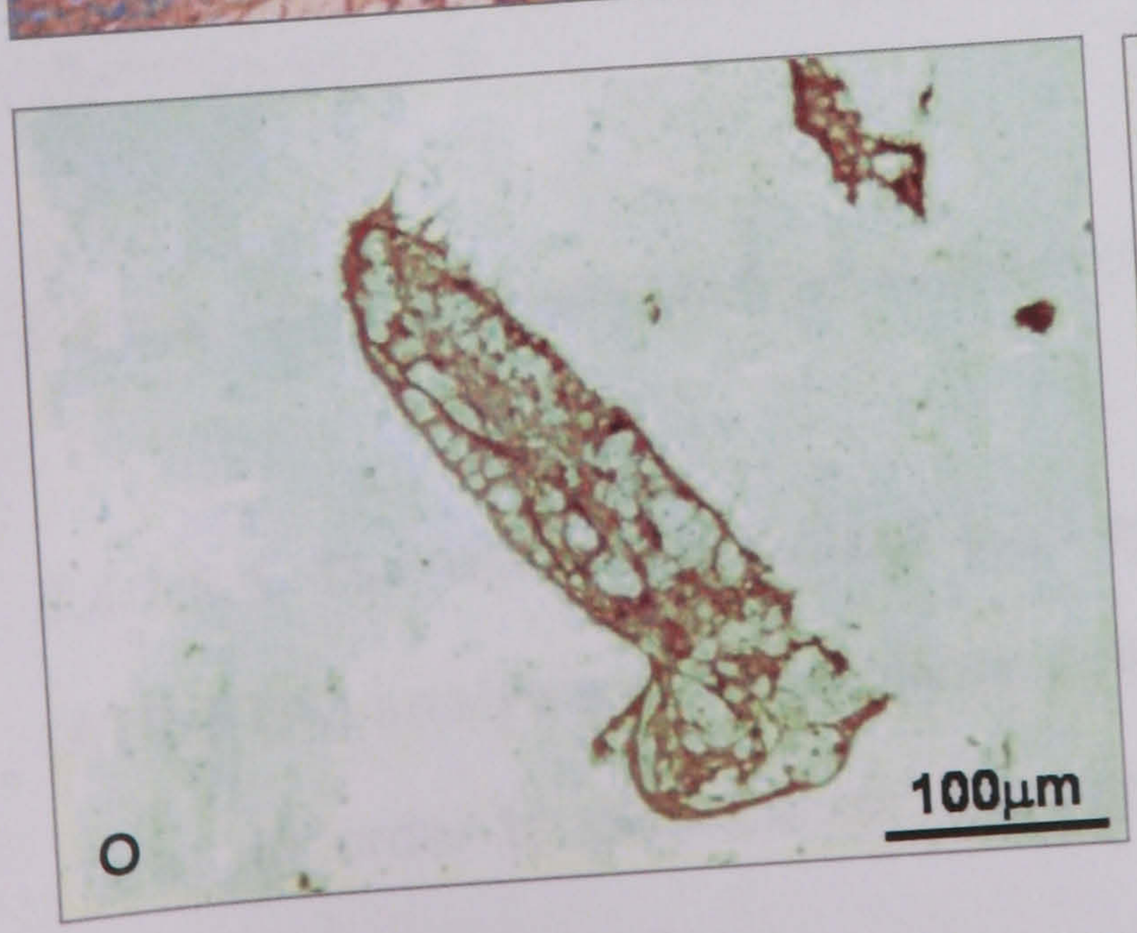

J
100μm

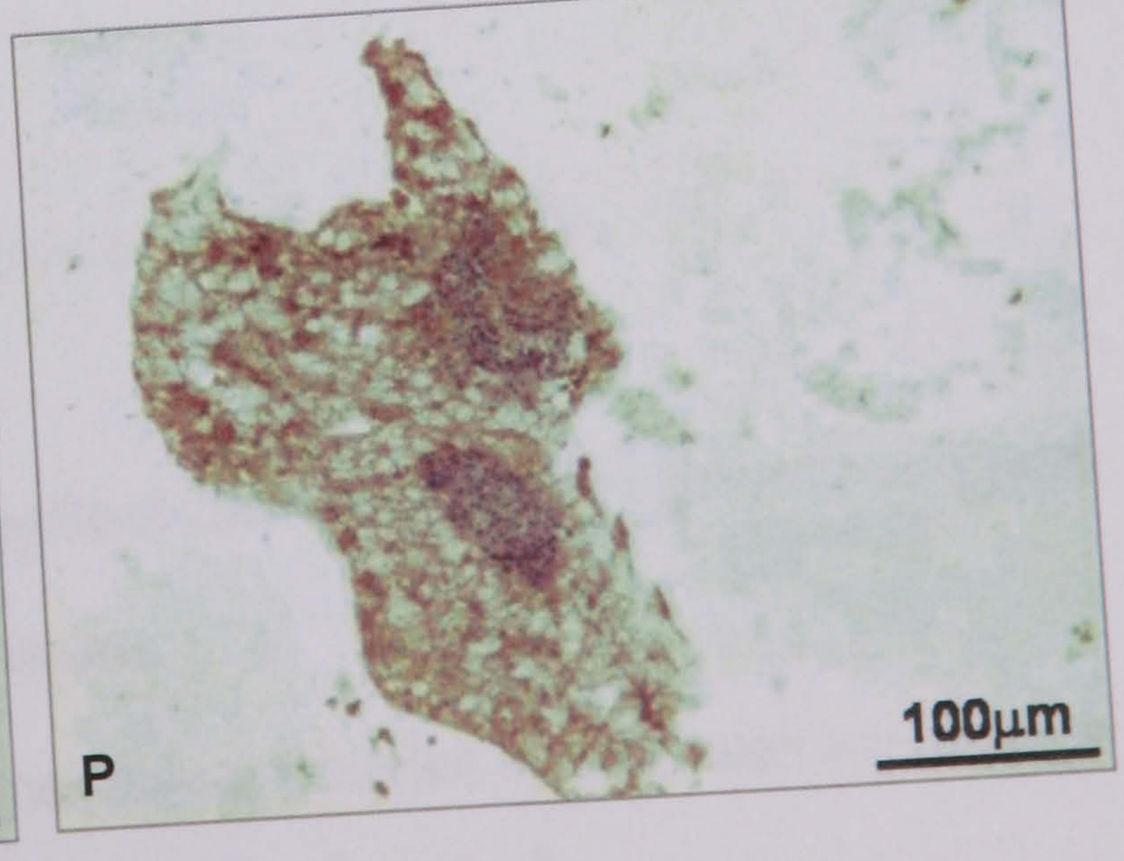

K
100μm


L
100μm


M
100μm


N
100μm


O
100μm


P
100μm

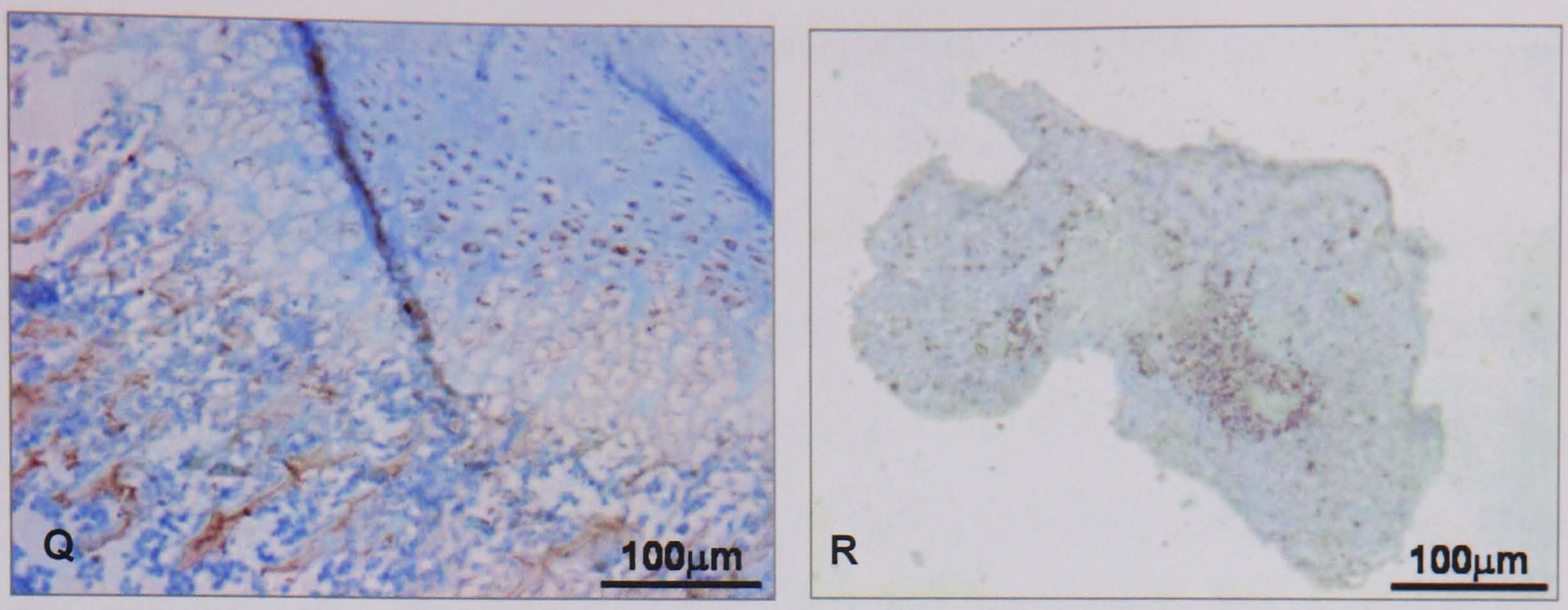


Figure 64. Various staining and immuno-staining for mineralised bone nodules and osteogenic differentiation. A-D: H&E staining, E-H: ARS staining, I: negative staining of ARS, J: positive staining of mouse bone tissue, K: positive staining of ARS and L: ARS positive staining representing fluorescence. M: type I collagen immuno-staining of mouse bone tissue, N: negative staining for type I collagen, O & P: type I collagen immuno-staining of 3D bone construct. Q: Osteocalcin immuno-staining of mouse bone tissue, R: negative staining for Osteocalcin, S & T: Osteocalcin immuno-staining of 3D bone construct. All alginate bead encapsulating cells were allowed to direct osteogenic differentiation for 21 days in HARV bioreactors.

6.4.2.5. Physicochemical characterisation of alginate beads

6.4.2.5.1. The micro attenuated total reflection-Fourier transformed infrared (ATR-FTIR) analysis of mineralised nodules

In order to characterise the mineralised nodules within alginate beads,

alginate beads encapsulating cells were collected to evaluate mineral components of mineralised nodules after 21 days of osteogenic culture using ART-FTIR analysis method in combination with a focal plane array (FPA) detector. Firstly, FTIR images were collected with this system, and FTIR imaging showed distinct presence of phosphate only in the sample of cells plus alginate bead directing osteogenic differentiation (Figure 65 C), not in pure alginate beads (Figure 65 A) and cells plus alginate beads (Figure 65 B) when the images were plotted by the integrated absorbance of PO_4 (between 970 cm^{-1} and 1035 cm^{-1}) and amide I (between 1565 and 1500 cm^{-1}). The FTIR spectrum of mineralised bone nodules showed characteristic functional groups of phosphate moieties. Phosphate peaks were observed between 970 cm^{-1} and 1035 cm^{-1}. This ATR-FTIR analyses of the mineralised nodules suggested that they are apatitic since the characteristic PO_4 (at 1016 cm^{-1}) vibrations were observed (Figure 66 E), which are typical of apatitic minerals [Granja PL 2005, Aparicio S 2002, Sandeep GH 2006]. Furthermore, two major additional peaks such as hydroxyl and H_2O peak, centred at around 1650 cm^{-1} and 3250 cm^{-1} were observed in FTIR spectrum (Figure 65 E), which could be derived from control alginate beads and media in sample evaluation (Figure 65 D). Another interesting bands in this evaluation was amide I (between 1565 and 1500 cm^{-1}) regarding whether the mineralised nodule was derived from cellular origin, but the amide I peak was not characterised due to shielding effect by high peak of H_2O from sample media. In addition, another minor peak that can be considered as carbonyl (CO_3^{2-}) peak regarding its peak band [Aparicio S 2002], indication biological mineralisation of bone tissue. It has been well proved that in the biological mineralization of bone tissue, hydroxyl ions and PO_4^{3-} is substituted in the apatite structure by CO_3^{2-} or HPO_4^{2-} [Sandeep GH 2006].

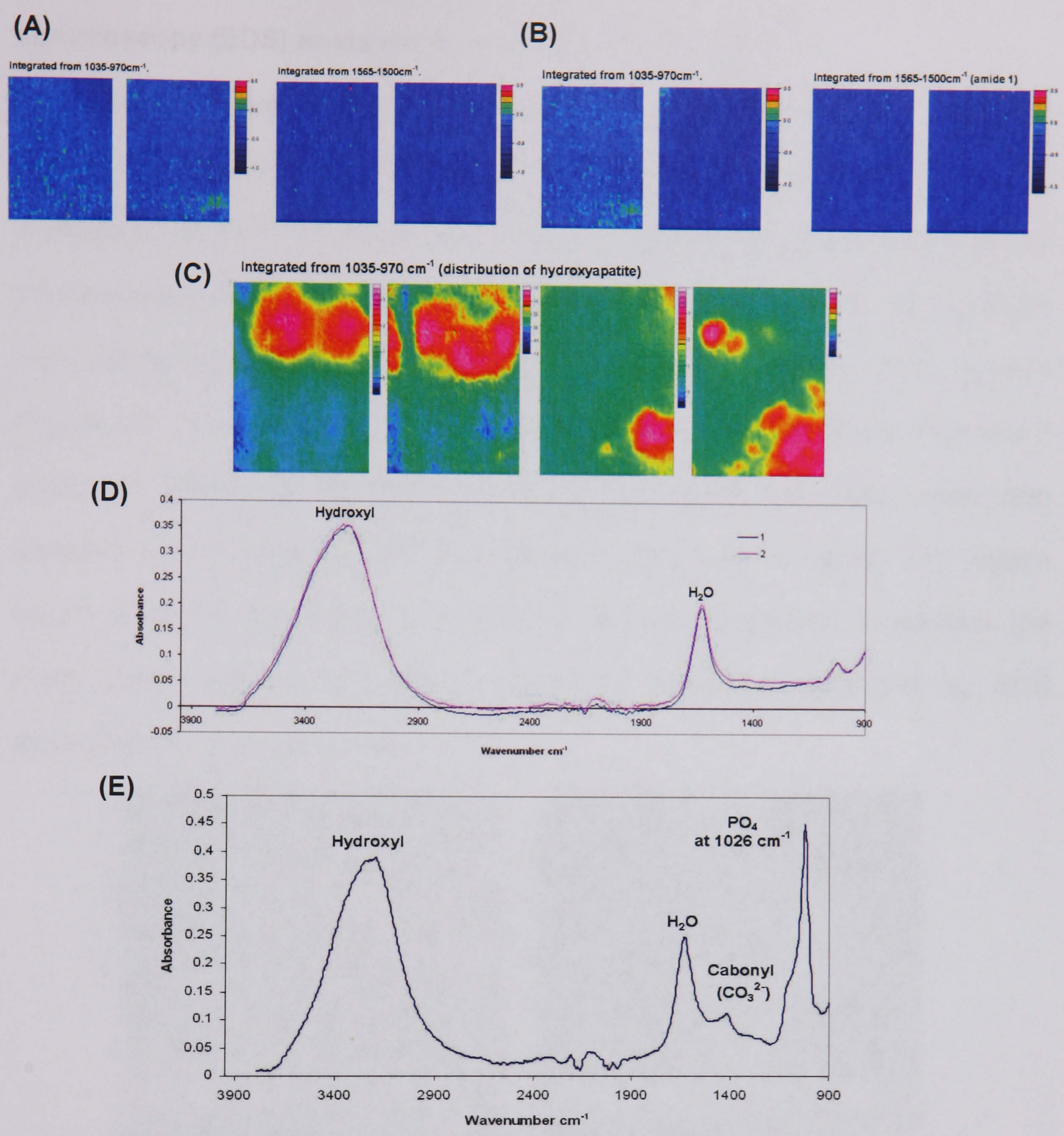


Figure 65. The FTIR images and ATR-FTIR spectra of cell + alginate construct; generated by plotting the integrated absorbance of PO_4 (between 970 cm^{-1} and 1035 cm^{-1}) and amide I (between 1565 and 1500 cm^{-1}) over the imaged area; the colour scale bar shows the value of the integrated absorbance. (A) Chemical image of pure alginate beads. (B) Chemical image of alginate beads encapsulating cells. (C) Chemical image of alginate beads encapsulating cells directed into osteogenic differentiation. (D) ATR-FTIR spectra of pure alginate beads analysed. (E) ATR-FTIR spectra of alginate beads encapsulating cells directed into osteogenic differentiation analysed.

6.4.2.5.2. Scanning Electron Microscope (SEM) and Energy Dispersive spectroscopy (EDS) analysis of mineralised bone nodules

When viewed by SEM, many mineralized deposit were observed within alginate hydrogels encapsulating cells after osteogenic culture. In the X-ray analysis observation, SEM pictures showed the presence of non-stoichiometric mineralised deposits, and mineralised bone nodules within alginate hydrogels were mainly composed of calcium and phosphorous, proved by EDS analysis (Figure 66). The EDS spectrum of mineralised nodules showed specific Ca and P peaks. In addition, in the spectrum, minor magnesium and sodium were also detected as one of component. A relatively higher peak of carbon and oxygen might be due to the cellular component or alginate component. In addition, the Ca/P molar ratio of the calcium phosphate formed, as analysed by EDS microanalysis, was about 1.23.

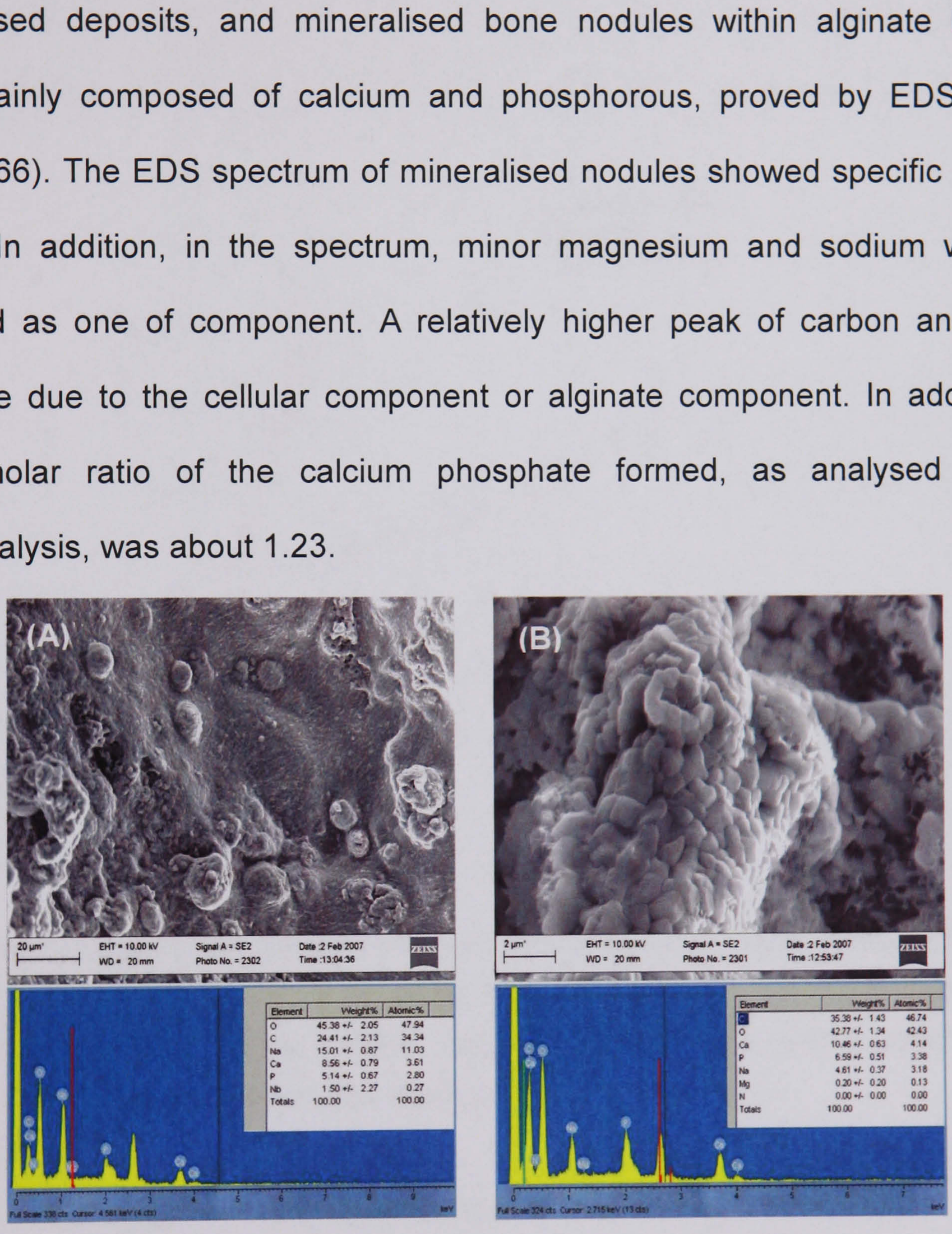
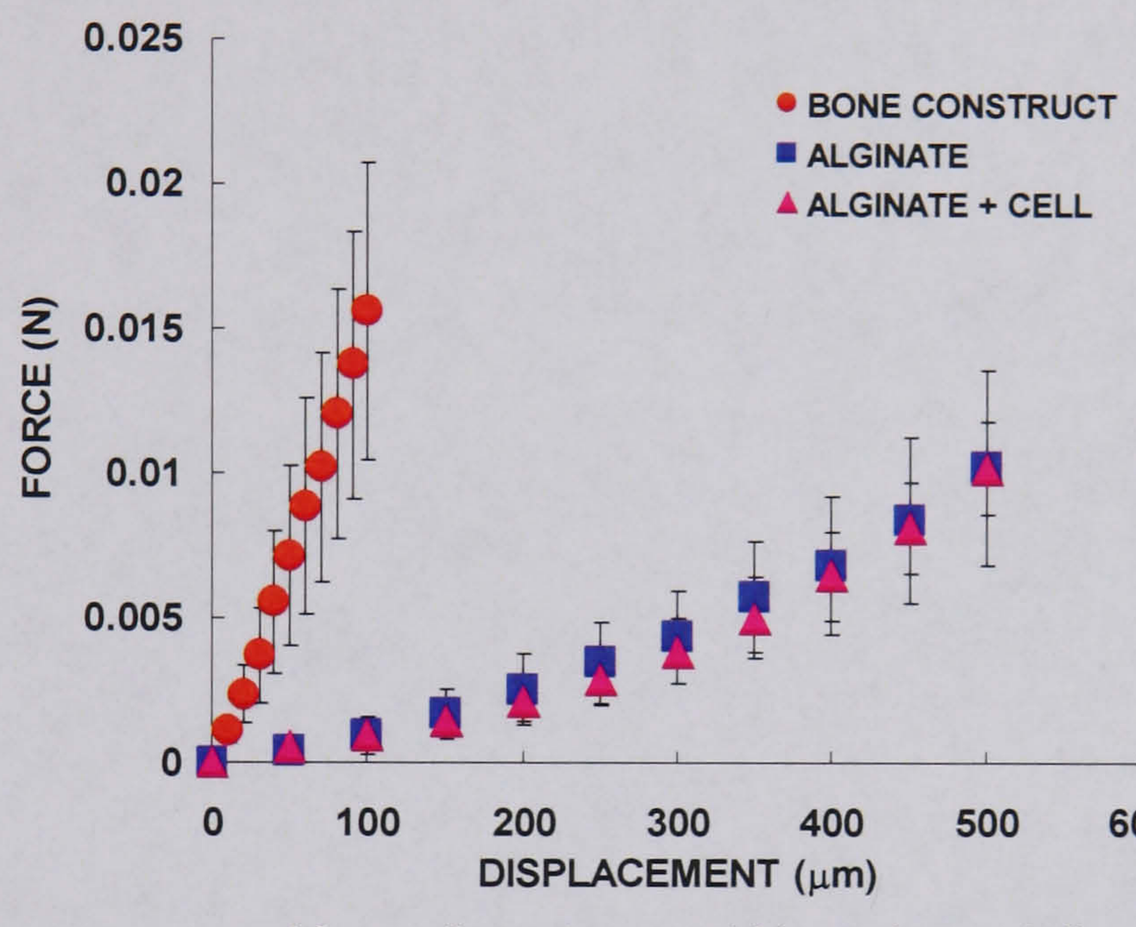


Figure 66. SEM and EDS microanalysis spectra for the composition of mineralised bone nodules formed within alginate beads in the osteogenic culture of mESCs after 21 days. (A): Low magnified SEM observation and its EDS analysis. (B): High magnified SEM observation and its EDS analysis.

6.4.2.5.3. Mechanical property of 3D bone like construct

The mechanical property of bone like construct was characterised by compression testing. The compressive modulus was measured for each test materials including controls, and the bone constructs, which were formed by the osteogenic culture of mESCs for 21 days in HARV bioreactor following alginate encapsulation, was stiffer than the controls, pure alginate beads and alginate bead encapsulating undifferentiated mESCs with same cell density as bone construct



Mean diameters and Young's moduli

Particle	Mean diameter (μm)	Calculated Young's modulus (kPa)
Alginate	3059 ± 79	35.2
Alginate + Cell	3548 ± 59	29.3
Bone Construct	3154 ± 49	666.2

Figure 67. Mechanical strength of bone like construct. Bone construct: 21 days osteogenic culture of mESCs encapsulated with alginate. Alginate: pure alginate bead without cells. Alginate + Cells: Alginate bead encapsulating undifferentiated mESCs with same cell density as Bone construct.

6.4.3. *In vitro* single step 3D chondrogenesis in a HARV bioreactor

6.4.3.1. Observation of cell viability

As shown in figure 68, at day 5 of chondrogenic culture, most of cells within alginate beads showed intensified green fluorescence indicating live cells with very few yellow or orange fluorescence, and as culture time passed,

population of dead cells was gradually increase, but the size of cell aggregation with tissue like structure was also increased. In addition, comparing with cell viability within alginate beads in HARV bioreactor, the cells within alginate bead in static culture condition at day 5 of culture showed much higher population of dead cells (Figure 68G).

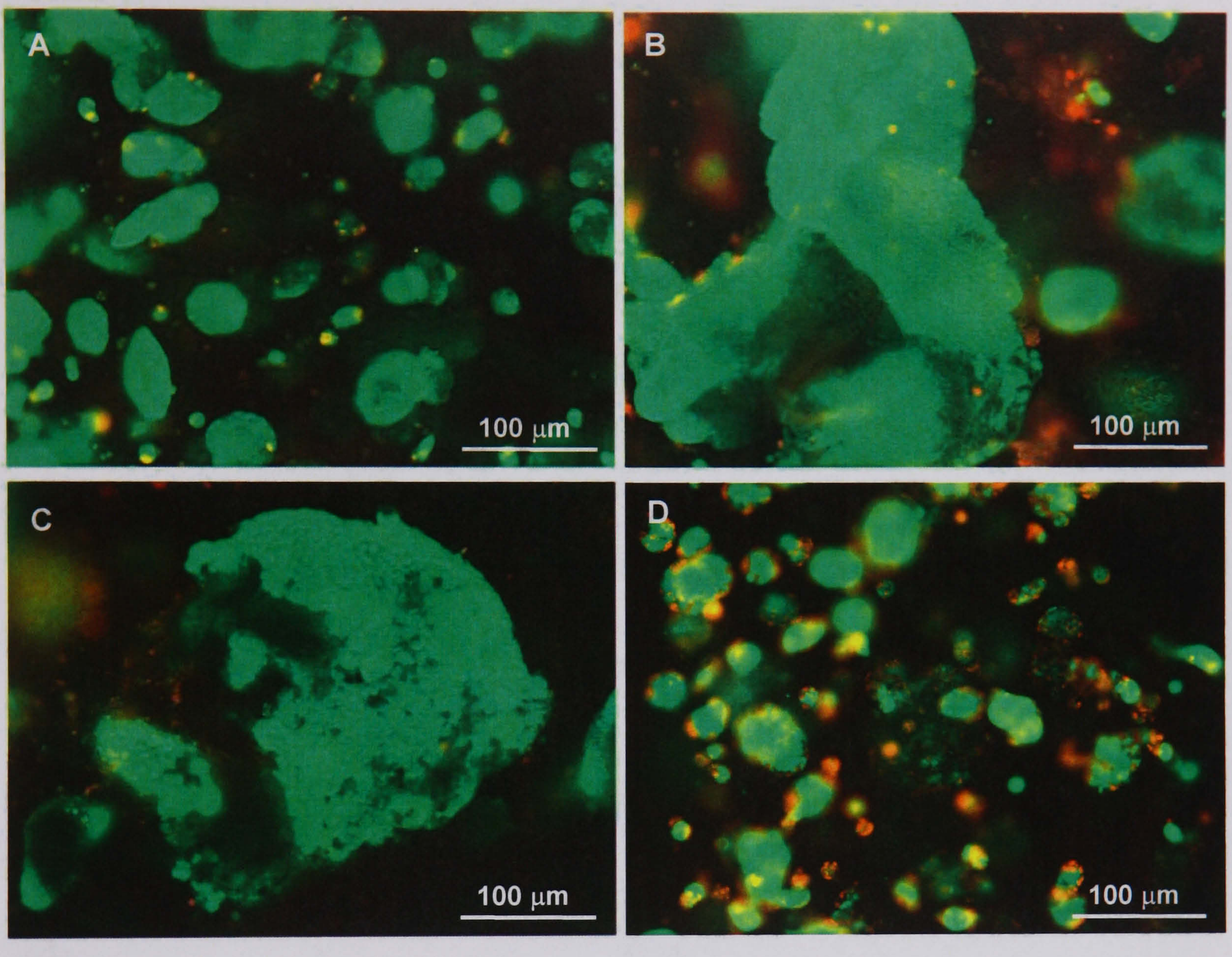


Figure 68. Live/dead assay and morphology of cells within alginate beads. A, B and C; CM-mESCs in alginate beads at day 5, day 10 and day 15 of chondrogenic culture in HARV bioreactor. G: CM-mESCs in alginate beads at day 5 of chondrogenic culture in 2D static culture condition.

6.4.3.2. Bioprofiling

Following live and dead assay, in order to evaluate the growth kinetics of CM-mESCs within alginate beads indirectly, consumption of nutrient in the chondrogenic media in a HARV bioreactor was evaluated by measuring time-course concentration of glucose, ammonia, and lactate and by detecting pH of media during whole culture. In this study, the chondrogenic media was refreshed

every two days just after measuring the concentration of nutrients in cultured media using a bio-profiler. In pH kinetics, even though the fresh medium was supplied every two days, pH of Medium gradually decreased from 7.6 to 7.0 as culture time passed. In glucose consumption kinetics, glucose concentration in medium was also reduced rapidly from 22 mM to around 10 mM even at day 2 of chondrogenic culture without further reduction in concentration for following culture period. In an opposite pattern with pH and glucose, ammonia concentration went up rapidly from 0.55 mM to 1.65 mM even at day 2 of chondrogenic culture and increased finally up to 2.45 mM at day 15, and lactate concentration went gradually from 0 mM up to 22.6 mM in medium, indicating ammonia and lactate production and release though metabolism of cells within alginate beads into medium. (Figure 69)

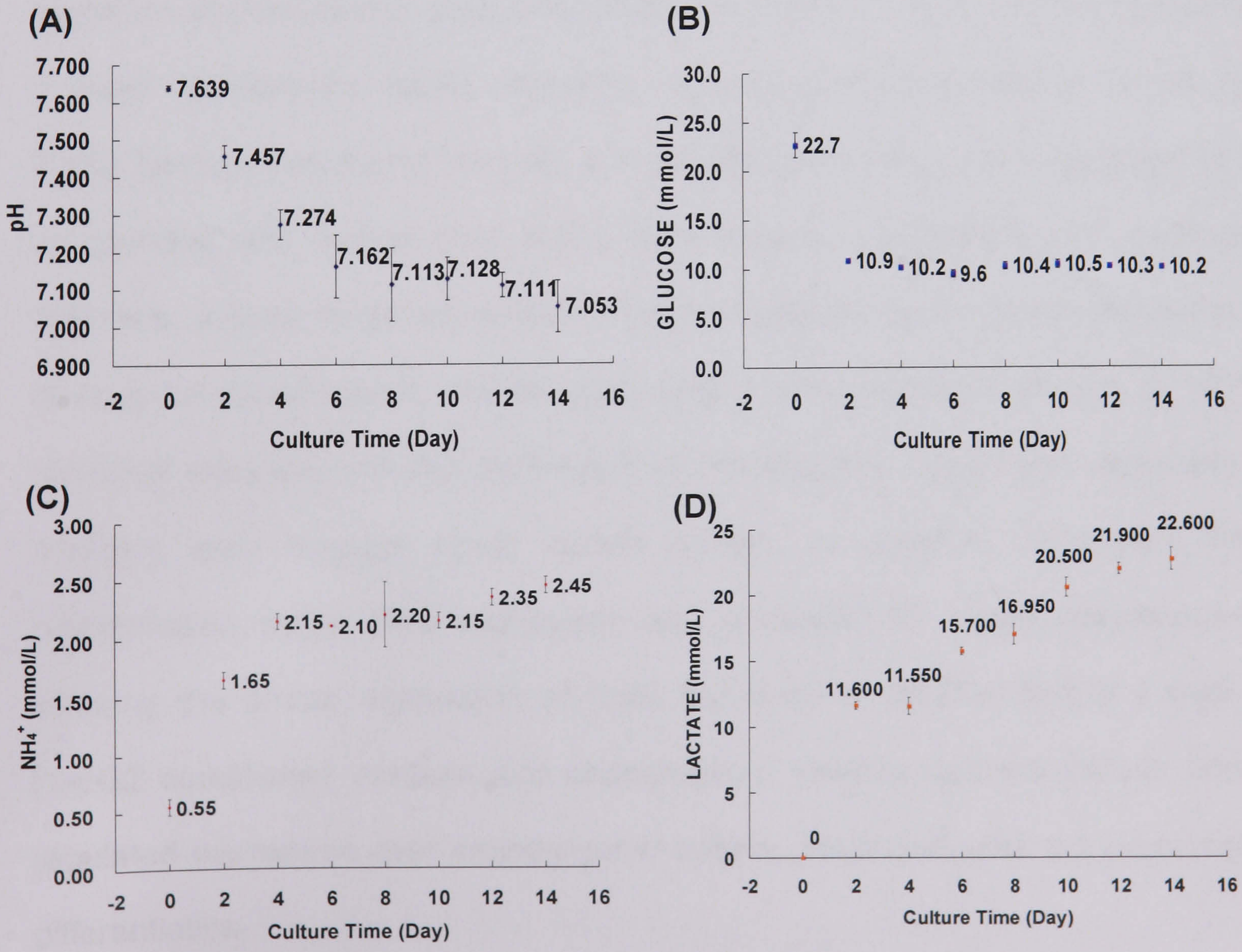


Figure 69. The change of pH, glucose, ammonia and lactate concentration in

medium in accordance with culture time during 3D chondrogenesis. (A) pH change, (B) Change of glucose concentration, (C) Change of ammonia concentration, (D) Change of lactate concentration.

6.4.3.3. Chondrogenic gene expression

For the validation of 3D chondrogenesis, chondrogenic differentiation were characterised by genotypic profiling of chondrogenic markers in this study using RT-PCR at different culture time points, as shown in figure 70. Upon chondrogenic differentiation, type II collagen, aggrecan and link protein transcript, which are major structural component of cartilage [Sandell LJ 1991, Watanabe H 1998, Rodriguez E 2005, Neame PJ 1994], were readily detectable during chondrogenic culture. These expressions except aggrecan were not detected in normal mESCs, but, when mESCs were cultured in HepG2 conditioned medium for 3 days, aggrecan and link-protein was upregulated. Furthermore, Sox-9 mRNA expression, a major transcription factor controlling chondrogenic differentiation [Kulyk KM 2000], become detectable from day 5 of chondrogenic culture, and appeared to be upregulated with culture time during chondrogenic differentiation. In particular, Scleraxis, a basic helix-loop-helix (bHLH) transcription factor to be expressed in developing chondrogenic cell lineages during embryogenesis [Brown D 1999], transcript were also induced from day 5 of chondrogenic culture and expressed in constant level through whole culture period. In addition, to confirm their differentiation stage, Oct4 expression was evaluated for whole culture period, showing the strong expression of Oct4 transcript of mESCs before culture in HepG2 conditioned medium and chondrogenic medium and the distinct down-regulated expression over chondrogenic culture, which indicates the progressive differentiation.

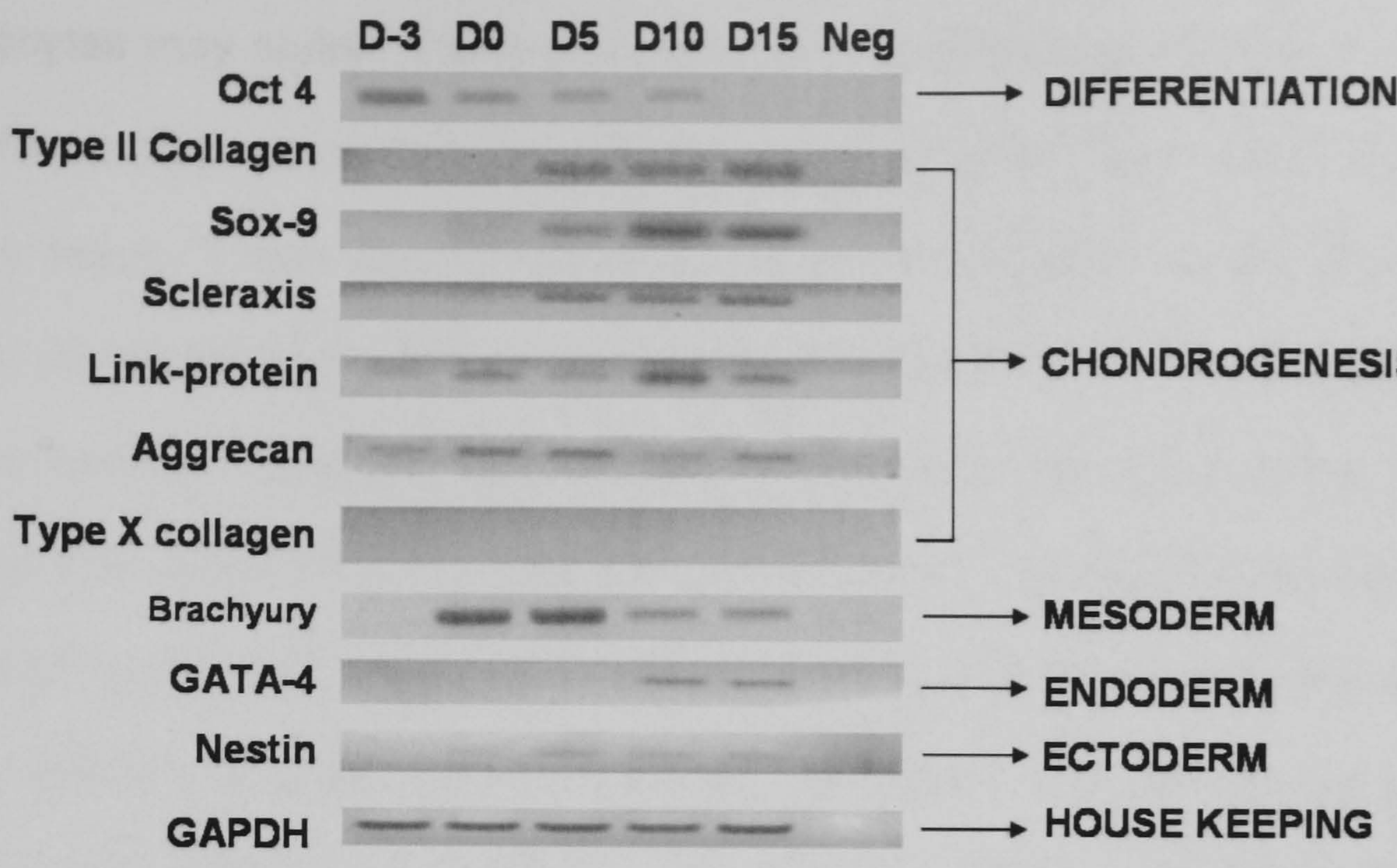
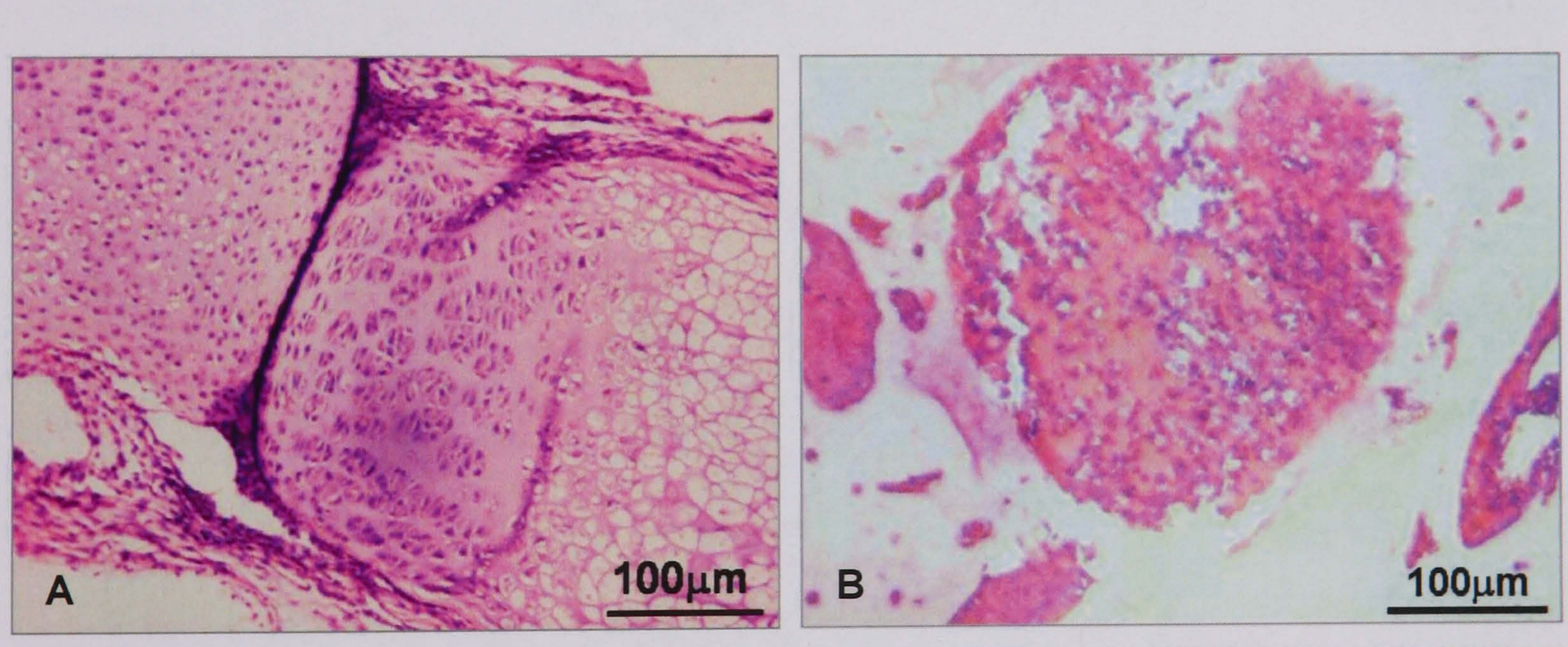


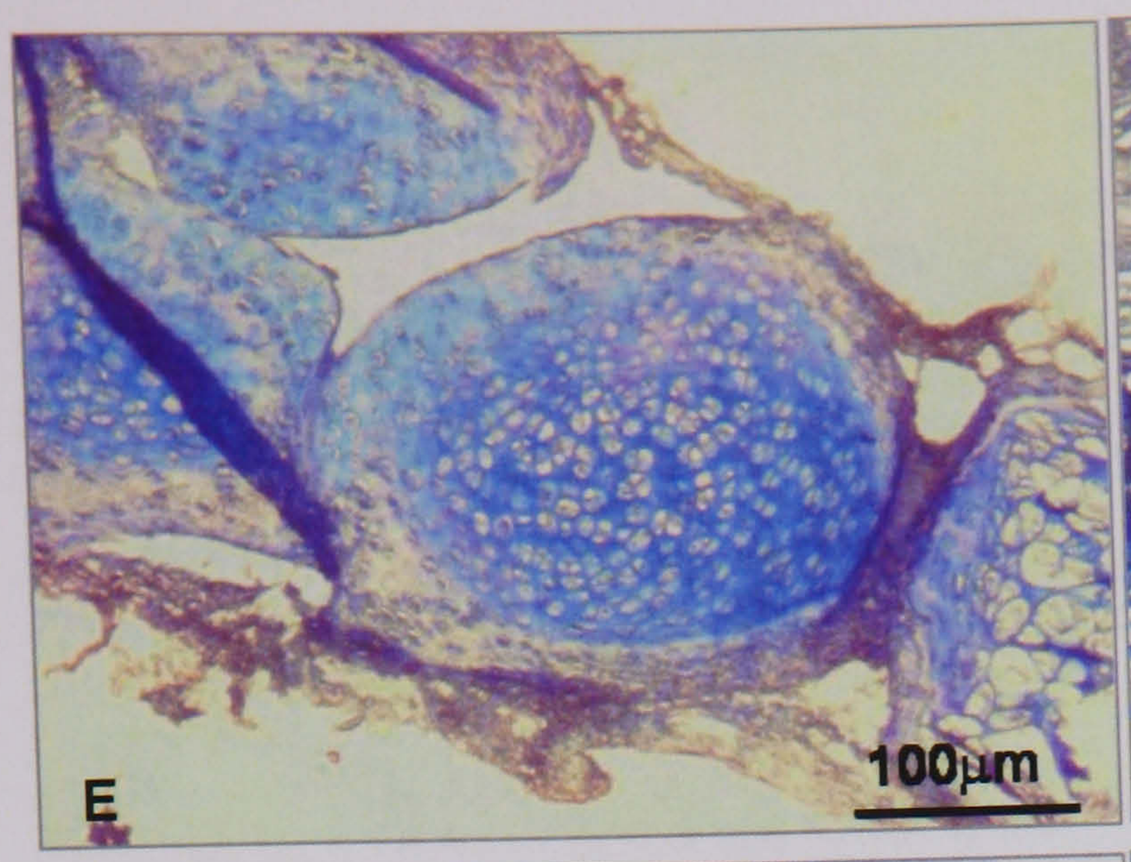
Figure 70. RT-PCR analysis of chondrogenic gene expression in 3D chondrogenesis.

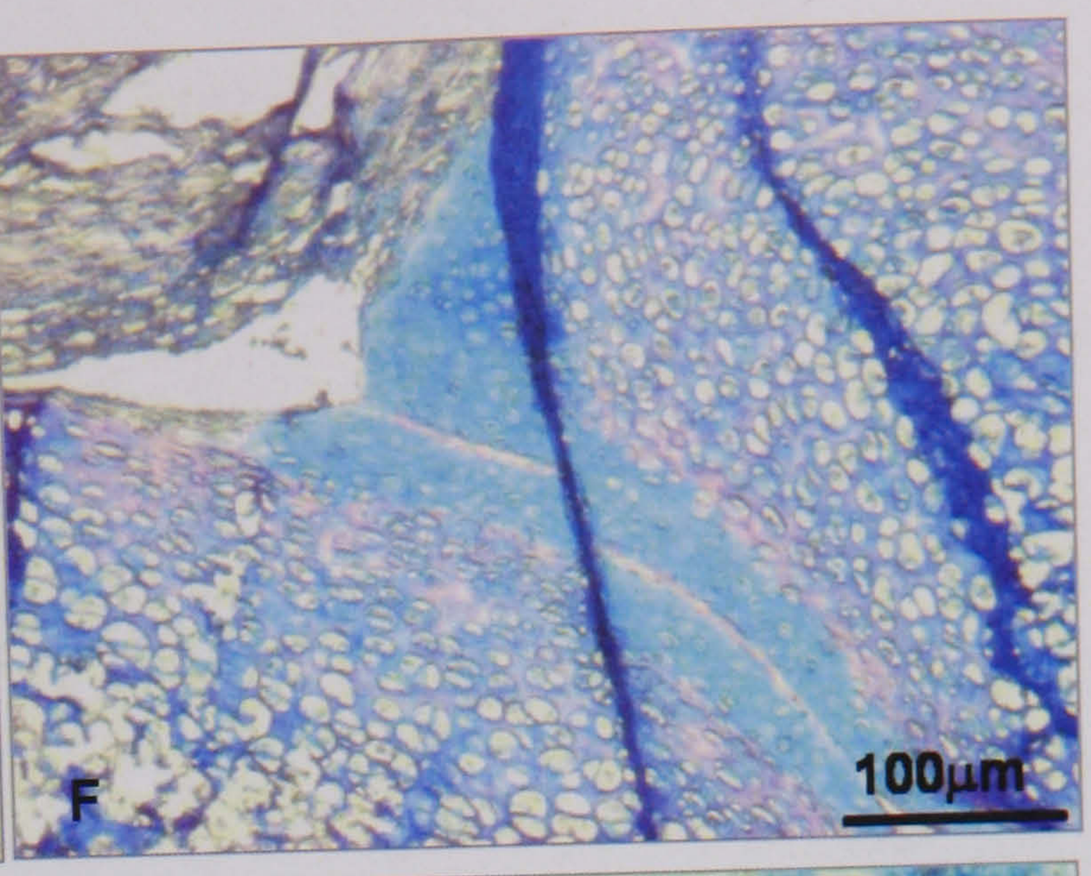
6.4.3.4. Staining and immuno-staining

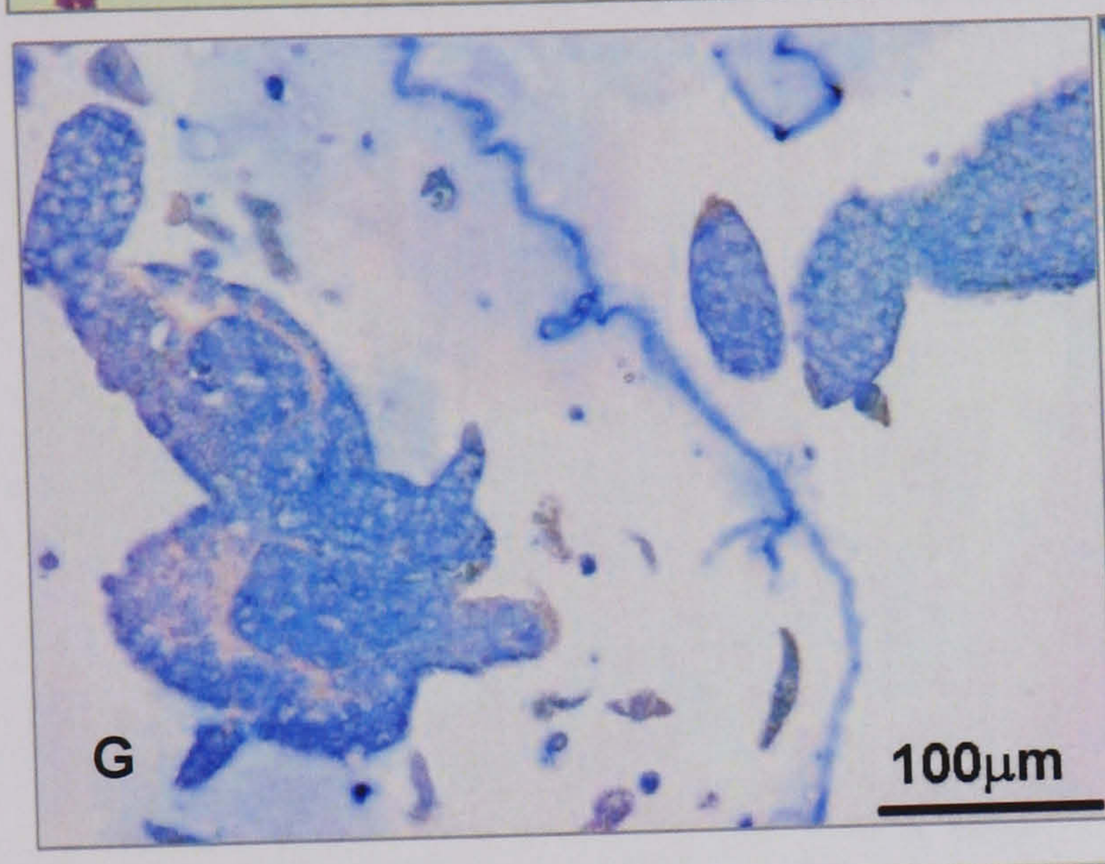
In our previous study, early differentiated mESCs (CM-mESCs) formed mineralised bone nodules in vitro in 2D culture system without EB formation process. Therefore, we addressed whether the CM-mESCs were also capable of forming cartilage like tissues in 3D culture system using alginate beads and a HARV bioreactor. The encapsulated mESC were subjected to be cultured in HepG2 CM in order to induce early differentiation into specific cell population with high chondrogenic capacity and then to differentiate directly into chondrogenic lineage in replaced chondrogenic medium in suspension culture system within bioreactor. The H&E staining showed well developed three dimensional tissue formation within alginate beads with size variation, which some of large tissues represents 200-400 μm in diameter or length, after 15 days of chondrogenic culture (Figure 71B-D). When the chondrocytes secrete their extracellular matrix, they become trapped within the matrix. In a histological preparation the

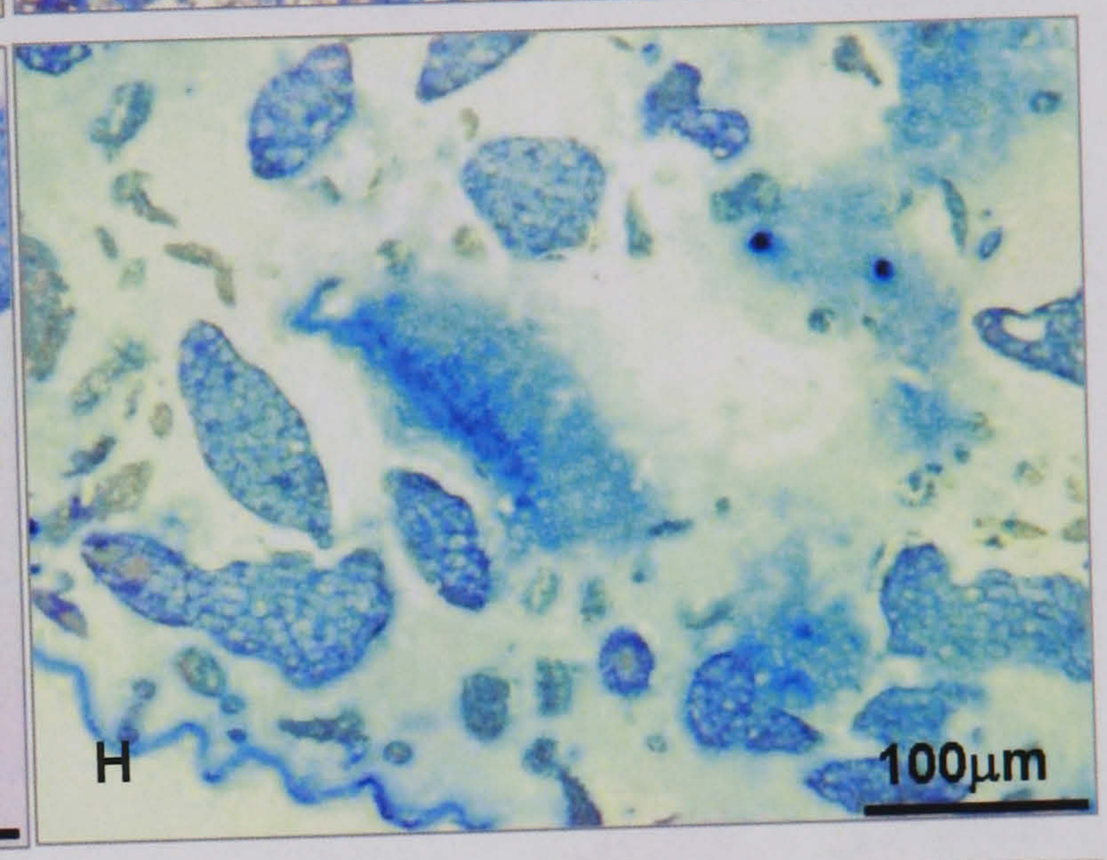
chondrocytes may shrink, thereby revealing the small spaces, called lacunae, in which they reside, which can be a distinct characteristic of histological section of cartilage tissue. These lacunae structure could be observed in H&E staining. In addition, Alcian blue and Safranin O staining were done for the characterisation of cartilage tissues. These staining represent represents overall area that stained dark-blue with Alcian blue and dark-red with Safranin O, which became noticeable throughout whole area of the tissues, indicating an extensive deposition of GAG that are one of the major ECM in cartilage. In addition, chondrocyte-like lacunae structure was evident in the sections and could be detected with Alcian Blue and Safranin O (Figure 71G-L, O-P). For further confirmation, the sections were stained with anti-type II collagen (Figure 71Q-T). Most of the areas expressed abundant extracellular immunoreactivity for type II collagen.

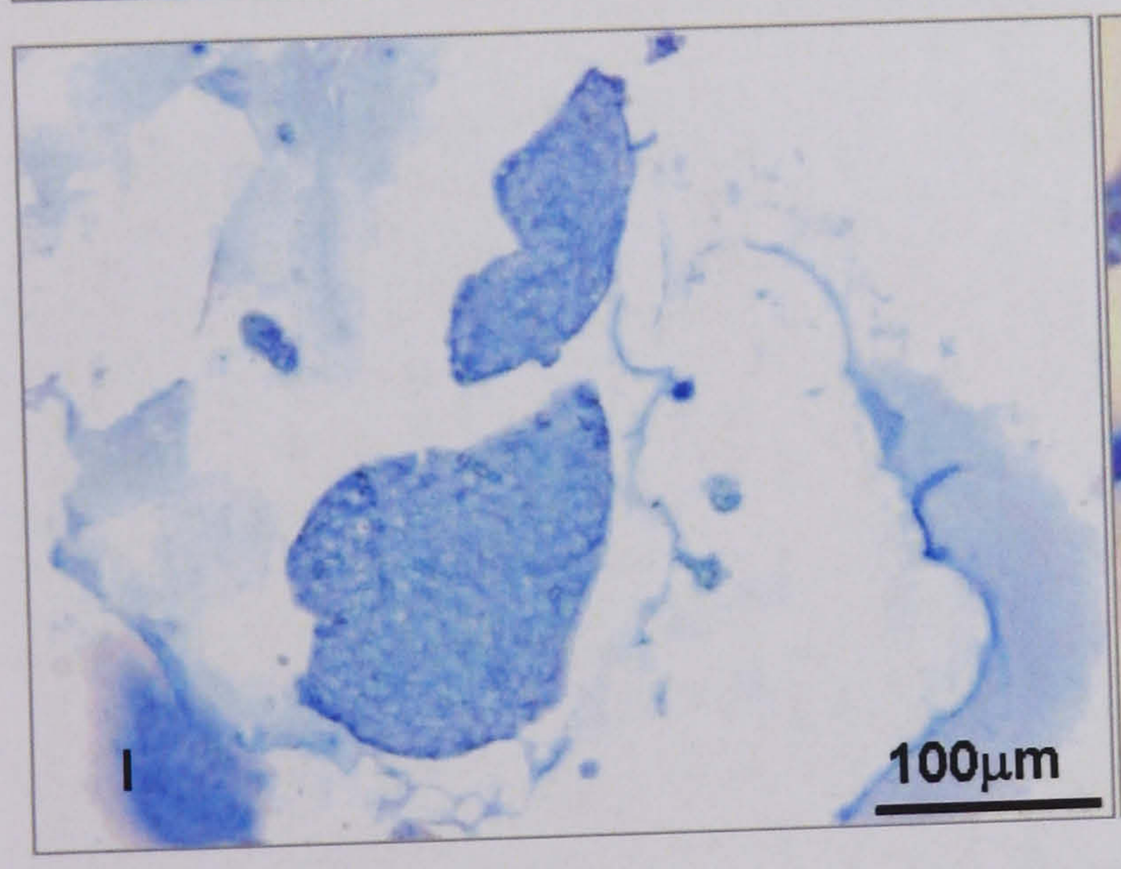


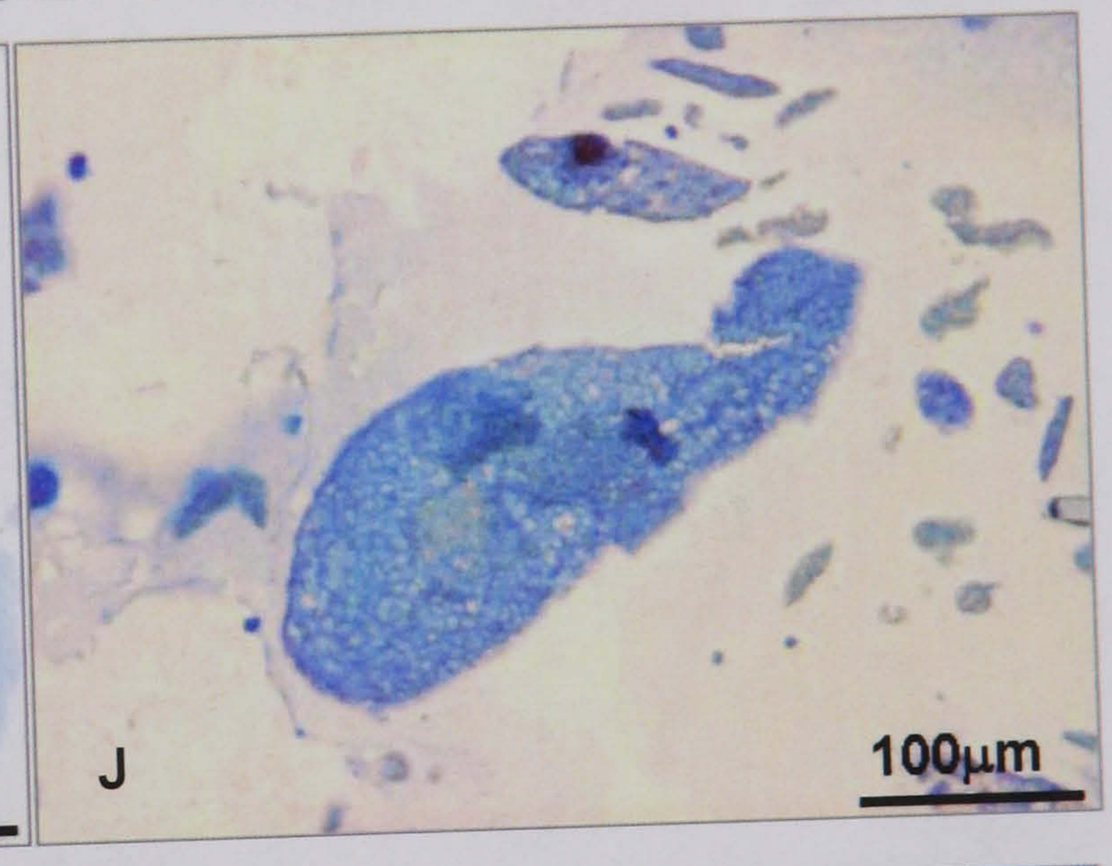

E
100μm

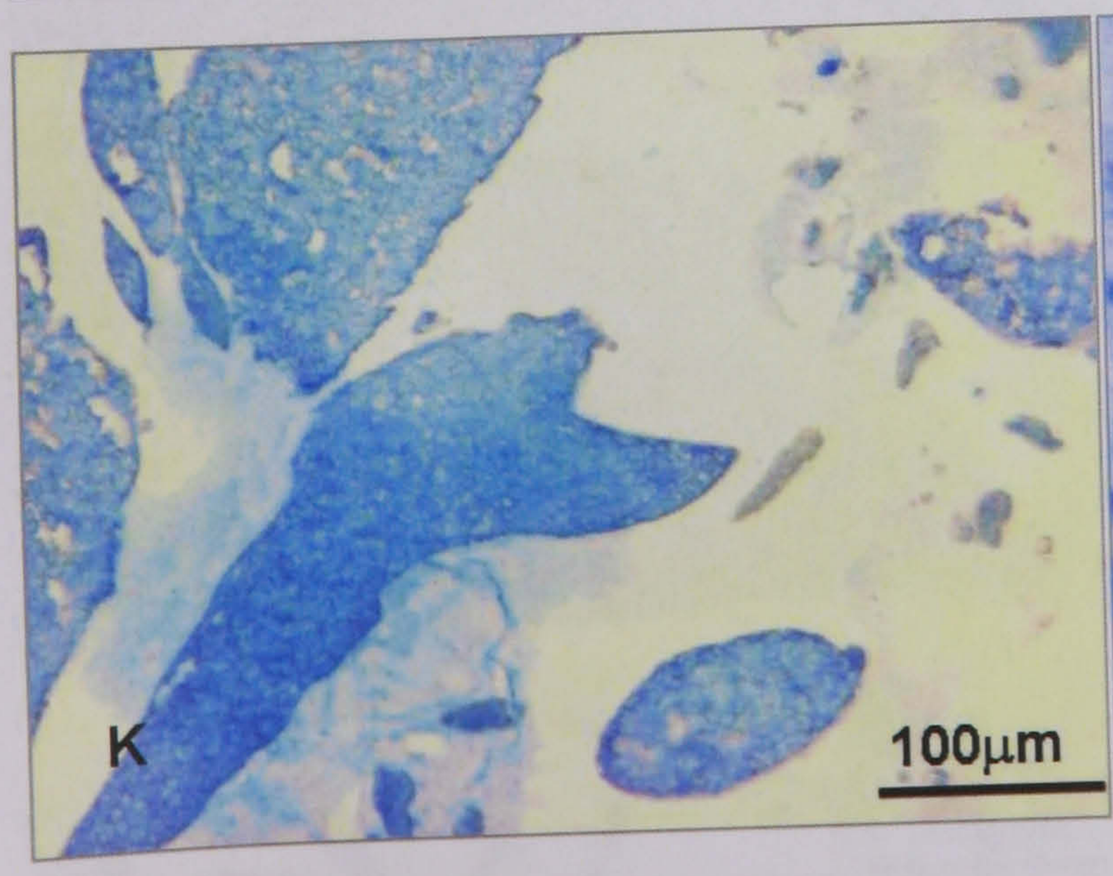

F
100μm

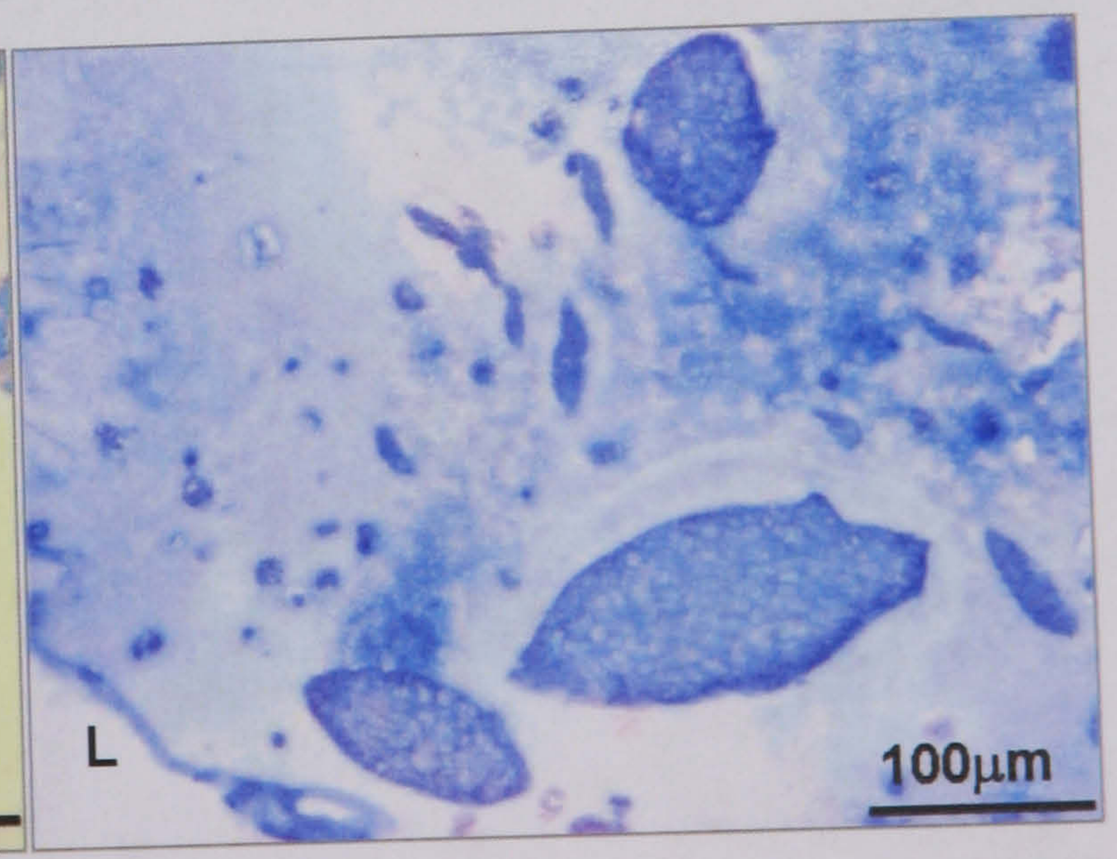

G
100μm


H
100μm

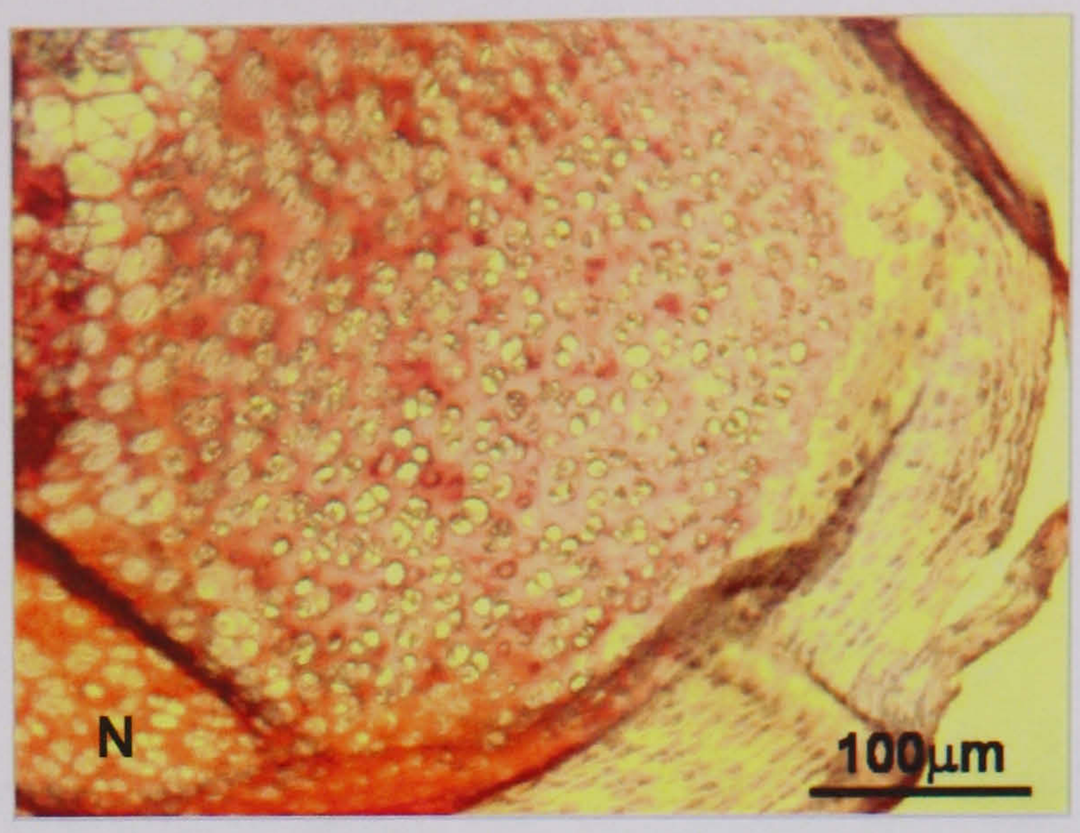

I
100μm

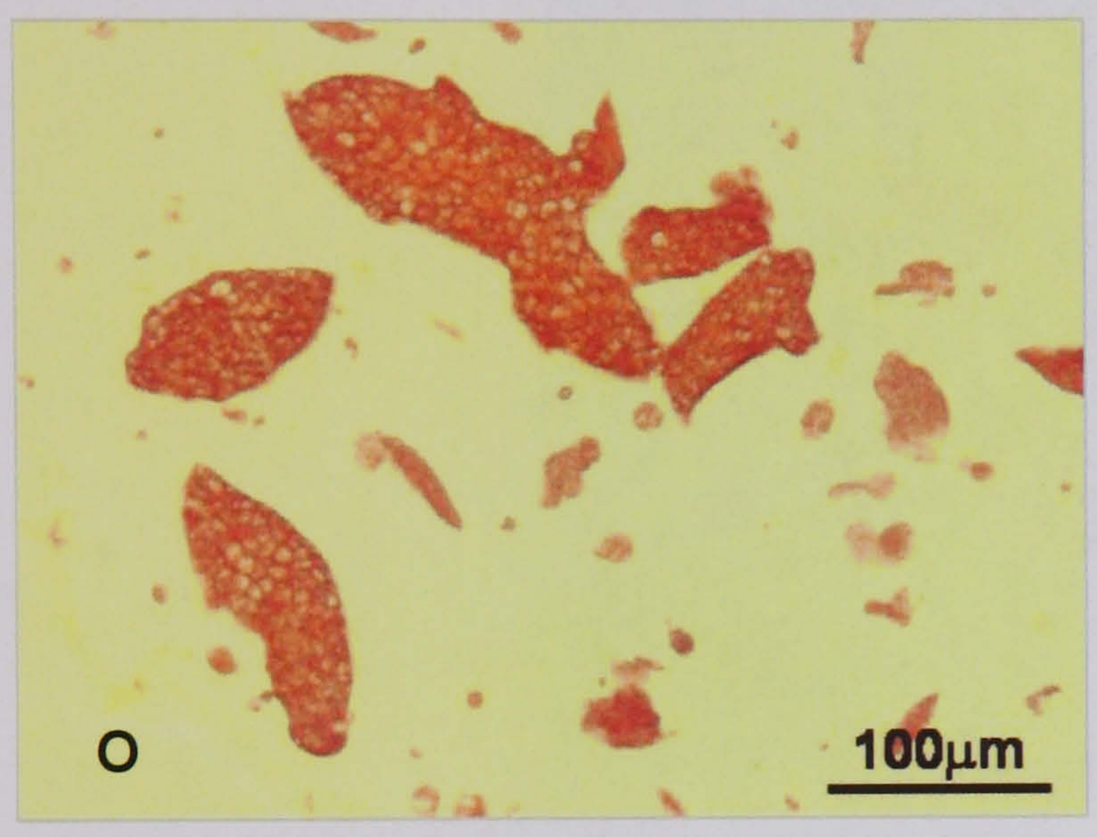

J
100μm

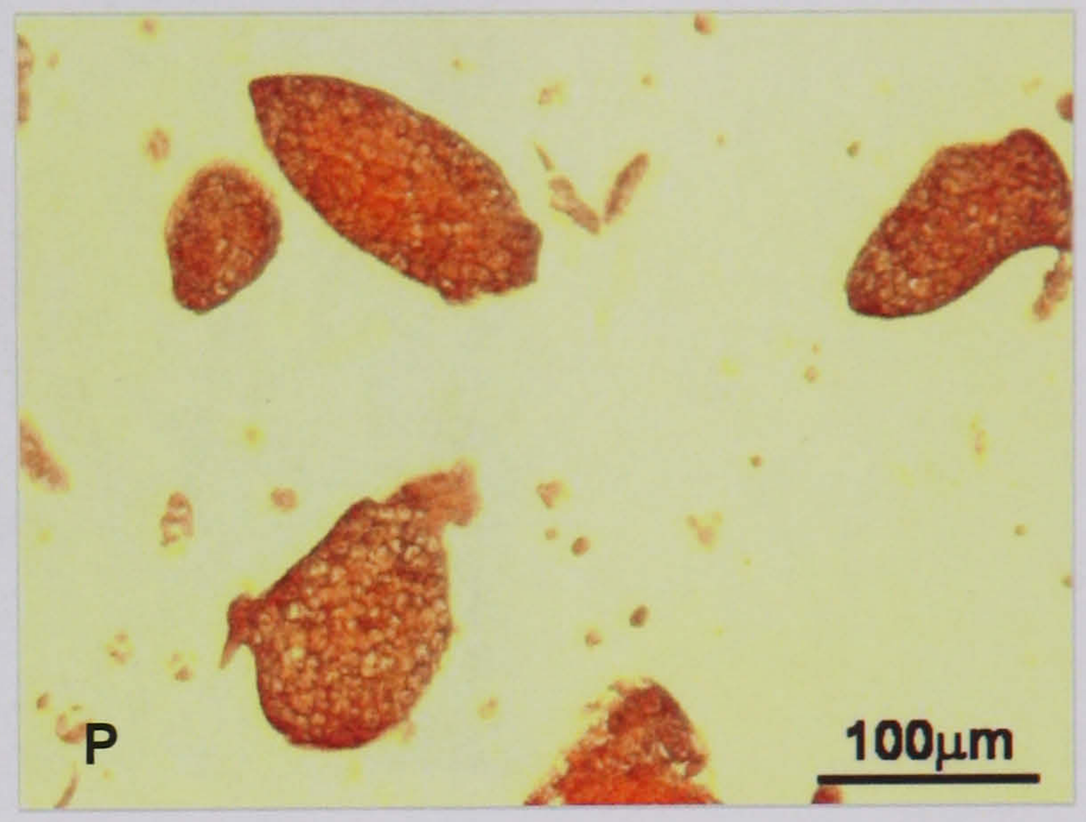

K
100μm

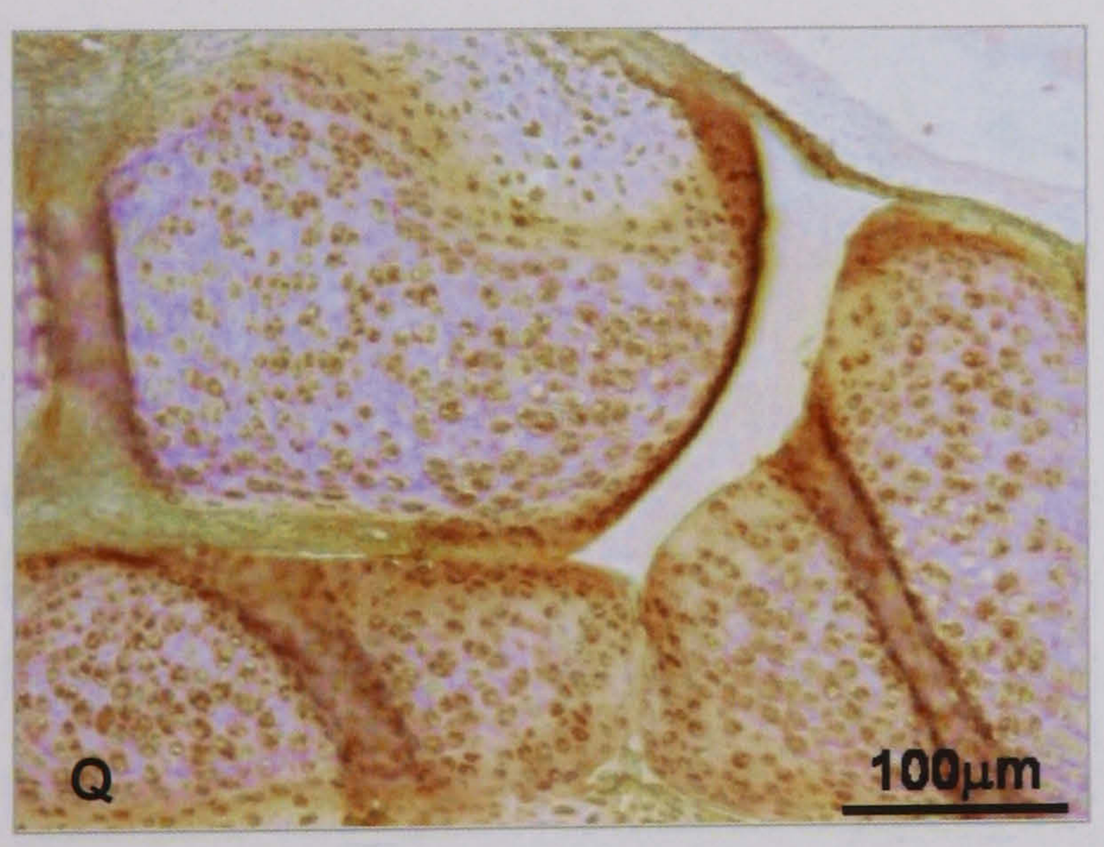

L
100μm

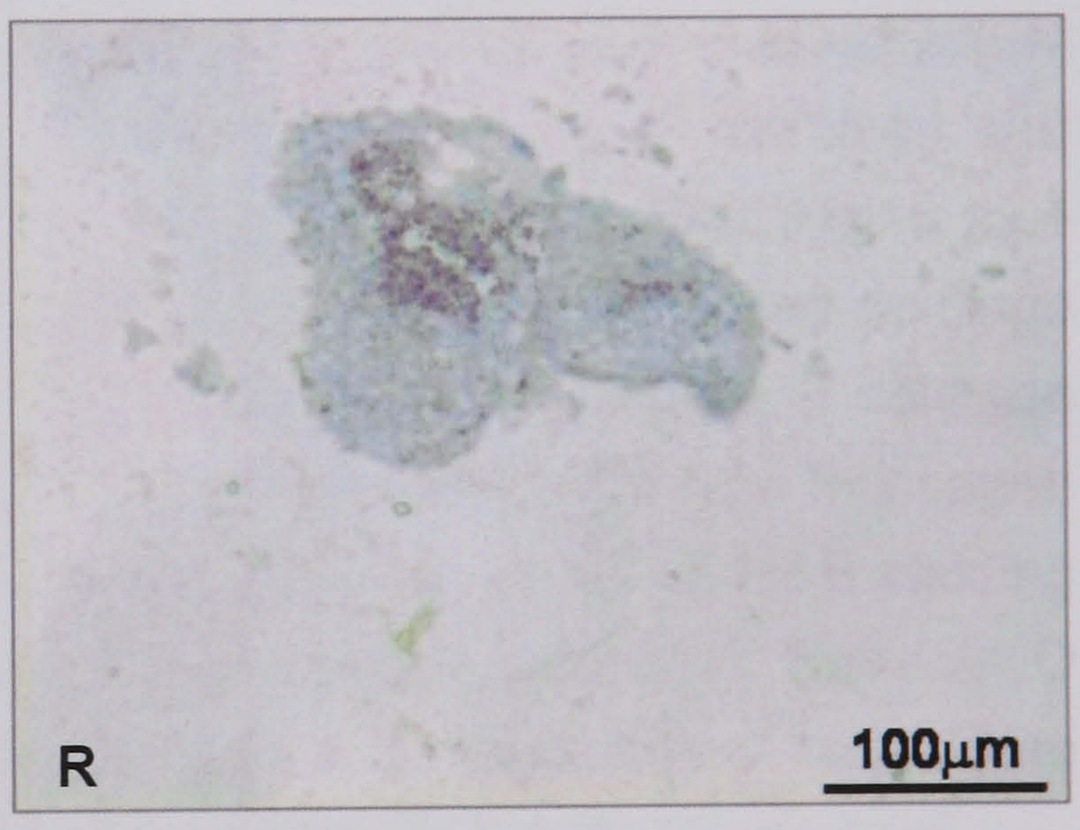

M
100µm

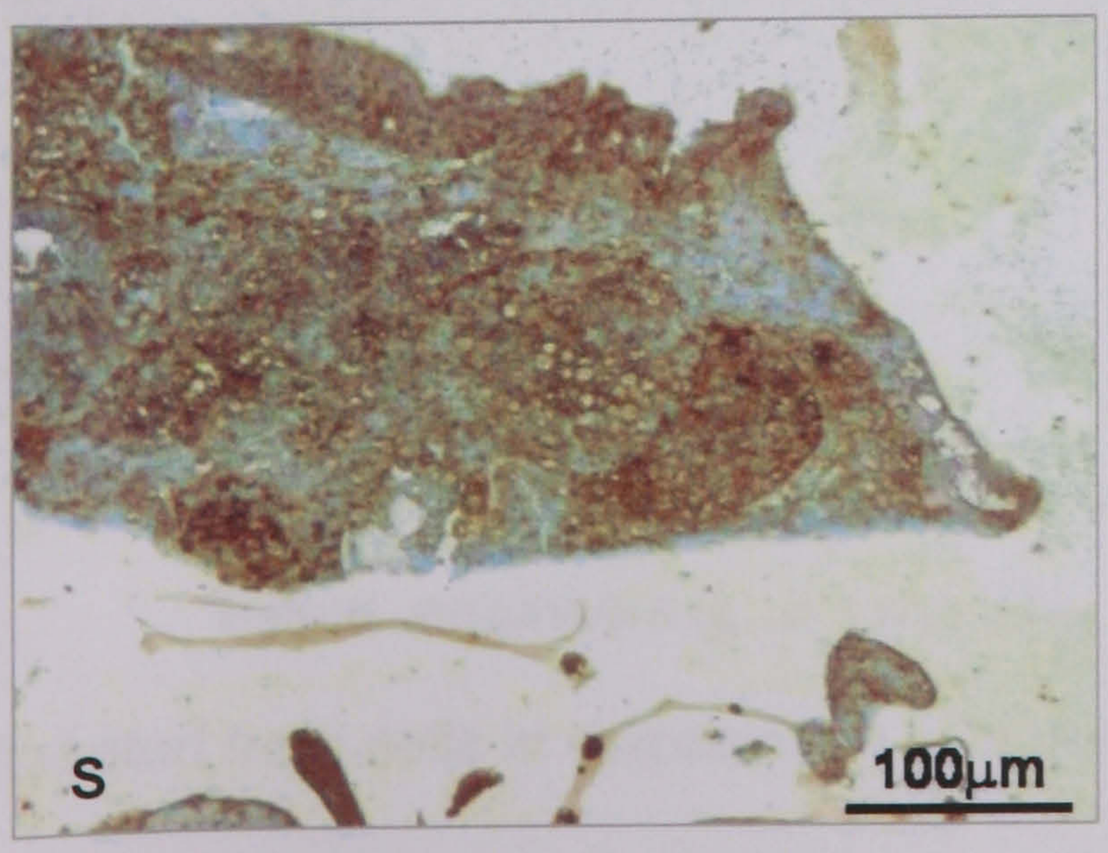

N
100µm

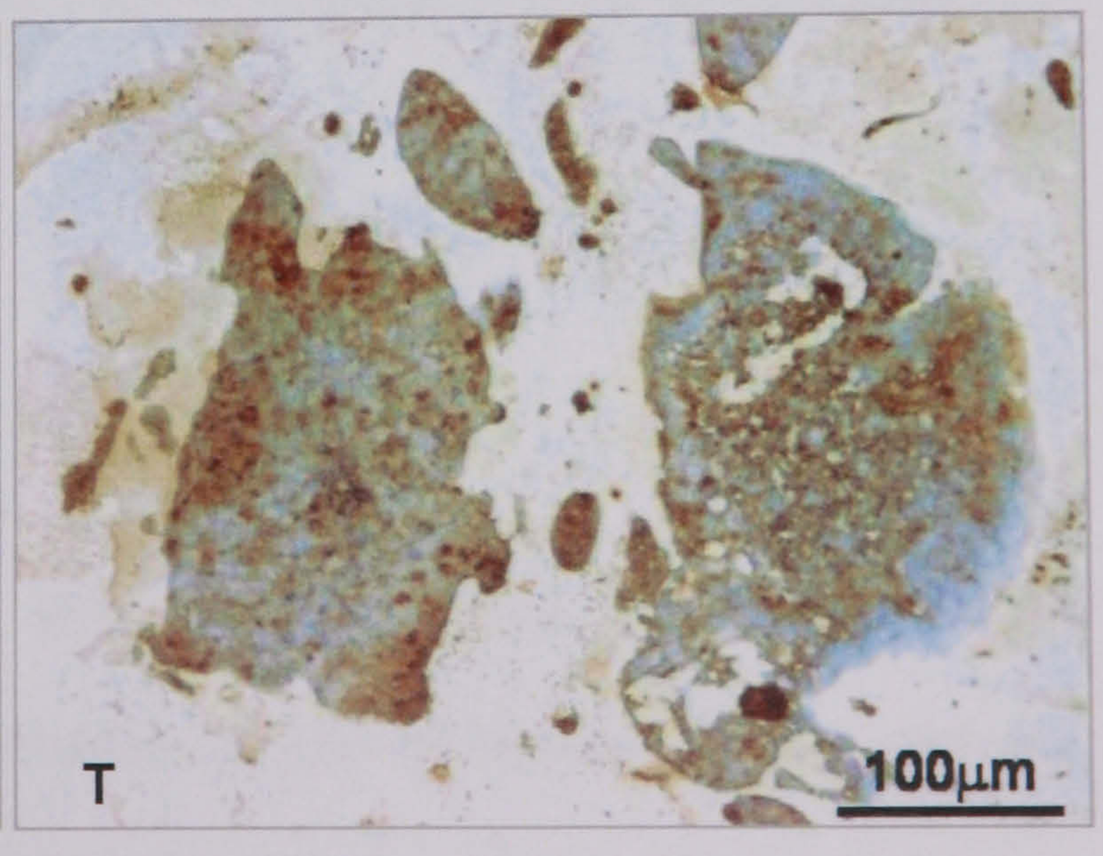

O
100µm


P
100µm


Q
100µm


R
100µm


S
100µm


T
100µm

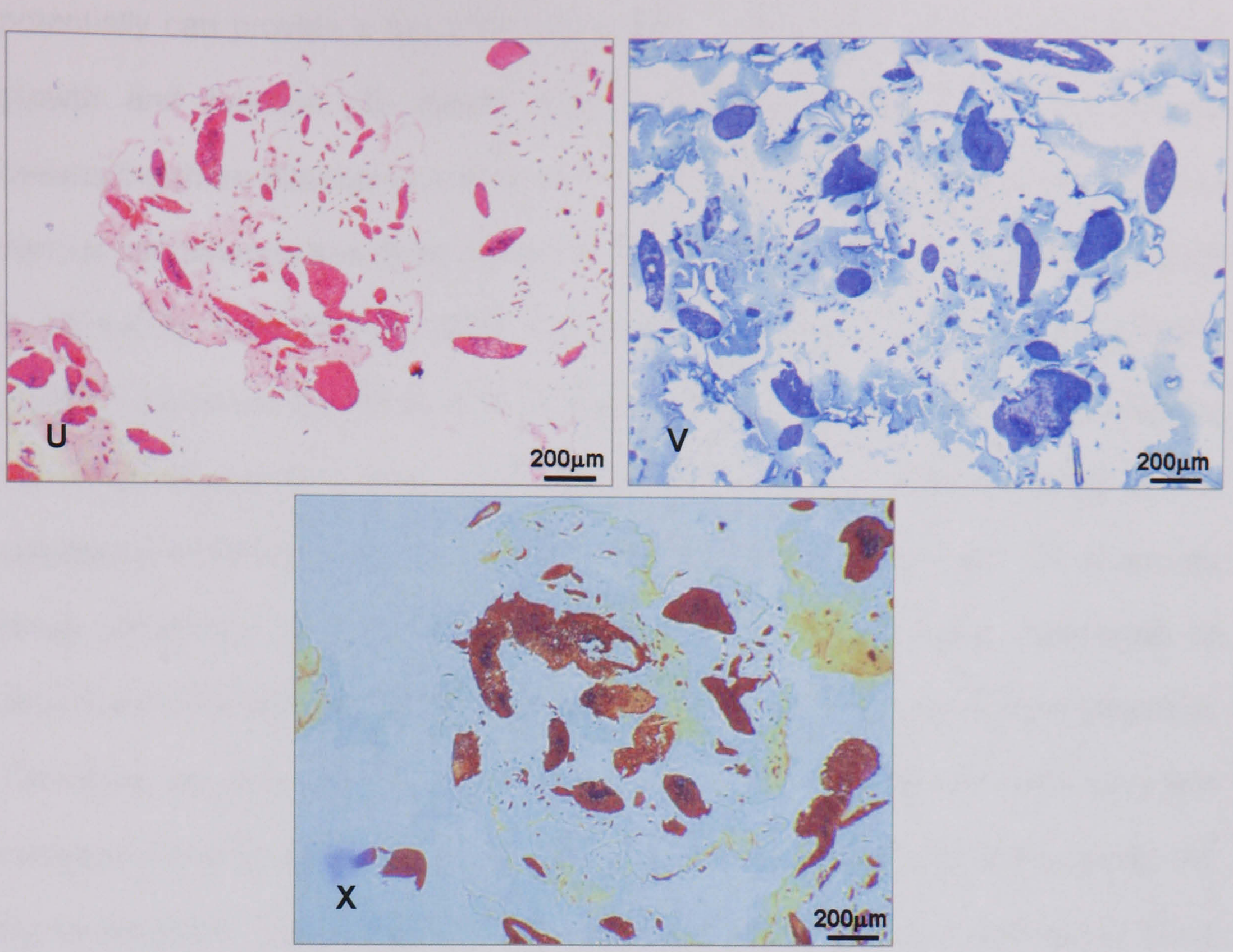


Figure 71. Various staining and immuno-staining for 3D cartilage like construct. A: H&E staining of mouse cartilage tissue. B-D: H&E staining of cartilage like constructs. E & F: Alcian blue staining of mouse cartilage tissue. G-L: Alcian blue staining of cartilage like construct, M & N: Safranin O staining of mouse cartilage tissue. O & P: Safranin O staining of cartilage like construct, Q: type II collagen immuno-staining of mouse cartilage tissue. R: negative staining for type II collagen S & T: type II collagen immuno-staining of cartilage like construct. U: H&E staining (Low magnification). V: Alcian blue staining (Low magnification). X: Safranin O staining (Low magnification). All alginate hydrogels encapsulating cells were allowed to direct chondrogenic differentiation for 15 days in HARV bioreactors.

6.5. Discussion

Tissue engineering, a new field that enables tissue equivalents to be created from cells in combination with biomaterials and bioreactor culture vessels,

potentially can provide a basis for systematic, controlled *in vitro* studies of tissue growth and function. To dates, there have been extensive researches for developing three dimensional bone and cartilage tissue like construct by studying various cell sources and three dimensional biomimic scaffold in 2D culture system in laboratory scale [Suh H 2000, Suh H 2001, Ceuninck FD 2004, Hwang NS 2006(1)]. However, the 2D culture system has not been successful for constructing 3D tissue equivalent due to some limitations of nutrient mass transport and of controlling mechanical forces to induce differentiation and growth. To overcome these limitations, recently bioreactor culture system has been developed to enhance and develop three dimensional growth of cells in proper culture condition. Therefore, we developed a culture system to create three-dimensional bone and cartilage like tissues based on mESCs, alginate bead, and HARV bioreactor. As far as we know, this is the first study demonstrating the three dimensional bone and cartilage like tissue formation from individual cell suspension of mESCs in a bioreactor system, and, thus, could have widespread applications in bone and cartilage tissue engineering.

In this study, mESCs were prepared in suspension and encapsulated with 1.1% alginate mixed with 0.1% gelatin, and then the encapsulated mESCs were placed to culture in suspension environment within vessels of HARV bioreactors, a kind of Rotating Wall Vessel (RWV) bioreactor, whereas the bioreactor maintains controlled *in vitro* culture conditions that permit tissue growth and development. This RWV bioreactor optimize suspension culture circumstance by producing laminar flow and minimizing shear and turbulence which can be the stresses on cells in culture, while providing sufficient nutrition and oxygenation that supports three dimensional tissue growth [Hammond TG 2001]. In our study, live and dead assay showed increased cell aggregation size in accordance with culture time and

finally well developed tissue formation within alginate beads in both osteogenic and chondrogenic culture. In addition, in brief comparison study with static culture of mESCs within alginate beads, 3D culture system using a bioreactor showed much higher cell viability. The relatively lower cell viability in static culture system in comparison with 3D culture system might be due to potential mass transfer limitations including external and internal mass transfer limitation with respect to the supply of oxygen and medium components, which transport of nutrient in static culture mainly depends on diffusion, which can not satisfy the metabolic requirement of cells on three dimensional scaffolds for long culture period [Mueller SM 1999]. This difference can be explained by that mass transfer limitations involved during *in vitro* culturing of three dimensional constructs result in limited cell growth into the three dimensional construct [Ishaug-Riley SL 1998, Holy CE 2000].

Tissues constructs formed by cell growth within alginate beads consisted of viable and metabolically active cells, which were evaluated by measuring pH change, glucose consumption, lactate and ammonia production in osteogenic and chondrogenic medium during cultures. It has been well reported that these metabolites profile and pH can provide a kind of metabolic parameters to be used to modulate cell metabolism such as ECM synthesis and tissue growth and morphology for developing optimal culture condition for cell growth [Obradovic B 1999]. Mammalian cells utilize glucose and glutamine as one of major energy sources. Glucose uptake was from culture medium and then is converted to lactate as a by-product through glycolysis under anaerobic condition, yielding 2 mol of adenosine triphosphate (ATP) per mole of glucose, or to CO_2 and H_2O through the tricarboxylic acid (TCA) cycle in aerobic condition, yielding 36 mol of ATP per mole of glucose. Lactate is mostly produced by glycolysis of glucose, and only a small

amount is derived from glutamine [Glacken 1986, Zielke 1980]. Glutamine is utilized by catabolism through the TCA cycle, producing ammonia as a by-product. The amount of ammonia can be used as an indicator of glutamine utilization and TCA cycle activity [Miller 1987, Siano 1991].In our study of 3D osteogenesis and 3D chondrogenesis, glucose consumption kinetics showed rapid decrease in glucose concentration in medium, implying rapid cell growth and active metabolism in cells. Furthermore, rapid reduction of glucose concentration to ground level in osteogenesis might be due to initial low concentration of glucose in osteogenic medium, and the glucose was consumed to constant level at 10 mM in chondrogenesis, which might be due to relatively much higher initial concentration of glucose in chondrogenic medium. Lactate and ammonia profile showed fast decline in their concentration at day 2 of culture in both 3D osteogenesis and 3D chondrogenesis, but, in 3D osteogenesis, lactate was consumed to constant level at around 10 or 11 mM for further culture period, and, in 3D chondrogenesis, the lactate concentration in medium was increased gradually up to 22.6 mM, which might be related with the difference in initial concentration of glucose in osteogenic and chondrogenic medium, and the accumulation of lactate matches the decrease of glucose, and ammonia production might be from the metabolism of glutamine contained in medium (α-MEM) as basal concentration, 2mM. In addition, medium pH is another key parameter in cell culture as it affects cell viability, cell growth, and metabolic activity. In our study, the pH in osteogenic and chondrogenic medium decreased with culture time and with increasing lactate and ammonia concentration, which is consistent with that ammonia and lactate production alters intracellular and external pH in medium [Barngrover D 1985]. However, the pH change was within the proper pH range (7.0-7.4) of cell culture media, implying no strong influence on cell growth and function. From these results, we suggests that

the more concise control of culture condition should be necessary for achieving optimal culture system in regard of nutrient consumption profile and cellular metabolism in a bioreactor.

Recently, there have been tissue engineering based approaches in development of three dimensional bone and cartilage like construct using mESCs, three dimensional scaffold systems and appropriate growth factors in static culture system, showing the potential use of ESCs for bone and cartilage tissue regeneration [Hwang NS 2006(1), Hwang NS 2006(2), Hwang NS 2006(3), Tanaka H 2004, Garreta E 2006]. In most these current researches, mESCs were allowed to form EBs, then mESCs derived EBs were encapsulated with synthetic hydrogels, and cultured in 2D static culture environment with various osteogenic and chondrogenic supplements, showing successful achievement of bone and cartilage like structure. However, in spite of these successful approaches for 3D osteogenic and chondrogenic differentiation of ESCs, attempts to direct the differentiation of ESCs into desired cell types though intermediate EB formation have been limited. To dates, limited knowledge exists concerning the culture conditions and requirements for culturing EBs and differentiation mechanism and cellular interactions within EB, resulting in difficulty to control homogenous differentiation. In other words, little is known about the process guiding the development of three germ layers and specific lineage of cells within the EB. Current approaches for the differentiation through intermediate EB formation give rise to a mixture of different cell types due to spontaneously formed three germ layers [Khoo MLM 2005]. It has been well proved that ESC differentiation into osteogenic lineage cells without an EB step can be used to derive large quantities of functional osteogenic cells for bone tissue engineering [Karp JM 2006]. Therefore, to develop more efficient culture system for skeletal tissue engineering

application, our culture system was designed to induce early differentiation of mESCs encapsulated with alginate and subsequent osteogenic and chondrogenic differentiation by the culture in HepG2 conditioned medium and osteogenic and chondrogenic medium in a HARV bioreactor, for achieving 3D bone and cartilage like construct. 3D osteogenesis and chondrogenesis was characterised at a gene expression level by examining expression of osteocalcin, Cbfa1/Runx2, osterix, type II collagen, aggrecan, link protein, scleraxis, sox-9 and Oct4. These osteogenic, osteocalcin, Cbfa1/Runx2, osterix, and chondrogenic, type II collagen, aggrecan, link protein, scleraxis, Sox-9, gene expression showed substantial level throughout whole osteogenic and chondrogenic culture period, indicating well developed *in vitro* osteogenic and chondrogenic differentiation, which progressive differentiation was confirmed by the gradual downregulated expression of Oct4 transcript for osteogenic and chondrogenic culture which strongly expressed in undifferentiated mESC. Interestingly, the mESCs culture in HepG2 conditioned media for first 3 days prior to culture in osteogenic medium also showed relatively weak expression of osteogenic maker, osteocalcin and Cbfa1/Runx2. It has been well reported that Cbfa1/Runx2, a transcription factor that is the earliest marker of osteogenesis, is expressed in early mesenchymal origin [Ducy P 1997, Banerjee C 2001], and osteopontin (OPN), a specific protein expressed in osteogenesis with similar function with osteocalcin (OCN), can be also expressed in undifferentiated or early differentiated ESCs through coordinated action with other molecules controlling undifferentiation stage of ESCs, Oct4 and cd9 [Koestenbauer S 2006, Oka M 2002, Botquin V 1998]. However, further researches for their expression in early differentiated mESCs are needed. In addition, aggrecan or link protein transcript were also expressed in relatively low level in both undifferentiated and early differentiated mESCs, which might be related with that aggrecan and link

protein can be also expressed by other cell lineage and non-cartilaginous tissue [Carulli D 2007, Binette F 1994]. In spite of these finding, the distinct expression of osteogenic and chondrogenic specific gene, such as osterix, an osteoblast-specific transcription factor required for the differentiation of osteoprogenitors into mature osteoblasts [Nakashima K 2002, Guanping T 2004], type II collagen, one of major macromolecules produced by chondrocyte [Poole AR 2001], Sox-9, one of the most important transcription factors that are expressed during early chondrogenesis [Kulyk KM 2000], and scleraxis, one of major transcription factor, is expressed in mesenchymal progenitors and during chondrogenesis [Brown D 1999], represents well developed osteogenic and chondrogenic differentiation in our 3D culture system.

Finally, for further validation of 3D osteogenesis and 3D chondrogenesis, the 3D cell plus alginate construct after osteogenic and chondrogenic culture was characterised by histological and immuno-staining. Histological staining of sectioned 3D construct in 3D osteogenesis showed well distributed tissue growth with a few hundreds μm in size within alginate beads, and ARS staining indicated mineral deposition on those tissues, and mineral deposits that stained strongly with ARS and showed fluorescence was shown to be formed mainly at centre area of tissues. Immuno-staining of these tissues represented type I collagen and osteocalcin accumulation at peripheral region. In further physicochemical characterisation of mineralised deposit, mineral deposits formed by osteogenic cells within alginate hydrogels were evaluated by ATR-FTIR analysis, SEM-EDS microanalysis and mechanical analysis. ATR-FTIR analysis showed distinct peaks of phosphate and carbonyl, indicating the presence of hydroxyapatite ($Ca_{10}(PO_4)_6(OH)_2$) like mineral deposits within alginate hydrogels, which is major component of bone mineral [Hunter GK 1983], within alginate hydrogels.

Previously, it has been reported that mineral deposits are formed *in vitro* by β-glycerophosphate as an additional source of phosphate ions [Chang YL 2000], and it was also reported that phosphate ions were made available in places where ALPase was present, thereby reducing the possibility of non-specific mineral precipitation, suggesting that a controlled mineralization process is operating by osteogenic cells in proper culture condition [Tenenbaum HC 1982], which is consistent with our result that mineralised deposit formation was confined only within tissues in histochemical studies. Mineralisation could also be confirmed by SEM-EDS microanalysis, showing distinct mineral morphology and around 1.23 in the Ca/P molar ratio of the mineral deposit. The morphology and Ca/P molar ratio might indicate the formation of calcium phosphate-based minerals, regarding that Ca/P molar ratio of the representative calcium phosphate minerals is 1.00 in Dicalcium phosphate dihydrate, 1.33 in octacalcium phosphate, 1.50 in tricalcium phosphate and 1.67 in hydroxyapatite [Campbell AA 1996, Wang H 2002, Rodríguez-Lugo V 2005]. This mineral deposit formation within the 3D constructs influenced their mechanical properties, as shown by the compression strength testing. The Youngs modulus of the 3D bone constructs, formed by the osteogenic culture of mESCs for 21 days in HARV bioreactor following alginate encapsulation, was much higher than the controls, pure alginate hydrogels and alginate hydrogel encapsulating undifferentiated mESCs with the cell density of approximate 1,800,000 cells, which are almost identical to the cell number in 3D bone construct after 21 days of osteogenic culture, indicating much higher stiffness of the 3D bone constructs. It is therefore concluded that these mechanical experiments confirm the presence of mineralised tissue with superior mechanical properties formed by the osteogenic culture of mESCs in the alginate hydrogels.

In 3D chondrogenesis, histological analysis represented well-developed

and distributed tissue growth with various sizes within alginate hydrogels after 15 days of chondrogenic culture. Clusters of cells were surrounded by significant amounts of extracellular matrix that stained strongly with alcian blue and safranin O, and tissues formed within alginate hydrogels showed a lacunae structure which is typical cartilage tissue structure. In addition, immuno-staining of these tissues represented type II collagen accumulation on tissues. Finally, these histological characterisation and physicochemical characterisation demonstrated the formation of well-developed 3D bone and cartilage like construct by the osteogenic and chondrogenic culture of mESCs in alginate hydrogel and HARV bioreactors.

6.6. Conclusion

The bioprocessing for directing 3D osteogenic and chondrogenic differentiation of mESCs in alginate hydrogels and HARV bioreactors described here enabled the formation of 3D bone and cartilage-like constructs. Osteogenic and chondrogenic differentiation could be directed from the early differentiated mESCs, which induced by HepG2 conditioned medium treatment, and by the culture in osteogenic and chondrogenic environment. Alginate based cell encapsulation and HARV bioreactor culture system provided suspension culture environment suitable for 3D cell and tissue growth. In addition, removing the EB formation step in directing 3D osteogenesis and chondrogenesis resulted in more efficient and easy bioprocess than the conventional EB mediated differentiation culture method. This culture system described here would provide an efficient and easy culture system for applying to bone and cartilage tissue engineering in the context of macroscopic bone and cartilage formation.

CONCLUSIONS
AND
FUTURE WORK

CONCLUSIONS

In this thesis, we have developed a novel culture strategy for deriving *in vitro* osteogenesis and chondrogenesis from murine ESCs and a bioprocess for the formation of 3D bone- and cartilage-like constructs for application to skeletal tissue engineering. For the application of ESCs to bone and cartilage tissue engineering, the efficient derivation of osteogenic and chondrogenic lineage cells from pluripotent ESCs is a prerequisite. Regarding ESCs early differentiation strategy into three germ layers; endoderm, mesoderm and ectoderm, well-organised induction of mesoderm formation from undifferentiated ESCs is an important intermediate step for further terminal differentiation into osteogenic and chondrogenic lineage cells. Hence, early differentiation of mESCs was induced by the treatment with conditioned medium from the HepG2 cell line (human hepatocarcinoma) with similar biological function with visceral endoderm, which plays a key role in mesoderm formation during embryogenesis since it induces and enhances mesoderm formation. mESC stimulation by the HepG2 conditioned medium produced a cell population with a similar gene expression profile to primitive streak/nascent mesoderm, which was signified by the increased expression of brachyury, cripto and goosecoid transcripts. Furthermore, the gene expression profile during EB formation showed relatively enhanced and rapid induction of mesoderm formation in comparison with normal mESCs. Finally, the HepG2 conditioned medium-treated cells demonstrate the capacity of reversible differentiation into the undifferentiation stage in certain culture conditions. Following enhanced early differentiation of mESCs into mesoderm, mESCs were allowed to form EBs for 5 days, and then dissociated EB-derived cells to differentiate into osteogenic lineage cells in the presence of osteogenic

supplements. However, increased beating colony formation in the HepG2 CM treated mESCs, which was probably due to spontaneous cardiogenic differentiation, was observed that was accompanied by bone nodule formation with no significant difference in comparison to the untreated mESCs, suggesting the need to modulate culture condition for enhancing osteogenic and chondrogenic differentiation. Hence, we have designed new culture strategy to enhance osteogenic and chondrogenic differentiation selectively and reduce spontaneous cardiogenic differentiation. Controlling the EB formation period of the mESCs treated with HepG2 conditioned medium resulted in the preferential stimulation of cardiogenic, osteogenic and chondrogenic differentiation, respectively. Specifically, reducing EB formation time resulted in the distinct reduction of cardiogenic differentiation and simultaneously the almost exclusive osteogenic and chondrogenic differentiation, which was superior to the conventional EB formation process.

Following the control of skeletal lineage differentiation of mESCs, the need to develop a more efficient culture method led to the investigation of direct differentiation of mESCs by bypassing EB formation, which was suggested from the finding that HepG2 conditioned medium-treated mESCs showed early inducted gene expression profile for mesoderm. Therefore, mESCs early differentiation was induced by culture in HepG2 conditioned medium. Subsequently, osteogenic and chondrogenic differentiation was induced by osteogenic or chondrogenic media without EB formation. Removing the EB formation step resulted in the almost exclusive osteogenic or chondrogenic differentiation. This novel approach represents a more efficient and less time- and labour-intensive process than the conventional EB-mediated differentiation method. Finally, using this novel differentiation strategy, direct 3D osteogenesis or chondrogenesis of mESCs

through encapsulation in alginate hydrogels and culture in HARV bioreactors was achieved which enabled the formation of 3D bone or cartilage-like constructs. This novel bioprocess would provide an efficient, integrated, and easily scalable and automatable culture system for applying to bone and cartilage tissue engineering for potential therapeutic applications.

FUTURE WORK

In this thesis, a novel culture strategy and bioprocess was established for mESC differentiation. However, from a therapeutic point of view, application of this culture strategy and bioprocess for bone and cartilage tissue engineering and regenerative medicine requires further characterization and development.

First, the HepG2 conditioned medium requires to be characterized, which would enable the identification of the active factors that trigger ESC differentiation and enhance mesoderm formation. Since cell line-derived conditioned media may cause transmission of pathogens and vary in the quality depending on the cell passage number as well as the cell's physiological status, it is imperative to identify the biological molecules in order to produce a defined medium, thus rendering its utilisation clinically relevant. The combination of two-dimensional electrophoresis coupled to mass spectrometry with matrix-assisted laser desorption ionization (MALDI) has become as a powerful tool in the differential analysis of proteoms. Therefore, characterization of the active factors in the HepG2 conditioned medium using proteomics is essential in developing a novel, defined medium that contains the active factors able to enhance mesoderm formation.

Second, cell purification through cell sorting in order to purify osteogenic cells or chondrogenic cells specifically from the heterogeneous cell population may be required. Specifically, Fluorescence Activated Cell Sorting (FACS) could be applied. FACS selects the desired cell type from a heterogeneous population based upon the intensity of fluorescence which desired cells emit. This requires the generation of suitable monoclonal antibodies can be selectively used to identify the desired cell type. In particular, specific markers and antibodies relating

to the ESC differentiation stage are required, because, to date, only OB cadherin (Cadherin 11) has been available to identify and select cells with mesenchyme origin.

Finally, for the practical application of this culture system, which established using mESCs, to human ESC (hESC)-based biotechnology, this culture strategy and system should be tested and modified in terms of the difference in culture condition between mESCs and hESCs. Generally, hESC culture is based on the use of feeder cell layers with mouse origin and FBS free environment. Preliminary, HepG2 growth was tested in the FBS-free condition in comparison with FBS-containing condition, and there is no significant difference in HepG2 growth between FBS-free and FBS-containing culture condition (Appendix 8), suggesting the potent use of FBS-free HepG2 conditioned medium in hESC early differentiation with slight modification. In addition, feeder cell layer free culture system will be developed to remove the possibility of cross-contamination between human origin and mouse origin for the final purpose of medical application, and more concise culture condition will be developed to derive and control hESC differentiation into osteogenic and chondrogenic lineage, and finally hESC derived 3D bone and cartilage tissue construct will be fabricated by the use of our established integrated bioprocess with slight modification.

REFERENCES

Abe Y, Aida Y, Abe T, Hirofuji T, Anan H, Maeda K. Development of mineralized nodules in fetal rat mandibular osteogenic precursor cells: Requirement for dexamethasone but not for beta-glycerophosphate. Calcif Tissue Int. 2000;66:66-69.

Ahrens PB, Solursh M, Reiter RS. Stage related capacity for limb chondrogenesis in cell culture. Dev Biol. 1977;60:69-82.

Andrei DC, Briscoe BJ, Luckham PF, Williams DR. The deformation of microscopic gel particles. J Chim Phys PCB. 1996;93(5):960-976.

Aparicio S, Dotty SB, Camacho NP, Paschalis EP, Spevak L, Mendelsohn R, Boskey AL. Optimal method for processing mineralized tissues for fourier transform infrared microspectroscopy. Calcif Tissue Int. 2002;70:422-429.

Arai A, Yamamoto K, Toyama J. Murine cardiac progenitor cells require visceral embryonic endoderm and primitive streak for terminal differentiation. Dev Dyn 1997;210;344-353.

Asou Y, Nifuji A, Tsuji K, Shinomiya K, Olson EN, Koopman P, Noda M. Coordinated expression of scleraxis and sox-9 genes during embryonic development of tendons and cartilage. J Ortho Res. 2002;20:827-833.

Atala A. Technology Insight: applications of tissue engineering and biological substitutes in urology. Nat Clin Prac Urol. 2005;2:143-149.

Baker J, Liu JP, Robertson EJ, Efstratiadis A. Role of insulin-like growth factors in embryonic and postnatal growth. Cell. 1993;7:73-82.

Banerjee C, Javed A, Choi JY, Green J, Rosen V, van Wijnen AJ, Stein JL, Lian JE, Stein GS. Differential regulation of the two principal Runx2/Cbfa1 N-terminal isoforms in response to bone morphogenetic protein-2 during development of the osteoblast phenotype. Endocrinology. 2001;142(9):4026-4039.

Barbosa I, Garcia S, Barbier-Chassefiere V, Caruelle JP, Martelly I, Papy-Garcia D. Improved and simple micro assay for sulfated glycosaminoglycans quantification in biological extracts and its use in skin and muscle tissue studies. Glycobiology. 2003;13:647-653.

Barngrover D, Thomas J, Thilly WG. High density mammalian cell growth in Leibovitz biocarbonate-free medium: effects of fructose and galactose on culture biochemistry. J Cell Set. 1985;78:173-189.

Baxter MA, Wynn RF, Jowitt SN, Wraith JE, Fairbairn LJ, Bellantuono I. Study of telomere length reveals rapid aging of human marrow stromal cells following *in vitro* expansion. Stem Cells. 2004;22:675-682.

Beattie GM, Lopez AD, Bucay N, Hinton A, Firpo MT, King CC, Hayek A. Activin A maintains pluripotency of human embryonic stem cells in the absence of feeder layers. Stem Cells. 2005;23:489-495.

Becker TA, Kipke DR, Brandon T. Calcium alginate gel: A biocompatible and mechanically stable polymer for endovascular embolization. J Biomed Mater Res. 2000;54:76-86.

Bellows CG, Aubin JE, Heersche JNM. Initiation and progression of mineralization of bone nodules formed *in vitro*: the role of alkaline phosphatase and organic phosphate. Bone Miner. 1991;14:27-40.

Bellows CG, Aubin JE, Heersche JNM, Antosz ME. Mineralized bone nodules formed *in vitro* from enzymatically released rat calvaria cell populations. Calcif. Tissue Int. 1986;38:143-154.

Ber S, Kose GT, Hariici V. Bone tissue engineering on patterned collagen films: an *in vitro* study. Biomaterials. 2005;26:1977-1986.

Betz RR. Limitations of autograft and allograft: new synthetic solutions. Orthopaedics. 2002;25(Suppl 5):S561-570.

Bianco P, Robey PG. Stem cells in tissue engineering. Nature. 2001;414:118-121.

Bielby RC, Pryce RS, Hench LL, Polak JM. Enhanced derivation of osteogenic cells from murine embryonic stem cells after treatment with ionic dissolution products of 58S bioactive sol-gel glass.Tissue Eng. 2005;11(3-4):479-488.

Bielinska M, Narita N, Wilson DB. Distinct roles for visceral endoderm during embryonic mouse development. Int J Dev Biol. 1999;43:183-205.

Bienaime C, Barbotin JN, Nava-Saucedo JE. How to build an adapted and bioactive cell microenvironment? A chemical interaction study of the structure of Ca-alginate matrices and their repercussion on confined cells. J Biomed Mater Res. 2003;67A(2):376-388.

Binette F, Cravens J, Kahoussi B, Haudenschild DR, Goetinck PF. Link protein is ubiquitously expressed in non-cartilaginous tissues where it enhances and stabilizes the interaction of proteoglycans with hyaluronic acid. J Biol Chem. 1994;269(29):19116-19122.

Binderman I, Greene RM, Pennypacker JP. Calcification of differentiating skeletal mesenchyme *in vitro.* Science. 1979;206:222-224.

Blaker JJ, Maquet V, Jerome R, Boccaccini AR, Nazhat SN. Mechanical properties of highly porous PDLLA/Bioglass composite foams as scaffolds for bone tissue engineering. Acta Biomater. 2005;1(6):643-52.

Bloor DJ, Metcalfe AD, Rutherford A, Brison DR, Kimber SJ. Expression of cell adhesion molecules during human preimplantation embryo development. Mol Hum Reprod. 2002;8:237–245.

Bobic V. Current status of the articular cartilage repair. J Regen Med. 2000;1(4):37-41.

Boheler KR, Czyz J, Tweedie D, Yang HT, Anisimov SV, Wobus AM. Differentiation of pluripotent embryonic stem cells into cardiomyocytes. Circ Res. 2002;91:189–201.

Bonab MM, Alimoghaddam K, Talebian F, Ghaffari SH, Ghavamzadeh A, Nikbin B. Aging of mesenchymal stem cell in vitro. BMC Cell Biol. 2006;10:7-14.

Bosnakovski D, Mizuno M, Kim G, Takagi S, Okumura M, Fujinaga T. Chondrogenic Differentiation of Bovine Bone Marrow Mesenchymal Stem Cells (MSCs) in Different Hydrogels: Influence of Collagen Type II Extracellular Matrix on MSC Chondrogenesis. Biotechnol Bioeng. 2006;93(6):1152-63.

Bosnakovski D, Mizuno M, Kim G, Ishiguro T, Okumura M, Iwanaga T, Kadosawa T, Fujinaga T. Chondrogenic differentiation of bovine bone marrow mesenchymal stem cells in pellet cultural system. Exp Hematol. 2004;32(5):502-509.

Botchwey EA, Pollack SR, Levine EM, Laurencin CT. Bone tissue engineering in a rotating bioreactor using a microcarrier matrix system. J Biomed Mater Res 2001;55:242–253.

Botquin V, Hess H, Fuhrmann G, Anastassiadis C, Gross MK, Vriend G, Scholer HR. New POU dimer configuration mediates antagonistic control of an osteopontin preimplantation enhancer by Oct-4 and Sox-2. Genes Dev. 1998;12:2073–2090.

Briscoe BJ, Liu KK, Williams DR. Adhesive contact deformation of a single microelastomeric sphere. J Col Inter Sci. 1998;200(2):256-264.

Brittberg M, Lindahl A, Nilsson A, Ohlsson C, Isaksson O, Peterson L. Treatment of deep cartilage defects in the knee with autologous chondrocyte transplantation. N Engl J Med. 1994;331:889–895.

Brittberg M, Tallheden T, Sjorgren-Jansson B, Lindahl A, Peterson L. Autologous chondrocytes used for articular cartilage repair: an update. Clin Orthop. 2001;391:S337–348.

Brook IM, Craig GT, Lamb DJ. *In vitro* interaction between primary bone organ cultures, glass-ionomer cements and hydroxyapatite/tricalcium phosphate ceramics. Biomaterials. 1991;12(2):179-186.

Brown D, Wagner D, Li X, Richardson JA, Olson EN. Dual role of the basic helix-loop-helix transcription factor scleraxis in mesoderm formation and chondrogenesis during mouse embryogenesis. Development. 1999;126:4317-4329.

Buckwalter JA. Articular cartilage injuries. Clin Orthop. 2002;402:21-27.

Burdsal CA, Damsky CH, Pedersen RA. The role of E-cadherin and integrins in mesoderm differentiation and migration at the mammalian primitive streak. Development. 1993;118:829-844.

Buttery LD, Bourne S, Xynos JD, Wood H, Hughes FJ, Hughes SP, Episkopou V, Polak JM. Differentiation of osteoblasts and in vitro bone formation from murine embryonic stem cells. Tissue Eng. 2001;7:89-99.

Calhoun JD, Rao RR, Warrenfeltz S, Rekaya R, Dalton S, McDonald J, Stice SL. Transcriptional profiling of initial differentiation events in human embryonic stem cells. Biochem Biophys Res Commun. 2004;323:453-464.

Campbell AA, Fryxell GE, Linehan JC, Graff GL. Surface-induced mineralization: A new method for producing calcium phosphate coatings J Biomed Mat Res. 1996;32:111-118.

Cancedda R, Dozin B, Giannoni P, Quarto R. Tissue engineering and cell therapy of cartilage and bone. Matrix Biol. 2003;22:81-91.

Cao T, Henga BC, Ye CP, Liu H, Toh WS, Robson P, Li P, Hong YH, Stanton LW. Osteogenic differentiation within intact human embryoid bodies result in a marked increase in osteocalcin secretion after 12 days of *in vitro* culture, and formation of morphologically distinct nodule-like structures. Tissue Cell. 2005;37:325–334.

Caplan AI. Mesenchymal stem cells: Cell-based reconstructive therapy in orthopedics. Tissue Eng. 2005;11(7/8):1198-1211.

Carulli D, Rhodes KE, Fawcett JW. Upregulation of aggrecan, link protein 1, and hyaluronan synthases during formation of perineuronal nets in the rat cerebellum, J Comp Neurol. 2007;501(1):83-94.

Ceuninck FD, Lesur C, Pastoureau P, Caliez A, Sabatini M. Culture of chondrocytes in alginate beads. Methods Mol Med. 2004;100:15-22.

Chan KLA, Kazarian SG. New opportunities in micro- and macro-attenuated total reflection infrared spectroscopic imaging: spatial resolution and sampling versatility. Appl Spectrosc. 2003;57:381-389.

Chang YL, Stanford CM, Keller JC. Calcium and phosphate supplementation promotes bone cell mineralization: Implications for hydroxyapatite(HA)-enhanced bone formation. J Biomed Mater Res. 2000;52:270-278.

Chen OZ, Thompson ID, Boccaccini AR. 45S5 Bioglass-derived glass-ceramic scaffolds for bone tissue engineering. Biomaterials. 2006;27(11):2414-2425.

Chen CY, Schwartz RJ. Recruitment of the tinman homolog Nkx-2.5 by serum

response factor activates cardiac α-actin gene transcription. Mol Cell Biol. 1996;16(11):6372–6384.

Chen Y, Bal BS, Gorski JP. Calcium and collagen binding properties of osteopontin, bone sialoprotein, and bone acidic glycoprotein-75 from bone. J Biol Chem. 1992;267:24871–24878.

Cheng SL, Lecanda F, Davidson KM, Warlow MP, Zhang FS, Zhang L, Suzuki S, St John T, Civitelli R 1998 Human osteoblasts express a repertoire of cadherins, which are critical for BMP-2-induced osteogenic differentiation. J Bone Miner Res. 1998;13:633–644.

Colnot C. Cellular and molecular interactions regulating skeletogenesis. J Cell Biochem. 2005;95:688–697.

Coucouvanis E, Martin GR. Signals for death and survival: a two step mechanism for cavitation in the vertebrate embryo. Cell. 1995;83:279–287.

Dabiri GA, Turnacioglu KK, Sanger JM, Sanger JW. Myofibrillogenesis visualized in living embryonic cardiomyocytes. Proc. Natl. Acad. Sci. 1997;94: 9493–9498.

Dahéron L, Opitz SL, Zaehres H, Lensch WM, Andrews PW, Itskovitz-Eldor P, Daley GQ. LIF/STAT3 signaling fails to maintain self-renewal of human embryonic stem cells. Stem Cells. 2004;22:770-778.

Dang SM, Gerecht-Nir S, Chen J, Itskovitz-Eldor J, Zandstra PW. Controlled, scalable embryonic stem cell differentiation culture. Stem Cells. 2004;22:275-282.

Daniels K, Reiter R, Solursh M. Micromass cultures of limb and other mesenchyme. Methods Cell Biol. 1996;51:237-247.

Dodson SA, Bernard GW, Kenney EB, Carranza FA. *In vitro* comparison of aged young osteogenic and hemopoietic bone marrow stem cells and their derivative colonies. J Periodontol. 1996;67:184–196.

Doevendans PA, Kubalak SW, An RH, Becker DK, Chien KR, Kass RS. Differentiation of cardiomyocytes in floating embryoid bodies is comparable to fetal cardiomyocytes. J Mol Cell Cardiol. 2000; 32:839–851.

Dono R, Scalera L, Pacifico F, Acampora D, Persico MG, Simeone A. The murine cripto gene: expression during mesoderm induction and early heart morphogenesis. Development. 1993;118:1157-1168.

Du A, Sanger JM, Linask KK, Sanger JW. Myofibrillogenesis in the first cardiomyocytes formed from isolated quail precardiac mesoderm. Dev Biol. 2003;257:382–394.

Ducy P, Zhang R, Geoffroy V, Ridall AL, Karsenty G. Osf2/Cbfa1: A transcriptional activator of osteoblast differentiation. Cell. 1997;89:747-754.

Eldor JI, Schuldiner M, Karsenti D, Eden A, Yaneka O, Michal A, Soreq H, Benventisty N. Differentiation of human embryonic stem cells into embryoid bodies comprising the three embryonic germ layers. Mol Med. 2000;6:88-95.

Endres M, Hutmacher DW, Salgado AJ, Kaps C, Ringe J, Reis RL, Sittinger M, Brandwood A, Schantz ZT. Osteogenic induction of human bone marrow-derived mesenchymal progenitor cells in novel synthetic polymer-hydrogel matrices.Tissue Eng. 2003;9(4):689-702.

Erlebacher A, Filvaroff EH, Gitelman SE, Derynck R. Toward a molecular understanding of skeletal development. Cell. 1995;80:371-378.

Evans MJ, Kaufman MH. Establishment in culture of pluripotential cells from mouse embryos. Nature. 1981;292(5819):154-156.

Fisher EM, Layrolle P, Van Blitterswizk CA, De Bruijin JD. Bone formation by mesenchymal progenitor cells cultured on dense and microporous hydroxyapatite particles. Tissue Eng. 2003;9(6):1179-1188.

Flechon JE, Degrouard J, Flechon B. Gastrulation events in the prestreak pig embryo: ultrastructure and cell markers. Genesis. 2004;38:13-25.

Frank Eamesa B, Sharpeb PT, Helmsa JA. Hierarchy revealed in the specification of three skeletal fates by Sox9 and Runx2. Dev Biol. 2004;274:188– 200.

Freed LE, Langer R, Martin I, Pellis NR, Vunjak-Novakovic G.Tissue engineering of cartilage in space. Proc Natl Acad Sci.1997;94:13885–13890.

Friedenstein AJ, Latzinik NW, Grosheva AG, Gorskaya UF. Marrow microenvironment transfer by heterotopic transplantation of freshly isolated and cultured cells in porous sponges. Exp Hematol. 1982;10(2):217-227.

Garreta E, Genove E, Borro's S, Semino CE. Osteogenic differentiation of mouse embryonic stem cells and mouse embryonic fibroblasts in a three-dimensional self-assembling peptide scaffold. Tissue Eng. 2006;12(8):2215-2227.

Gertow K, Wolbank S, Rozell B, Sugars R, Andang M, Parich CL, Imreh MP, Wendel M, Ahrlung-Richter L. Organized development from human embryonic stem cells after injection into immunodeficient mice. Stem Cells Dev. 2004;13:421-435.

Giannoudis PV, Dinopoulos H, Tsiridis E. Bone substitutes: an update. Injury. 2005;36(Suppl 3):S20-27.

Glacken MW, Fleischaker RJ, Sinskey AJ. Reduction of waste product excretion via nutrient control: Possible strategies for maximizing product and cell yields on serum in cultures of mammalian cells. Biotechnol Bioeng. 1986;28:1376–1389.

Glowacki J, Mizuno S, Greenberger JS. Perfusion enhances functions of bone marrow stromal cells in three-dimensional culture. Cell Transplant. 1998;7:319–326.

Goldring MB, Tsuchimochi K, Jiri K. The control of chondrogenesis. J Cell Biochem. 2006;97:33–44.

Granja PL, De Jéso D, Bareille R, Rouais F, Baquey C, Barbosa MA. Mineralization of regenerated cellulose hydrogels induced human bone marrow stromal cells.Eur Cells Mater. 2005;10:31-39.

Gregory CA, Gunn WG, Peister A, Prockop DJ. An Alizarin red-based assay of mineralization by adherent cells in culture: comparison with cetylpyridinium chloride extraction. Anal Biochem. 2004;329:77-84.

Grigoriadis AE, Aubin JE, Heersche JN. Effects of dexamethasone and vitamin D3 on cartilage differentiation in a clonal chondrogenic cell population. Endocrinology. 1998;125: 2103-2110.

Grover A, Adamson ED. Roles of extracellular matrix components in differentiating teratocarcinoma cells. J Bio Chem. 1985;260(22):12252-12258.

Guanping T, Polak JM, Bishop AE, Christodoulou I, Buttery LDK. Differentiation of osteoblasts from murine embryonic stem cells by overexpression of the transcriptional factor osterix. Tissue engineering. 2004;10(9/10):1456-1466.

Gu F, Amsden B, Neufeld R. Sustained delivery of vascular endothelial growth factor with alginate beads. J Controll Rel. 2004;96:463– 472.

Hall BK, Miyake T. The membranous skeleton: the role of cell condensations in vertebrate skeletogenesis. Anat Embryol.1992;186:107–124.

Hall BK, Miyake T. All for one and one for all: Condensations and the initiation of skeletal development. Bioessays. 2000;22:138–147.

Hambly K, Bobic V, Wondrasch B, Van Assche D, Marlovits S. Autologous chondrocyte implantation postoperative care and rehabilitation: science and practice. Am J Sports Med. 2006;34(6):1020-1038.

Hammond TG, Hammond JM. Optimized suspension culture: the rotating-wall vessel. Am J Physiol Renal Physiol. 2001;281:F12–F25.

Harley CB, Futcher AB, Greider CW. Telomeres shorten during aging of human fibroblasts. Nature. 1990;345:458–460.

Hegert C, Kramer J, Hargus G, Muller J, Guan K, Wobus AM, Muller K, Rohwedel J. Differentiation plasticity of chondrocytes derived from mouse embryonic stem cells. J Cell Sci. 2002;115:4617-4628.

Heng BC, Cao T, Stanton LW, Robson P, Olsen B. Strategies for directing the differentiation of stem cells into the osteogenic lineage *in vitro*. J Bone Miner Res. 2004;19(9):1379-1394.

Hennessy B, Körbling M, Estrov Z. Circulating stem cells and tissue repair. Panminerva Med. 2004;46(1):1-11.

Herrmann BG. Expression pattern of the Brachyury gene in wholemount TWis/TWis mutant embryos. Development. 1991;113:913-917.

Hollinger JO, Winn S, Bonadio J. Options for tissue engineering to address challenges of the aging skeleton. Tissue Eng. 2000;6(4):341-350.

Holy CE, Shoichet MS, Davies JE. Engineering three-dimensional bone tissue in vitro using biodegradable scaffolds: investigating cell density and culture period. J Biomed Mater Res. 2000;51:376-382.

Hosseinkhani H, Hosseinkhani M, Tian F, Kobayashi H, Tabata Y. Ectopic bone formation in collagen sponge self-assembled peptide–amphiphile nanofibers hybrid scaffold in a perfusion culture bioreactor. Biomaterials. 2006;29:5089-5098.

Huber BTL, Zhou Y, Mead PE, Zon LI. Cooperative effects of growth factors involved in the induction of hematopoietic mesoderm. Blood. 1998;92(11):4128-4137.

Humphrey RK, Beattie GM, Lopez AD, Bucay N, King CC, Firpo MT, Rose-John S, Hayek A. Maintenance of pluripotency in human embryonic stem cells Is STAT3 independent. Stem Cells. 2004;22:522-530.

Hunter GK, Goldberg HA. Nucleation of hydroxyapatite by bone sialoprotein. Proc Natl Acad Sci. 1983;90:8562-8565.

Hutmacher DW. Scaffolds in tissue engineering bone and cartilage. Biomaterials. 2000;21:2529–2543.

Hwang NS, Kim MS, Sampattavanich S, Baek JH, Zhang Z, Elisseeff J. Effects of three-dimensional culture and growth factors on the chondrogenic differentiation of murine embryonic stem cells. Stem Cells. 2006;24:284–291. (1)

Hwang NS, Varghese S, Zhang Z, Elisseeff J. Chondrogenic differentiation of human embryonic stem cell–derived cells in arginine-glycine-aspartate–modified hydrogels. Tissue Eng. 2006;12(9):2695-2706. (2)

Hwang NS, Varghese S, Theprungsirikul P, Canver A, Elisseeff J. Enhanced chondrogenic differentiation of murine embryonic stem cells in hydrogels with glucosamine. Biomaterials. 2006;27(36):6015-6023. (3)

Ishaug-Riley SL, Crane-Kruger GM, Yaszemski MJ, Mikos AG. Three dimensional

culture of rat calvarial osteoblasts in porous biodegradable polymers. Biomaterials. 1998;19:1405-1412.

James CB, Uhl TL. A review of articular cartilage pathology and the use of glucosamine sulfate. J Athl Train. 2001;36(4):413-419.

Johansson BM, Wiles MV. Evidence for involvement of activin A and bone morphogenetic protein 4 in mammalian mesoderm and hematopoietic development. Mol Cell Bio. 1995;15(1):141–151.

Jones CM, Kuehn MR, Hogan BLM, Smith JC, Wright CVE. Nodal-related signals induce axial mesoderm and dorsalize mesoderm during gastrulation. Development. 1995;121:3651-3662.

Karen JLB, Scott P, James FK. Biomaterial developments for bone tissue engineering. Biomaterials. 2000;21:2347-59.

Karp JM, Ferreira LS, Khademhosseini A, Kwon AH, Yeh J, and Langer R. Cultivation of human embryonic stem cells without the embryoid body step enhances osteogenesis *in vitro.* Stem Cells. 2006;24(4):835-843.

Kawaguchi J, Kii I, Sugiyama Y, Takeshita S, Kudo A. The Transition of Cadherin Expression in Osteoblast Differentiation from Mesenchymal Cells: Consistent Expression of Cadherin-11 in Osteoblast Lineage. J Bone Miner Res. 2001;16:260 –269.

Kawaguchi J, Mee PJ, Smith AG. Osteogenic and chondrogenic differentiation of embryonic stem cells in response to specific growth factors. Bone. 2005;36(5):758-69.

Kehat I, Gepstein A, Spira A, Itskovitz-Eldor J, Gepstein L. High-resolution electrophysiological assessment of human embryonic stem cell-derived cardiomyocytes: a novel in vitro model for the study of conduction. Circ Res. 2002;91: 659–661.

Khoo MLM, McQuade LR, Smith MSR, Lees JG, Sidhu KS, Tuch BE. Growth and differentiation of embryoid bodies derived from human embryonic stem cells: effect of glucose and basic fibroblast growth factor. Bio Reprod. 2005;73:1147–1156.

Kii I, Amizuka N, Shimomura J, Saga Y, Kudo A. Cell–Cell Interaction Mediated by Cadherin-11 Directly Regulates the Differentiation of Mesenchymal Cells Into the Cells of the Osteo-Lineage and the Chondro-Lineage. J Bone Miner Res. 2004;19:1840–1849.

Kimelman D, Christian JL, Moon RT. Synergistic principles of development: overlapping patterning systems in Xenopus mesoderm induction. Development. 1992;116:1–9.

King A, Sandler S, Anderson A. The effect of host factors and capsule composition on the cellular overgrowth on implanted alginate capsules. J Biomed Mater Res. 2001;57:374-383.

Kingsley DM, Bland AE, Grubber JM, Marker PC, Russell LB, Copeland NG, Jenkins NA. The mouse short ear skeletal morphogenesis locus is associated with defects in a bone rnorphogenetic member of the TGF superfamily. Cell. 1992;71:399-410.

Kispert A, Herrmann B. Immunohistochemical analysis of the Brachyury protein in wild-type and mutant mouse embryos. Dev Biol. 1994;161:179-193.

Knudson CB. Knudson W. Cartilage proteoglycans. Semin Cell Dev Biol. 2001;12: 69-78.

Koestenbauer S, Zech NH, Juch H, Vanderzwalmen P, Schoonjans L, Dohr G. Embryonic stem cells: similarities and differences between human and murine embryonic stem cells. Am J Reprod Immunol. 2006;55:169–180.

Kramer J, Klinger M, Kruse C, Faza M, Hargus G, Rohwedel J. Ultrastructural analysis of mouse embryonic stem cell-derived chondrocytes. Anat Embryol. 2005;210:175-185.

Kramer J, Hegert C, Guan K, Wobus AM, Muller PK, Rohwedel J. Embryonic stem cell-derived chondrogenic differentiation in vitro: activation by BMP-2 and BMP-4. Mech Dev. 2000;92:193-205.

Kuettner KE, Pauli BU, Gall G, Memoli VA, Schenk RK. Synthesis of Cartilage Matrix by Mammalian Chondrocytes In Vitro. I. Isolation, Culture Characteristics, and Morphology. J Cell Biol. 1982;93:743-750.

Kulyk KM, Franklin JL, Hoffman LM. Sox9 expression during chondrogenesis in micromass cultures of embryonic limb mesenchyme. Exp Cell Res. 2000;255:327-332.

Kuo CK, Ma PX. Ionically crosslinked alginate hydrogels as scaffolds for tissue engineering: Part 1. Structure, gelation rate and mechanical properties. Biomaterials. 2001;22:511–521.

Lake J, Rathjen J, Remiszewski J, Rathjen PD. Reversible programming of pluripotent cell differentiation. J Cell Sci. 2003;113:555-566.

Lawson A, Schoenwolf GC. Epiblast and primitive-streak origins of the endoderm in the gastrulating chick embryo. Development. 2003;130(15):3491-3501.

Leahy A, Xiong JW, Kuhnert F, Stuhlmann H. Use of developmental marker genes to define temporal and spatial patterns of differentiation during embryoid body formation. J Exp Zoo. 1999;284(1):67–81.

Lecanda F, Cheng SL, Shin CS, Davidson MK, Warlow P, Avioli LV, Civitelli R. Differential regulation of cadherins by dexamethasone in human osteoblastic cells. J. Cell Biochem. 2000;77:499-506.

Lee YS, Stott NS, Jiang TX, Widelitz RB, Chuong CM. Early events during precartilage condensation in limb bud micromass cultures. Cell Mater. 1998;8:19-32.

Li S, Harrison D, Carbonetto S, Fässler R, Smyth N, Edgar D, Yurchenco PD. Matrix assembly, regulation, and survival functions of laminin and its receptors in embryonic stem cell differentiation. J Cell Biol. 2002;157(7):1279–1290.

Li WJ, Cooper JA, Jr Mauck RL, Tuan RS. Fabrication and characterization of six electrospun poly(alpha-hydroxy ester)-based fibrous scaffolds for tissue engineering applications. Acta Biomater. 2006;2(4):377-385.

Lints TJ, Parsons LM, Hartley L, Lyons I, Harvey RP. Nkx-2.5: a novel murine homeobox gene expressed in early heart progenitor cells and their myogenic descendants. Development. 1993;119:419–431.

Liu KK, Williams DR, Briscoe BJ. The large deformation of a single micro-elastomeric sphere. J Phy D App Phy. 1998;31(3):294-303.

Lu CC, Brennan J, Robertson EJ. From fertilization to gastrulation: axis formation in the mouse embryo. Cur Opin Gene Dev. 2001;11:384–392.

Luegmayr E, Glantschnig H, Varga F, Klaushofer K. The organization of adherens junctions in mouse osteoblast-like cells (MC3T3-E1) and their modulation by triiodothyronine and 1,25-dihydroxyvitamin D3. Histochem Cell Biol. 2000;113:467-478.

Mahmoudifar N, Doran PM. Tissue engineering of human cartilage in bioreactors using single and composite cell-seeded scaffolds. Biotechnol Bioeng. 2005; 91:338–355.

Malaval L, Liu F, Roche P, Aubin JE. Kinetics of osteoprogenitor proliferation and osteoblast differentiation *in vitro*. J Cell Biochem. 1999;74:616–627.

Maleski MP, Knudson CB. Hyaluronan-mediated aggregation of limb bud mesenchyme and mesenchymal condensation during chondrogenesis. Exp Cell Res. 1996;225:55–66.

Mankani MH, Kuznetsov SA, Avila NA, Kingman A, Robey PG. Bone formation in transplants of human bone marrow stromal cells and hydroxyapatite-tricalcium phosphate: prediction with quantitative CT in mice. Radiology. 2004;230(2):369-376.

Marler JJ, Upton J, Langer R, Vacanti JP. Transplantation of cells in matrices for tissue regeneration. Adv Drug Del Rev. 1998;33:165–182.

Martin JA, Buckwalter JA. Aging, artilcular cartilage chondrocyte senescence and osteoarthritis. Biogerontology. 2002;3:257-264.

Martin JA, Buckwalter JA. Telomere erosion and senescence in human articular cartilage chondrocytes. J Gerontol Series A: Biol Sci Med Sci. 2001;56:B172-B179.

Martinsen A, Skjak-Braek G, Smidsrod O. Alginate as immobilization material. I. Correlation between chemical and physical properties of alginate gel beads. Biotechnol. Bioeng. 1989;33:79–89.

Masuda K, Sah RL, Hejna MJ,, Thonar EJMA. A novel two-step method for the formation of tissue-engineered cartilage by mature bovine chondrocytes: the alginate-recovered-chondrocyte (ARC) method. J Ortho Res. 2003;21:139-148.

Matsuda T, Nakamura T, Nakao K, Arai T, Katsuki M, Heike T, Yokota T. STAT3 activation is sufficient to maintain an undifferentiated state of mouse embryonic stem cells. EMBO J. 1999;18(15):4261-4269.

Mauro LJ, Foster DN, Regulators of Telomerase Activity. Am J Respir Cell Mo Biol. 2002;26:21–52.

Mbalaviele G, Nishimura R, Myoi A, Niewolna M, Reddy VS, Chen D, Feng J, Roodman D, Mundy RG, Yoneda T. Cadherin-6 mediates the heterotypic interactions between the hemopoietic osteoclast cell lineage and stromal cells in a murine model of osteoclast differentiation. J Cell Biol. 1998;141:1467–1476.

Midura RJ, Wang A, Lovitch D, Law D, Powell K, Gorski JP. Bone acidic glycoprotein-75 delineates the extracellular sites of future bone sialoprotein accumulation and apatite nucleation on osteoblastic cultures. J Biol Chem. 2004;279: 25464-25473.

Mierisch CM, Anderson PC, Balian G, Diduch DR. Treatment with Insulin-Like Growth Factor-1 Increases Chondrogenesis by Periosteum *In Vitro*. Connec Tiss Res. 2002;43:559–568.

Miller WM, Wilke CR, Blanch HW. Effects of dissolved oxygen concentration on hybridoma growth and metabolism in continuous culture. J Cell Physiol. 1987;132:524–530.

Morali OG, Jouneau A, McLaughlin KJ, Thiery JP, Larue L. IGF-II promotes mesoderm formation. Dev Biol. 2000;227:133–145.

Morishita T, Honoki K, Ohqushi H, Kotobuki N, Matsushima A, Takakura Y.Tissue engineering approach to the treatment of bone tumors: three cases of cultured bone grafts derived from patients' mesenchymal stem cells. Artif Organs. 2006;30(2):115-118.

Mouw JK, Case ND, Guldberg RE, Plaas AH, Levenston ME. Variations in matrix

composition and GAG fine structure among scaffolds for cartilage tissue engineering. Osteoarthritis Cartilage. 2005;13:828–836.

Mueller SM, Mizuno S, Gerstenfeld LC, Glowacki J. Medium perfusion enhances osteogenesis by murine osteosarcoma cells in three-dimensional collagen sponges. J Bone Mineral Res. 1999;14:2118–2126.

Mummery C, Ward D, van den Brink CE, Bird SD.; Doevendans PA, Opthof T, Brutel de la Riviere A, Tertoolen L, van der Heyden M, Pera M. Cardiomyocyte differentiation of mouse and human embryonic stem cells. J Anat. 2002;200:233-242.

Muschler GF, Nakamoto C, Griffith LG. Engineering principles of clinical cell based tissue engineering. J Bone Joint Surg Am. 2004; 86:1541—1558.

Nakashima K, Zhou X, Kunkel G, Zhang Z, Deng JM, Behringer RR, Crombrugghe BD. The novel zinc finger-containing transcription factor osterix Is required for osteoblast differentiation and bone formation. Cell. 2002;108:17–29.

Nakayama N, Duryea D, Manoukian R, Chow G, Han CY. Macroscopic cartilage formation with embryonic stem-cell-derived mesodermal progenitor cells. J Cell Sci. 2003;116:2015-2028.

Neame PJ, Barry FP. The link proteins. EXS.1994;70:53-72.

Nichols J, Zevnik B, Anastassiadis K, Klewe-Nebenius ND, Chambers I, Schöler H, Smith A. Formation of pluripotent stem cells in the mammalian embryo depends on the POU transcription factor Oct4. Cell. 1998;95(3):379-391.

Niederlander C, Walsh JJ, Episkopou V, Jones CM. Arkadia enhances nodal-related signalling to induce mesendoderm. Nature. 2001;410:830-834.

Niehrs C, Steinbeisser H, De Robertis EM. Mesodermal patterning by a gradient of the vertebrate homeobox gene goosecoid. Science. 1994;63:817-820.

Niwa H, Miyazaki J, Smith A. Quantitative expression of Oct-3/4 defines differentiation, dedifferentiation or self-renewal of ES cells. Nat Genet. 2000;24(4):372-376.

Obradovic B, Carrier RL, Vunjak-Novakovic G, Freed LE. Gas exchange is essential for bioreactor cultivation of tissue engineered cartilage. Biotechnol Bioeng. 1999;63:197–205.

Ohyabu Y, Kida N, Kojima H, Taguchi T, Tanaka J, Uemura T. Cartilaginous tissue formation from bone marrow cells using rotating wall vessel (RWV) bioreactor. Biotchnol Bioeng. 2006;95(5):1003-1008.

Oka M, Tagoku K, Russell TL, Nakano Y, Hamazaki T, Meyer EM, Yokota T, Terada N. CD9 Is associated with leukemia inhibitory factor mediated maintenance of embryonic stem cells. Mol Biol Cell. 2002;13:1274–1281.

Percival M. Bone health & osteoporosis. Appl Nut Sci Rep. 1999;5(4):1-6.

Pesce M, Gross MK, Scholer HR. In line with our ancestors: Oct-4 and the mammalian germ. Bioessays. 1998;20(9):722-732.

Petite H, Viateau V, Bensaid W, Meunier A, de Pollak C, Bourguignon M, Oudina K, Sedel L, Guillemin G. Tissue-engineered bone regeneration. Nat Biotechnol. 2000;18(9):959-963.

Pfendler KC, Catuar CS, Meneses JJ, Pedersen RA. Overexpression of *nodal* promotes differentiation of mouse embryonic stem cells into mesoderm and endoderm at the expense of neuroectoderm formation. Stem Cells. 2005;14:162-172.

Pittenger MF, Mackay AM, Beck SC, Jaiswal RK, Douglas R, Mosca JD. Multilineage potential of adult human mesenchymal stem cells. Science 1999;284:143–147.

Poliard A, Nifuji A, Lamblin D, Plee E, Forest C, Kellermann O. Controlled conversion of an immortalized mesodermal progenitor cell towards osteogenic, chondrogenic, or adipogenic pathways. J Cell Biol. 1995;130(6):1461-1472.

Pollack SR. Meany DF. Levine EM. Litt M. Johnston ED. Numerical model and experimental validation of microcarrier motion in a rotating bioreactor. Tissue Eng. 2000;6(5):519-530.

Poole AR, Kojima T, Yasuda T, Mwale F, Kobayashi M, Laverty S. Composition

and structure of articular cartilage: a template for tissue repair. Clin Orthop Relat Res. 2001;391;S26-33.

Przyborski SA. Differentiation of human embryonic stem cells after transplantation in immune-deficient mice. Stem cells. 2005;23(9):1242-1250.

Qi X, Li TG, Hao J, Hu J, Wang J, Simmons H, Miura S, Mishina Y, Zhao GQ. BMP4 supports self-renewal of embryonic stem cells by inhibiting mitogen-activated protein kinase pathways. Proc Natl Acad Sci. 2004;101;6027-6032.

Qiu QQ, Ducheyne P, Ayyaswamy PS. Fabrication, characterization and evaluation of bioceramic hollow microspheres used as microcarriers for 3-D bone tissue formation in rotating bioreactors. Biomaterials 1999;20:989–1001.

Raghunath J, Salacinski HJ, Sales KM, Butler PE, Seifalian AM. Advancing cartilage tissue engineering: the application of stem cell technology. Cur Opin Biotech. 2005;16:503–509.

Rando TA. Stem cells, ageing and the quest for immortality. Nature. 2006;441(7097):1080-1086.

Rathjen J, Lake JA, Bettess MD, Washington JM, Chapman G, Rathjen PD. Formation of a primitive ectoderm like cell population, EPL cells, from ES cells in response to biologically derived factors. J Cell Sci. 1999;112:601-612.

Rathjen PD, Nicholas J, Toth S, Edwards DR, Heath JK, Smith AG. Developmentally programmed induction of differentiation inhibiting activity and the control of stem cell populations. Genes Dev. 1990;4(12B):2308-2318.

Raz R, Lee CK, Canizzaro LA, d'Eustachio P, Levy DE. Essential role of STAT3 for embryonic stem cell pluripotency. Proc Natl Acad Sci.1999;96(6):2846-51.

Robertson EJ. Derivation and maintenance of embryonic stem cell cultures. Methods Mol Biol. 1997;75:173-184.

Rodriguez E, Roughley P. Link protein can retard the degradation of hyaluronan in proteoglycan aggregates. Osteoarth Cartil. 2006;14(8):823-829.

Rodríguez-Lugo V, Sanchez Hernández J, Arellano-Jimenez MJ, Hernández-

Tejeda PH, Recillas-GispertS. Characterization of hydroxyapatite by eectron microscopy. Microsc Microanal. 2005;11:516–523.

Rossert J, Crombrugghe BE. Type I collagen. In: Principles of Bone Biology. Bilezikian JP, Raisz LG, Rodan GA, eds. Academic Press, San Diego, 2002. 189-209.

Rudy-Reil D, Lough J. Avian precardiac endoderm/mesoderm induces cardiac myocyte differentiation in murine embryonic stem cells. Circ Res. 2004;94(12):107-116.

Sandeep GH, Varma K, Kumary TV, Suresh Babu S, John A. Characterization of novel bioactive glass coated hydroxyapatite granules in correlation with in vitro and in vivo. Trends Biomater Artif. Organs. 2006;19(2);99-107.

Sandell LJ, Morris N, Robbins JR, Goldring MB. Alternatively spliced type II procollagen mRNAs define distinct populations of cells during vertebral development: differential expression of the amino-propeptide. J Cell Biol. 1991;114:1307-1319.

Saito S, Liu B, Yokoyama K. Animal embryonic stem (ES) cells: self-renewal, pluripotency, transgenesis and nuclear transfer. Human Cell. 2004;17(3):107-115.

Salgado AJ, Coutinho OP, Reis RL. Bone tissue engineering: state of the art and future trends. Macromol Biosci. 2004;4:743—765.

Schmid TM, Linsenmayer TF. Immunohistochemical localization of short chain cartilage collagen (type X) in avian tissues. J Cell Biol. 1985;100:598-605.

Schnabel M, Marlovits S, Eckhoff G, Fichtel I, Gotzen L, Vecsei V, Schlegel J. Dedifferentiation-associated changes in morphology and gene expression in primary human articular chondrocytes in cell culture. Osteoarthritis Cartilage. 2002;10:62–70.

Schreiber RE, Ratcliffe A. Tissue engineering of cartilage. Methods Mol Biol. 2000;139:301–309.

Schumann D, Kujat R, Nerlich M, Angele P. Mechanobiological conditioning of stem cells for cartilage tissue engineering. Biomed Mater Eng. 2006;16(Suppl

4):S37-52.

Seeman E, Delmas PD. Bone quality. The material and structural basis of bone strength and fragility. N Engl J Med. 2006;354:2250-2261.

Siano SA, Mutharasan R. NADH fluorescence and oxygen uptake response of hybridoma cultures to substrate pulse and step changes. Biotechnol Bioeng. 1991;37:141–159.

Smith AG, Heath JK, Donaldson DD, Wong GG, Moreau J, Stahl M, Rogers D. Inhibition of pluripotential embryonic stem cell differentiation by purified polypeptides. Nature. 1988;336(6200):688-690.

Sodek J, Ganss B, McKee MD. Osteopontin. Crit Rev Oral Biol Med. 2000;11:279-303.

Sottile V, Thomson A, McWhir J. *In vitro* osteogenic differentiation of human ES cells. Clon Stem Cells. 2003;5:149-155.

South-Paul JE. Osteoporosis: Part I. Evaluation and assessment. Am Fam Physician. 2001;63:897-908.

Suemori H, Kadodawa Y, Goto K, Araki I, Kondo H, Nakatsuji N. A mouse embryonic stem cell line showing pluripotency of differentiation in early embryos and ubiquitous beta-galactosidase expression. Cell Differ Dev. 1990;29(3):181-186.

Sugawara Y, Suzuki K, Koshikawa M, Ando M, Iida J. Necessity of enzymatic activity of alkaline phosphatase for mineralization of osteoblastic cells. Jpn. J. Pharmacol. 2002;88:262-269.

Suh H, Hwang YS, Song MJ, Lee WS, Han CD, Park JC. Behaviors of osteoblast-like cells (MC 3T3-E1) on collagen grafted porous poly L-lactic acid (PLLA) membranes with various pore sizes. Biomaterials Research. 2000;4(2):37-44.

Suh H, Hwang YS, Lee JE, Han CD, Park JC. Behaviors of osteoblasts on a type I atelocollagen grafted ozone oxidized poly L-lactic acid membrane. Biomaterials. 2001;22:219-230.

Suzuki A, Raya A, Kawakami Y, Morita M, Matsui T, Nakashima K, Gage FH, Rodríguez-Esteban C, Belmonte JCL. Maintenance of embryonic stem cell

pluripotency by Nanog-mediated reversal of mesoderm specification. Nature Clin Prac Cardio Med. 2006;3:S114-S122.

Takahashi T, Lord B, Schulze PC, Fryer RM, Sarang SS, Gullans SR, Lee RT. Ascorbic acid enhances differentiation of embryonic stem cells Into cardiac myocytes. Circulation. 2003;107;1912-1916.

Tam PP, Williams EA, Chan WY. Gastrulation in the mouse embryo: ultrastructural and molecular aspects of germ layer morphogenesis. Microsc Res Tech. 1993;26(4):301-328.

Tam PP, Loebel DA. Gene function in mouse embryogenesis: get set for gastrulation. Nat Rev Genet. 2007;8(5):368-381.

Tamura S, Kataoka H, Matsui Y, Shionoya Y, Ohno K, Michi KI . The effects of transplantation of osteoblastic cells with bone morphogenetic protein (BMP) / carrier complex on bone repair. Bone. 2001;29:169–75.

Tanaka H, Murphy CL, Murphy C, Kimura M, Kawai S, Polak JM. Chondrogenic differentiation of murine embryonic stem cells: Effects of culture conditions and dexamethasone. J Cell Biochem. 2004;93:454–462.

Temenoff JS, Mikos AG. Review: tissue engineering for regeneration of articular cartilage. Biomaterials 2000;21:431–440.

Tenenbaum HC, Heersche JNM. Differentiation of osteoblasts and formation of mineralized bone *in vitro*. Calcif Tissue Int. 1982;34:76-79.

Thomson JA, Itskovitz-Eldor J, Shapiro SS, Waknitz MA, Swiergiel JJ, Marshal VS, Jones JM. Embryonic stem cell line from human blastocysts. Science. 1998;282:1145–1147.

Togari A, Arakawa S, Arai M, Matumoto S. Inhibition of in vitro mineralization in osteoblastic cells and in mouse tooth germ by phosphatidylinositol-specific phospholipase C. Biochem Pharmacol. 1993;46:1668-1670.

Tsuji T, Hughes FJ, McCulloch CA. The effects of donor age on osteogenic cells of rat marrow *in vitro*. Mech. Ageing Dev. 1990;51:121–132.

Tuan RS. Biology of developmental and regenerative skeletogenesis. Clin Orthop Relat Res. 2004;427:S105–S117.

Vacanti CA, Langer R, Schloo B, Vacanti JP. Synthetic polymers seeded with chondrocytes provide a template for new cartilage formation. Plast Reconstr Surg. 1991; 88:753–759.

Vacanti JP, Langer R. Tissue engineering: the design and fabrication of living replacement devices for surgical reconstruction and transplantation. Lancet. 1999;354(Suppl 1):SI32–134.

Valdimarsdotter G, Mummery C. Functions of the TGF-β superfamily in human embryonic stem cells. APMIS. 2005;113: 773–789.

Viereck V, Siqqelkow H, Tauber S, Raddatz D, Schutze N, Hufner M. Differential regulation of Cbfa1/Runx2 and osteocalcin gene expression by vitamin-D3, dexamethasone, and local growth factors in primary human osteoblasts. J Cell Biochem. 2002;86(2):348-356.

Vincent SD, Dunn NR, Hayashi S, Norris DP, Robertson EJ. Cell fate decisions within the mouse organizer are governed by graded nodal signals. Genes Dev. 2003;17:1646-1662.

Wang H, Lee JK, Moursi A, Lannutti JJ. Ca/P ratio effects on the degradation of hydroxyapatite *in vitro.* J Biomed Mater Res (Part A). 2002;67A(2): 599-608.

Wang Y, Kim UJ, Blasioli DJ, Kim HJ, Kaplan DL. *In vitro* cartilage tissue engineering with 3D porous aqueous-derived silk scaffolds and mesenchymal stem cells. Biomaterials. 2005;26(34):7082-7094.

Watanabe H, Yamada Y, Kimata K. Roles of aggrecan, a large chondroitin sulfate proteoglycan, in cartilage structure and function. J Biochem (Tokyo). 1998;124:687-693.

Weiner S, Traub W. Bone structure: from angstroms to microns. FASEB J. 1992;6(3):879-885.

Wenger KH, Woods JA, Holecek A, Eckstein EC, Robertson JT, Hasty KA. Matrix remodeling expression in anulus cells subjected to increased compressive load.

Spine. 2005;30:1122–1126.

Westfall MV, Pasyk KA, Yule DI, Samuelson LC, Metzger JM. Ultrastructure and cell-cell coupling of cardiac myocytes differentiating in embryonic stem cell cultures. Cell Motil Cytoskeleton. 1997;36:43–54.

Wexler SA, Donaldson C, Denning-Kendall P, Rice C, Bradley B, Hows JM. Adult bone marrow is a rich source of human mesenchymal 'stem' cells but umbilical cord and mobilized adult blood are not. Br J Haematol. 2003;121(2):368-374.

Wilkinson DG, Bhatt S, Herrmann BG. Expression pattern of the mouse T gene and its role in mesoderm formation. Nature. 1990;343:657-659.

Woll NL, Heaney JD, Bronson SK. Osteogenic nodule formation from single embryonic stem cell-derived progenitors. Stem Cells Devel. 2006;15:865-879.

Woll NL, Bronson SK. Analysis of embryonic stem cell-derived osteogenic cultures. Methods Mol Biol. 2006;330:149-159.

Wolpert L. Positional information and the spatial pattern of cellular differentiation. J Theor Biol. 1969;25:1–47.

Wozney JM. The bone morphogenetic protein family and osteogenesis. Mol Reprod Dev. 1992;32:60-167.

Wuthier RE, Register TC. Role of alkaline phosphatase, a polyfunctional enzyme, in mineralizing tissues. In The Chemistry and Biology of Mineralized Tissues. Butler WT, editor. EBSCO Media, Birmingham, AL. 1985. 113-124.

Xu C, Police S, Rao N, Carpenter MK. Characterization and enrichment of cardiomyocytes derived from human embryonic stem cells. Circ Res. 2002;91: 501–508.

Yates A, Chambers I. The homeodomain protein Nanog and pluripotency in mouse embryonic stem cells. Biochem Soc Trans. 2005;33(6):1518-1521.

Yoo J, Johnstone B. Mesenchymal cell transfer for articular cartilage repair. Exp Opin Biol Ther. 2001;1(6):915-921.

Yoshikawa M, Suzuki K, Kajii T, Koshikawa M, Imai T, Matsumoto A. quantitative analysis of alkaline phosphatase activity and mineralization of a clonal osteoblast-like cell MC3T3-E1. J Hard Tissue Biol.1999;8:37-42.

Zhou HY, Takita H, Fujisawa R, Mizuno M, Kuboki Y. Stimulation by bone sialoprotein of calcification in osteoblast-like MC3T3-E1 cells. Calcif Tissue Int. 1995;56:403–407

Zhou X, Quann E, Gallicano IG. Differentiation of nonbeating embryonic stem cells into beating cardiomyocytes is dependent on downregulation of PKCβ and ζ in concert with upregulation of PKCω. Dev Biol. 2003;255:407-422.

Zhu JX, Sasano Y, Takahashi I, Mizoguchi I, Kagayama M. Temporal and spatial gene expression of major bone extracellular matrix molecules during embryonic osteogenesis in rats. Histochem J. 2001;33:25–35.

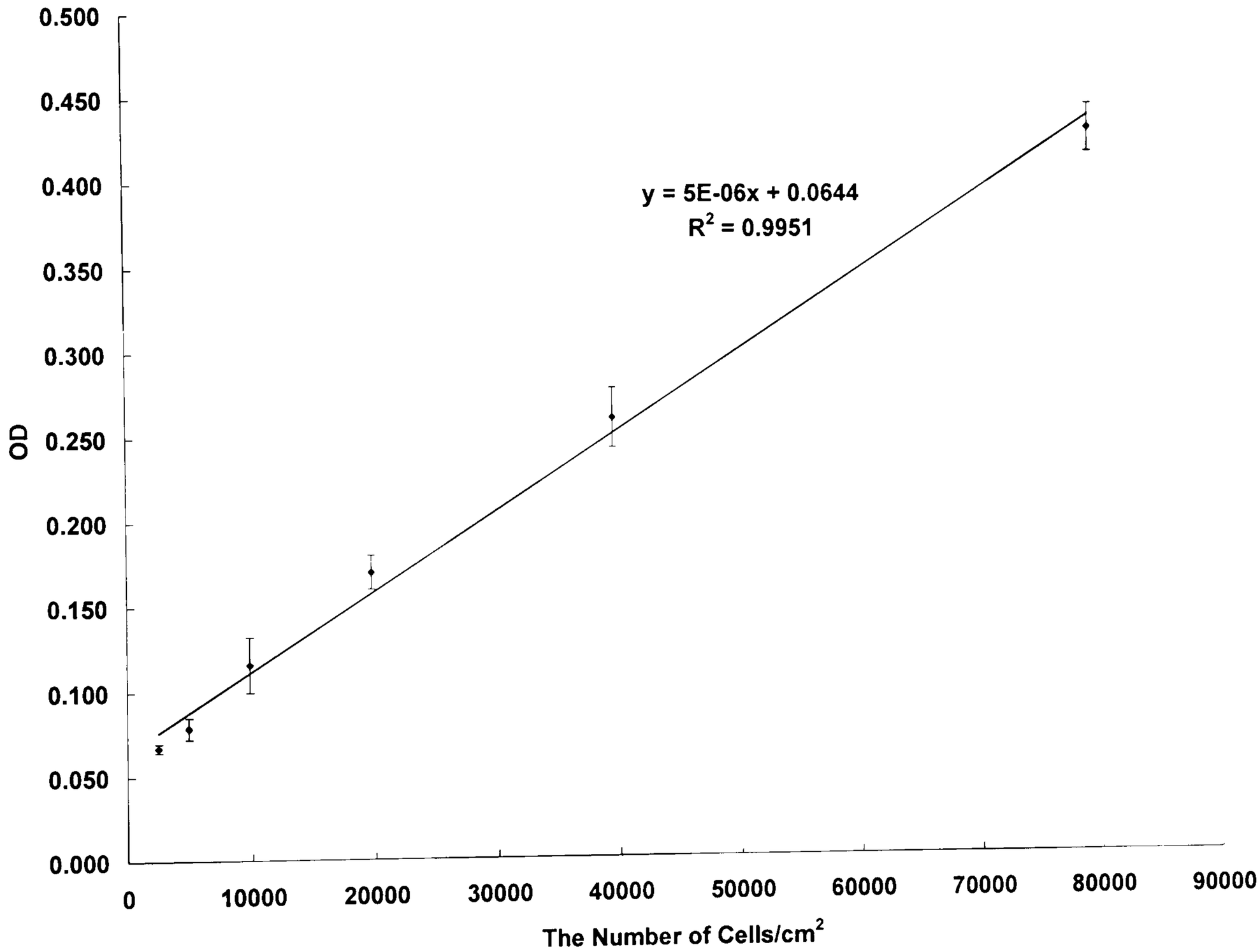
Zielke HR, Sumbilla CM, Sevdalian DA, Hawkins RL, Ozand PT. Lactate: A major product of glutamine metabolism by human diploid fibroblasts. J Cell Physiol. 1980;104:433–441.

Zur Nieden NI, Kempka G, Ahr HJ. *In vitro* differentiation of embryonic stem cells into mineralized osteoblasts. Differentiation. 2003;71:18-27.

APPENDIX

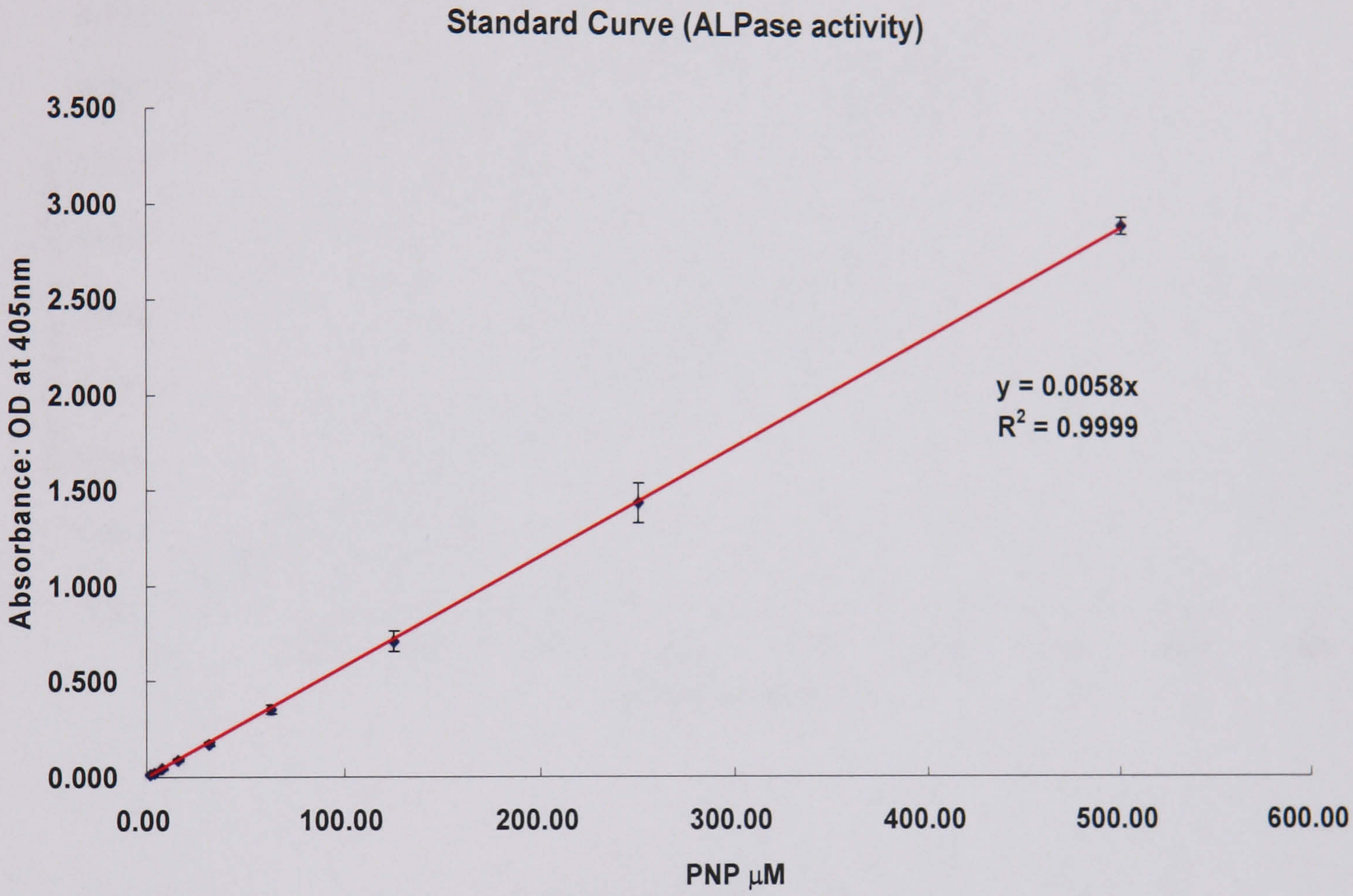
APPENDIX 1

A standard curve was generated by measuring the level of the endogenous mitochondrial dehydrogenase of mESCs after 4 hrs of seeding in accordance with serial cell seeding density using the CellTiter 96® AQueous non-radioactive cell proliferation assay according to previously described method in the section of 2.3.1.



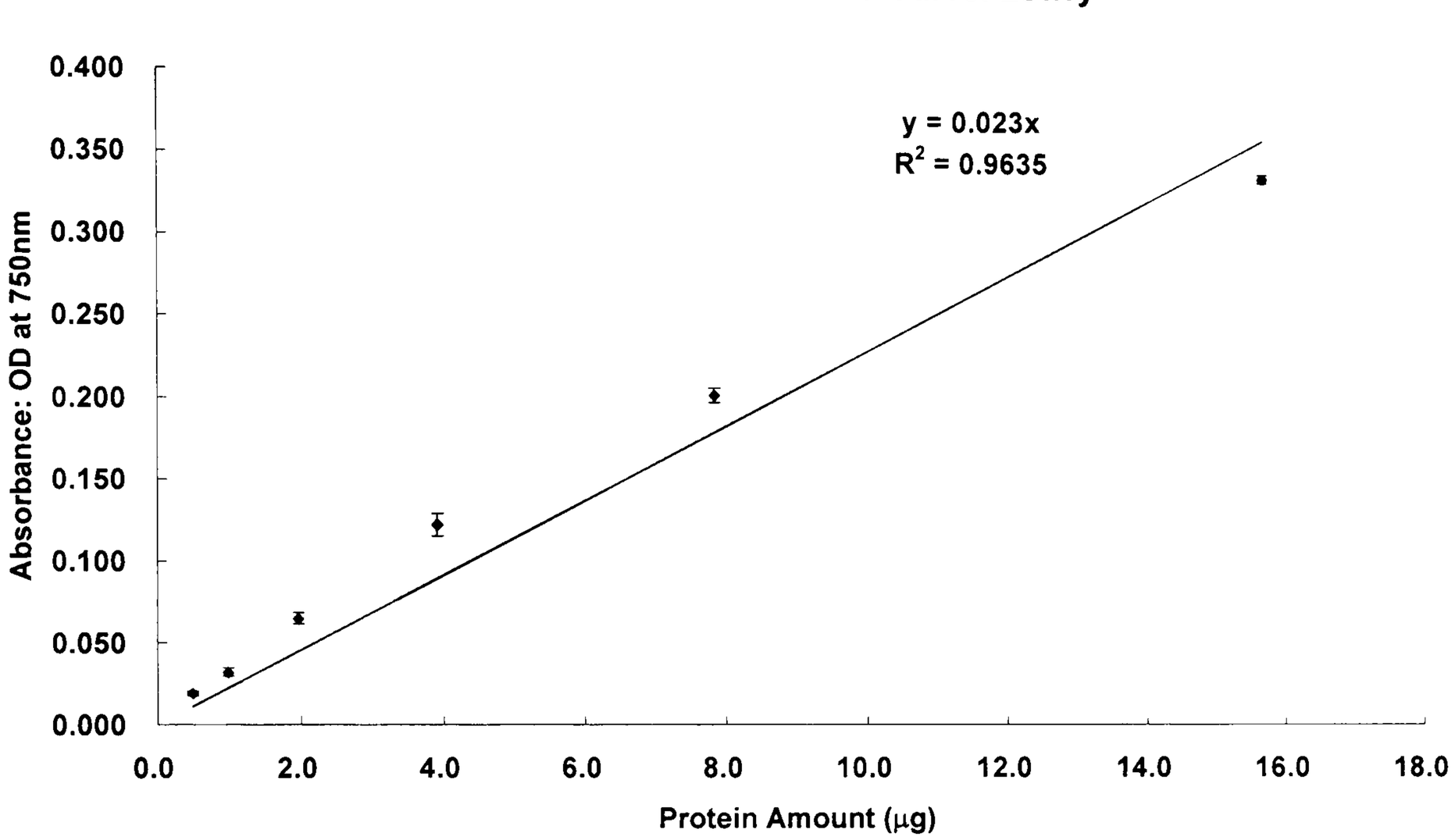
APPENDIX 2

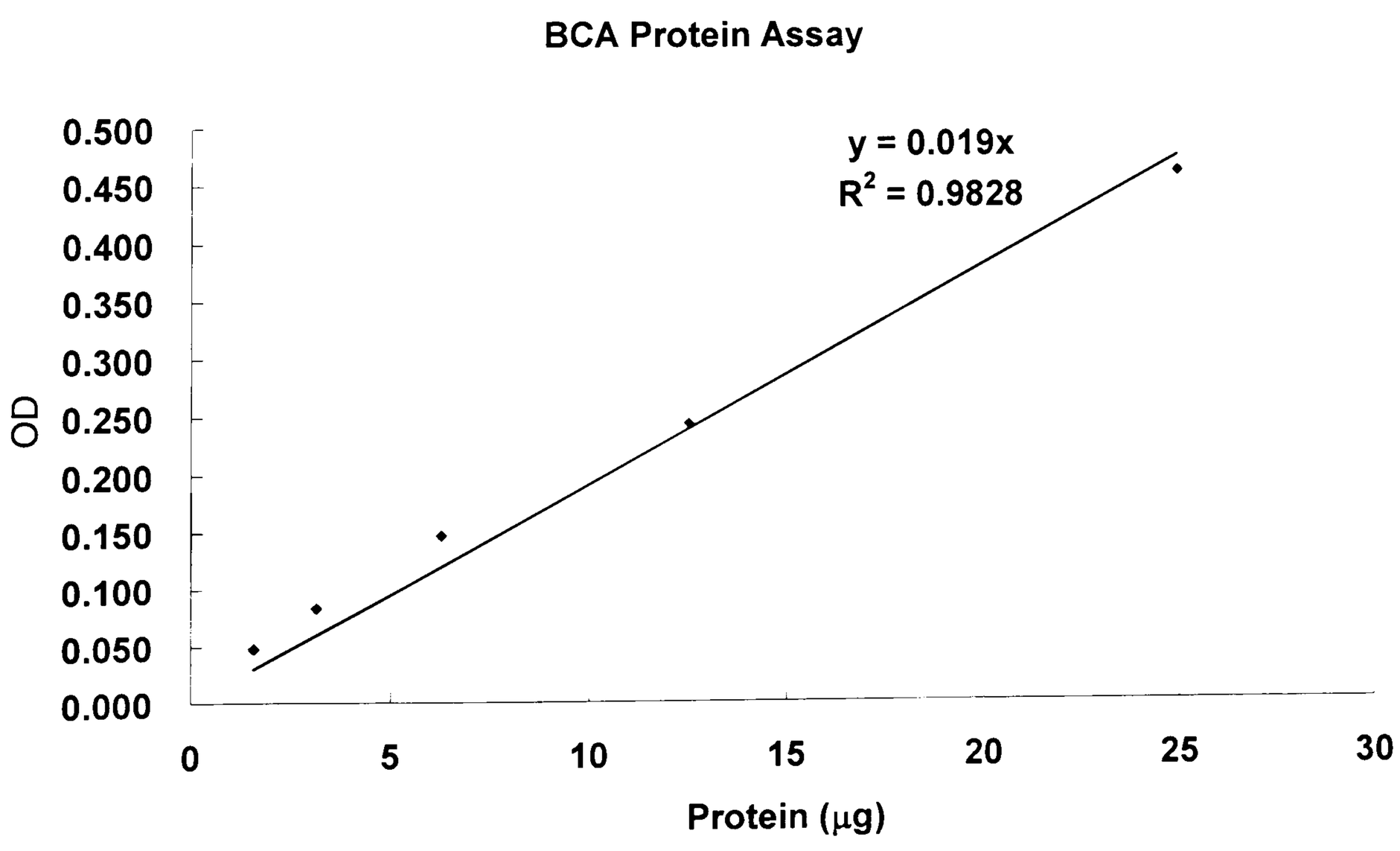
A calibration curve was generated using standard p-nitrophenol solution (Sigma, UK). The absorbance for serially diluted p-nitrophenol, ranged from 0 to 500 μM, was read at 405 nm.



APPENDIX 3

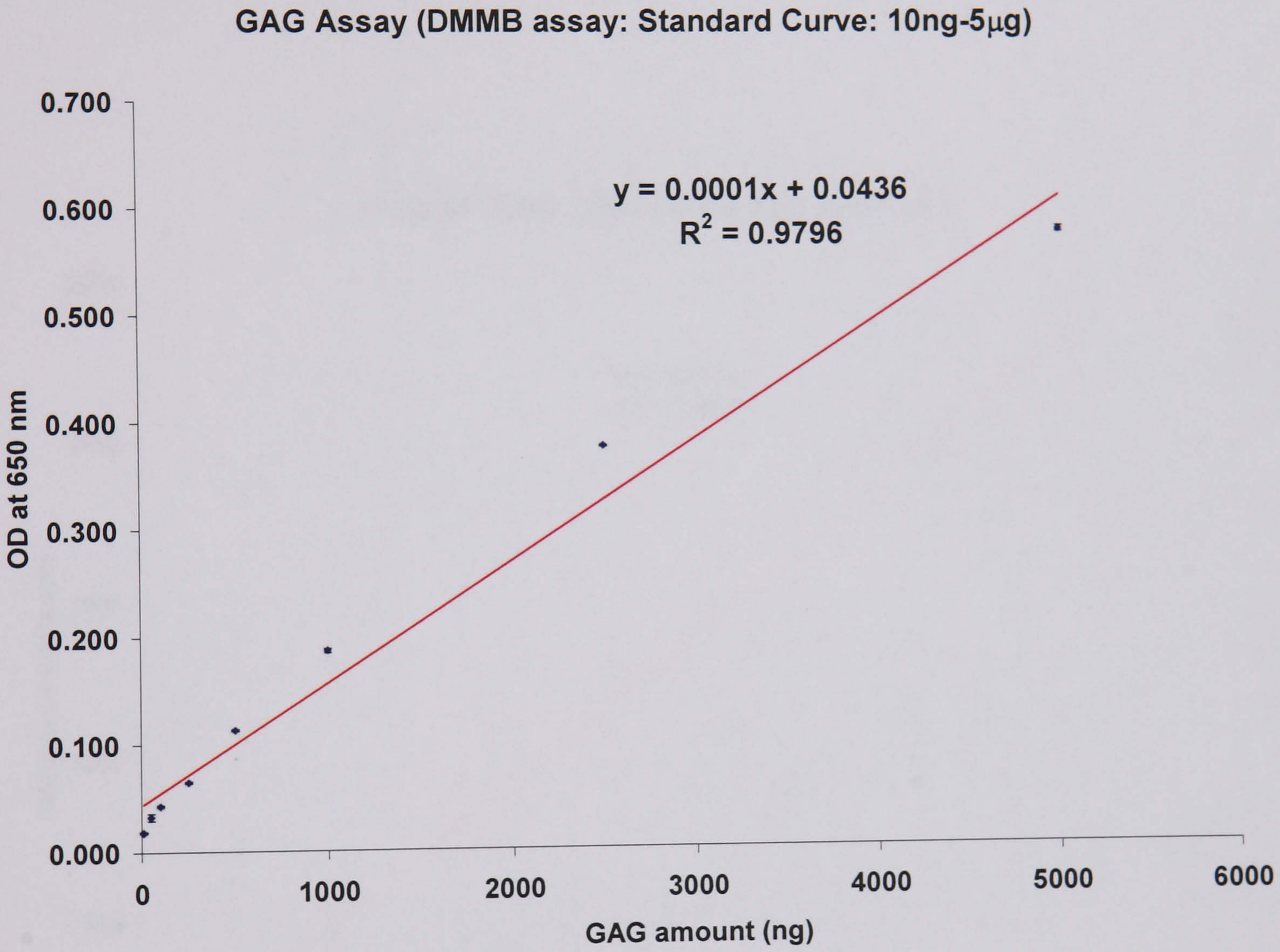
Calibration curves were generated using serially diluted bovine serum albumin (Sigma, UK) and Bio-Rad DC protein assay kit (Bio-Rad, USA) or BCA™ protein assay kit (Pierce, USA) according to the manufacturer's instruction.





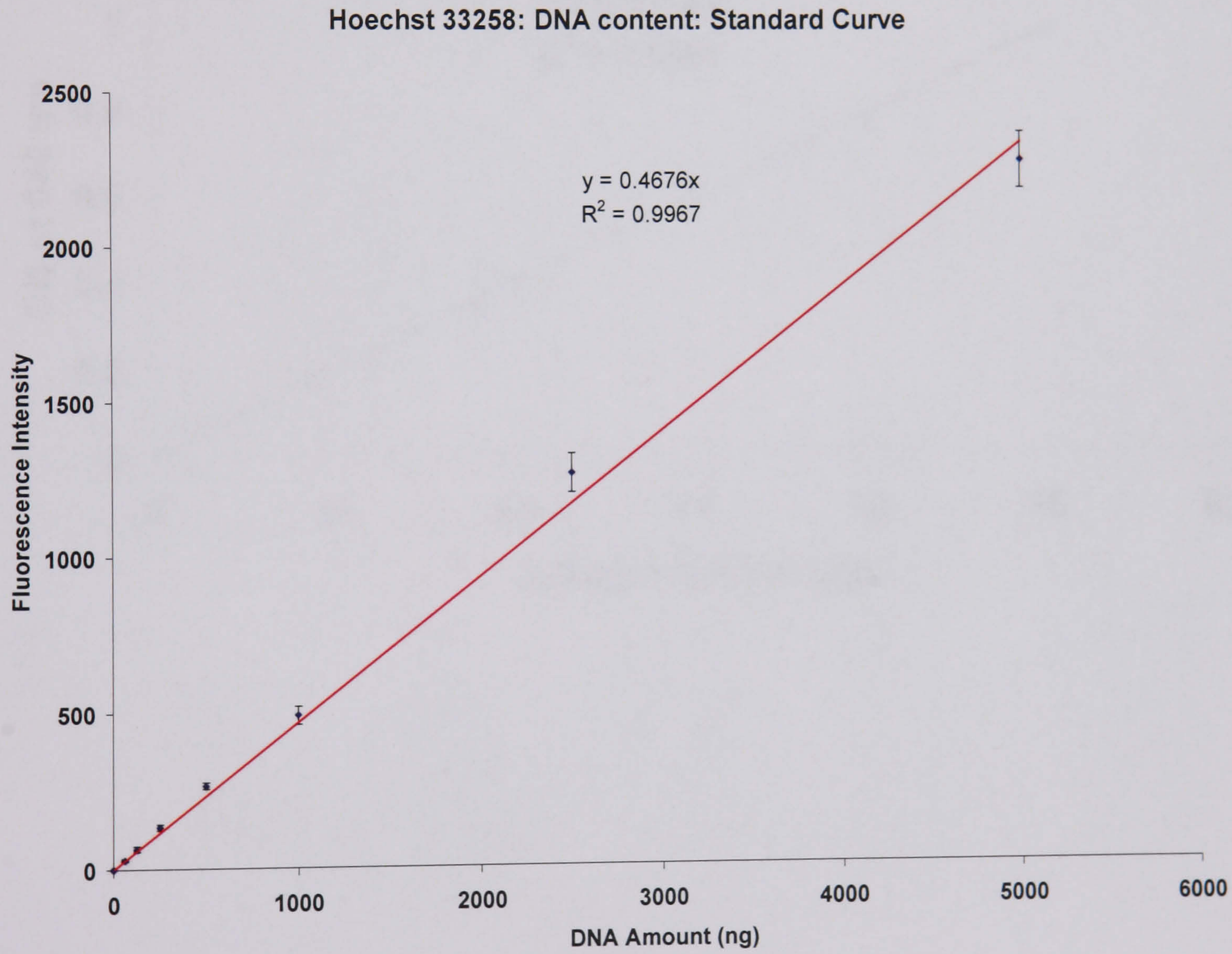
APPENDIX 4

A calibration curve was generated using the serially diluted chondroitin sulfate solution (Sigma, UK), and other procedure was done according to previously described method in the section of 2.4.2.5. Measurement of sulfated GAG content (1,9-Dimethlmethylene Blue (DMMB) assay) and DNA content, and the OD_{650} of the solution was measured.



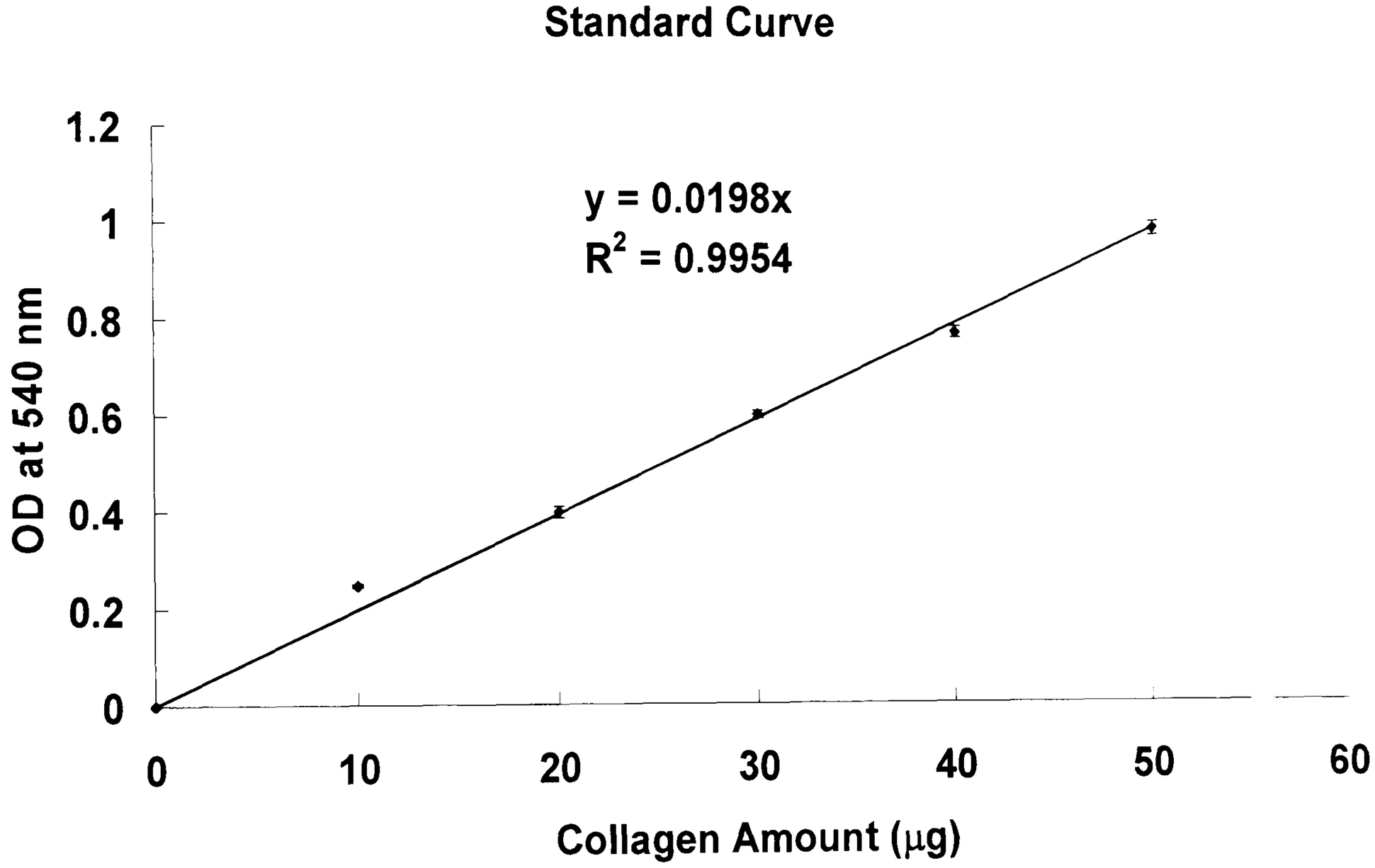
APPENDIX 5

A calibration curve was generated using highly polymerised calf-thymus DNA (Sigma, UK) and other procedure was done according to previously described method in the section of 2.4.2.5. Measurement of sulfated GAG content (1,9-Dimethlmethylene Blue (DMMB) assay) and DNA content. An aliquot (100μl) of the solution was then read using a microtiter plate fluorometer (MFX, Dynex Technology, Finland) with the excitation wavelength being at 365 nm and the emission wavelength at 460 nm.



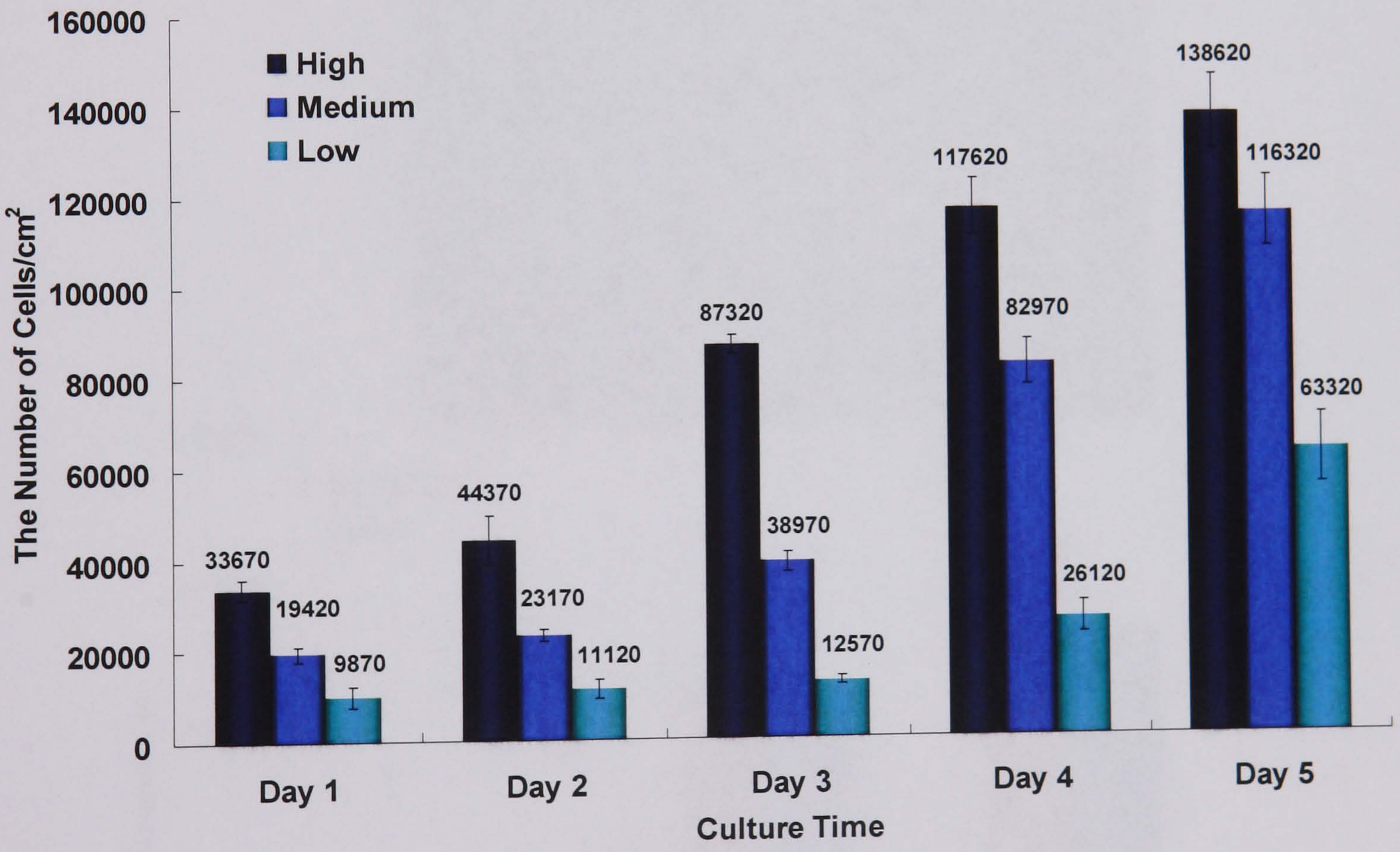
APPENDIX 6

A calibration curve was generated using the supplied reference collagen standard solution (Sircol Collagen Assay S 1000, Biocolor Ltd, Ireland), and other procedure was done according to previously described method in the section of 2.5.2.6. Measurement of collagen content and DNA content



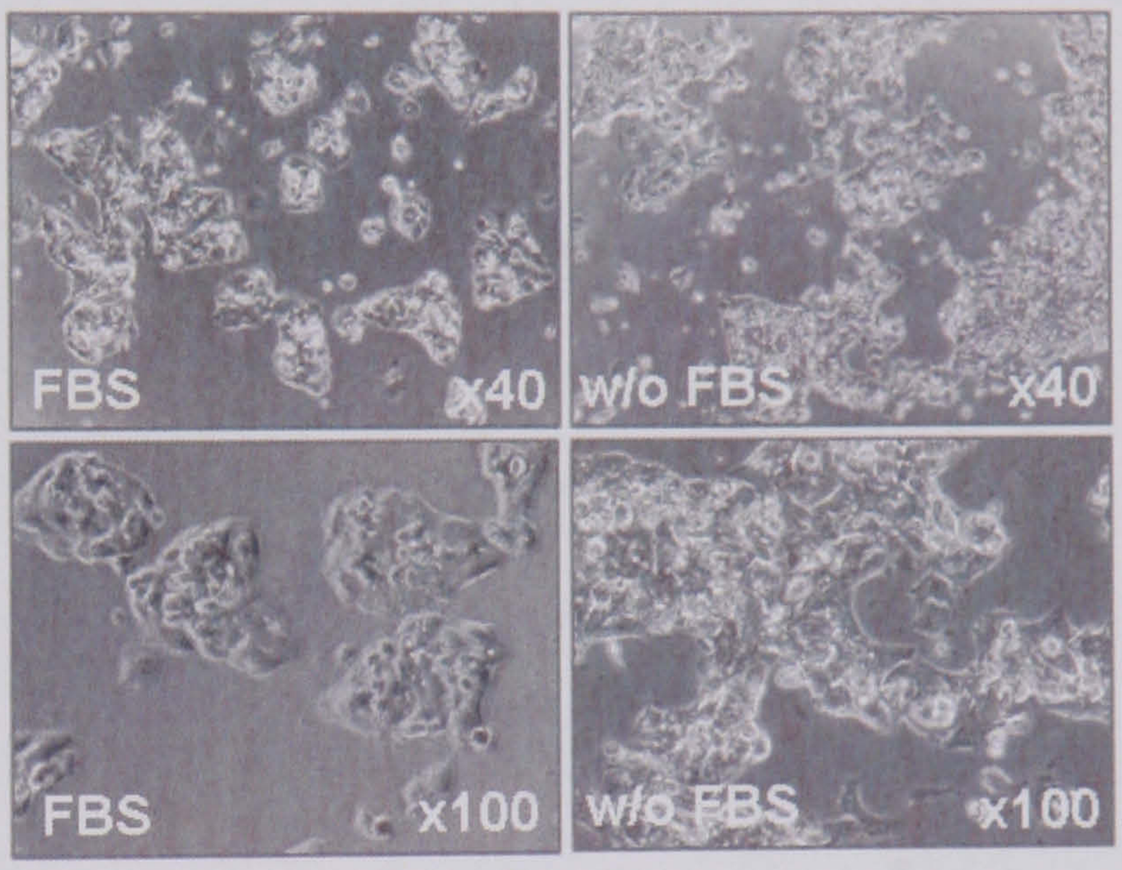
APPENDIX 7

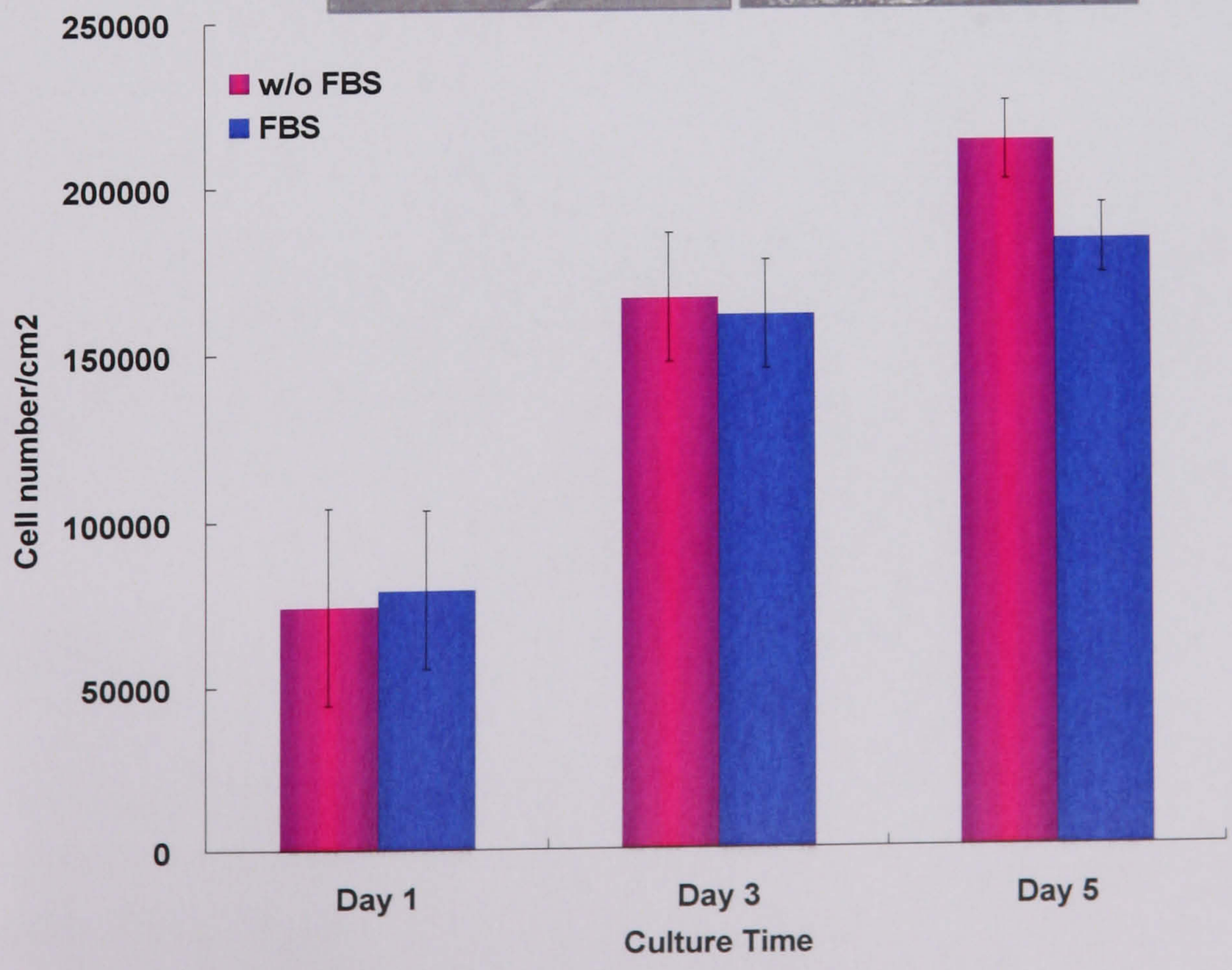
As a preliminary experiment, mESC (TG2a) growth was evaluated in accordance with initial cell seeding density for achieving optimal cell density for further researches. mESCs were seeded onto the plates at various concentration of 1.0×10^4 cells/cm^2, 2.0×10^4 cells/cm^2 and 3.0×10^4 cells/cm^2, and cultured for 1, 2, 3, 4, and 5 days in standard mESC maintenance culture medium at 37°C in a 5% CO_2 humidified incubator. Unattached cells were removed by thoroughly washing 3 times with 1X PBS. Cell growth were evaluated using the CellTiter 96® AQueous non-radioactive cell proliferation assay according to previously described method in the section of 2.3.1. mESCs, with initial cell seeding density of 3.0×10^4 cells/cm^2, reached almost 90% confluence and showed higher growth rate at early culture period. From this previous experiment, the cell density of 3.0×10^4 cells/cm^2 was used for further studies.



APPENDIX 8

For the further researches about the application of our developed cell culture system to human ESCs, as a previous experiment, we evaluated HepG2 cell growth in FBS free culture condition. HepG2 cells were seeded on culture plate with initial cell seeding density of 5 X 10^4 cells/cm^2 and cultured in HepG2 maintenance media containing FBS and in HepG2 maintenance media without FBS for 1, 3, and 5 days. Cell growth were evaluated using the CellTiter 96® AQueous non-radioactive cell proliferation assay according to previously described method in the section of 2.3.1. As shown in below figure, there was no significant difference in HepG2 growth between FBS containing medium and FBS free medium, suggesting that the FBS free conditioned medium from HepG2 culture can be applied to hESCs early differentiation.





ACHIEVEMENTS

DERIVED FROM THIS STUDY

PUBLICATIONS

1. **YS. Hwang**, WL. Randle, RC. Bielby, JM. Polak, A. Mantalaris "Enhanced osteogenic differentiation of murine embryonic stem cells: application to skeletal tissue engineering" Tissue Engineering (2006:12(6); p1381-1392)

2. **YS. Hwang**, A. Bishop, JM. Polak, A. Mantalaris "Enhanced chondrogenic differentiation of murine embryonic stem cells for cartilage tissue engineering" Biotechnology and Bioprocess Engineering (2007;12(6):696-706)

3. **YS. Hwang**, Y.Kang, A. Mantalaris "Directing embryonic stem cell differentiation into osteogenic/chondrogenic lineage *in vitro*" Biotechnology and Bioprocess Engineering: (2007;12(1):p15-21)

4. **YS. Hwang**, JM. Polak, A. Mantalaris "*In vitro* direct osteogenesis of murine embryonic stem cells without embryoid body formation" Stem Cell and Development (Accepted)

5. **YS. Hwang**, JM. Polak, A. Mantalaris "*In vitro* direct chondrogenesis of murine embryonic stem cells without embryoid body formation" Stem Cell and Development (Accepted)

6. **YS. Hwang**, JH. Cho, KLA. Chan, J. Heng, AR. Boccacini, SG. Kazarian, D. Williams, JM. Polak, A. Mantalaris "Bioprocessing three dimensional bone construct from murine embryonic stem cells using bioreactor" Stem Cells (Submitted)

7. **YS. Hwang**, JM. Polak, A. Mantalaris "Bioprocessing three dimensional cartilage construct from murine embryonic stem cells using bioreactor" Biomaterials (Submitted)

PRESENTATIONS

1. **YS. Hwang**, MR. Placzek, JM. Cha, A. Chan, SG. Kazarian, JM. Polak and A. Mantalaris "3-D Bone and Cartilage Constructs in Alginate Hydrogels from Murine Embryonic Stem Cells" 2007 September 9-11 International Nanomedicine Conference, Chalkidiki, Greece [Oral Presentation]

2. **YS Hwang**, MR. Placzek, JM Cha, A Chan, SG. Kazarian, JM. Polak, A. Mantalaris "Bioprocessing of 3-D bone and cartilage constructs from murine embryonic stem cells" 2007 June 17-20 5th Annual Meeting of the International Society for Stem Cell Research, Cairns, Queensland, Australia [Poster presentation]

3. **YS. Hwang**, J.M. Polak, A. Mantalaris "Enhanced chondrogenic differentiation from embryonic stem cells: Applications for cartilage tissue engineering" 2005 7th International Conference on Cellular Engineering (ICCE, IFMBE), Seoul, Korea [Oral presentation]

4. **YS. Hwang**, WL. Randle, R.C. Bielby, ND. Evans J.M. Polak, A. Mantalaris "Controlling mesodermal development of murine embryonic stem cells results in enhanced osteogenic and chondrogenic differentiation: Applications for skeletal tissue engineering" 2005 3rd Annual Meeting of the International Society for Stem Cell Research, Sanfrancisco, USA [Poster presentation]

5. **YS. Hwang**, R.C. Bielby, J.M. Polak, A. Mantalaris "Mesodermal Cell development from embryonic stem cell using HepG2 conditioned medium" 2004 Annual Meeting of Tissue and Cell Engineering Society, Bermingham, UK [Oral presentation]

PATENT

1. Title: Methods for production of mesodermal lineage cells, Patent pending (2005) PCT application number: PCT/GB2005/050089

HONORS AND AWARDS

- Young Investigator Award in 2005 7th International Conference on Cellular Engineering (ICCE, IFMBE), Seoul, Korea

- Research Assistantship: 2005-2008: DTI, "Developing Practical Applications of Stem Cell Technology"

- Winner of top 20 runners in Entrepreneurs' Challenge for the Business Plan of Cartilage Injectables. Tanaka Business School, Imperial College London (2004)